University of Southampton

Faculty of Environmental and Life Sciences

Ocean and Earth Sciences

Multi-scale investigations of cold-water coral habitat using novel technology and advanced image analysis.

by

David Michael Price

B.Sc., Bangor University

ORCID ID 0000-0001-7907-8457

Thesis for the degree of Doctor of Philosophy

February 2021

University of Southampton

Abstract

Faculty of Environmental and Life Sciences

Ocean and Earth Science

Doctor of Philosophy

Multi-scale investigations of cold-water coral habitat using novel technology and advanced image analysis.

by

David Michael Price

Cold-water corals, like their shallow-water counterparts are capable of forming reef habitats that are important for their local environment. Cold-water corals are under increasing anthropogenic pressure and thus, the need to map their occurrence and understand their fundamental ecological role is essential in order to plan effective conservation measures. Cold-water coral reefs promote biodiversity with the introduction of structural complexity and substrate heterogeneity. Whilst the role of structural complexity is important and is a key criterion of Vulnerable Marine Ecosystem designation, we typically lack high-resolution data that can quantify such metrics. Ship-borne multibeam echosounder (MBES) data is typically low resolution, missing vital geomorphological features and the detailed video coverage is minimal in comparison. This results in Ill-matched datasets for mapping coral extent through predictive mapping and insufficient resolution to quantify cold-water coral reef structural complexity. We deployed an Autonomous Underwater Vehicle to collect high-resolution MBES data and Remotely Operated Vehicles to collect images for Structure from Motion (SfM) to bridge the gaps in data resolution and undertake novel fine-scale investigations.

The results in this thesis show that by resolving fine-scale geomorphological features with high-resolution bathymetry, additional locations suitable for cold-water coral growth can be identified. The results further highlighted the importance of vertical walls in Explorer Canyon, NE Atlantic, as a habitat for cold-water coral. This thesis also demonstrates how SfM can be used to quantify cold-water coral structural complexity. Cold-water coral reef in Explorer Canyon introduces significant structural complexity on a centimetric scale, promoting local biodiversity and providing a distinct cold-water coral habitat when coral coverage was greater than 30%. Further investigations reveal that cold-water coral associated taxa are not randomly distributed within cold-water coral reefs, instead local geomorphic properties such as rugosity and inferred biotic interactions are conducive to localised clustering of reef associated species. The combination of scales of analysis quantitively depict how important cold-water coral are to their local environment and more accurately indicate their true spatial extent providing useful information for marine spatial planning.

Table of Contents

Table of Tables

Table of Figures

Table of Figures

Research Thesis: Declaration of Authorship

Print name: David Michael Price

Title of thesis: Multi-scale investigations of cold-water coral habitat using novel technology and advanced image analysis.

I declare that this thesis and the work presented in it are my own and has been generated by me as the result of my own original research.

I confirm that:

1. This work was done wholly or mainly while in candidature for a research degree at this University;
2. Where any part of this thesis has previously been submitted for a degree or any other qualification at this University or any other institution, this has been clearly stated;
3. Where I have consulted the published work of others, this is always clearly attributed;
4. Where I have quoted from the work of others, the source is always given. With the exception of such quotations, this thesis is entirely my own work;
5. I have acknowledged all main sources of help;
6. Where the thesis is based on work done by myself jointly with others, I have made clear exactly what was done by others and what I have contributed myself;
7. Parts of this work have been published as:

Price, D.M., Robert, K., Callaway, A., Lo Iacono, C., Hall, R.A., Huvenne, V.I.A. Using 3D photogrammetry from ROV video to quantify cold-water coral reef structural complexity and investigate its influence on biodiversity and community assemblage. Coral Reefs 38, 1007–1021 (2019). https://doi.org/10.1007/s00338-019-01827-3

Signature: 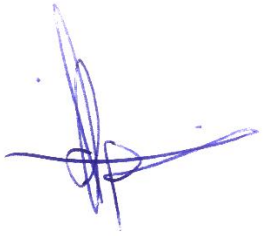 Date: 12/02/2021

Acknowledgements

First and foremost, I wish to thank my primary supervisor Dr Veerle Huvenne for supporting my work and providing a rich learning experience. This was especially important in the final months of the PhD, I'm not sure I would have finished this work without Veerle's technical and moral support! I thank Dr Alex Callaway for his unbelievable eye for detail and technical support (and regular grammar lessons!). I thank Dr Claudio Lo Iacono, Dr Rob Hall and Dr Antony Jensen for their continued help, guidance and encouragement! I thank Dr Katleen Robert, Dr Aaron Lim, Dr Markus Eichhorn and Prof Andy Wheeler for their data contributions and statistical support for my PhD research. All of the above mentioned have contributed so much to my scientific thinking! I thank the captain and crew of the scientific cruises undertaken to collect the data presented in the thesis.

I have made many friends within the GSNOCs and NEXUSS community, and in our office, whom I am grateful for their friendship throughout this journey. In particular I was lucky enough to share my office with Dr. Tabitha Pearman and Guillem Corbera who have become amongst my closest of friends. Without you guys, it would have been impossible. So many laughs were shared!

I was lucky enough to visit many countries to broaden my scientific perspective through conferences and fieldwork. I met so many wonderful scientists along the way and enjoyed lots of productive, insightful discussions. In particular, I would like to thank boss man Lim and Andy for hosting me at UCC, Ireland. I enjoyed the fruitful learning experience and I had maximum craic with the lads in the office!

2020 was a challenging year for everyone. I was lucky enough to have spent lockdowns with some of the best people. I wish to thank Sarah Breimann, Stephen Cooper and Milla Kalasnikova for keeping me sane during lockdown v1, Matthew Johnson, Helen Harrison and especially Thelma for keeping me sane during lockdown v2 and my parents for keeping me sane during lockdown v2.5 and v3. Furthermore, the regular online chats with my family and the Barmby lot during lockdowns were always uplifting!

Last but most certainly not least, I wish to thank my parents, Alan and Julia, my nan, Joan, and family (Nina, Jenny, Dave), for their continued support, encouragement and for believing in me! This support has been evident throughout and has kept me motivated. Thank you to Alan Price for proofreading various parts of drafts over the years.

Definitions and Abbreviations

AIC ..... Akaike's Information Criterion

AUC ..... Area Under the Receiver Operating Curve

AUV ..... Autonomous Underwater Vehicle

BPI ..... Bathymetric Positioning Index

DEM ..... Digital Elevation Model

GAM ..... Generalised Additive Model

GCP ..... Ground Control Point

MBES ..... Multibeam echosounder

MCZ ..... Marine Conservation Zone

MPA ..... Marine Protected Area

PPA ..... Point Pattern Analysis

PCF ..... Pair Correlation Function

PPM ..... Point Pattern Modelling

ROV ..... Remotely Operated Vehicle

SDM ..... Species Distribution Modelling

SfM ..... Structure from Motion

SSS ..... Side-scan sonar

VME ..... Vulnerable Marine Ecosystem

VRM ..... Vector Ruggedness Measure

Chapter 1 Introduction

1.1 Coral

Corals are marine invertebrates best known for their reef formations and vivid colours. Corals can form reefs which are important for biodiversity, human food resource, economy (tourism), medicinal discovery and coastal protection. A range of natural and anthropogenic stressors put pressure on these habitats, locally and globally (Wilkinson, 1999), and as coral are slow growing organisms, recovery from damage is sluggish (Knowlton et al, 2001). Whilst the tropical, shallow-water corals are the most well-known types, corals are found globally, across a range of depths, even beyond the photic zone, where they are no less susceptible to anthropogenic stressors (Davies et al., 2007). Therefore, ecological research is essential in order to understand their distribution and functioning, even in the locations that are difficult to reach, such as the deep-sea.

Corals are found within the phylum Cnidaria, which consists of more than 11,000 species according to the World Register of Marine Species (WORMS), including jellyfish, coral and anemones. The class Anthozoa consists of fully sessile species, and is split into 3 sub-classes: Hexacorallia, Octocorallia and Ceriantharia. Corals are found within the Hexacorallia and Octocorallia. Hexacorallia have 6 or fewer axes of symmetry, Octocorallia have 8-fold symmetry. Hexacorallia contains hard corals (Scleractinia), black corals (Antipatharia), anemones (Actinaria), Zoanthids (Zoantharia) and Corallimorpharia. Octocorallia consist of soft coral (Alcyonacea), Helioporacea, and sea pens (Pennatulacea).

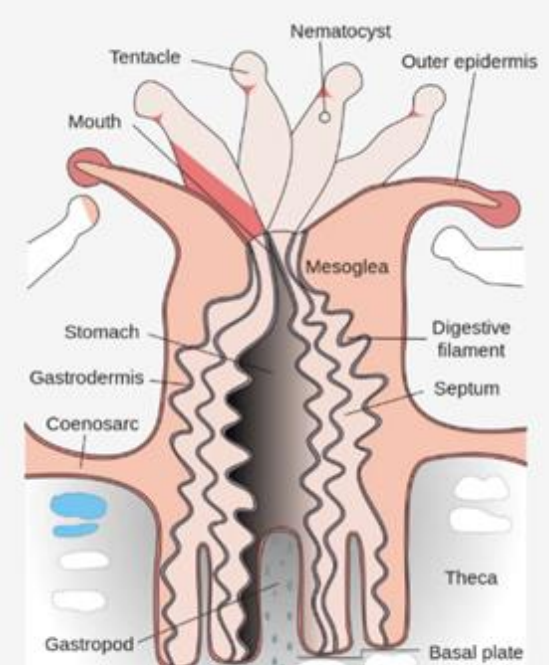

Figure 1.1. Schematic of an individual coral polyp. Figure from Wikipedia Commons.

Corals are sessile animals and are capable of forming colonies consisting of individual polyps (Figure 1.1). Stony (hard) corals secrete calcium carbonate to form a skeleton, providing the colony with a stable structure and protection. Soft corals do not produce such hard skeleton, instead groups like Alcyonacea spp. rely on calcium carbonate sclerites and proteins for structure. Polyps are typically connected through a coenosarc and can showcase colonial behaviour in terms of polyp extension and movement. Shallow-water corals, usually found in tropical waters are most well-known due to their relative accessibility and vivid colours. In such habitats, corals form symbiotic relationships with

algae, which provide sustenance of the coral via photosynthesis and give rise to those vivid colours. However, not all coral species form these relationships to become zooxanthellate (algae harbouring). In fact, more than 66% of coral species are found in waters deeper than 50 m, defined as the deep-sea (Cairns, 2007). This would typically suggest a global dominance of those species that do not possess the symbiotic algae: azooxanthellate coral types. These groups are known as cold-water corals (also deep-sea corals).

1.2 Cold-water coral - background

Cold-water corals are filter feeders that rely on passing food such as zooplankton and organic particulate matter, meaning they are not restricted to the shallow, light saturated waters. Instead, cold-water corals can be found as deep as 6, 328 m (Keller, 1976). Cold-water corals were first observed following the advent of deep-sea fishing techniques in the 1700's and first documented in the scientific literature in 1755 by Erich Pontoppidan in "The Natural history of Norway". Soon after, cold-water corals such as "*Madrepora pertusa*" (Linnaeus, 1758) were described. Sars (1865) was the first to describe a major coral bank in the Oslo Fjord that consisted of dead coral, though they were previously well known by Norwegian and French fishermen (Teichert, 1958). Charles Wyville-Thomson later led the famous worldwide expedition aboard HMS Challenger, which led to the discovery that deep-sea life was indeed widespread, and included corals, despite early notions that life did not occur below 300 fathoms (550 m). Compared to their shallow-water counterparts, cold-water corals remain a relatively lesser studied group. This is owing to the costs, time and technological restraints of studying deep-sea organisms. However, the recent development of research technology has progressed our understanding of these habitats by using imagery, underwater acoustics and targeted physical sampling. Since the 1970's, cold-coral coral habitats have garnered great scientific interest (Roberts et al., 2009). The rapid expansion of research focusing on cold-water corals has greatly increased our understanding of their distribution, functioning and vulnerability. This is timely because of the threats that the Anthropocene poses to cold-water corals, such as fishing, climate change and pollution, and therefore understanding cold-water coral habitats is essential if we are to effectively protect them.

1.3 Development of cold-water coral reefs

More than half of the 5, 080 known coral species are cold-water coral (Cairns et al., 2007). Most research has focussed on the reef building scleractinians of which there are several main species; *Desmophyllum pertusum* (Synonym: *Lophelia pertusa*), *Madrepora oculata*, *Enallopsammia rostrata*, *E. profunda*, *Oculina varicose, Bathelia candida*, *Goniocorella dumosa*, and *Solenosmilia*

variabilis. *L. pertusa* has recently transferred genus and been named as *Desmophyllum pertusum* (Addamo et al., 2016) which has been accepted in WoRMS. However, due to the cautiousness of taxonomists to embrace this nomenclature until further molecular data is available (Cairns, 2019 note in WoRMs; Cairns and Hourigan, 2020) and for harmony with the plethora of research undertaken since the 70's, this thesis hereafter refers to *L. pertusa* (Figure 1.2). These species are focussed on due to their ability to form three-dimensional, structurally complex frameworks which provide structural complexity and substrate heterogeneity to the seafloor, which is an important provisioning to the ecosystem. These colonies can either be isolated or under suitable conditions can form reefs and mounds.

Figure 1.2. Closeup image of *Lophelia pertusa*. Image from CODEMAP ROV dive 254.

Hard substrate is a prerequisite for initial settlement (Wilson 1979) and in areas where hard substrate is sparse, small boulders or dropstones may suffice (Wilson 1979; Wheeler et al., 2008). Upon metamorphosis of coral larvae that have settled, a holdfast is created and polyps can grow outwards and bud, secreting a calcium carbonate skeleton with a linear extension growth rate up to 33 mm $year^{-1}$ (Mortensen and Rapp, 1998; Gass and Roberts, 2006; Orejas et al., 2008; Brooke and Young, 2009; Orejas et al., 2011). Over time, outward growth leads to the senescence of older polyps found deeper in the framework due to sedimentation, water stagnation and poor food accessibility from the overlying water column, as seen in shallow-water coral (Chamberlain and Graus, 1975), and they eventually die leaving dead coral skeleton framework behind. Through asexual reproduction of coral (fragmentation and budding) and accumulation of surrounding colonies, aggregations called thickets are formed (Squires, 1964; Wilson, 1979). Thickets are precursors for lateral expansion of cold-water coral resulting in underlying dead colonies which

subsequently collapse and coral debris (or rubble) is formed through biological and physical erosion, resulting in a "coppice" stage. When the coral rubble accumulates, together with baffled sediment, coral banks are subsequently formed which are characterised by live coral at the top, the presence of coral debris (rubble) and a compact mass of coral debris and mud (Squires 1964). More recently the terms reef and mound are commonly used to describe coppices and coral banks (Roberts et al., 2009; Mackay et al., 2014). The term reef was originally coined to describe submerged objects that a ship may strike (Roberts et al., 2009). However, in modern ecology and policy, the term reef is liberally applied to cold-water coral bioherms. In this context a "cold-water coral reef" is considered a biogenic reef which is a self-sustaining habitat that has a positive expression on the seafloor, alters the local hydrodynamic regime and provides a habitat for benthic organisms (Roberts et al., 2009).

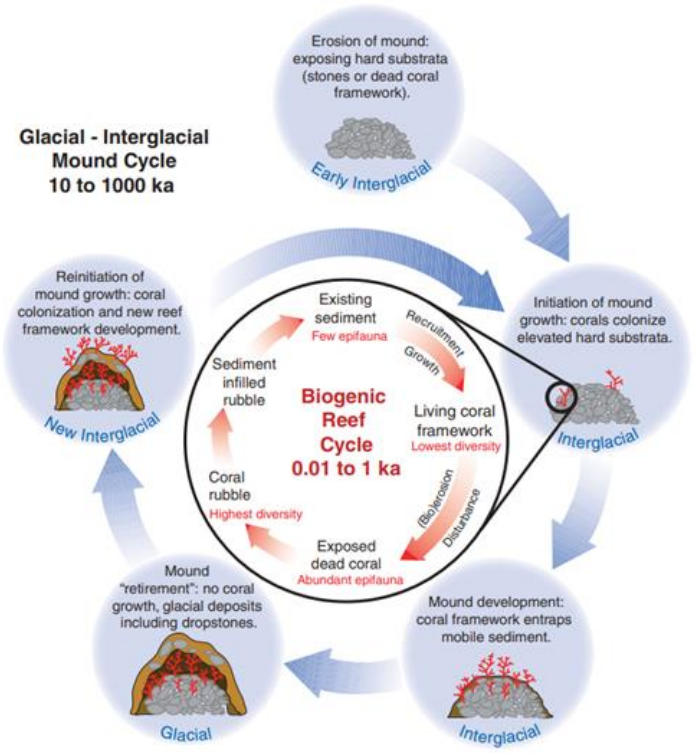

Figure 1.3. A schematic to demonstrate the development of carbonate mounds. Figure from Roberts et al., 2006.

Extensive cold-water coral reefs were first intensively studied in the North East Atlantic, including the large continuous reef formations on the Norwegian shelf (Mortensen et al., 1995; Hovland et al., 1998; Fossa et al., 2002; Freiwald et al., 2002). Throughout glacial and interglacial time periods, coral reefs experienced suitable and unsuitable environmental conditions and in some cases over time grew to form carbonate mound features (Figure 1.3; Wilson, 1979; Hovland et al., 1994; De Mol et al., 2002; Masson et al., 2003; Kenyon et al., 2003). Mounds can vary in size from a few metres high (Masson et al., 2003; Wheeler et al., 2011a) to hundreds of metres high (Kenyon et al., 2003; Huvenne et al., 2003; O'Reilly et al., 2003; van Weering et al., 2003). Carbonate mounds form provinces in the North East Atlantic, e.g., the Rockall Trough (Kenyon et al., 2003; van Weering et al., 2003; Mason et al., 2003) and the Porcupine Seabight (De Mol et a., 2002; Van Rooij et al., 2003), and in other regions of the Atlantic Ocean; offshore Namibia and Angola (Hanz et al., 2017), offshore Mauritania (Wienberg et al., 2018), in the southern Gulf of

Mexico (Matos et al., 2019), offshore Argentina (Steinmann et al., 2020) and offshore Brazil (Raddatz et al., 2020), and in the Mediterranean sea (Corbera et al., 2019). The South Atlantic, Indian and Pacific Oceans are under-investigated in terms of mapping cold-water coral reefs (Lim et al., 2021), and could support further undiscovered reef and mound systems. For example, recent surveys have revealed coral mounds in the Indian Ocean (Reolid et al., 2017). In addition, recent examples of reef-building scleractinians have also been observed in the Pacific Ocean (Baco et al., 2017), though the ocean chemistry is thought to be unsuitable for wide spread scleractinian coral occurrence (Guinotte et al., 2006).

1.4 The role of cold-water coral reefs in promoting biodiversity

Early scientific investigations into the biodiversity of cold-water coral reefs relied on fishing techniques such as dredging. Teichert (1958) described early studies which found 190 species associated with cold-water coral reefs. Burdon-Jones and Tambs-Lyche (1960) utilised dredge hauls to collect 300 species from Norwegian reefs (as cited in Teichert, 1958). However, less destructive sampling methods to quantify biodiversity are now more commonplace and include video assisted grabs (Mortensen et al., 2000), videos (e.g. Pearman et al., 2020) and images (e.g. van den Beld et al., 2017). This range of survey approaches has enabled us to study the association between cold-water coral and other species, from mega- to microfauna. For example, we now know that over 1,300 species in the North East Atlantic alone have been associated with cold-water coral reefs (Roberts et al., 2006).

Corals are autogenic ecosystem engineers that are able to alter their local physical environment with consequences for the local biodiversity (Jones et al., 1994). It is therefore unsurprising that reefs and aggregations of reef-building coral are hotspots of biodiversity because they provide various niches for other organisms to occupy (Roberts et al., 2006). Even within cold-water coral

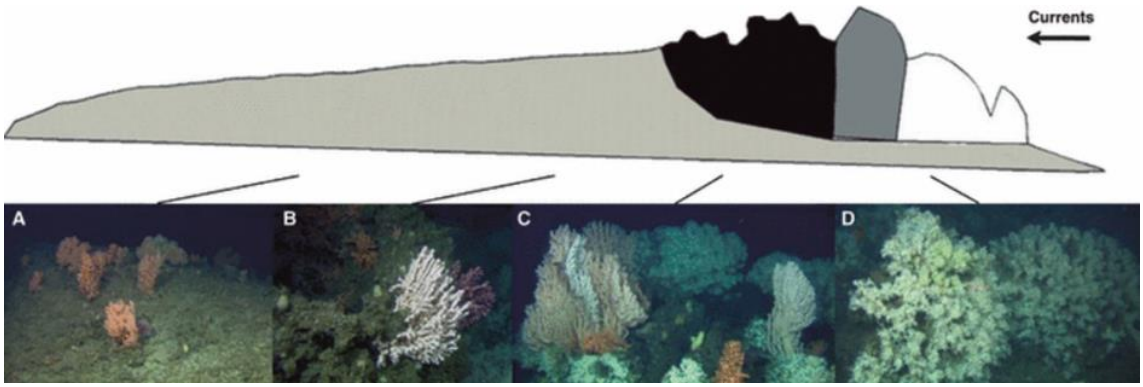

Figure 1.4 Schematic of the Zonation in a cold-water coral reef under a unidirectional current: A) Tail of the reef composed of coral rubble. B) Dead coral framework. C) Recently dead coral framework. D) Live coral framework. Figure from Buhl-Mortensen et al. (2010).

reef habitats, live coral framework, dead coral framework and coral rubble all provide distinct macro- to mesohabitats (metres to tens of metres) and introduce spatial heterogeneity (Figure 1.4). Furthermore, Mortensen et al. (1995) proposed that smooth living coral, detritus laden coral skeleton, skeleton cavities and vacant space between coral skeleton provides multiple micro-habitats.

Cold-water coral reefs are diverse habitats supporting distinct associated communities (Jonsson et al., 2004; Mortensen and Fossa, 2006; Henry and Roberts, 2007; Roberts et al., 2008) and early studies made comparisons with shallow-water coral reef in terms of biodiversity (Jensen and Frederiksen, 1992; Rogers, 1999). Most studies observe that species richness and abundance of associated species is greater on than off reefs and mounds (e.g. Jonsson et al., 2004; Henry and Roberts, 2007; Roberts et al., 2008; Mienis et al., 2014). Two fundamental drivers of biodiversity in cold-water coral reefs are considered in this thesis 1) provision of hard substrate, and 2) structural complexity.

Hard substrate provides a point of contact for sessile organisms to settle upon (Henry and Roberts, 2017), which may otherwise be lacking in the area. This typically occurs on dead coral framework which appears to support a greater number of species compared to living framework of reef. For example, cold-water corals host a wide variety and abundance of encrusting species and biofilm communities within the framework (Freiwald et al., 2004; Beuck et al., 2007; van Oevelen et al., 2009). Sessile megafauna such as sponges appear to commonly occur within coral reef habitat (Van Soest et al., 2007; De Clippele et al., 2018), notably *Aphrocallistes* spp. (Henry and Roberts, 2007; Buhl-Mortensen et al., 2017; Boolukos et al., 2019). Soft corals and other filter feeders are additionally found colonising the dead coral framework (Beuck et al., 2007; Henry and Roberts, 2007; De Clippele et al., 2019; Corbera et al., 2019). Associated taxa seldom colonise the living portion of the framework (Mortensen 2001; Mortensen and Fossa, 2006), due to live polyps and tissue (coenosarc) covering the skeleton which is unsuitable for larvae to settle upon. However, due to surface patchiness of live reef, some dead framework is always exposed (Wilson, 1979), meaning even reefs with high live coral cover are able to support sessile taxa which utilise the hard substrata of dead coral framework (Mortensen et al., 1995).

Structural complexity is another product of cold-water coral framework which introduces multiple niches and provides physical shelter from currents and predation. In shallow-water coral reefs, structural complexity is a promoter of biodiversity (Friedlander and Parrish, 1998; Gratwicke and Speight, 2005). The link between cold-water coral structural complexity and associated taxa is more difficult to establish, due to the challenge of quantifying structural complexity at depth. Structural complexity is likely to enhance shelter for organisms from predation, for example, it has been

inferred that *Cidaris cidaris* utilise the structure of cold-water coral framework to avoid predation (Stevenson et al., 2015). In addition, many observations note that demersal fish benefit from structure provided by cold-water coral (Ross and Quattrini, 2007; Fernholm and Quattini, 2008; Soffker et al., 2011; Purser et al., 2013; Kutti et al., 2014). Cold-water coral reef structure may provide a refuge for adult fish (Henry et al., 2013; Henry and Roberts, 2017) but has particular suitability as nursery grounds for juveniles (Costello et al., 2005; Henry et al., 2013; Corbera et al., 2019). The links between cold-water coral and fish are not functionally unique (Auster 2005): other structurally complex habitat such as boulder fields, sponge grounds and other topographically complex features can provide comparable habitat for reef associated species (Auster, 2005; Harter et al., 2009; Miller et al., 2012). However, this supports the argument that structural complexity promotes deep-sea mobile taxa abundance and diversity, which can be provided by cold-water coral reefs.

In addition to providing physical shelter, the structure of the framework has a direct effect on the immediate overlaying water by increasing drag and thus reducing the boundary layer flow velocity (Mienis et al., 2019). In general, near bottom flow velocities are lower within reef areas compared to outside reef areas, as has been observed at the Tisler reef where flow velocity was up to 2.4 times greater outside the coral framework area (Guihen et al., 2013). Mienis, et al. (2019) observed that the water-framework interface was turbulent which enhanced vertical momentum and flow velocity was drastically reduced within and downstream of the coral patches (Mienis et al., 2019). This interruption of flow provides additional micro-habitats (Buhl-Mortensen et al., 2010) and turbulence allows vertical transport of food particles to individual animals inhabiting the reef, including the reef building coral itself. The reduced boundary current within coral framework and immediate areas around coral framework is likely to provide suitable feeding conditions for some sessile organisms including reef-building corals themselves, by reducing the chances of flow induced deformed polyps or particles ripping off the tentacles before ingestion (Purser et al., 2010), which result in low feeding efficiency (Purser et al., 2010; Orejas et al., 2016). Though this is specific to certain species as some cold-water corals' feeding efficiency are not so impacted by local current flow (e.g. Gori et al., 2015). These mechanisms may explain why cold-water coral reefs support greater numbers of filter feeders than surrounding proximal habitats (Johnsson et al., 2004; Henry and Roberts, 2007). In addition, it is possible that the reduced flow could aid larval entrainment to the framework, as suggested by De Clippele et al. (2018). For example, it has been noted that micro-structural complexity induces turbulence and eddies, aiding the entrainment of coral larvae (Hata et al., 2017). Furthermore, Boxshall (2000) and Harri and Kayanne (2002) demonstrated larval settling abilities of some shallow-water species are greater in low flow regimes. It is likely similar mechanisms may aid settlement of some reef-builder larvae in cold-water coral framework,

especially for mature larvae which swim at higher swimming speed (Larsson et al., 2014) which combined with lower flow speeds could increase the distance covered and settlement success through the increased hard substrate encounter potential.

The fundamental drivers of structural complexity and hard substrate provide the basis and creation of a food chain, thus attracting predators. Biofilms including bacteria, foraminifera and small epifauna are likely to support predatory macrofauna such as polycheates, crustaceans and echinoderms (van Oevelen et al., 2009). Furthermore, fishes are observed foraging and feeding around cold-water coral reefs (Husebro et al., 2002; D'onghia et al., 2012), probably taking advantage of increased prey abundance.

These relationships generally relate to well-developed cold-water coral framework structures. Coral rubble is less structurally complex and may not provide as stable a hard substrate, depending on the hydrodynamic regime. However, coral rubble and debris still form an important habitat for some species such as squat lobsters (Mortensen et a., 1995), deposit feeders (Mortensen and Fossa, 2006) and distinct meiofauna assemblages (Bongiorni et al., 2010).

1.5 Environmental controls on cold-water coral distribution

Cold-water corals are observed in all oceans (Figure 1.5), and are often found associated with geomorphological features such as fjords (Buscher et al., 2019; Brooke and Jarnegren, 2013), continental slopes (Thiem et al., 2006), submarine canyons (Huvenne et al., 2011; De Mol et al., 2011; Gori et al., 2013; van den Beld et al., 2017) and seamounts (Koslow et al., 2001; Duineveld et al., 2004; Baco et al., 2017). Distribution of cold-water coral is driven by their ecological niche which is defined by biological, chemical, hydrodynamic and geological factors.

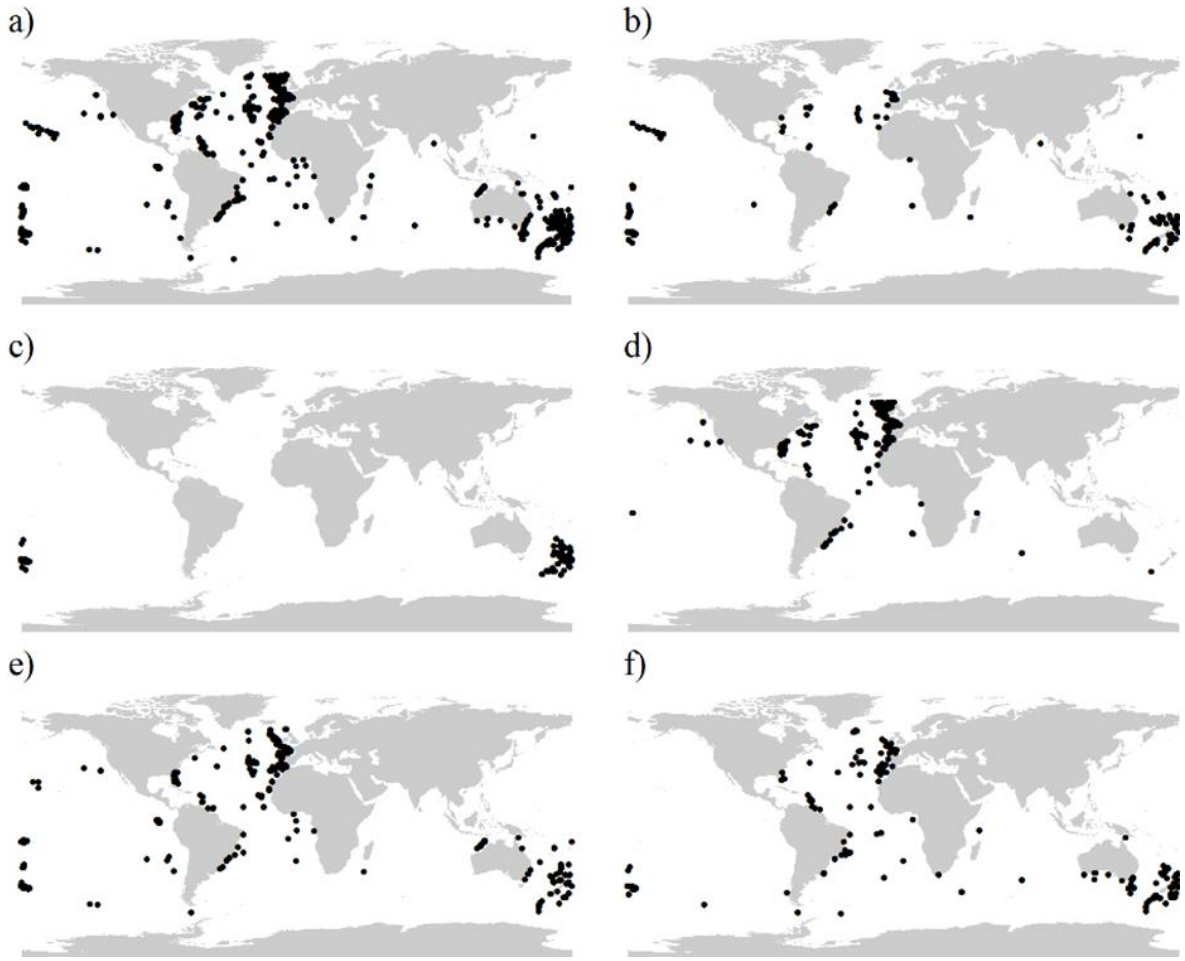

Figure 1.5 Global distribution of reef forming cold-water corals A) Five reef-forming cold-water coral species, B) *Enallopsammia rostrata*, C) *Goniocorella dumosa*, D) *Lophelia pertusa*, E) *Madrepora oculata*, F) *Solenosmillia variabilis*. Figure from Davies and Guinotte (2011)

1.5.1 Substrate

Hard substrate is a prerequisite for cold-water coral occurrence due to the need for hard substrate for larvae settlement. *L. pertusa* larvae, for example, are planktotrophic, active swimmers, and 3-5 weeks after fertilisation, bottom probe until a suitable settlement site is chanced upon (Larsson et al., 2014). Dead coral skeleton is also an important settlement medium (Roberts et al., 2009). Small mobile substrata are unsuitable for attachment and subsequent growth.

1.5.2 Water mass properties

Oceanic water masses are bodies of water characterised by specific ranges of physical and chemical properties, such as temperature, salinity, oxygen and pH. Some of these properties have fundamental physiological impacts on cold-water coral and thus may influence their distribution. For example, *L. pertusa* increases its oxygen consumption by 50% under a 2°C warming,

demonstrating great sensitivity (Dodds et al. 2007). Aragonite, a "polymorph" of calcium carbonate, forms the skeleton of scleractinian cold-water corals. As low pH can dissolve calcium carbonate structure, the pH of the water influences cold-water coral physiology (Hennige et al., 2014), and skeleton structure (Hennige et al., 2015; 2020). Whilst some *ex situ* experiments have found physiological acclimation in aragonite undersaturated waters (Maiar et al., 2019), the scarcity of reef forming cold-water coral in the Pacific, which is largely undersaturated, is palpable (Guinotte et al., 2006). These examples establish that water composition is important for cold-water coral presence and distribution. This was further demonstrated by Dullo et al., (2008) who found that thriving *L. pertusa* in the NE Atlantic was only found in a density "envelope" of 27.35 to 27.65 kg m^3 in the NE Atlantic which may influence larvae and food transport. However, cold-water corals are still found outside of this optimal density envelope in other regions (Western Atlantic: Davies et al., 2010; Mediterranean: Gori et al., 2013; Taviani et al., 2017; Angeletti et al., 2020) and under variable hydrodynamic regimes whereby the water column properties and particle retention within pycnoclines may be influenced by various, more localised, hydrodynamic mechanisms (Huvenne et al., 2011).

1.5.3 Oceanography as a distribution driver

Even the earliest observations of cold-water coral reefs noted that cold-water coral distribution was linked with oceanography. Cold-water coral 'banks' were located where "Atlantic water wells upward and surges around promontories" (Dons, 1934 as cited in Teichert, 1958). Hydrodynamics influence coral at different scales (Monismith 2007), from the scale of individual polyps to coral distribution over 100's of kilometres.

1.5.3.1 10 km – 100's km

Large oceanic circulation currents are important in the dispersal of larvae and connectivity between reefs (Buhl-mortensen et al., 2015), and have facilitated the endurance of cold-water coral reefs over wide geographic areas (Henry et al., 2014). The larvae of cold-water corals such as *L. pertusa* can drift in the water column for 3-5 weeks, providing scope for extensive transport (Larsson et al., 2014). Regional currents provide links between populations as seen in and around the Gulf of Mexico (Morrison et al., 2011) and in the NE Atlantic (Le Goff-Vitry et al., 2004; Fox et al., 2016). In addition, it is assumed that coral larvae transported via the Mediterranean Outflow Water, supplied NE Atlantic reefs during inter-glacial periods (De Mol et al., 2005; Flot et al., 2013), particularly for *L pertusa* (Boavida et al., 2019), which provided a stepping stone for dispersal to Norwegian reefs (Henry et al., 2014). However, at broader scales such as trans-North Atlantic, connectivity may be inhibited by geographic barriers such as depth difference isolation and oceanography that retains

larvae (Morrison et al., 2011). This demonstrates that even if all other conditions are suitable, such as a plentiful food source, coral presence and distribution still relies on larval supply from other areas.

Large scale internal waves which propagate along water density contrasts, can reflect or break due to shallowing of the shelf. The turbulence caused by the break is thought to resuspend material and cause wide-scale mixed zones, which are suspected to be an important food supply and mound growth mechanism to Faroe Islands reefs and NE Atlantic mounds (Frederiksen et al., 1992; White et al., 2010). Furthermore, internal waves that are reflected upwards may enhance surface primary production via mixing and the transport of nutrients to the surface, which ultimately may end up as sustenance for coral via vertical transport on a more local scale.

1.5.3.2 10's of metres to km

As sessile organisms, cold-water corals rely on water movement to supply food from outside the reef area to the reef vicinity. Complex topography and internal waves cause enhanced near-bottom current speeds (Genin et al., 1986; Davies et al., 2009) which may reach over 100 cm s^{-1} in the local vicinity around cold-water coral reef habitats (Lim et al., 2020). Accelerated near-bottom currents around reefs are thought to supply reefs with resuspended matter for sustenance (Duineveld et al., 2004; Thiem et al., 2006; Mienis et al., 2009; Davies et al., 2009), which is subsequently entrained through the baffling effect of reef structures on boundary layer currents, resulting in a more suitable feeding environment for individual polyps.

Many reef locations show evidence for surface productivity as a prominent food source. Larger topographic forms such as mounds and seamounts may enhance surface productivity by mixing water, pushing nutrient rich deep waters to the surface (White et al., 2005). Taylor caps which are bodies of water retained above localised high-profile topography as a conical vortex and can be found around banks and seamounts. It is suspected that Taylor caps retain surface productivity above the seamount or bank, allowing Ekman drainage where dense water drains through the benthic boundary layer to transport surface productivity to cold-water coral habitats on the flanks (White et al., 2005, 2007; Duineveld et al., 2007).

Active downwelling is also an important food supply mechanism. For example, at the relatively shallow (~100-150 m depth) Mingulay reef, a tidally-driven hydraulic jump causes downwelling of surface water, which is subsequently washed over reefs on the turn of the tide (Davies et al., 2009). Tisler reef (Norway, 70-160 m depth) also exhibits similar hydrology, though downwelling is driven by residual flows rather than tidal currents and can occur at both sides of the reef (Wagner et al., 2011). In addition, large coral mounds have the ability to create local downwelling and mixing,

leading to surface and mid water intruding down to the mounds, potentially providing nutrient-rich shallower water to reefs covering the flanks of the mounds (Cyr et al., 2016; Soetaert et al., 2016).

1.6 Using environmental variables to predict cold-water coral

Collecting data on cold-water coral presence is spatially restricted by the time and expense of reaching survey sites and deployment of platforms to collect samples or images of the seafloor. Therefore, various modelling approaches based on known species-environment relationships have been deployed to extrapolate information obtained at discrete data points to surrounding areas. This methodology is known as Species Distribution Modelling (SDM) or Habitat Suitability Modelling. SDM is based upon multivariate regression statistics such as Generalised Additive Models, or on machine learning approaches such as Random Forest to accommodate multiple environmental factors that have non-linear relationships with the species of interest. SDM of reef building coral has been undertaken on a global (Davies et al., 2008; Davies and Guinotte, 2012), regional (Rengstrof et al., 2013; Mienis et al., 2014; Georgian et al., 2014; Guinotte and Davies, 2014; Anderson et al., 2016a, b; Tracey et al., 2011; Ross and Howell, 2013) and local scale (Dolan et al., 2008; Guinan et al., 2009; Howell et al., 2011; Robert et al., 2015; De Clippele et al., 2017; Lo Iacono et al., 2018; Bargain et al., 2018) with varying data resolutions. These spatial predictions are important outputs in aiding spatial management planning (Howell et al., 2011; Reiss et al., 2015). Furthermore, SDM can be used to predict what the effects of climate change will be on cold-water coral distribution (Jackson et al., 2014; Morato et al., 2020), which in turn may be beneficial for future proofing marine spatial planning (Jackson et al., 2014).

Oceanographic variables are important for cold-water coral distribution but information is seldom available in sufficient spatial resolution due to sparse data points and temporal variability of the data points which is difficult to incorporate with spatial data. However, hydrodynamic models are being increasingly used to support SDM, improving the SDM performance and accuracy (Pearman et al., 2020). They have shown that cold-water coral is predicted to occur in areas of intense current velocity (Rengstorf et al., 2014; Mohn et al., 2014; De Clippele et al., 2017; Bargain et al., 2018; Pearman et al., 2020), which is consistent with *in situ* benthic monitoring of hydrodynamic regimes around cold-water coral reefs which reveal coral reefs may experience currents in excess of 40 cm s^{-1} (e.g. Mienis et al., 2014; Lim et al., 2020).

Some of the most common datasets used in SDM for cold-water coral are geomorphic terrain variables derived from bathymetric data collected by acoustic mapping. These variables include depth, slope, curvature, Bathymetric Positioning Index (BPI), rugosity and aspect. These variables act as proxies for many variables known to influence cold-water coral distribution. Slope can be a

proxy for substrate type (Dove et al., 2020), stability of substrate (Lecours et al., 2016), current flow (Genin et al., 1986) and breaking internal waves (Frederiksen et al., 1992). Bathymetric Positioning Index, which quantifies localised bathymetric elevation or depression, can relate to substrate composition (Lundblad et al., 2006) and exposure to hydrodynamic regime (De Clippele et al., 2017). Rugosity (roughness) variables relate to habitat heterogeneity, shelter provision (Lecours et al., 2016) and substrate composition (Dunn and Halpin, 2009). Curvature quantifies the shape of the slope and may relate to convergence or divergence of water flow (Vierod et al., 2014). Aspect, or orientation, may influence the exposure of the seafloor inhabitants to prevailing currents (Lecours et al., 2016).

1.7 Mapping cold-water coral in high-resolution

Bathymetric maps are required to locate and quantify cold-water coral reef formations, to place them in their 'seascape' context, and provide means to derive geomorphic terrain variables for SDM as described above. In the 1800's, original depth soundings were collected with a lead line (e.g. Thomson, 1874), a technique used during the HMS Challenger expedition (Wölfl et al., 2019). The advent of single beam echosounders, which measured the time taken for a single acoustic signal to reach the seafloor and reflect back, progressed our ability to resolve geomorphological features (Laughton et al., 1960) from the early 1900s. In the 1970s, multibeam echosounders (MBES) became accessible (Glenn, 1970) and more common in the 1990s (Lim et al., 2021), and the application of multiple acoustic signals significantly increased the footprint of a survey area. The increased swath size improved our ability to resolve seafloor features over a larger area with a resolution of metres to 100's of metres. Side-scan sonar (SSS) is another acoustic mapping technique that came to prominence in the 60s. Side-scan sonar is a form of mapping that measures the intensity of the return signal from the side which can indicate the texture and roughness of the substrate providing useful data to map cold-water coral mounds (Huvenne et al., 2002). However, this technique is becoming rarer in cold-water mapping with the widespread adoption of MBES (Lim et al., 2021).

Low-resolution data is often seen as the limiting factor for SDM (Vierod et al., 2014; Anderson et al., 2016a). This is essentially due to a mismatch between the size of bathymetric data pixels and ground truth data. Bathymetry pixels typically have a size of 25 to 50 m per pixel from data collected by ship board MBES in water depths that cold-water corals are found. On the other hand, video footage or physical sample collection via cores only cover a fraction of each bathymetric pixel and therefore SDM is associates ecological relationships without full ground truth of a bathymetric pixel. In light of this resolution mismatch, new approaches are required to collect high-resolution bathymetry. The benefit of collecting high-resolution bathymetry for SDM, is the ability to better

represent different ecological processes which are scale-dependant (Levin, 1992; Lecours et al., 2015). Furthermore, low-resolution bathymetry may miss key geomorphological features that are important coral habitats such as vertical walls and mounds (Rengstorf et al., 2012; Robert et al., 2019). The MBES derived map resolution is a function of depth due to the increase in the spread of beams with depth and sound attenuation. MBES data resolution can be improved by narrowing the swath, increasing the number of beams and increasing the frequency of each beam. These result in a small swath area and a narrower footprint of the individual beam. However, high frequency sound rapidly attenuates in water and thus low frequency beams are used to map seafloor features far away at greater depth. Therefore, maps of deep-sea habitats, such as cold-water coral reefs, collected from surface vessels, tend to be low resolution. To bypass these trade-offs, the proximity of MBES and the seafloor needs to be reduced. The advancement of technology in recent years has enabled the integration of MBES into Remotely Operated Vehicles (ROVs) and Autonomous Underwater Vehicles (AUVs) to collect high-resolution bathymetric data at depth.

1.8 ROVs

ROVs are user operated robots that were initially developed for military use (Huvenne et al., 2018), and have become important tools in deep-sea research (Figure 1.6). A tether between the ROV and the user, usually situated in on a vessel or a water-side platform, provides a communication link for a high degree of manual control. Equipped with multiple thrusters, ROVs can be intricately manoeuvred to navigate and survey structurally complex subjects. Large working class ROVs are usually equipped with cameras and manipulator arms and may have a capability to reach 6,000 m water depth (Yoerger et al., 2000; Rigaud, 2007; Marsh et al., 2013).

1.9 AUVs

AUVs are self-contained, untethered robots that undertake surveys with pre-programmed instructions (Figure 1.6). As AUVs are untethered, AUV surveys can free the “mothership” to undertake other research missions, thus saving time and costs (Benoist et al., 2019). There are two types of AUV: 1) Survey-class AUVs 2) Hover-class AUVs. Survey-AUVs are torpedo shaped robots designed to cover large distances, powered by a single propeller (Wynn et al., 2014). Hover-AUVs have additional propellers and thrusters to provide additional precise controlled manoeuvrability during slow paced surveys (Huvenne et al., 2018).

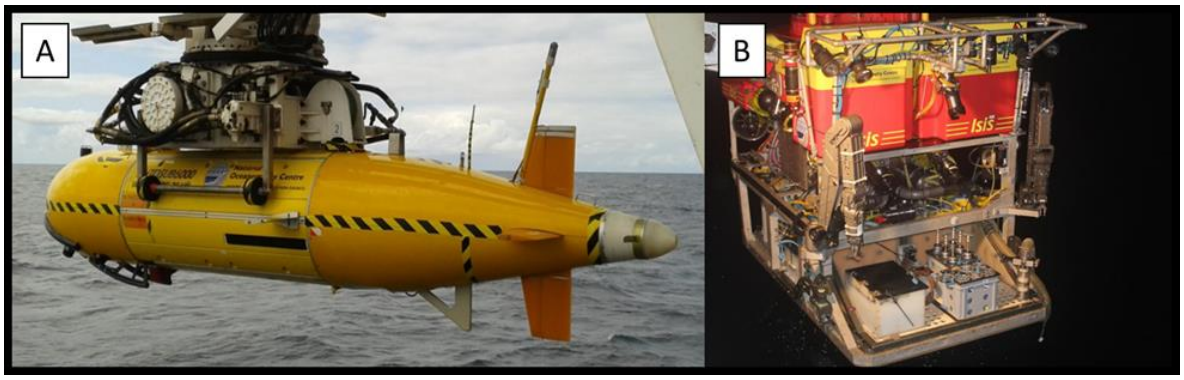

Figure 1.6. Examples of AUVs and ROVs A) The AUV *Autosub6000*. B) The ROV *ISIS*. Both vehicles operated by the National Oceanography Centre. Images from Huvenne et al., 2016a and noc.ac.uk.

1.10 High-resolution acoustics

Both AUVs and ROVs can be fitted with MBES in order to achieve bathymetric data with a metric or sub-metric pixel resolution. Cold-water coral reef habitats have been mapped in high-resolution using AUV mounted MBES (Grasmueck et al., 2006; Ludvigsen et al., 2014; Wynn et al., 2014; Corbera et al., 2019). In addition, ROV mounted MBES have collected even higher resolution maps of cold-water coral habitat (Dolan et al., 2008; Huvenne et al., 2011; Foubert et al., 2011; De Clippele et al., 2017; Lim et al., 2018a). These high-resolution data improved our understanding of ecological drivers of community structure, geological processes and anthropogenic impact. Notably, Dolan et al. (2008) utilised ROV-derived bathymetry for SDM of cold-water coral on a sub-metre resolution bathymetric dataset to reveal that fine-scale terrain derivatives influence the distribution of cold-water coral patches on the flank of a carbonate mound. These studies demonstrate the importance of investigating high-resolution datasets.

Furthermore, an overlooked use of deploying ROVs and AUVs is the ability to map features in full 3D, rather than from nadir (orthogonal to the horizontal subject). For example, vertical wall structures are an important and under-quantified geomorphological feature for cold-water coral habitats (Robert et al., 2019). This was first demonstrated by Huvenne et al. (2011) who used forward facing, ROV mounted MBES to map out cold-water coral assemblages on a canyon wall. This ability to survey vertically or obliquely reveals a larger footprint of seafloor and habitats that could only previously be observed with a small footprint via a ROV video survey. AUVs can also be ballasted to collect angled bathymetric data and resolve vertical features better (e.g. Robert et al., 2017). These studies demonstrate how unoccupied underwater vehicles fitted with MBESs can be used to quantify habitats difficult to observe with traditional surveying techniques.

1.11 Structure from Motion and photomosaicing

Data derived from acoustic instruments lack the optical information and resolution that enable analysis on the scale of individual cold-water coral colonies. This centimetric scale of observation is traditionally undertaken with underwater cameras. Progress in camera technology has driven costs down, and image quality up, resulting in a plethora of use for scientific studies. The collection of images in the deep-sea has revolutionised our ability to identify taxa and benthic patterns in cold-water coral habitats. However, the field of view in images can be small and lack 3D information about the scene. More recently, image processing methods have enabled greater spatial analysis with the use of photomosaicing and Structure from Motion (SfM). Photomosaicing involves the combination of multiple, overlapping images using common features for matching, to create a large single 2D image with a greater footprint (e.g. Marsh et al., 2012).

Structure form Motion is the use of a single camera to create a 3D reconstruction of the scene. SfM utilises an algorithm called Scale Invariant Feature Transform (SIFT) to feature-match common points in a series of overlapping images. The geometry of the 3D structure is then resolved whilst simultaneously triangulating the relative position of the camera (Westoby et al., 2012), using a bundle adjustment algorithm. A 3D scene is reconstructed at this stage but requires scaling and geographic positioning. This is undertaken with the use of Ground Control Points (GCPs) and camera position to provide accurate X, Y and Z context. The 3D model can be texturized by parameterising the surface to create a texture atlas. Orthorectified photo mosaics and Digital Elevation Model (DEM) are produced for projection on the 2D plane, based on the dense point cloud of the 3D model. The use of DEMs in particular has gained traction in terrestrial geosciences and geomorphology studies (e.g. Lane, 2000; Keutterling and Thomas, 2006). However, collecting comparable data from the marine environment is challenging due to the difficulties of image acquisition underwater due to visibility issues, collecting scale and geographic meta-data and maintaining stable control to perform the survey in the chosen pattern (Kwasnitschka et al, 2013).

1.11.1 Platform

Most terrestrial photogrammetry surveys are undertaken on foot (e.g. Krosley et al., 2006) or with Unoccupied Aerial Vehicles (UAVs) (e.g. Marzolff and Poesen, 2009). The same approaches can be applied to the intertidal marine habitat (Muffit et al., 2017; Collin et al., 2019; D'Urban Jackson et al., 2020), however the vast majority of the marine habitat is subtidal. Whilst UAVs can be used to produce orthomosaics in clear, shallow water (Ventura et al., 2018), the generation of SFM derived DEMs are only possible under perfect atmospheric conditions (Cassella et al., 2017; Fallati et al., 2020) or with the use of bespoke advanced hardware (Chirayeth and Earle, 2016; Chirayeth and

Instrella, 2019). Instead, snorkelers, SCUBA divers, motorboats and Autonomous Surface Vehicles (ASV) are used to collect imagery of shallow-water habitats such as tropical coral reefs and seagrass. (Leon et al., 2015; Burns et al., 2015; Raoult et al., 2017; Raber and Schill, 2019; Mohamed et al., 2020). However, to collect images for SfM surveys on cold-water coral reefs beyond recreational SCUBA depths and most saturation technical diving operations, ROVs, AUVs or towed platforms are required.

Deep-sea SfM surveys using ROVs are now becoming more commonplace (Figure 1.7; Sedlazeck et al., 2009; Kwasnitschka et al., 2013; Thornton et al., 2016; Robert et al., 2017, 2019; Price et al., 2019; Gerdes et al., 2019; Mitchell and Harris, 2020; Lim et al., 2020). Alternatively, Remotely Operated Towed Vehicles (ROTV) can be deployed for SfM surveys at depth (Prado et al., 2019a, b; Rios et al., 2020). Survey-AUVs have seldom been utilised for SfM surveys due to the required close proximity to the seafloor, which represents a collision danger when navigating complex terrain. Hover-AUVs may resolve this issue by providing means of a slower and carefully controlled survey, but this technology is not yet readily available. Nonetheless, survey-AUVs have been used to create photomosaics of more topographically simple abyssal plains (Simon-Lledo et al., 2019) and sponge grounds (Meyer et al., 2019), and SfM reconstructions of rocky substrata and coral reefs in shallower water (Johnson-Roberson et al., 2010; Bryson et al., 2013). More recently, for the first time, an AUV was used to undertake SfM surveys of cold-water coral reefs (Huvenne and Thornton, 2020).

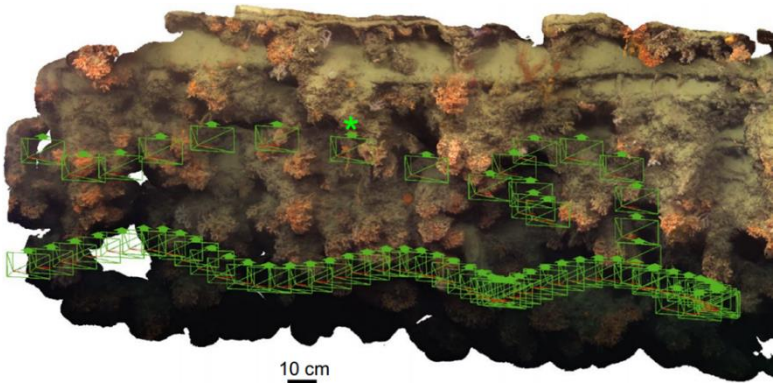

Figure 1.7. A 3D reconstruction of a cold-water coral assemblage found on a vertical wall in the NE Atlantic. Figure from Robert et al., 2019

1.11.2 Relevance of 3D photogrammetry for the study of cold-water coral habitat and ecology

SfM can provide a basis on which to monitor benthic change through spatial or classification studies, but also through measuring colony growth (Ferrari et al., 2017) and reef rugosity change (Fallati et al., 2020). For high-resolution in-situ growth measurements, rigorous georeferencing and precise scaling is required to ensure accuracy (Rossi et al., 2019), which is challenging with an ROV or AUV.

However, Bennecke et al. (2016) has utilised 3D models to measure linear and cross-sectional area growth of octocorals, demonstrating the monitoring potential for cold-water coral habitats.

Rugosity in shallow-water coral reefs is a well-documented influencer of coral reef biodiversity (Friedlander and Parrish, 1998; Gratwicke and Speight, 2005; Wilson et al., 2007; Graham and Nash, 2013; Richardson et al., 2017). Whilst observations show that the structure of cold-water coral influences the community (Purser et al., 2013), structural complexity has never been quantified in cold-water coral habitats. This is because geomorphic quantification of rugosity traditionally requires the use of a chain along the seafloor to calculate rugosity, which is a challenging operation to undertake with an ROV. SfM is one way that structural complexity of cold-water coral reefs can be quantified.

The fine-scale spatial organisation of cold-water corals has seldom been quantified. Initial studies have utilised photomosaics to identify patterns around small mounds in the NE Atlantic (Lim et al., 2017), revealing hotspots of live coral and sponge aggregations (Conti et al., 2019). This reveals the power of benthic classification of photomosaics in quantifying the spatial organisation of the benthic habitat. Another approach is the use of landscape ecology techniques to reveal further interactions, which has successfully been applied in shallow-water reef settings with point pattern analysis (Edwards et al., 2017) and in cold-water coral habitats by applying landscape metrics on classified high-resolution sidescan sonar maps (Robert et al., 2014). Point Pattern Analysis (PPA) has recently been applied to deep-sea habitats with SfM (Prado et al., 2019a, b; Mitchel and Harris, 2020), and may provide valuable information on the biotic and abiotic drivers of distribution and benthic organisation of cold-water coral reef. Whilst 2D analysis from linear video transects can be used to identify clustering patterns of cold-water coral (Orejas et al., 2009; Gori et al., 2011a), little is known on a wider area or 3D environment, and in particular how species interact and aggregate around cold-water coral reef structure.

Overall, 3D photogrammetry can provide novel measurements of cold-water coral habitats, previously impossible before the application of SfM and photomosaicing. These techniques are in their infancy but are rapidly gaining traction in deep-sea ecology research. SfM combined with acoustic data can produce a 3D, multi-resolution overview of deep-sea habitats for monitoring and ecological insight (Robert et al., 2017).

1.12 Scale in cold-water ecology

Collecting data across the scales from centimetres and kilometres is easier than ever with the progress of technology and analytical techniques, cumulating into a range of acoustic and optical spatial data. This has resulted in the ability to undertake “multi-designed” studies that attempt to

quantify species-environment relationships through multiple scales (Lecours et al., 2015). The progressing attempts to quantify relationships at different scales is important as ecological processes are scale-dependant (Levin et al., 1992). This is exemplified by the interactions of flow velocity in cold-water coral whereby high flow velocities are required for food supply, but polyps only feed at a low flow velocity. Theoretically, without studying cold-water coral at fine scales, it could have easily been concluded that cold-water coral prefer high flow velocities without any further consideration of the baffling effect of the framework and how fine-scale topographic steering may influence the very local distribution of cold-water coral.

A single resolution of data is typically used in SDM. Any specific bathymetric resolution is likely to reflect the scale of a subset of specific ecological processes and different resolution SDM outputs are likely to present slightly different spatial predictions (Vierod et al., 2014). Therefore, the consideration of multiple resolutions is pertinent for spatial planning. The extent of the predicted species distribution is likely to change between model resolutions, and thus precautionarily accepting the largest predicted spatial extent should be considered (Ross et al., 2015), or perhaps a combination of the predicted distribution extent generated by different models.

The advantage of combining resolutions to identify the ecological patterns of benthic habitats is that no single scale of analysis is solely considered, and a more thorough investigation is undertaken in order to capture different processes happening at varying spatial scales. For example, Robert et al., 2017 combined AUV, ROV based MBES data and SfM to quantify spatial parameters of vertical cold-water coral habitats. This enabled the observation of different environmental variables acting on the communities present at different resolutions. This was only possible owing the advancement of technology enabling high-resolution acoustic data acquisition and development of SfM.

1.13 Rationale of the PhD

Little is known about the fundamental ecology of cold-water coral reefs, yet they have not escaped the reach of human presence. Bottom contact fishing has a negative impact on benthic habitat (Jennings and Kaiser, 1998), including cold-water coral reefs (Fossa et al., 2002), which have low capacity for recovery (Althaus et al., 2009; Huvenne et al., 2016b). In addition to localised or regional stressors, 80% of warming from climate change has dissipated into the oceans (Levitus et al., 2005), including deep water (Barnett et al., 2005). Temperature influences reef building cold-water coral physiology (Dodds et al., 2007) and changes associated with climate change may lead to loss of cold-water coral habitat (Morato et al., 2020). Furthermore, ocean acidification is leading to the shoaling of the aragonite saturation horizon with implication for coral skeletal structure and reef structural complexity (Hennige et al., 2015; 2020), and the distribution of cold-water coral in

general (Guinnote et al., 2006). Furthermore, there are several other anthropogenic impacts that may impact cold-water coral, such as hydrocarbon drilling discards (Rogers, 1999), litter and plastic pollutants (Chapron et al., 2018; Soares et al., 2020). The need for improved knowledge about cold-water coral ecology and distribution is essential in order to develop robust protection strategies. This is particularly evident when considering that conservation efforts and distribution estimates are usually based on ill-matched datasets such as broad-scale bathymetry together with detailed, but out of context video and photo transects. SDM bridges the gap between the two observational resolutions but more closely matched resolutions of environmental and species data are required. The use of unoccupied vehicles can achieve this by collecting very high resolution bathymetric and optical data. By collecting acoustic and optical data from a range of platforms (vessels to ROVs), a range of scales of the habitat present a more accurate overview of cold-water coral habitats. This multi-designed or multi-scale approach to scientific observations of deep-sea habitats is crucial as different ecological process occur at different scales (Levin 1992)

Before conservation efforts are undertaken, the definition and justification for protection is required. On an international level, cold-water coral reefs are listed as a Vulnerable Marine Ecosystem (VME) (FAO, 2009) and meet the criteria of Ecologically and Biologically Significant Areas (EBSAs) (CBD, 2010). VMEs are vulnerable to destructive fishing practices and are classified on their rarity, functional significance, fragility, life history traits and structural complexity (FAO, 2009). The presence of cold-water coral may indicate a VME, but a regional threshold for VME designation is so far only based on fishing bycatch thresholds. This is not a sustainable approach to VME presence and extent assessment. Using imagery is one possibility of sustainably identifying VMEs and opens up an abundance of additional data (Baco-Taylor et al., 2020).

Identifying important features that require protection, such as VMEs, is difficult. Not only is high-resolution data needed on the spatial distribution, an understanding of how important the cold-water coral reef is for the area and how developed the reef is, is also required. For this, typically image surveys are undertaken to quantify the biodiversity of a reef and asses reef status. One feature that is often touted as an important variable is structural complexity, which is a prerequisite for VME status but is difficult to quantify *in situ*.

Within regional policies, Marine Protected Areas (MPAs) can be designated to protect cold-water coral. The first known cold-water coral MPA was designated off the coast of Florida to protect *Oculina varicosa* reefs (Roberts and Cairns, 2014), although did not prove effective in deterring illegal fishing (Reed et al., 2005; 2007). In the NE Atlantic, an emergency fishing closure was declared at the Darwin Mounds in 2003 (Davies et al., 2007) upon discovery of significant trawling damage (Wheeler et al., 2005a). However, an intense flurry of trawling undertaken just before the fisheries

closure was in place led to long term damage to the coral reefs, with little evidence of recovery, even eight years later (Huvenne et al., 2016b). These case studies demonstrate that MPAs require sufficient enforcement and a long-term protection in order to reach the goal of habitat recovery. To fully understand where to position MPA boundaries and to achieve an optimum compromise between all stakeholders, estimates of cold-water coral abundance and distribution estimates are required, which could be achieved by targeted SDM to identify locations of utmost importance (e.g. Rowden et al., 2017). High-resolution data may be useful in capturing fine-scale heterogeneity in predictive mapping (Lo Iacono et al., 2018) which is useful for marine spatial planning (Howell et al., 2011).

1.14 Scientific objectives and research questions

Cold-water coral reefs are of high ecological importance and effective management is required. To fully understand the ecology of cold-water corals, the use of recently developed technology is required to collect high-resolution data. In spatially nested surveys, cold-water coral distribution and ecological importance in a system can be quantified, taking into account the role of scale in driving local biodiversity. In this thesis, I deploy technologically advanced marine robotics to collect high-resolution optical and acoustic data to identify cold-water coral distribution and the reefs' influence on biodiversity and associated taxa, with an emphasis on how these data help spatial management and status designation of an MPA.

Chapter 2

The aim of this chapter is to use an AUV in a submarine canyon to produce high-resolution SDMs of cold-water coral. By comparing lower resolution data collected from a shipboard MBES with AUV-borne bathymetry, I explore the role of resolution in SDM. The study site is located in the Explorer Canyon, NE Atlantic, which is part of a Marine Conservation Zone in the UK. The spatial prediction of cold-water coral will help with spatial management plans, highlight the role that AUVs can play in marine conservation and demonstrate the importance of collecting high-resolution bathymetry.

Chapter 3

In this chapter I aim to quantify cold-water coral structural complexity, its role in the associated community and its application in quantifying the importance of the reef in the local area. I will apply SfM to linear video transects along a cold-water coral reef in Explorer Canyon to compare rugosity metrics. Multivariate approaches will be used to evaluate how the rugosity introduced by the cold-water coral reef influences the megabenthic community, aiding our understanding of how a reef

Chapter 1

becomes an important habitat. These data will feed into an argument that SfM can help asses reef status and provide important information for conservation policy.

Chapter 4

The aim of this chapter is to investigate the role that cold-water coral reef structure has on the benthic organisation of associated taxa. Using landscape ecology statistical descriptors, I analyse how biotic and abiotic interactions influence the fine-scale distribution of benthic taxa. This chapter emphasises the heterogeneous nature of cold-water coral reefs in terms of geomorphology and ecology, with the use of novel advanced image processing and statistical analysis.

Chapter 5

The final chapter will synthesise the results from the thesis to demonstrate how spatially nested surveys, from a few centimetres to tens of metres, can improve our understanding of the role and distribution of cold-water coral reefs. I discuss how the analytical gains from high-resolution data collected by advanced technology will improve our ability to designate cold-water coral reef as important habitats and develop useful maps to aid marine spatial planning.

Chapter 2 High-resolution predictions of cold-water coral distribution in Explorer Canyon (NE Atlantic) with the use of an Autonomous Underwater Vehicle (AUV).

This chapter is in preparation for submission to a peer-reviewed journal as Price, D.M., Callaway, A., Robert, K., Lo Iacono, C., Hall, R., Huvenne, V.A.I. High-resolution predictions of cold-water coral distribution in Explorer Canyon (NE Atlantic) with the use of an Autonomous Underwater Vehicle (AUV).

Author contributions: DP and VH conceptualised the study. DP processed AUV bathymetry, generated environmental raters, undertook all statistical analysis and wrote the manuscript. KR contributed annotated video data. VH collected the data during the JC125 CODEMAP cruise. All authors reviewed and commented on chapter.

2.1 Abstract

Ecological research in deep-water environments has historically seen a trade-off between data resolution and data coverage. To achieve comprehensive, broad-scale coverage the resolution of data is necessarily low. Yet when examining key fine-scale features the data resolutions are comparatively, incredibly high, though over very small areas. This results in fine-scale relationships being extrapolated across broad-scale data although the implications of doing so are rarely considered due to the lack of an alternative approach. Recent implementation of multibeam echosounder (MBES) survey techniques from underwater robotic systems such as Remotely Operated Vehicles (ROVs) and Autonomous Underwater Vehicles (AUVs) has enabled acquisition of fine-scale information over broad-scale areas in deep water allowing the implication of resolution on biodiversity to be interrogated more effectively.

During the JC125 expedition, multi-scale MBES data in Explorer Canyon, NE Atlantic, were collected. Explorer Canyon is a Marine Conservation Zone, designated on the occurrence of cold-water coral habitat. However, a lack of knowledge about the distribution of cold-water coral in Explorer Canyon presents challenges for marine spatial planning and identifying areas to target for further investigation. A combination of ship and AUV (*Autosub6000*) acquired bathymetry was analysed to explore the role of terrain at different scales (metres to 10s of metres) in Explorer Canyon, which is part of the wider Whittard Canyon complex. Using the ROV *Isis*, two video transects were collected to identify cold-water coral occurrence within the vicinity of the MBES survey for subsequent use of Species Distribution Modelling. The AUV collected bathymetry data at 5 m bathymetric resolution, revealing cold-water coral mounds and vertical walls which were missed in the ship-borne bathymetry. The ability to resolve smaller geomorphological features progresses our ability to identify locations that are likely to support cold-water coral assemblages. Comparing these scales give us greater insight into the canyon system as a cold-water coral habitat and demonstrates the advantage of collecting high resolution data from AUVs.

2.2 Introduction

Cold-water corals are ecosystem engineers that are typically found in the deeper regions of the oceans (Jones et al., 1994). Scleractinian cold-water corals such as *Lophelia pertusa* (recently changed to *Desmophyllum Pertusum* (Addamo et al., 2016)), *Solenosmilia variabilis* and *Madrepora*

oculata are coral species that can construct reef structures and carbonate mounds (Wilson et al., 1979; De Mol et al., 2002; Roberts et al., 2006). It is well documented that these reef habitats promote a diverse and abundant community (Jensen and Frederiksen, 1992; Mortensen et al., 1995; Costello et al., 2005; Henry and Roberts, 2007; Purser et al., 2013; Bongiorni et al., 2010), and therefore attract scientific and conservation interest. Cold-water coral habitats are classified as "Vulnerable Marine Ecosystems (VME)" (FAO, 2009) due to their susceptibility to the detrimental impacts of bottom contact fishing practises (Fossa et al., 2002, Wheeler et al., 2005a; Davies et al., 2007; Althaus et al., 2009; Huvenne et al., 2016b). Furthermore, cold-water corals are exposed to environmental challenges associated with climate change, such as ocean acidification (Turley et al., 2007; Hennige et al., 2014). Consequently, it is likely that the spatial suitability for cold-water coral longevity will change, locally and globally (Guinotte et al., 2006; Jackson et al., 2014; Morato et al., 2020).

Cold-water coral habitats have been observed globally (Davies et al., 2008, Davies and Guinotte, 2011) and are often located on complex bathymetric features such as seamounts (Duineveld et al., 2004; Tracey et al., 2011), shelf slopes and edges (Thiem et al., 2006), fjords (Brooke and Jarnegren, 2013) and submarine canyons (Huvenne et al., 2011; Gori et al., 2013; Van de Beld et al., 2017). Submarine canyons can provide important habitat for cold-water corals and associated assemblages as well as other VMEs (Orejas et al., 2009; Fabri et al., 2014; Robert et al., 2015; 2019; Lo Iacono et al., 2018; Moccia et al., 2020), due to favourable hydrodynamic conditions and geomorphic features such as vertical walls and gullies (Pearman et al., 2020). These geomorphic features may provide natural protection to cold-water coral from bottom trawling (Huvenne et al., 2011), though may still be prone to trawling-induced gravity flows and resuspension (Palanques et al., 2006; Martin et al., 2014). Submarine canyon research has only more recently gained traction (Huvenne and Davies et al., 2014; Matos et al., 2018) and 13.6% of known canyons have some form of protection spanning >10% of their area (Fernandez-Arcaya et al., 2017), but information on cold-water coral distribution within these features is still lacking.

Spatial information of cold-water coral prevalence is limited but their distribution appears to be dictated by environmental conditions such as water properties (Dullo et al., 2008), terrain characteristics (Guinan et al., 2009; Robert et al., 2015) and hydrodynamic regime (Davies et al., 2009; De Clippele et al., 2018). Species Distribution Modelling (SDM) has become an important tool for quantifying these known relationships to predict cold-water coral distribution, aiding marine spatial planning (Ross and Howell, 2013) and predicting the effect of anthropogenic impacts (Jackson et al., 2014; Morato et al., 2020). Terrain variables, which may act as a proxy for oceanographic variables and substrate type, are commonly used predictors of cold-water coral distribution (Dolan et al., 2008; Robert et al., 2015; Lecours et al., 2016; Lo Iacono et al., 2018). The

underpinning pixel resolution of bathymetric data used to derive terrain variables is commonly 25 to 50 m, collected with a ship board multibeam echosounder (MBES) (e.g. Howell et al., 2011; Guinan et al., 2009; Robert et al., 2015). However, bathymetry data on a scale of 10s of metres may not resolve finer-scale geomorphological features (Wilson et al., 2007; Masson et al., 2011; Paull et al., 2013) which can have consequences on the subsequent accuracy of SDM results (Veirod et al., 2014; Lecours et al., 2015; Anderson et al., 2016a). Some fine-scale features that can be omitted include features that are known to support cold-water corals such as vertical walls (Lo Iacono et al., 2018; Robert et al., 2020) and mounds (Rengstorf et al., 2012), leading to inaccurate and imprecise predictions.

To address the issue of bathymetry data resolution, MBES data collected from Remotely Operated Vehicles (ROVs; Dolan et al., 2008; Foubert et al., 2011; De Clippele et al., 2017; Lim et al., 2018a) and Autonomous Underwater Vehicles (AUVs; Grasmueck et al., 2006; Corbera et al., 2019) have been used to investigate cold-water coral reefs. Recent spatially nested studies of cold-water coral habitat have additionally incorporated 3D photogrammetry surveys to complement MBES data, providing data across all scales (e.g. Robert et al., 2017). Whilst bathymetry collected from ROV can produce sub-metre maps, their spatial extent is limited and ROV surveys restrict research vessels from conducting other research due to a tether connected to the ship (Huvenne et al., 2018). AUVs on the other hand are self-powered and cost-saving, liberating the ship for other surveys whilst collecting MBES data over a large area (Wynn et al., 2014). AUVs present the means for covering large areas and are a suitable tool for monitoring of benthic habitat. Data acquisition within structurally complex features, such as canyons, presents navigation issues for AUVs due to the topographic heterogeneity, presenting collision hazards. However, the need to survey such features in high resolution is paramount in order to develop robust predictive models of cold-water coral and other VME distribution.

To overcome the challenges presented, we deployed an AUV equipped with a collision avoidance system into Explorer Canyon, NE Atlantic, to collected high resolution MBES bathymetry data. High-resolution bathymetry and 3D reconstructions were used to visualise the structure of cold-water coral reefs, to provide the first description of coral topped mounds in Explorer Canyon. Using the AUV and ship derived bathymetry in tandem with ROV video transects, we here formulate SDMs based upon broad- and fine-resolution bathymetric terrain variables to predict the distribution of cold-water coral occurrence. The objective is to understand how the application of AUVs can contribute to more accurate spatial predictions of cold-water coral occurrence within a canyon in order to aid spatial planning procedures within a Marine Protected Area (MPA).

2.3 Methods

2.3.1 Explorer Canyon

The Whittard Canyon complex experiences strong internal wave activity (Vlasenko et al., 2014; Hall et al., 2017; Aslam et al., 2018), which is strongly linked with the local fauna distribution and abundance (Pearman et al., 2020). Explorer Canyon is a tributary of the Eastern Whittard Canyon branch (Figure 2.1). Explorer Canyon incises the continental shelf in the Bay of Biscay, NE Atlantic, with a water depth ranging from ~200m to 2000 m (Figure 2.1).

Explorer Canyon and neighbouring Dangaard Canyon are found on the edge of the UK mainland Exclusive Economic Zone and have been designated as a Marine Conservation Zone (MCZ) due to the occurrence of 'Deep-sea bed', 'Cold-water coral reefs', 'Coral gardens' and 'Sea-pen and burrowing megafauna communities', which are of conservation importance (Ministerial order/DEFRA, 2013, 2019). Explorer Canyon provides refuge to various VME indicator species, including reef-building scleractinian cold-water coral inhabiting a spur part way up the canyon (Davies et al., 2014; Stewart et al., 2014), which promotes local diversity (Price et al., 2019). Explorer Canyon also provides suitable conditions for cold-water coral in other locations such as vertical wall features supporting three scleractinian species, *L. pertusa*, *M. oculata* and *S. variabilis* (Robert et al., 2020). Moreover, cold-water corals are predicted to occur along the flanks near the Explorer/Whittard Canyon junction (Pearman et al., 2020). In addition, Stewart et al. (2014) described 'mini-mound' features on the interfluves surrounding Explorer Canyon. These mini-mounds are degraded due to fishing or environmental change, comprising of coral rubble, but support the argument that the general region has been important for reef-forming cold-water coral over time. As such, further exploration of Explorer Canyon should seek to expand our knowledge on potential cold-water coral distribution.

2.3.2 Multibeam echosounder mapping

Bathymetry data were collected at 50 m resolution from a shipboard Simrad EM120 MBES mounted on RS James Cook during the CODEMAP cruise in 2015. The data were processed using CARIS HIPS and SIPS and exported with a pixel resolution of 50 m. In order to collect higher resolution bathymetric data, an AUV was deployed. *Autosub6000* is a large survey AUV, fitted with an integrated Kongsberg EM2040 MBES (McPhail, 2009). As canyon systems are steep, traditional nadir/orthogonal acquisition methods may miss information along steep walls and overhangs. As such, the AUV mission (M98) was undertaken with a -20 degree roll offset in order to capture these steep features accurately with survey lines positioned in a spiral pattern with the multibeam swath

angled away from the spiral centre, collecting 84.7 km of angled data (Figure 2.1 C; also see Robert et al., 2017). A section towards the head of Explorer Canyon was chosen for the survey in order to map areas of known cold-water coral presence. The AUV was monitored during its descent, and its position recorded using an Ultra-short baseline acoustic positioning system (USBL). When the vehicle reached the survey altitude, it received a command to move to the correct start position. From that point onwards, it used Doppler dead-reckoning for navigation and the science party carried on with other sampling and surveying work at another location. The MBES frequency was set to 200 kHz and beam count to 400. Due to the topographically complex nature of canyon systems, a collision avoidance system was developed (Huvenne et al., 2016a). The horizontal collision avoidance system was deployed providing a horizontal avoidance range of 120 degrees and a range of 250m with a weak spike filter strength. Doppler dead-reckoning navigation is prone to drift over time, which may cause survey lines to incorrectly align, resulting in bathymetric error. Therefore, due to navigation drift, roll offset and motion sensor placement discrepancy, the GLOBE V1.15.16 software (IFREMER) was used to process the data due to high level of user interaction enabled. The outputs were exported as geotiffs at a pixel resolution of 5 m.

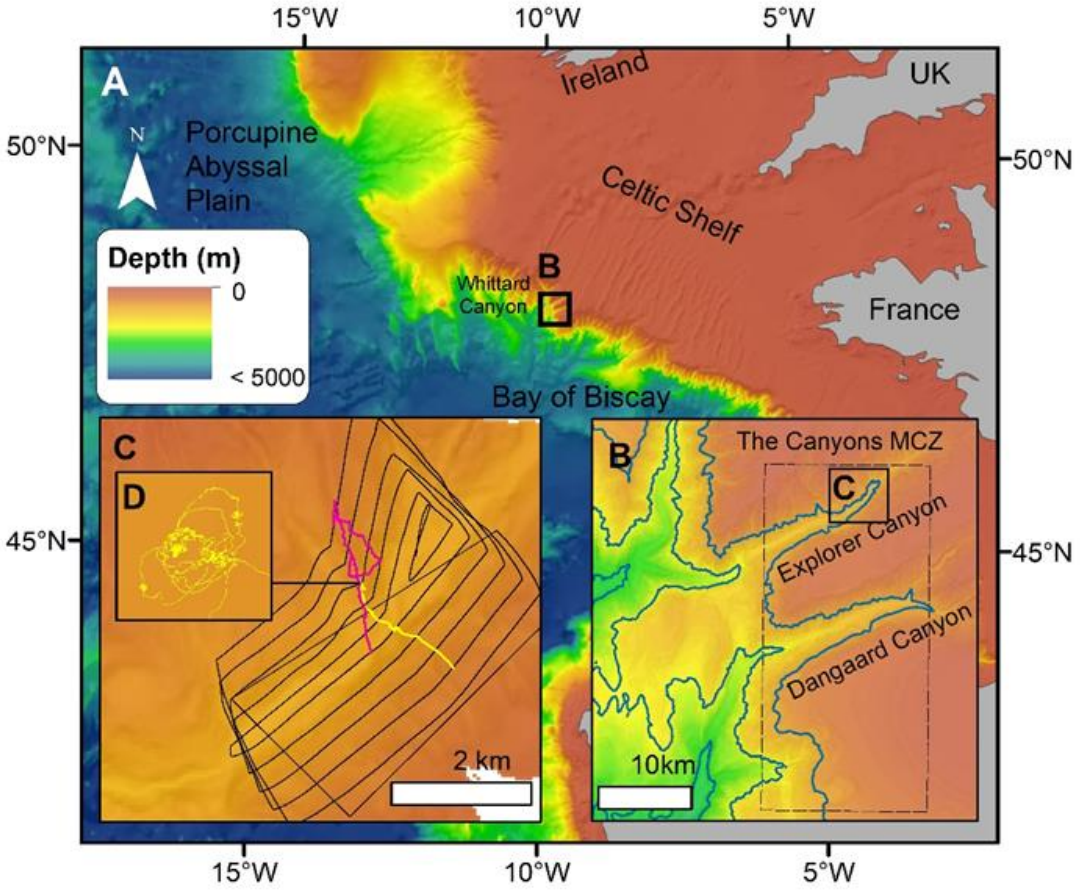

Figure 2.1 Map of the NE Atlantic and Explorer Canyon. Bathymetry obtained from General Bathymetric Chart of the Oceans (GEBCO) compilation group (2019). B. Eastern Whittard Complex. Bathymetry obtained from EMODnet Bathymetry Consortium (2018). Contours located at 1000,

2000 and 3000 m water depth. Dashed outline represents the "The Canyons" Marine Conservation Zone. C. Doppler navigation of *Autosub6000* during Mission 98 (black lines). USBL navigation from ROV video transects from dive 246 (Pink lines) and 254 (yellow lines). D. Close up of USBL navigation when ROV circled a cold-water coral mound for a 3D photogrammetry survey.

2.3.3 ROV video data

ROV *Isis* was used to survey the sea floor during two transects (Figure 2.1; Dive 246 and 254). *Isis* is a 6,000 m depth rated work-class ROV. *Isis* is fitted with 3 HD cameras and two 7-function manipulator arms (Marsh et al., 2013). A Sonardyne USBL system was used for navigation. The Ocean Floor Observation Protocol (OFOP) software was used to log the XY positions of organisms observed on the SCORPIO camera. SCORPIO is a HD video (1080p) camera and is set at a fixed angle and position, and was kept at a fixed zoom level in order to provide a consistent field of view of the seafloor. Three reef building scleractinians (*L. pertusa*, *M. oculata* and *S. variabilis*) were considered. All three species were concatenated as "Cold-water coral". *L. pertusa* and *M. oculata* were additionally considered independently. *S. variabilis* was not considered separately due to its rarity. Live reef building scleractinian coral heads were counted and converted into presence/absence data, as is common in Species Distribution Modelling (SDM) studies (e.g. Guinan et al., 2009). The transects were split into 50 m sections to match the 50 m resolution shipboard bathymetry. For the 5 m resolution dataset, 10 m sections were used as equivalent 5 m sections did not cover a large enough area of the seabed to be representative. The centre point of each section was used to provide a single point position according to the ROV USBL position. To reduce the influence of spatial autocorrelation, a quarter of datapoints were retained from the 10 metre sections, by systematically removing groups of 3 consecutive data points to ensure maximum possible distance between data points. Spatial autocorrelation appeared much less influential when analysing the 50 m transects. Sections in which the ROV was stationary for sampling purposes, visibility was poor or close up imagery was undertaken, were removed.

In addition to the two linear transects, a 3D photogrammetry survey was undertaken in a spiral pattern around a small mound at the start of transect 254 (Figure 2.1). A frame every 3 seconds was taken from the video and a 3D photogrammetry model generated in Agisoft Photoscan (now Metascan). The protocol followed Robert et al., (2017) and Price et al., (2019). An orthomosaic and Digital Elevation Model (DEM) was generated for use as visual aids in this manuscript to demonstrate the vertical relief of the mound and coral cover.

2.3.4 Terrain variables

All data were imported into ArcMap 10.4 and projected in UTM zone 29N projected co-ordinate system prior analysis. From the bathymetry rasters (Figure 2.2), Slope (Figure 2.2 H, J), Curvature (general), Northness (Figure 2.2 L, N), Eastness, Vector ruggedness measure (VRM) and Bathymetric Positioning Index (BPI) (Figure 2.2 D, F) were generated using RSOBIA (Le Bas et al., 2016) and Benthic Terrain Modeller extensions (Wright et al., 2005). Slope calculates the terrain gradient at each pixel, measured in degrees. General curvature quantifies the slope as a concave or convex surface. Northness and Eastness quantifies the aspect of each pixel in its respective direction. VRM, which calculates the orientation variation of the pixels, independent of the slope (Sappington et al., 2007), was generated with neighbourhoods of 3, 9 and 15 pixels to represent terrain rugosity. Finally, BPI is a variation of Topographic Position Index, which measures a location position relative to the surrounding area vertically, helping quantify if the position is locally elevated (positive values), or locally depressed (negative values). Three scales of Bathymetric Position Index were calculated at inner and outer radii of 5-10, 2-10 and 10-40 pixels.

2.3.5 Species Distribution Modelling

Two predictive modelling approaches were undertaken: 1) Generalised Additive Models (GAM) and 2) Random Forest, as both have been used in the past to create high quality predictions of cold-water coral distribution and are suitable for non-linear relationships (e.g. Pearman et al., 2020). Furthermore, using both approaches gives insights with two different modelling types; regression-based analysis to estimate the relationship between variables and machine learning classification-based analysis which uses classification trees.

Generalised Additive Models were undertaken using the MGCV package in R with a binomial family distribution and logit link function. Data exploration according to Zuur et al., (2009; 2012) was undertaken prior to analysis. Correlations between environmental variables were detected via the Variance Inflation Factor (USDM package) and removed using a cut off value of 3. In addition, the remaining variables were compared using Pearson correlation with a cut off value of r = 0.5 (Pearman et al., 2020). This resulted in a restricted number of variables considered (Table 2.1). GAMs were fitted with remaining variables which were sequentially removed and compared with Akaike Information Criterion (AIC) to identify the most parsimonious model. Restricted Maximum Likelihood (REML) was used to define smoothing parameters (Wood, 2011).

Random Forest (package: random forest) was used as it has been demonstrated to be a strong machine learning approach to predict coral occurrence (e.g. Robert et al., 2015; Pearman et al., 2020). Random forest uses random subsamples of both response and independent variables to

create multiple decision trees, which are split to create smaller groupings based on the most influential variable. Random Forest makes no assumptions of the variable response distributions and therefore is therefore less sensitive to variable collinearity and non-linearity in the response variables. The model was run in classification mode with 1500 trees and number of node splits was the square root of the number of variables (default).

Both GAM and Random Forest methods are prone to spatial autocorrelation (e.g. Sinha et al., 2019). To detect the presence of spatial autocorrelation, variograms (full spatial range and up to 300 m) and spline correlograms of the model residuals were assessed. Spline correlograms visualise Moran's I as a continuous and non-linear function of distance. Confidence envelopes (95%) were calculated by bootstrapping the data (100 resamples).

Table 2.1 Chosen variables for the GAMs and correlated values group with their strongest relationship according to Pearson r correlation

Retained variables	Correlation (r > 0.5)
5 m resolution	
Depth	BPI (10-40)
Slope	
Curvature	BPI (5-10), BPI (2-20)
Northness	
Eastness	
VRM15	VRM3, VRM9
50 m resolution	
Depth	BPI(5-10), BPI(2-20), BPI(10-40)
Slope	Northness
Curvature	
Eastness	
VRM15	VRM3, VRM9

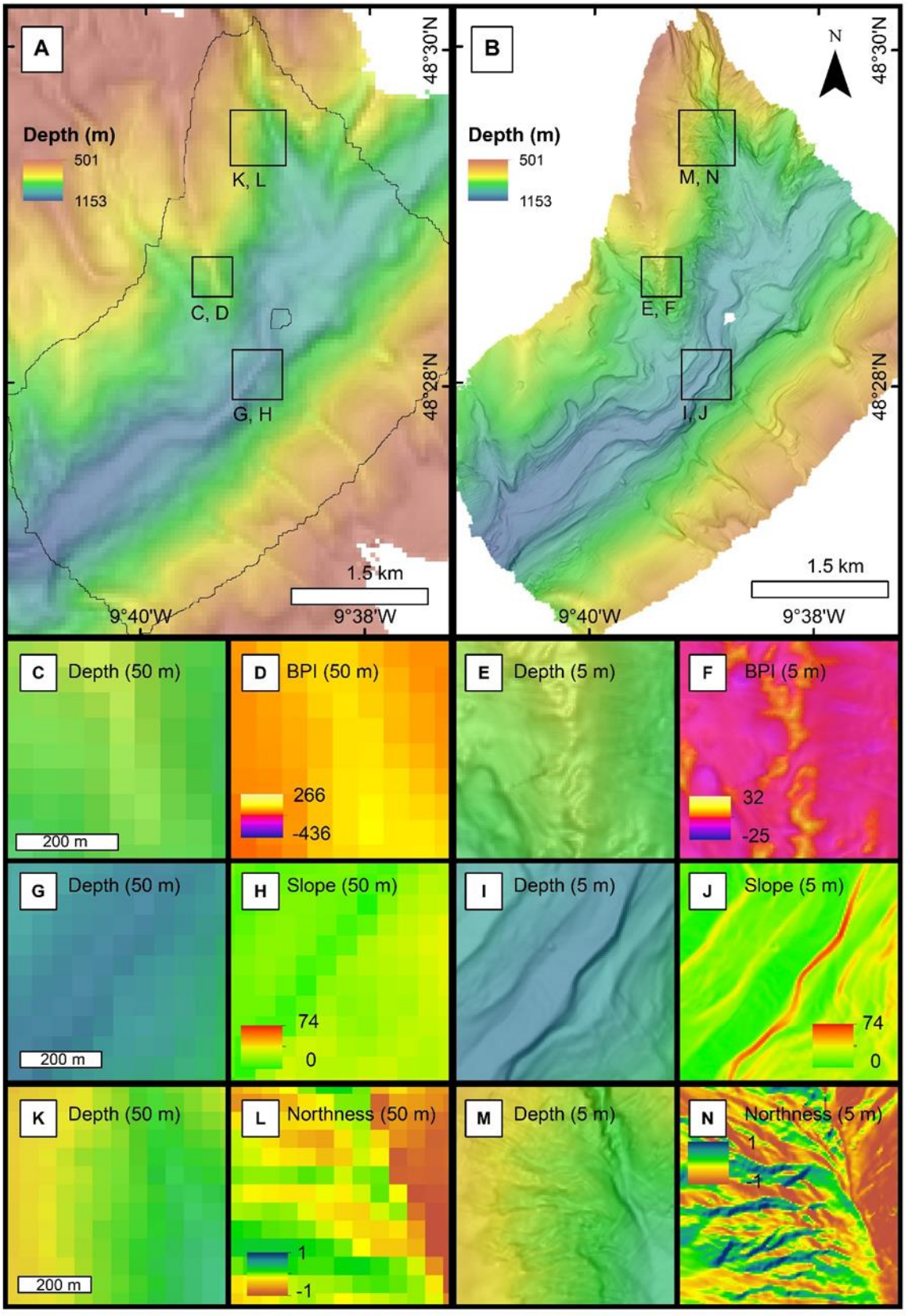

Figure 2.2. Bathymetry data acquired in Explorer Canyon at 50 m (shipboard MBES) and 5 m (AUV MBES) pixel resolution plus associated derivatives. Subsequent maps illustrate examples of the additional terrain information obtained with the two bathymetry resolutions. A. 50 m pixel

resolution bathymetry with AUV survey outline. B. 5 m pixel resolution bathymetry of Explorer Canyon. C. Depth (50 m pixel resolution). D. Fine-scale bathymetric positioning index (50 m pixel resolution). E. Depth (5 m pixel resolution). F. Fine-scale BPI (50 m pixel resolution). G. Depth (50 m pixel resolution). H. Slope (50 m pixel resolution). I. Depth (5 m pixel resolution). J. Slope (5 m pixel resolution). K. Depth (50 m pixel resolution). L. Northness (50 m pixel resolution). M. Depth (5 m pixel resolution). N. Northness (5 m pixel resolution). Scale bars for C-N are located in C, G & K, with horizontal rows showing same extent and scale.

2.3.6 Model evaluation

All data were randomly split into training (70%) and test (30%) data prior modelling to perform cross validation. Area under the curve (AUC) was used on both training and testing data. AUC is a common method to gauge performance of presence-absence models in the form of a single number (Vierod et al., 2014). Less than 0.5 signifies poor model performance and greater than 0.7 signifies adequate model performance. Further, sensitivity and specificity metrics were generated which measure the fraction of correctly predicted presences and absences respectively. In addition, Out Of Bag error (OOB) (Random Forest) and R^2 (GAM) were assessed.

2.4 Results

2.4.1 Bathymetry

The 5 m resolution bathymetry enabled the identification of many geomorphological features that were otherwise unresolved in the 50 m resolution data set. In Figure 2.2 (C & F), mounds are observed on a spur and quantified by BPI in the 5 m dataset. Such features were not observed in the 50 m dataset. Wall features and a series of consecutive terraces were observed on the south flank in the 5 m resolution bathymetry. However, in the 50 m dataset, slope was more gradual as areas of wall were smoothened by the lower resolution (Figure 2.2 H). A series of gullies in the north east of the survey were observed in the 5 m resolution data, but were not resolved in the 50 m resolution data. Northness values ranged from nearly -1 to nearly 1 in the 5 m resolution data, but only ~ 0 to ~-0.75 in the 50 m resolution data.

2.4.2 Cold-water coral occurrence

A total of 270 sections (189 training, 81 testing) were used to predict coral species distributions across the 50 m resolution dataset. Cold-water coral colonies were observed in 120 of the 270 transects. 104 and 114 sections containing *L. pertusa* and *M. oculata* were observed. A total of 319

sections (223 training, 96 testing) were used to predict coral species distribution across the 5 m resolution dataset. Cold-water coral colonies were observed in 100 of the 319 sections. 87 and 90 sections containing *L. pertusa* and *M. oculata* were observed. Cold-water coral colonies ranged from scattered colonies to developed reefs forming small mounds on the spur found on the north flank of the survey area (Figure 2.3). One thousand, two hundred and forty-one images were utilised to create the 3D photogrammetry model which revealed dense coral cover on top of a mound between 869 and 874 m water depth. Large hummocks of coral colonies were observed at the peak of the mound, characterised by a high quantity of live coral cover. Cold-water colonies were also found on vertical walls and overhangs (Figure 2.4).

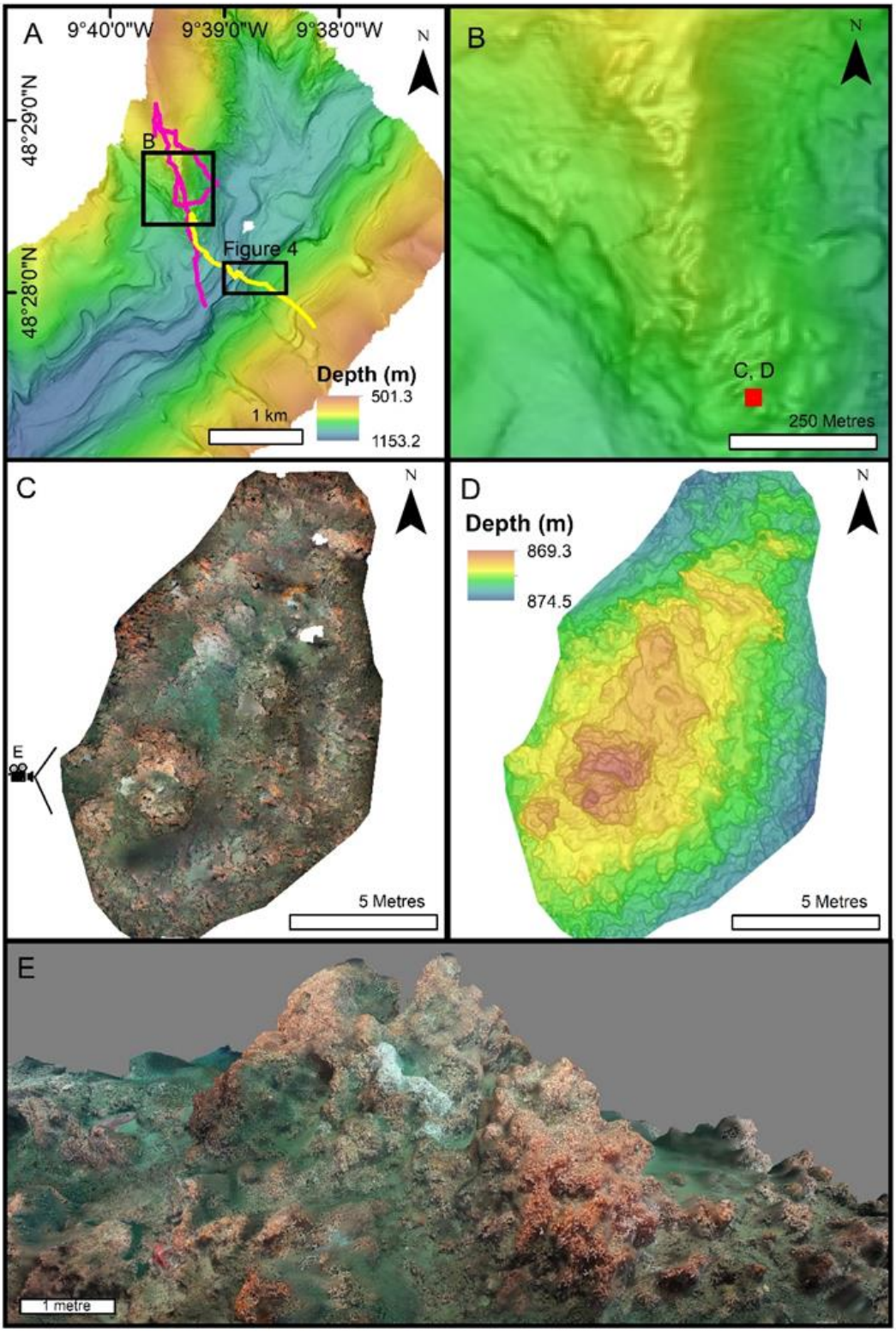

Figure 2.3. Cold-water coral formations in Explorer Canyon. A) Bathymetry of Explorer Canyon collected by *Autosub6000* at 5 m resolution. B) A close up of cold-water coral mound formations. C) Orthomosaic of the top of a mound. D) Digital Elevation Model of the top of a cold-water coral mound. E) Side view of the cold-water coral mound reconstructed in 3D.

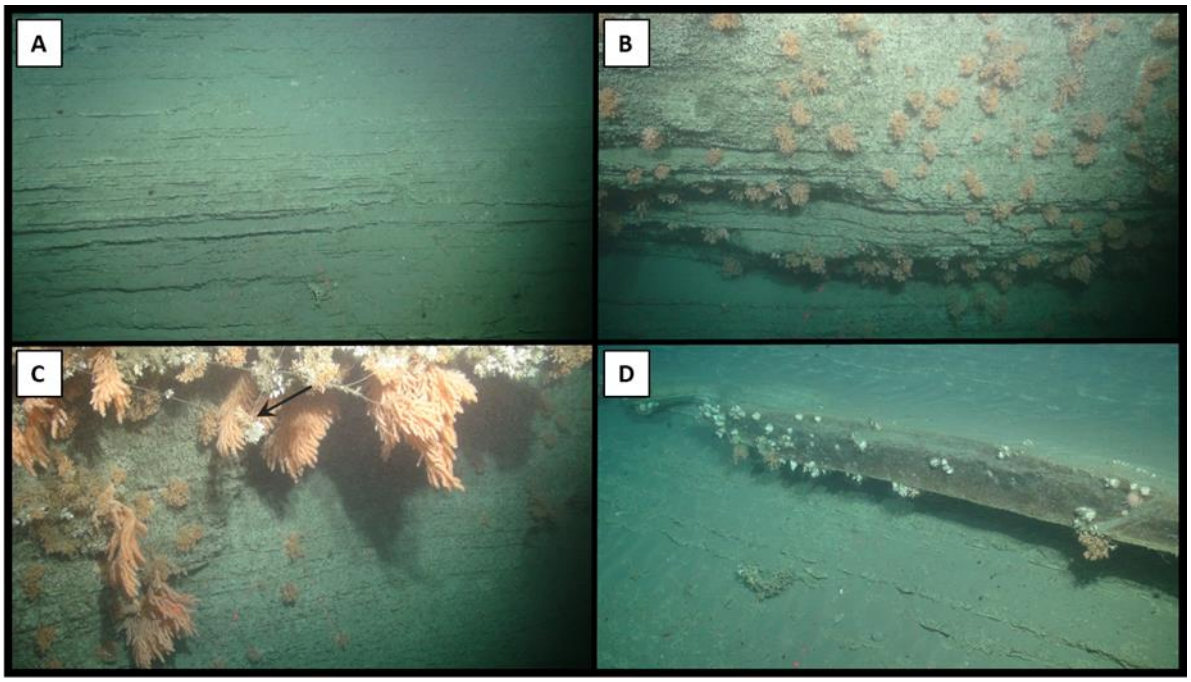

Figure 2.4. Images of cold-water coral assemblages found on vertical walls. A) Bare vertical wall with dead Scleractinia skeletons fallen from further up the cliff. B) Cold-water colonies (predominantly *M. oculata*) found on the vertical wall. Note that A and B were separated 14 m vertically. C) *M. oculata* and *Primnoa* sp. found on an overhang. Arrow is used to draw the reader's attention to scleractinian coral hanging from a fishing line. D) Filter feeders (including *M. oculata* and *L. pertusa*) colonising small areas of exposed vertical and overhang rock. Image locations found on the south flank within the outlined area in Figure 2.3 A.

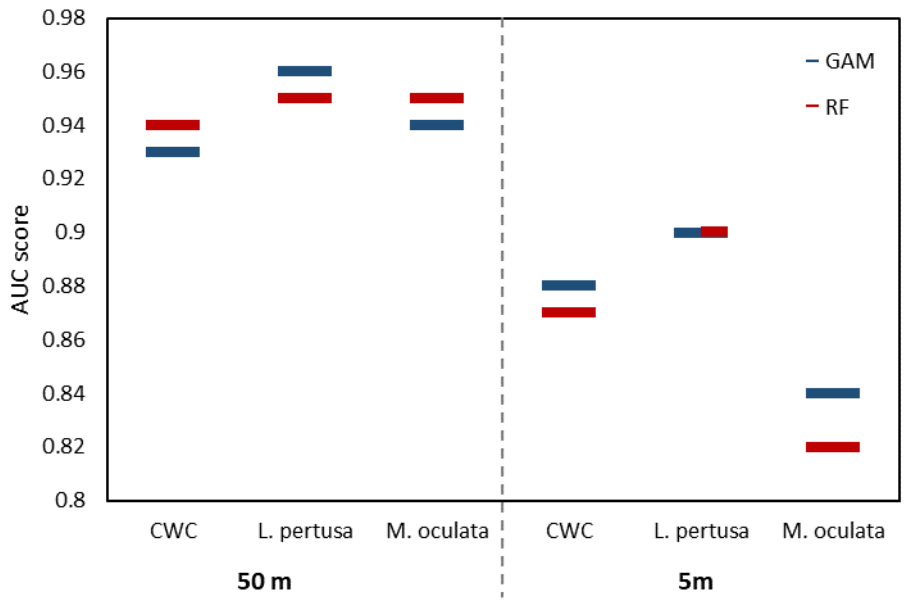

Figure 2.5 AUC values of models applied to validation datasets.

2.4.3 Modelling

Table 2.2 shows that modelling undertaken on the 50 m resolution dataset generally had a higher Adj R^2 and deviance explained, and lower OOB errors, compared with the 5 m resolution dataset (Table 2.2). All models performed excellent with an AUC score >0.8 (Table 2.3, Figure 2.5). AUC ranged from 0.93 – 0.96 (50 m) and 0.82 – 0.9 (5 m), on the testing data (Table 2.3). Sensitivity ranged from 0.79 – 0.88 (50 m) and 0.52 – 0.69 (5 m) on the testing data (Table 2.3). Specificity ranged from 0.86 – 0.94 (50 m) and 0.85 – 0.89 (5 m), on the testing data (Table 2.3). The 50 m dataset had higher AUC scores than the 5 m dataset (Figure 2.5). The AUC was higher for *M. oculata* and cold-water coral predictions using Random Forest at 50 m resolution, whereas at 5 m, the GAM performed slightly better. For *L. pertusa*, the GAM performed the best at 50 m resolution and performed the same as Random Forest at 5 m resolution.

Table 2.2. Summary of model performance, calculated from the test data.

		GAM		Random Forest
		Adj R^2	Deviance explained	OOB error (%)
50m	Cold-water coral	0.749	71.8	8.47
	L. pertusa	0.884	86.3	4.23
	M. oculata	0.69	65.9	12.7
5m	Cold-water coral	0.59	54	12.11
	L. pertusa	0.69	64.8	11.21
	M. oculata	0.64	61.7	13.45

2.4.4 Generalised Additive Model

The relationships between depth and all species at both resolutions were similar, peaking between 800 and 1000 m water depth (Appendix 2.2). Slope was significant for *L. pertusa*, indicating that a slope angle of around 10-20 was the optimum angle. Probability of coral occurrence increased with VRM (15) for all species at both resolutions. Eastness was an important variable for all species at 50

m resolution, whereas Northness was important to explain the occurrence of *L. pertusa* and cold-water coral at 5 m resolution.

2.4.5 Random forest variable importance

Depth was the most important variable in the Random Forest models at 50 m resolution for all species (Appendix 2.1). BPI (10-40) followed by VRM (15) were the next most influential for all species for 50 m resolution models. All other variables were much less influential.

The most important variables in the Random Forest models at 5 m resolution were more evenly distributed. Depth, VRM15, VRM9, BPI (5-10, 2-20, 10-40) were the most influential variables for all species (Appendix 2.1).

Table 2.3. Sensitivity, specificity and AUC scores of all models performed using both training and testing validation datasets

			Training			Testing		
			Sensitivity	Specificity	AUC	Sensitivity	Specificity	AUC
50m	Random Forest	Cold-water coral	0.87	0.95	0.98	0.79	0.86	0.94
		L. pertusa	0.92	0.98	0.96	0.85	0.94	0.95
		M. oculata	0.81	0.92	0.94	0.81	0.87	0.95
	GAM	Cold-water coral	0.89	0.94	0.98	0.79	0.86	0.93
		L. pertusa	0.96	0.98	0.99	0.88	0.92	0.96
		M. oculata	0.87	0.93	0.97	0.81	0.87	0.94
5m	Random forest	Cold-water coral	0.75	0.93	0.91	0.64	0.89	0.87
		L. pertusa	0.77	0.93	0.93	0.69	0.89	0.9
		M. oculata	0.69	0.93	0.92	0.52	0.85	0.82
	GAM	Cold-water coral	0.81	0.95	0.94	0.58	0.87	0.88
		L. pertusa	0.89	0.95	0.97	0.69	0.89	0.9
		M. oculata	0.80	0.94	0.96	0.55	0.85	0.84

2.4.6 Cold-water coral spatial predictions

The GAM and Random Forest model outputs showed broadly similar predicted patterns at 50 m resolution. For example, both models predicted coral at the spur, where the mounds were observed (Figure 2.3). Furthermore, along the opposite flank, a steep, north facing wall was deemed to be suitable for cold-water coral. Towards the north-east, both models predicted cold-water coral occurrence, particularly the GAM revealing a large area within which it was likely that cold-water

coral would occur. Another hotspot is observed at the west side of the survey along the north flank (Figure 2.6).

The model outputs for the finer-scale 5 m resolution bathymetry showed broadly similar patterns to the 50 m outputs, such as a high probability of coral occurrence on the mounds located on the spur, north-east gullies and some areas that depict vertical walls. At 5 m resolution, individual gullies were identified as suitable for cold-water coral. The west side of the survey area was considered less suitable by the 5 m outputs and both models predicted a high probability of finding cold-water coral over a smaller footprint on the southern flank, compared to the 50 m resolution models.

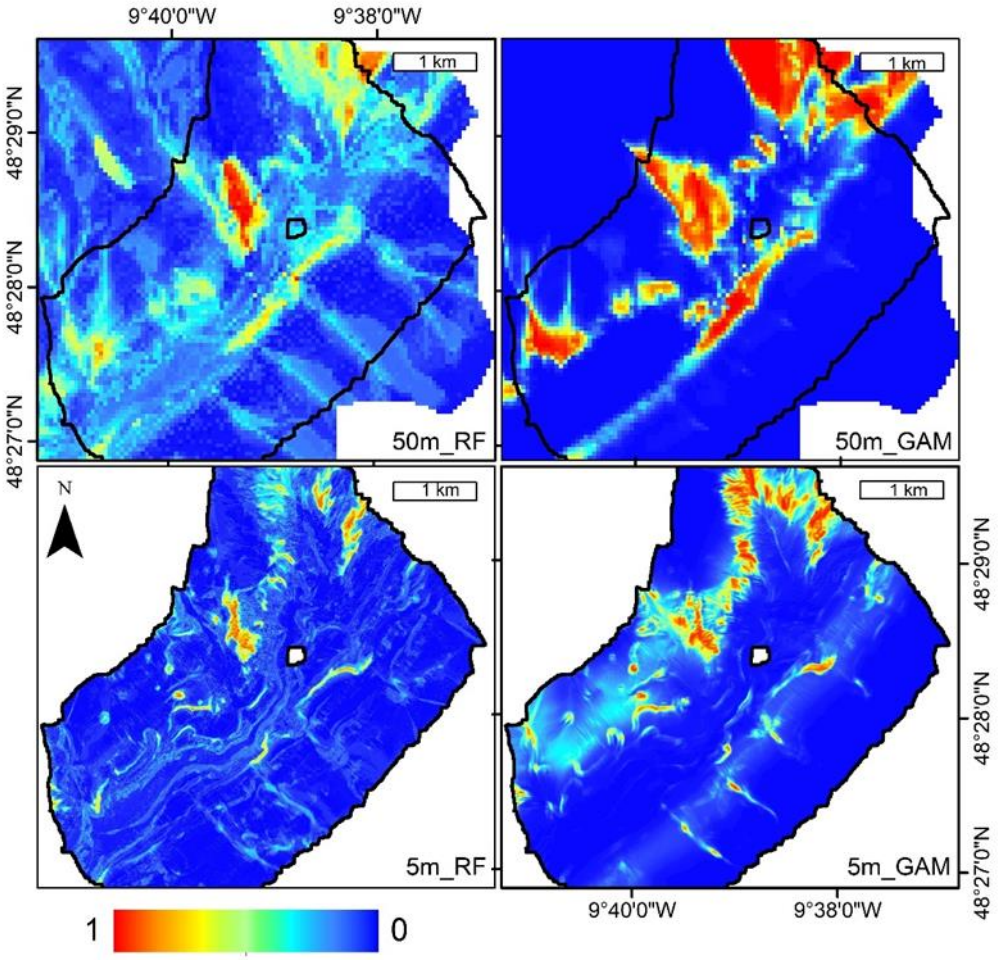

Figure 2.6. Probability of cold-water coral (*L. pertusa*, *M. oculata* and *S. variabilis* concatenated) occurrence based on 4 modelled outputs; Random Forest based on 50 m resolution data; Generalised Additive Model (GAM) based on 50 m resolution data; Random Forest based on 5 m resolution data; GAM based on 5 m resolution data.

2.4.7 *Lophelia pertusa* spatial predictions

The 50 m resolution data models were in general agreement, though the GAM spatial prediction showed a more extreme graduation between low to high probability of coral occurrence and areas of high probability of coral cover had a larger footprint. There were minor differences between the 5m and 50 m resolution data, with the 5 m resolution data predicting more spatially restricted *L. pertusa* extent. The Random Forest model predicted high probability of *L. pertusa* occurrence along the mini mound area, the north-eastern part of the survey and wall features along the south of the thalweg (Figure 2.7). The GAM revealed similar results, though also predicted coral in the gullies on the southern slope at 5 m resolution.

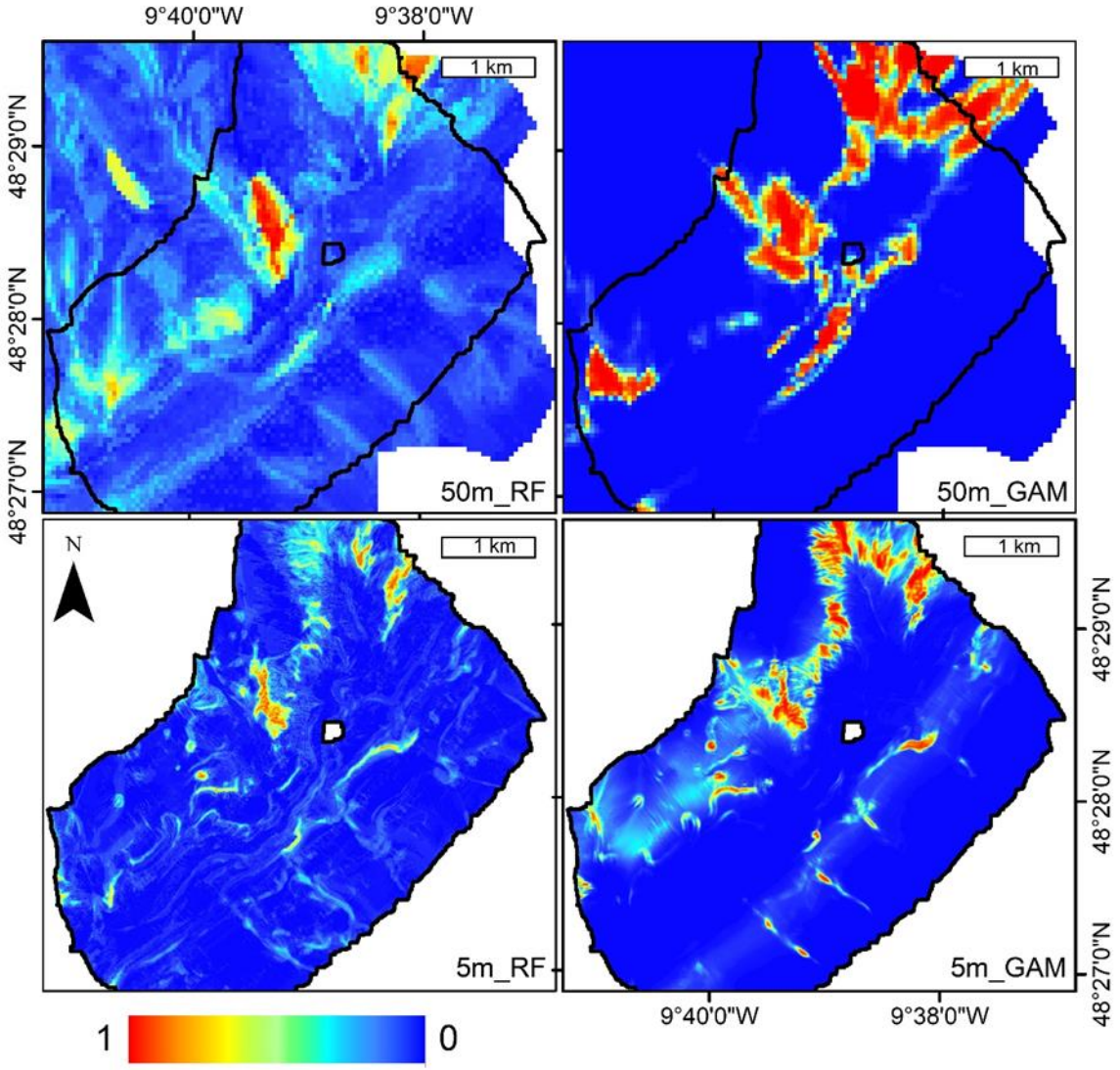

Figure 2.7. Probability of *L. pertusa* occurrence based on 4 modelled outputs; Random Forest based on 50 m resolution data; Generalised Additive Model (GAM) based on 50 m resolution data; Random Forest based on 5 m resolution data; GAM based on 5 m resolution data.

2.4.8 *Madrepora oculata* spatial predictions

The GAM predicted *M. oculata* on the spur, north-east gullies, south walls and west sections in the 50 m resolution dataset. The Random Forest indicated a high probability of *M. oculata* in similar areas, but the variability was more gradual and tended to predict more intermediate probabilities of observing *M. oculata*.

At the 5 m resolution, the predicted area was more restricted to the spur, north east gullies and north facing walls according to the Random Forest. The GAM additionally predicted a high probability of finding colonies along walls throughout the survey area (Figure 2.8).

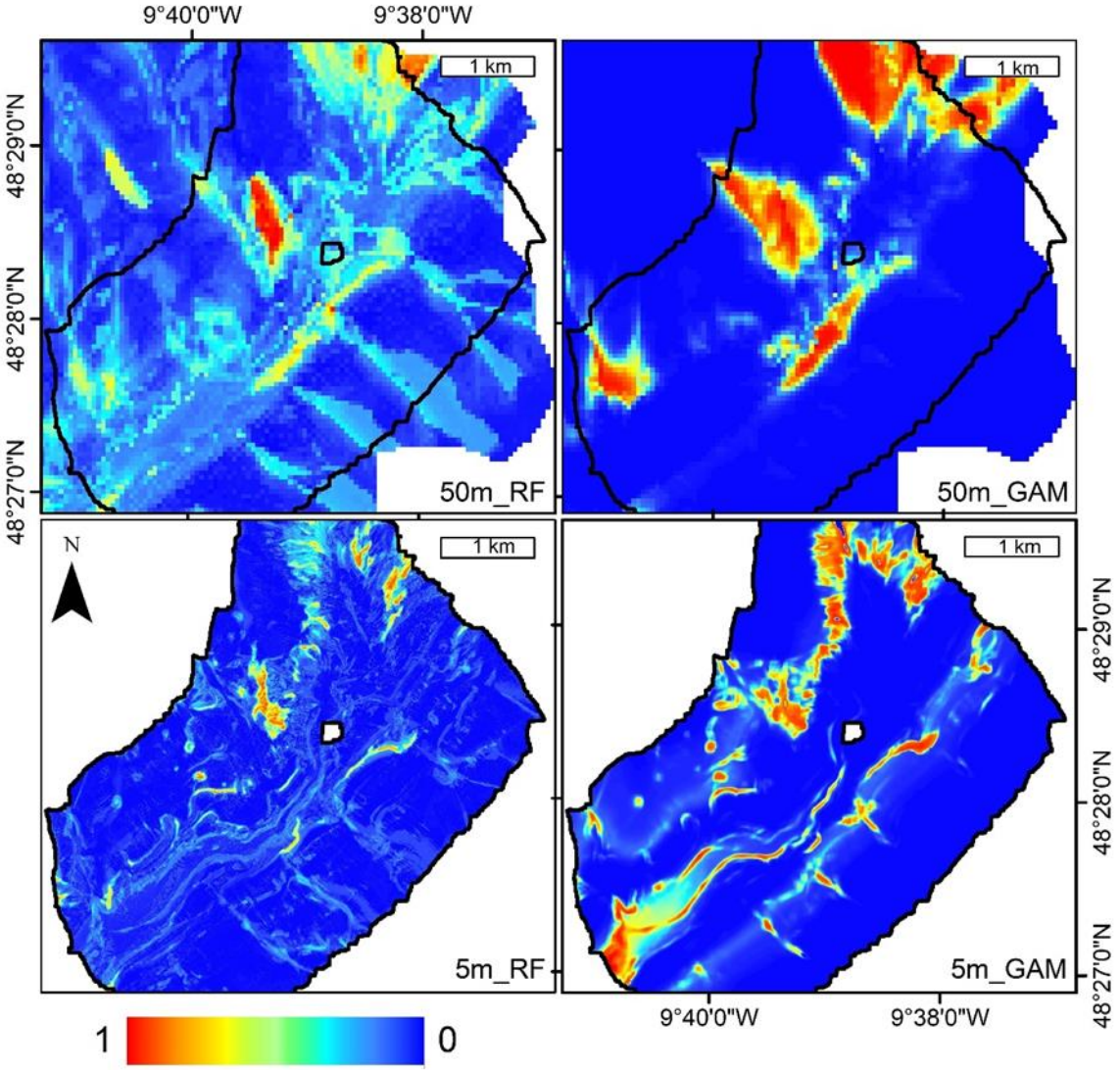

Figure 2.8. Probability of *M. oculata* occurrence based on 4 modelled outputs; Random Forest based on 50 m resolution data; Generalised Additive Model (GAM) based on 50 m resolution data; Random Forest based on 5 m resolution data; GAM based on 5 m resolution data.

2.4.9 Potential undiscovered mounds and habitats suitable for coral growth

Figure 2.9 highlights the slightly different predictions between modelling methods and data resolution. High probability of coral occurrence (in this study defined as 0.6) was predicted over a larger spatial extent in the models undertaken on the 50 m dataset, compared to the 5 m dataset (Figure 2.9). GAMs predicted a high probability of coral over a wider area compared to the random Forest predictions at both scales (Figure 2.9). Cold-water corals were predicted to occur along wall features in the 5 m datasets. However, this relationship was less clear in the models from the 50 m resolution dataset, whereby coral were predicted in the general vicinity, but not the precise wall features (e.g. Figure 2.9 A, C & E). In addition, 50 m resolution models predicted a lower probability of coral occurrence in the gullies immediately north of the spur (Figure 2.9).

The models derived from the 5 m resolution data set agreed in some locations that were not predicted by models using the 50 m dataset (Figure 2.9). In some of these locations (north flank and north east of the survey area), local topographic highs that resemble mounds, ridge features and walls were observed (Figure 2.10). These features are typical of cold-water coral habitat.

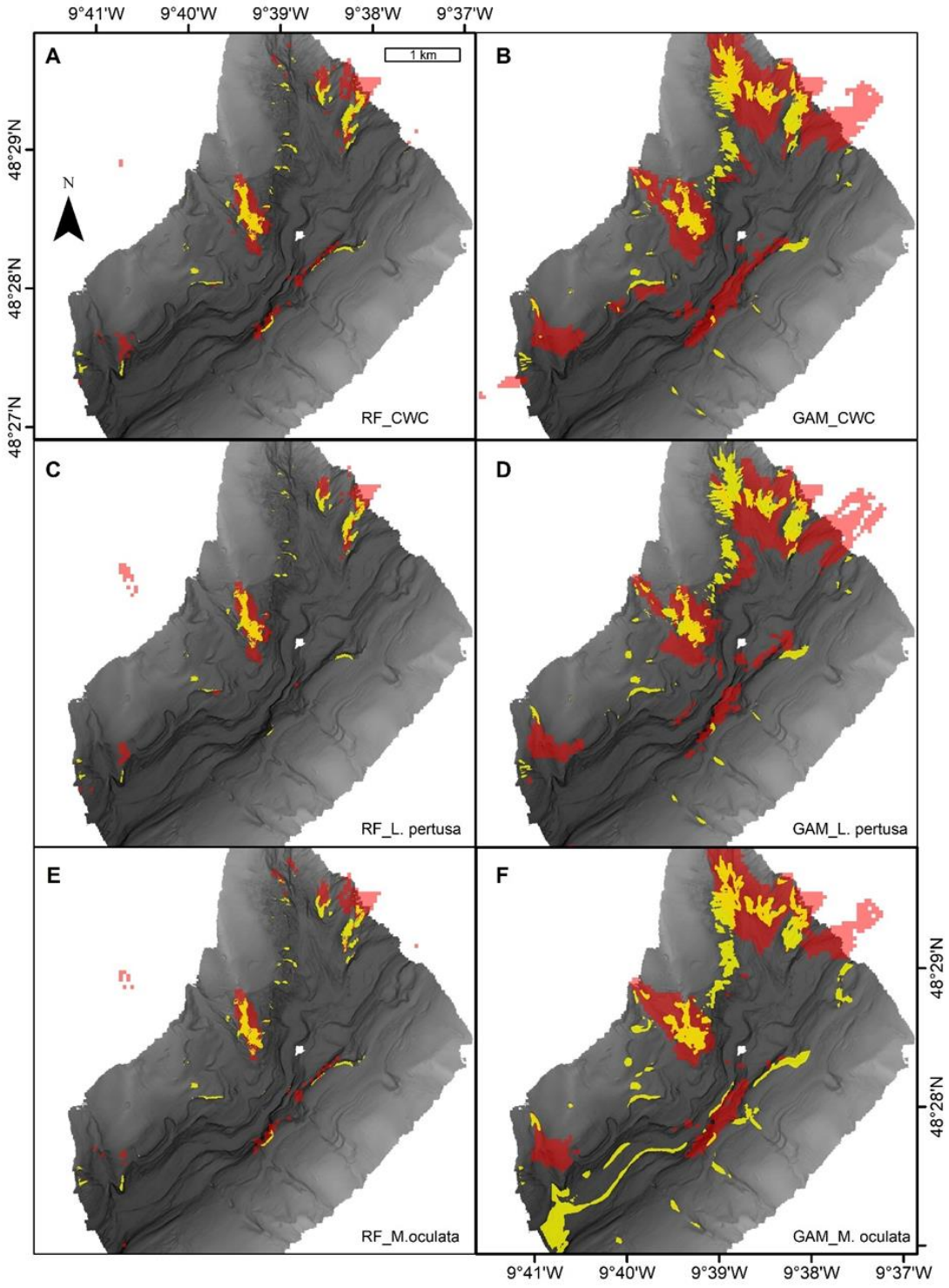

Figure 2.9. Model predictions: 5 m (yellow) and 50 m (red) resolution datasets, cut off point of 0.6 probability that cold-water coral occurs was chosen. A. Generalised Additive Models (GAMs) of Cold-water coral. B. Random Forest models of Cold-water coral. C. GAMs of *L. pertusa*. D. Random Forest models of *L. pertusa.* E. GAM models of *M. oculata*. F. Random Forest models of *M. oculata*.

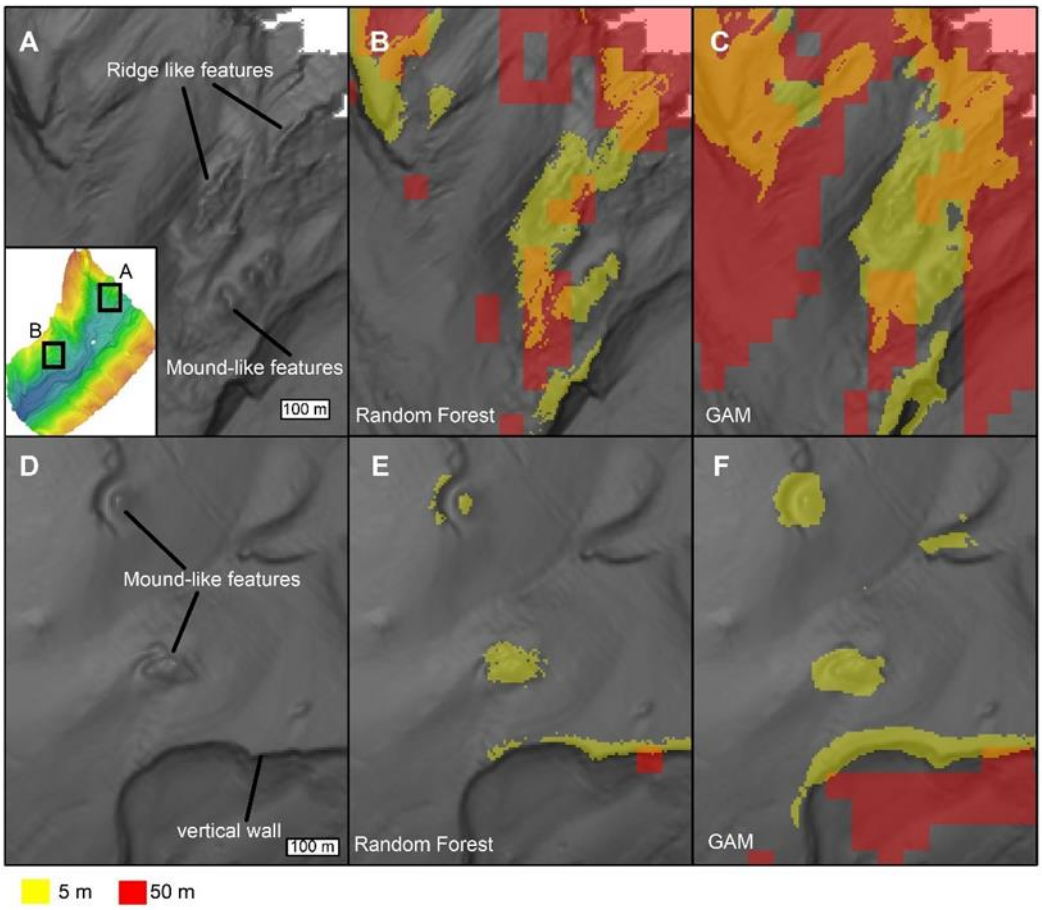

Figure 2.10. Spatial predictions and seabed features, depicted with slope (in grey). A. Close up of geomorphological features that may represent habitat suitable for cold-water coral. Subsequent maps illustrate predicted cold-water coral occurrence with a cut off of 0.6. B. Probability of Cold-water coral occurrence (Random Forest). C. Probability of Cold-water coral occurrence based on a Generalised Additive Model (GAM). D. Close up of geomorphological features that may represent habitat suitable for cold-water coral. E. Probability of Cold-water coral occurrence (Random Forest). F. Probability of Cold-water coral occurrence based on the GAM.

2.5 Discussion

Submarine canyons are seldom mapped to metre-scale resolutions. However, the few studies that have collect metre-scale resolution bathymetry of canyons have taught us a lot about canyon geological processes (e.g. Paull et al., 2011). Here we deployed an AUV in Explorer Canyon collect metre-scale resolution bathymetry to detect areas suitable for cold-water coral growth. High-resolution bathymetry resolved previously undiscovered geological features, contributing to spatial predictions of cold-water coral. We demonstrate the power of using spatially nested surveys to distinguish areas requiring further scientific and conservation interest to aid spatial management.

2.5.1 Model resolutions

All models had high Area Under the Curve (AUC) scores of greater than 0.8, indicating excellent model performance. Our training and validation dataset were spatially limited, suggesting spatial autocorrelation could have contributed to a higher AUC score, though this was minor in our study (see Appendix). When inspecting the spatial predictions, broad similarities between modelling techniques and resolutions gave high confidence of cold-water coral presence in areas such as the spur, which was identified to contain small coral mounds (Figure 2.3), and the north east gullies.

Surprisingly, the modelling undertaken on the 5 m resolution data did not achieve better results than the 50 m dataset from a statistical perspective, this is likely down to unquantifiable variables at the fine scale and geographical or navigation error. On finer scales, ecological processes driving benthic spatial organisation such as species interaction are influential, even on a centimetric scale (Price et al., in review/chapter 3), but may not be accounted for in SDMs (Vierod et al., 2014). Geographical error caused by manual feature matching during AUV bathymetry processing, and by USBL navigation of the ROV video dataset, which is accurate to 1% of depth, may introduce minor discrepancies between datasets. Due to the broad agreement between all models and high AUCs scores, this was not expected to have had a major influence on the spatial predictions.

Areas of disagreement between the model resolutions reveal the shortcoming of 50 m resolution predictions. Some geomorphological features such as vertical walls, ridges and mound-like structures which are strong candidates for coral habitat were only detected as being suitable for coral by the 5 m resolution predictions (Figure 2.10). The smoothing effect of low-resolution bathymetry is evident in Figure 2.2 H & J, and is reflected in the predictions whereby coral was predicted near but not on wall features (Figure 2.9 A, C & E). Cold-water corals were predicted over large areas in the 50 m resolution models compared with the 5 m predictions, particularly by the GAMs, which suggests an over-estimation of cold-water coral extent. In addition, cold-water coral absences in 50 m transects represent non-detection rather than true absences due to the narrow field of view of the video data (compared to 50 m x 50 m seafloor pixels) and hence are not necessarily representative (Du Preez et al., 2020), whereas absences are more realistic in the 10 m transects used with the 5 m x 5 m bathymetry. Therefore, whilst model accuracy was supposedly slightly better for the models undertaken on the 50 m resolution data, we suggest that the predictions from the AUV data may be more realistic.

2.5.2 Cold-water coral habitat in Explorer Canyon

Explorer Canyon provides suitable conditions for “Threatened and/or Declining Species and Habitats” (OSPAR, 2008) and is part of a designated Marine Conservation Zone (MCZ) (Marine and

Coastal Access Act, 2009). Whilst the physical complexity of submarine canyon features provides some natural shelter, protection is still required as long line fishing and trawling is likely prevalent in and around Explorer Canyon according to vessel monitoring system data (JNCC, 2012). Trawling and long line fishing may lead to physical abrasion of sensitive benthic fauna (Heifetz et al., 2009; Altheus et al., 2009; Huvenne et al., 2016b) and contribute to increasing the amount of marine litter (Pham et al., 2014) which was present in our video transect (Figure 2.4C; Huvenne et al., 2016a). For example, trawling on the interfluves may have already degraded other nearby cold-water coral habitats (Stewart et al., 2014; Amaro et al., 2016). The coral observed in Explorer Canyon may represent potential strongholds for future recolonization of such proximal degraded reefs (Robert et al., 2019) and require protection. Therefore, knowledge on the coral extent and health is of paramount importance. Our high-resolution bathymetric and optical data reveal that the cold-water corals form mounds with large living colonies, suggesting that the reef is healthy and is likely to be growing. SDMs strongly indicate that the area beyond the ROV field of view on the spur has a high probability of coral presence. This agrees with previous studies (Davies et al., 2014), but whilst confidence of cold-water coral reef presence and extent is “high” (JNCC, 2013), we show that further potential cold-water coral habitats are located within the MCZ boundaries. The cross-model agreement of coral occurrence on the north flank, north-east gullies and southern wall features point to a high likelihood of further coral assemblages in the study site, including potentially undiscovered coral mounds (Figure 2.10). It is considered that coarser resolution predictions should be utilised to create a more cautious network of MPAs (Ross et al., 2015). However, in the current study, the results suggest that whilst coarser resolution models perform well, they also miss potential cold-water coral habitats where features can only be resolved by high-resolution bathymetry (Figure 2.10). Therefore, we suggest that the inspection of multiple resolution SDM outputs should be used to detect and outline sensitive areas requiring further investigation and targeted protection.

A high probability of cold-water coral presence occurred between 750 and 950 m water depth, on structurally complex features such a spurs, gullies, vertical walls and mound features according to the 5 m resolution predictions (Figures 2.6, 2.7, 2.8, 2.9, 2.10). The presence of coral on complex terrain is well documented in SDM studies (Howell et al., 2011; Rengstorf et al., 2013; Robert et al., 2015; Bargain et al., 2018; Lo Iacono et al., 2018; Pearman et al., 2020). This relationship is likely derived from substrate heterogeneity and oceanographic interactions with the seafloor. For example, aspect and BPI may be proxies of current exposure (Guinan et al., 2009; Ismail et al., 2015; De Clippele et al., 2017; Lo Iacono et al., 2018), on which passive filter feeders such as cold-water corals are reliant for suspended food particles (Frederiksen et al., 1992; Mienis et al., 2007; Davies et al., 2009). Rugosity (in the form of VRM) was also an important variable in the modelling and

may relate to hard surfaces (Dunn and Halpin, 2009), vertical walls and coral mounds (Guinan et al., 2009). Depth was the most important variable. However, the depth range was well within normal known cold-water coral range in the Whittard Canyon area (Pearman et al., 2020), thus is it likely that one of the correlated variables such as BPI may be the true underlying cold-water coral distribution driver.

Pearman et al. (2020) noted an asymmetric prediction of cold-water coral distribution in Explorer Canyon as noted in other canyon systems (Lo Iacono et al., 2018), with the northern flank being more suitable for coral due to terrain complexity and current regime. Our results loosely support these patterns. The predicted cold-water coral extent on the southern flank was restricted to very steep areas or vertical walls. This could relate to higher sedimentation rates, lack of alternative terrain complexity or limited hard substrate availability. Vertical walls, cliffs and overhangs of varying sizes are often characterised by hard rock substrata which are suitable for cold-water coral (Huvenne et al., 2011; Robert et al., 2019) and provide shelter from turbidity currents, high sedimentation rates and bottom trawling (Huvenne et al., 2011; Gori et al., 2013; Brooke and Ross, 2014). In contrast with other locations in the Whittard Canyon complex (Robert et al., 2020), the vertical walls were more important for *M. oculata* than *L. pertusa*, especially on the southern flank of Explorer Canyon, which may reflect the slightly different niche they occupy (Arnaud-Haond et al., 2017; Lartaud et al., 2017). Therefore, it is important to ensure that spatial extent of distinct species is considered in future scientific and conservation efforts (Barbosa et al., 2020). However, not all wall features are suitable for cold-water coral, due to other competitive assemblages (e.g. deep-sea oysters and other clams; Van Rooij et al., 2010; Johnson et al., 2013), unsuitable surface properties or surfaces that are prone to erosion (e.g. Carter et al., 2018), none of which are likely to have been captured in the SDMs. This was observed in Explorer Canyon whereby different communities or bare wall (Figure 2.4) were observed just metres away from cold-water coral assemblages. In this example, the slight difference in terrain was observed (Figure 2.4 shows the wall to have a more convex, bulbous morphology), but also the deeper bare wall could be influenced by the sediment dynamics within the thalweg, an area known for sediment transport and turbidity currents, which may abrade communities within its path.

2.5.3 AUVs in conservation

The results show that AUVs can provide novel, high resolution data for indicating precise locations of potential cold-water coral occurrence in a geomorphologically complex setting. In particular, the high-resolution data allowed the identification of steep sided or vertical walls which are of interest as an under quantified cold-water coral habitat (Robert et al., 2019), but are receiving more acknowledgement in classification schemes used to inform ecosystem-based spatial management

(Davies et al., 2017). Orthorectified bathymetric data however underestimate the surface area of vertical walls and associated assemblages, as wall is depicted within a narrow ribbon. Therefore, AUV bathymetry can be collected at an angle to yield more accurate representation of the surface area of vertical walls, enabling fully three-dimensional interpretations (Robert et al., 2017). The application of using AUVs to survey walls is not restricted to the deep sea, as other assemblages can colonise vertical walls in shallower waters (e.g. Gori et al., 2011b, Rakka et al., 2020).

AUVs offer a time, cost and carbon emission efficient solution (Benoist et al., 2019) to map a relatively large area in high-resolution within regions of interest such as MPAs. Spatial predictions of species such as cold-water coral are useful tools to assist defining MPA boundaries (Howell et al., 2011; Reiss et al., 2015; Rowden et al., 2017). In particular, high resolution spatial predictions are important to understand what is happening within an MPA and fill the knowledge gaps around the extent and condition of features of interest. This is because communities are influenced by processes which act over a range of scales (Levin, 1992, Lecours et al., 2015) and this is more likely to be captured when undertaking a multi-resolution approach to SDM. Therefore, data from AUVs can be used to supplement SDM over broader areas in a spatially nested survey approach. AUVs also provide means for repeatable mapping for monitoring purposes (e.g. Huvenne et al., 2016b). Follow up surveys may identify terrain changes over time such as submarine landslides, or mechanical disturbance from trawling which is directly applicable in the monitoring of MPAs.

In addition to collecting high resolution bathymetry, AUV photographic surveys may be useful in spatially nested survey designs by means of providing ground truth data for benthic classification mapping (Zelada Leon et al., 2020), 3D photogrammetry (Johnson-Roberson, 2010), photomosaics (Meyer et al., 2019; Simon-Lledo et al., 2019), taxa identification (Morris et al., 2014; Boswarva et al., 2020) and possibly VME identification (Morato et al., 2018; Baco-Taylor et al., 2020). In topographically complex environments such as canyons, traditional survey AUVs do not possess the agility required to follow terrain variability at an optimum distance from the seafloor. Therefore, hover AUVs or untethered ROVs may provide a solution (Friedman et al., 2012; Wagner et al., 2013; Bowen et al., 2013), by navigating complex features in a similar way to how ROVs collect high resolution images to create mosaics and 3D models (e.g. Figure 2.3). SfM outputs can be used to demonstrate the structure of mounds and coral coverage (e.g. Figure 2.3), and such photographic surveys can be used to infer fine-scale relationships between benthic organisms and their environment (Lim et al., 2020), which will be explored in further chapters of this thesis. Photomosaic and 3D photogrammetry surveys can contribute information about benthic organisation using landscape ecology statistics, in order to quantify additional fine-scale drivers of distribution (Edwards et al., 2017). The combination of imagery and multi-resolution predictive

mapping is a powerful tool in the role of spatial planning and can be used to monitor cold-water coral habitats.

2.6 Conclusion

In this manuscript we demonstrate how an AUV survey can be integrated into a spatially nested SDM survey plan in order to extrapolate information obtained from ROV footage. By comparing low- and high-resolution surveys, the SDM approach deployed likely captured a range of species-environment relationships. Small mounds were observed for the first time on a spur part way up Explorer Canyon and described, and live coral were predicted to occur on gullies and vertical walls. Coral location appears strongly driven by terrain complexity and wall features that were only observed in the higher-resolution AUV bathymetry, showing the importance of collecting high resolution bathymetry. Multi-resolution consideration of benthic taxa distribution is a useful tool in marine spatial planning and AUVs provide the capability to perform the necessary spatially nested surveys.

2.7 Acknowledgements

We would like to thank the captain and crew of the expedition JC125. In particular thank you to the ROV team, whom without, this work would not have been possible. This work was funded by the European Research Council (CODEMAP: Grant no 258482) and NERC MAREMAP. DP is supported by NERC NEXUSS (NE/N012070/1). V. Huvenne was funded by MAREMAP, CODEMAP and IAtlantic.

Chapter 3 Using 3D photogrammetry from ROV video to quantify cold-water coral reef structural complexity and investigate its influence on biodiversity and community assemblage.

This chapter is published as:

Price, D.M., Robert, K., Callaway, A., Lo Iacono, C., Hall, R.A., Huvenne, V.I.A. Using 3D photogrammetry from ROV video to quantify cold-water coral reef structural complexity and investigate its influence on biodiversity and community assemblage. Coral Reefs 38, 1007–1021 (2019). https://doi.org/10.1007/s00338-019-01827-3

Author contributions: DP and VH conceptualised the study. DP created the 3D models, generated the geomorphic data, undertook statistical analysis and wrote the manuscript. DP and KR annotated the data. VH collected the data during JC125 CODEMAP cruise. All authors commented on the chapter.

3.1 Abstract

Fine-scale structural complexity created by reef-building coral in shallow-water environments is influential on biodiversity, species assemblage and functional trait expression. Cold-water coral reefs are also hotspots of biodiversity, often attributed to the hard surface and structural complexity provided by the coral. However, that complexity has seldom been quantified on a centimetric scale in cold-water coral reefs, unlike their shallow-water counterparts, and has therefore never been linked in a similar way to the reef inhabitant community. Structure from Motion techniques which create high-resolution 3D models of habitats from sequences of photographs are being increasingly utilised, in tandem with 3D spatial analysis to create useful 3D metrics, such as rugosity. Here, we demonstrate the use of ROV video transect data for 3D reconstructions of cold-water coral reefs at depths of nearly 1000 m in the Explorer Canyon, a tributary of Whittard Canyon, NE Atlantic.

We constructed 40 3D models of approximately 25 m length video transects using Agisoft Photoscan software, resulting in sub-centimetre resolution reconstructions. Digital elevation models were utilised to derive rugosity metrics and orthomosaics were used for coral coverage assessment. We found rugosity values comparable to shallow-water tropical coral reef rugosity. Reef and nearby non-reef communities differed in assemblage composition, which was driven by depth and rugosity. Species richness, epifauna abundance and fish abundance increased with structural complexity, being attributed to an increase in niches, food, shelter and alteration of physical water movement. Biodiversity plateaued at higher rugosity, illustrating the establishment of a specific reef community supported by more than 30% coral cover. The proportion of dead coral to live coral had limited influence on the community structure, instead within-reef patterns were explained by depth and rugosity, though our results were confounded to a certain extent by multi-collinearity. Fine-scale structural complexity appeared to be integral to local-scale ecological patterns in cold-water coral reef communities.

3.2 Introduction

Some colonial Scleractinian cold-water corals, such as *Lophelia pertusa* (recently synonymised to *Desmophyllum Pertusum* (Addamo et al., 2016)), *Madrepora oculata* and *Solenosmilia variablis*, are capable of forming complex 3D reef structures, ranging from patchy cover to massive carbonate mounds (Wilson, 1979; Wheeler et al., 2007). Cold-water coral reefs are predominantly found on continental slopes, seamounts and in fjords, but increasing evidence suggests submarine canyons also provide an important habitat (Orejas et al., 2009; Huvenne et al., 2011; De Mol et al., 2011; Lo Iacono et al., 2018). Due to their complex terrain, submarine canyons may provide important refugia for cold-water coral assemblages (Huvenne et al., 2011), that are vulnerable to destructive fishing practices elsewhere (Fossa et al., 2002; Davies et al., 2007; Althaus et al., 2009; Huvenne et al., 2016b).

Reef-building cold-water corals are autogenic ecosystem engineers according to the definition of Jones et al. 1994, and like shallow-water coral reefs, cold-water coral reefs are considered to be hotspots for biodiversity. Cold-water coral reefs support diverse habitat specific communities of epifauna and infauna (Johnsson et al., 2004; Mortensen and Fossa, 2006; Henry and Roberts, 2007; Bourque and Demopoulos 2018), with enhanced biodiversity and benthic biomass compared to adjacent substrate (Van Oevelen et al., 2009). For example, Shannon-Wiener indices of taxa associated with cold-water coral reefs on the Faroe shelves (North Atlantic) were approximately 5.5, a value which is comparable with shallow-water reef biodiversity (Jensen and Frederiksen, 1992). This biodiversity is associated with sessile and vagile taxa alike (Johnsson et al., 2004). Living portions of the reef harbour fewer, more specialised species (Mortensen and Fossa, 2006; Cordes et al., 2008), whilst the bare hard substrate of dead coral skeleton is often cited as a primary driver of reef biodiversity (Henry and Roberts, 2017). In addition, the structural complexity of the 3D framework provided by the coral skeleton is also considered an important variable contributing to cold-water coral reef assemblage and biodiversity (Johnsson et al., 2004; Cordes et al., 2008; Robert et al., 2017).

Coral reef structural complexity influences marine biodiversity and community structure at multiple scales (Friedlander and Parrish, 1998; Gratwicke and Speight, 2005; Wilson et al., 2007; Graham and Nash, 2013; Richardson et al., 2017). Broad-scale terrain rugosity has been cited as a driver of deep-sea biodiversity (Robert et al., 2015) and cold-water coral distribution (Lo Iacono et al., 2018). However, measuring fine-scale complexity of deep-sea habitats at a similar scale to that in shallow-water coral reef research is problematic owing to the difficulty of sampling at depth. Yet, based on qualitative observation, it is generally accepted that deep-sea benthic fish benefit from fine-scale structural complexity (Roberts et al., 2005; Soffker et al., 2011; Purser et al., 2013). Invertebrates

also benefit from structural complexity, for example, Stevenson et al., (2015) inferred the 3D structure created by cold-water coral was utilised by *Cidaris cidaris* in order to escape predation. At these fine scales, it is thought that the provision of a physically heterogeneous habitat offers multiple niches that organisms can utilise for shelter and/or feeding (Graham et al., 2013). Structural complexity can alter hydrodynamic properties such as current velocity, shear and turbulence, subsequently providing additional microhabitats (Buhl-Mortensen et al., 2010), influencing larval entrainment (De Clippele et al., 2018), larvae retention (Boxshall, 2000; Harii and Kayanne, 2002), suspension feeder feeding efficiency (Purser et al., 2010; Orejas et al., 2016) and infauna diversity (Bourque and Demopoulos, 2018).

Multibeam echosounders mounted on Remotely Operated Vehicles (ROVs) can acquire sub-metre resolution bathymetry of cold-water coral reefs (Huvenne et al., 2011; Foubert et al., 2011; De Clippele et al., 2017; Lim et al., 2018a). Yet, despite these novel techniques, a general lack of complexity measurements of cold-water coral reef framework (centimetric resolution) represents a knowledge gap which can be mitigated through the use of novel image analysis techniques. Structure from Motion (SfM), a form of 3D photogrammetry, is becoming more prevalent in marine imaging research in order to derive terrain variables such as coral reef rugosity (Leon et al., 2015; Storlazzi et al., 2016). This technique opens opportunities for the extraction of a plethora of fine-scale terrain variables that may contribute to the understanding of functioning of deep-sea habitats, such as cold-water coral assemblages (Robert et al., 2017). However, relatively few SfM surveys have been carried out in deep-sea habitats due to the difficulty of acquiring controlled images at depth with additional implications of strong currents and water column turbidity often associated with cold-water coral reef locations (Mienis et al., 2007; Davies et al., 2009; Duineveld et al., 2012). Unmanned underwater vehicles (ROVs, Autonomous Underwater Vehicles and towed platforms), however, can collect suitable images and data to implement SfM techniques (Johnson-Roberson et al., 2010; Robert et al., 2017; Purser et al., 2018).

Cold-water coral reefs are vulnerable to bottom contact fishing activities, and are thus classified as a 'Vulnerable Marine Ecosystem (VME)' (United Nations General Assembly Resolution 61/105), of which structural complexity is a defining characteristic (FAO, 2009). Yet the assignment threshold of VME status to cold-water coral reefs based on imagery is ambiguous, in part due to the lack of prerequisite information about the density at which a group of separate colonies alter the environment enough to form a habitat with distinct communities. Coral coverage values of more than 15 or 60% to detect a distinct coral reef or "coral framework" habitat have been used in previous studies (Rowden et al., 2017, Vertino et al., 2010), but no quantified consensus exists. This may be due to a lack of precise coral coverage and the associated structural complexity information required to identify a distinct habitat and VME threshold. As well as destructive fishing practices

mechanically reducing the reef structure, shallowing aragonite saturation horizon (Turley et al., 2007) geochemically degrades living and dead portions of the reef 3D structure (Hennige et al., 2015). These anthropogenic impacts would reduce the structural complexity with repercussions for the associated fauna and VME status, further highlighting a need to quantify reef characteristics on a framework scale.

In this study, we provide rugosity metrics from 3D reconstructions of cold-water coral reefs using SfM with video data collected from an ROV. We aim to (1) quantify the structural complexity introduced by cold-water coral reef patches, (2) identify the role of structural complexity in driving biodiversity and assemblage composition, (3) use fine-scale information to identify the threshold of coral cover and structural complexity required to form a distinct cold-water coral reef habitat and provide evidence for VME characteristics.

3.3 Methodology

3.3.1 Study area

Explorer Canyon is a tributary of the Whittard Canyon system in the North-East Atlantic (Figure 3.1). The canyon lies within the British exclusive economic zone (EEZ) and forms part of The Canyons Marine Conservation Zone (MCZ) (Ministerial order/DEFRA, 2013) which was designated based on the occurrence of deep-sea bed and cold-water coral reef habitats in accordance with the UK Marine and Coastal Access Act (2009). The canyon system is subject to energetic internal wave activity (Vlasenko et al., 2014; Hall et al., 2017; Aslam et al., 2018), upwelling (Porter et al., 2016) and provides suitable habitats for cold-water coral (Huvenne et al., 2011; Robert et al., 2017). Davies et al. (2014) located reef-building scleractinians on a spur midway up the Explorer Canyon branch at 795-940 m depth.

3.3.2 Video survey and data preparation

The data for this study were collected during a survey as part of the Expedition JC125 aboard the RRS James Cook (Huvenne et al., 2016a). The ROV *Isis* was used to conduct a video transect starting from the thalweg of the canyon and ascending along the Explorer Canyon slope and scarp (Figure 3.1). One frame per second was extracted from a High Definition obliquely angled camera (HDSCI) mounted on the ROV, using Quicktime 7 Pro (Apple inc.). The transect was divided into 25 m sections or sub-transects, estimated from the horizontal distance travelled based on the Sonardyne Ultra-Short Base Line (USBL) positioning system and the corresponding images were extracted for 3D reconstruction. Sections of 25 m were chosen as reconstructions along a single line tended to

accumulate positioning error with increasing distance and thus longer sub-transects became unreliable. Secondly, shorter sections might not have encompassed enough area for robust faunal counts of low density organisms such as fish. Finally, 25 m transects have also been used in shallow-water coral reef rugosity research (Friedlander and Parrish, 1998), thus aiding comparison with previous work.

The sloping and complex topography of the canyon prevented true nadir camera angle although the slightly angled ROV camera against the slope was determined to be favourable for 3D reconstructions during preliminary analysis. Whilst having the camera orthogonal to the subject is not a prerequisite for reconstructions, it is beneficial to ensure as much of the terrain is captured accurately as possible (Kwasnitschka et al., 2013). The images were manually assessed for lapses in quality and removed where necessary. De-interlacing of the frames was performed in Adobe Photoshop CS6.

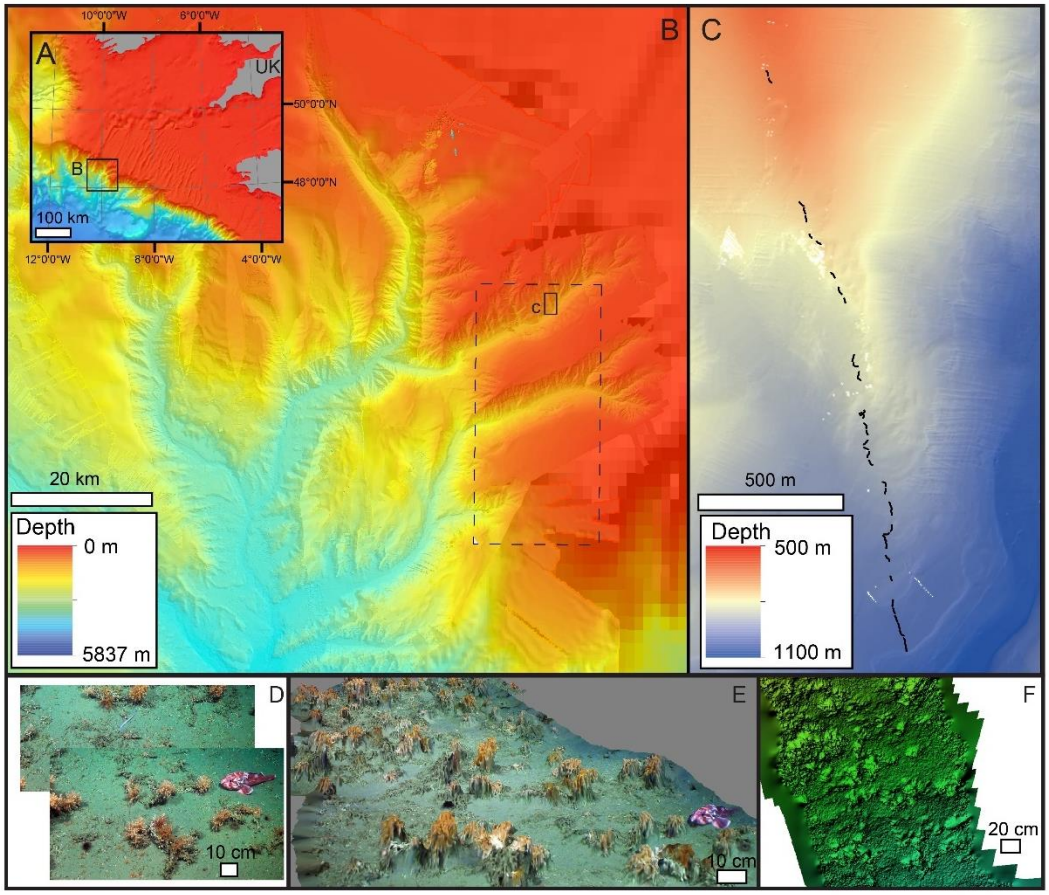

Figure 3.1. Study location. A) Geographical location, global bathymetry (GEBCO), with the Eastern Whittard Canyon outlined. B) Eastern Whittard Canyon with the Marine Conservation Zone boundary (dashed rectangle) and study site outlined (C). C) Spur in the Explorer Canyon (North part of MCZ). Black lines denote approximate 3D reconstructed sub-transects. D) Example image sequences. E) 3D reconstruction of a reef sub-transect. F) Digital elevation model of the coral reef

3.3.3 Reconstruction

The images were imported into Agisoft Photoscan Professional (v. 1.3.4.5067). The final step before processing involved masking the images to remove parts of the ROV equipment that were captured in the frame or black background beyond the light, improving image distortion residuals significantly. Optical aberrations caused by the water/glass interface were not calibrated due to lack of available information. However, Young et al. (2017) found that non-calibrated cameras produced accurate and precise reconstructions to a centimetric scale, suggesting Agisoft Photoscan performs adequately with non-calibrated cameras and distorted images. Each frame was paired with its USBL position for georeferencing (performed in R version 3.3.2), and lasers spaced 10 cm apart were used as a reference scale at multiple flat locations within each reconstruction.

The workflow was carried out as specified by Agisoft Photoscan Professional, using a 16 core, 64GB High Performance Computer (IRIDIS) node with two NVIDIA K20 graphics processors. High quality alignment via generic pre-selection was chosen. High quality dense clouds were created and optimised for scale and georeferenced, then reprocessed, followed by manual editing to remove outliers and noise. The models were screened visually for distortions and large georeferencing errors. The outputs were exported as digital elevation models (DEM) at a standard 5 mm pixel size for terrain analysis and orthomosaics at the highest resolution (predominantly <2 mm per pixel) to quantify coral coverage. Where gaps in the DEM were caused by tall coral colonies obstructing the camera view, these were addressed through interpolation (as used by Leon et al., 2015).

3.3.4 Biodiversity

The “SCORPIO” camera mounted on *Isis* recorded video footage in high definition which was used to count the organisms present using OFOP (Ocean Floor Observation Protocol) software. The SCORPIO camera was utilised as it was installed in a static position with fixed zoom for a consistent standardised analysis which was within the field of view of the HDSCI video footage. Organisms were recorded as morpho-species and then identified to the lowest possible taxonomic resolution. All species within the time frames of the image sequences used for reconstructions were binned to the respective sub-transect and standardised to sub-transect lengths (individuals per metre). Fish counts (for fish abundance only) were obtained from the HDSCI camera due to its wider field of view, providing a larger area for fish observations and all species were concatenated as few were observed (Purser et al., 2013). Species richness, Shannon Wiener index, total abundance and fish abundance were used for univariate data analysis. Reef building species were not included in community assemblage analysis due to their role as an independent variable in this study.

3.3.5 Rugosity

The DEMs were imported into ArcMap 10.5 and analysed using the Benthic Terrain Modeller tool (BTM; Wright et al. 2005). As the transect traversed a canyon slope, vector ruggedness measure (VRM) from the BTM was utilised as a measure of rugosity as this method decoupled ruggedness from slope angle (Sappington et al., 2007). To asses any measurement scale dependent relationships, VRM was calculated at different neighbourhood scales (1.5, 3.5, 5.5, 7.5, 9.5, 11.5, 13.5, 15.5, 17.5 and 19.5 cm), to investigate a full range of scales from individual polyps to colony scales. The mean ruggedness index value for each reconstruction was calculated to identify any scale dependent relationships.

A standard quantitative survey of shallow-water coral reef structural complexity is traditionally carried out using a chain laid out over the reef, and assessing the ratio of chain length:horizontal length to produce a rugosity index ratio (Graham and Nash, 2013). Rugosity index ratio values were calculated along a line through the middle of each sub-transect (for the full length), using the following formula in order to replicate the chain rugosity method:

$$Rugosity\ index\ ratio = \frac{3D\ line\ length}{2D\ line\ length}$$

The structural complexity measure that had the strongest relationship with coral cover and biodiversity was used in subsequent biodiversity and community assemblage analysis.

3.3.6 Substrate classification

A custom ImageJ macro code was used to randomly plot 250 points across each orthomosaic to assess percentage coral coverage and substrate type. Six classes of substrate were identified: 1) mixed sediment, 2) mudstone, 3) hard rock, 4) dead coral framework, 5) live coral or 6) litter. Mixed sediment consisted of fine and mobile material such as sand, silt and loose mud, with some areas of coarser sand, empty shells and small coral fragments. Mudstone and consolidated muds were considered separate from mixed sediment and hard rock due to a firmer surface compared to mixed sediment, but its propensity to erosion over time (Carter et al., 2018), and the presence of burrows. Fine layers of mixed sediment overlying flat parts of mudstone were considered mudstone due to the local hydrodynamics leading to sporadic sediment cover.

This type of coverage quantification was undertaken to (1) recognise a value of coral cover that may induce a reef community or influence biodiversity with the potential to identify a VME discrimination point and (2) utilise dead coral cover percentage as an abiotic factor for analyses of

with-in reef communities to discriminate between rugosity and hard substrate provision as a driving factor and (3) gain a broad overview of the substrate composition at each sub-transect.

3.3.7 Statistics

Linear Regression analysis and Pearson correlation were used to identify a relationship between coral cover and rugosity metrics (VRM and rugosity index ratio). Data exploration on biodiversity metrics was undertaken following the guidelines of Zuur et al. (2007, 2009). We utilised Generalized Additive Models (GAM) to investigate the relationship between the environmental variables (depth, VRM) and univariate biodiversity metrics (Species Richness, Shannon Index (H'), Total abundance and fish abundance). Collinearity was tested for by pairs plots and Variance Inflator Factor (VIF). Depth and rugosity were not correlated, but substrate type (in terms of percentage cover) was found to strongly correlate (>0.7 Pearson correlation; VIF >10) with depth and rugosity and was therefore not included in the analysis. Normality was tested for by Shapiro-Wilk test, total and fish abundance were $\sqrt{}$ and $\sqrt[3]{}$ transformed to meet normality assumptions for use of a Gaussian family distribution. VRM and Depth independently and combined were considered in the model building process and were assessed with corrected Akaike's Information Criterion value (AICc). Variance of the fitted residuals was inspected to ensure homogeneity. Variograms of the final models were explored to identify any evidence for spatial autocorrelation. Models were built using the package 'mgcv' in R (R core team 2012).

Multivariate analysis was carried out in PRIMER V6 with the PERMANOVA+ extension, on communities across all sub-transects and sub-transects with notable coral cover (>15% based on Rowden et al., 2017), to identify the drivers and the threshold where assemblage composition forms a distinct reef-associated community. Bray-Curtis similarity matrices of the communities were created after $\sqrt{}$ transformation of the data. Group average clustering was undertaken in order to explore community similarities between transects and statistically tested by ANalysis Of SIMilarity (ANOSIM). Depth, rugosity and dead:live coral ratio were normalised and Euclidean distance was used to create environmental similarity matrices. The relationship between each variable and the assemblage was investigated using a DISTance based Linear Model (DISTLM). The DISTLM results were coupled with a distance based Redundancy Analysis (dbRDA) to visualise the multidimensional spatial relationship. DISTLM tests each variable nominally which are then combined to create a multivariate structure. Final model choice was based on a stepwise AICc criteria method and BEST selection procedure.

3.4 Results

3.4.1 Image acquisition

A total of 40 reconstructions were produced utilising 8, 964 images and each sub-transect consisted on average of 224 (±13 SE) images (Table 3.1). The number of images depended on the speed of the ROV, ranging from approximately 0.06 to 0.24 m s^{-1}, which was an appropriate speed to utilise stills from video without blur or excessive image overlap. Mean georeference error was 1.53 m (± 0.07 m SE), which is within error estimates of USBL navigation (1% of Depth), and is relative to geographic location rather than within-model error (range: 0.7 – 3 mm). Continuous sampling along the entire ROV video transect was not always possible due to variations in ROV height inhibiting the camera view and monotone substrate that led to issues with camera positioning in the reconstructions. The mean reconstruction length was 26.8 m (±0.6 m SE). As point to point USBL positioning was used to identify the 25 m sub-transect lengths, true transect lengths were often longer than 25 m (as much as 40 m) due to an oscillating ROV path. In contrast, sub-transect A9 was only 18 m long but was retained for analysis to extend the range of rugosity measures as the coral cover was the highest. Sub-transect length had no effect on standardised species assemblages or species richness counts (considered as a variable in a BEST test and GAM (Appendix 3.4)).

3.4.2 Substrate classification

Deeper sub-transects (A-F, I-N) were characterised by mudstone with sporadically interspersed pockets of mixed sediment (2%-37% cover) (Figure 3.2). Sub-transects G and H were dominated by mixed sediment (>70% cover) whilst sub-transect O was the deepest where coral framework was observed (1071 m), but consisted of all dead framework. The regular occurrence of coral started at sub-transect U and continued until A9 at depths between 770 and 935 m. Coral cover ranged from 0% to 75% and mixed sediment usually covered most of the rest of the coral sub-transects. At shallower depths, mixed sediments were the dominant substrate (Figure 3.2). Hard substrate (rock) and litter cover (n=22; fishing gear and plastic sheets mostly) was negligible.

Table 3.1. Meta data of each sub-transect.

Sub transects	Total aligned images	Length (m)	Transect time	Number of dense cloud points	Georeference error (m)	Scale error (m)	DEM res (mm per pixel)	Ortho (mm per pixel)	Mean depth (m)
A	286	25.7	04:45	9659465	1.22	n/a	2.7	1.4	-1071
B	188	25	03:07	8912853	1.32	0.012	2.8	1.4	-1065
C	287	26.9	04:46	10894879	1.87	0.010	2.4	1.2	-1059
D	215	24.6	03:34	9529201	1.80	0.012	2.7	1.3	-1054
E	307	25.6	05:06	10350493	2.21	0.015	3.2	1.6	-1042
F	129	24.3	02:08	9501754	1.60	0.012	2.6	1.3	-1033
G	152	26.9	02:31	10134821	1.43	0.015	2.9	1.5	-1032
H	137	20	02:16	6196412	1.99	0.022	2.8	1.4	-1027
I	243	26.6	04:02	11079272	1.38	0.029	3.0	1.5	-1016
J	183	28.4	03:02	12349339	1.30	0.009	2.3	1.2	-1007
K	174	29.2	02:53	13307670	1.36	0.013	2.3	1.1	-1001
L	134	26.8	02:13	9407083	1.59	0.016	2.6	1.3	-998
M	163	26	02:42	11714816	1.75	0.169	2.3	1.1	-997
N	174	28.1	02:53	12617473	1.21	0.010	2.3	1.2	-993
O	208	27.3	03:27	14021270	1.48	0.013	2.4	1.2	-985
Q	274	22	04:33	11236523	1.93	0.023	2.3	1.2	-969
R	211	25.5	03:30	12467613	1.44	0.015	2.1	1.1	-964
S	161	23.8	02:40	11317261	1.14	0.012	2.2	1.1	-955
T	137	26.9	02:16	9764789	1.30	0.013	2.4	1.2	-945
U	230	29	03:49	13893585	1.56	0.013	2.3	1.2	-935
V	114	22.3	01:53	8261666	2.46	0.023	2.2	1.1	-928
W	152	23.7	02:31	10299492	1.53	0.016	2.6	13.1	-924
X	120	20.9	01:59	9887563	2.55	0.029	2.1	1.0	-915
Y	215	30.3	03:34	13884492	1.44	0.013	2.4	1.2	-910
Z	237	29.2	03:56	10961846	1.68	0.017	2.8	1.4	-898
A1	194	36.4	03:13	12896286	1.25	0.014	2.8	1.4	-895
A2	292	40.4	04:51	14474140	1.29	0.018	3.6	1.8	-868
A3	446	30.6	07:25	11653657	1.63	0.011	3.5	1.8	-852
A4	194	30.4	03:13	12254328	0.93	n/a	3.2	1.6	-839
A5	274	20.7	04:33	14974612	2.80	0.033	1.5	0.8	-818
A6	344	32	05:14	20569788	1.20	0.013	1.9	1.0	-810
A7	329	28.6	05:28	18821126	0.77	0.013	2.3	1.2	-795
A8	455	23.2	07:34	13659740	1.74	0.022	2.3	1.2	-780
A9	180	17.6	02:59	8434800	0.64	0.001	3.5	1.8	-770
A10	317	27.1	05:16	13649729	1.21	0.012	2.4	1.2	-767
A11	237	27	03:56	11298246	1.41	0.007	2.8	1.4	-756
A12	223	25.5	03:42	8461635	1.04	0.008	2.7	1.4	-753
A13	125	22.7	02:04	11625973	1.73	0.017	2.0	1.0	-726
A14	317	23.8	05:16	10488154	1.39	0.020	2.2	1.1	-648
A15	206	22.9	03:25	9965094	1.60	0.022	2.1	1.0	-646

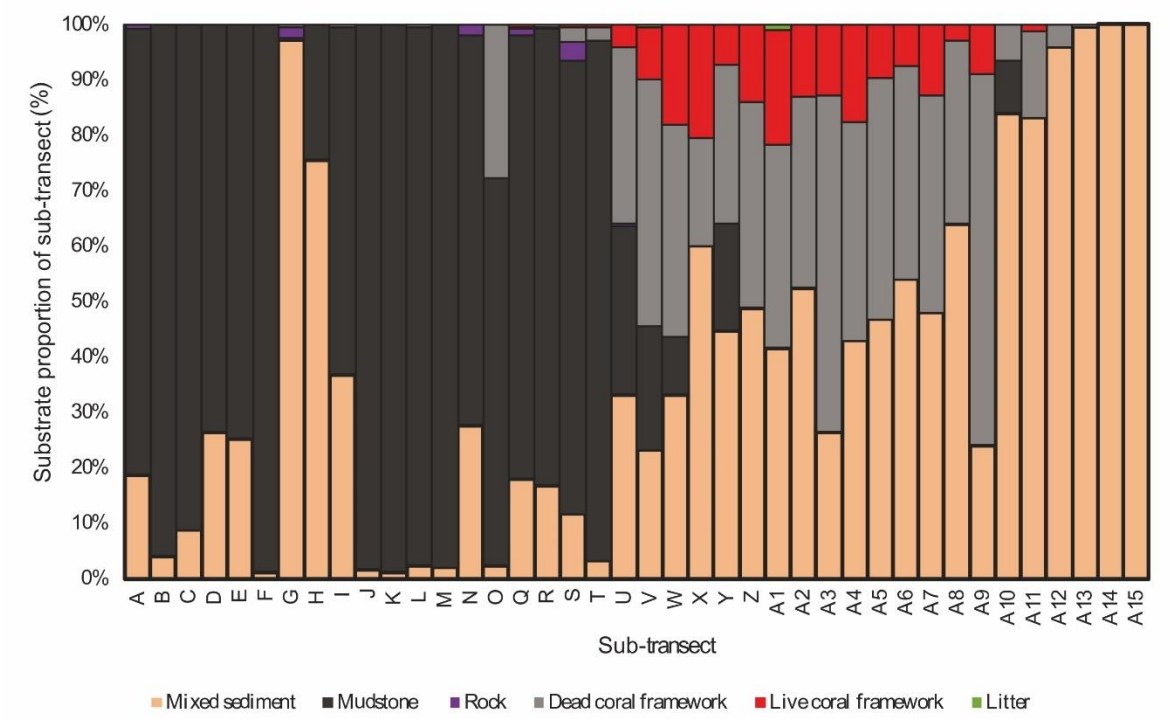

Figure 3.2. Substrate cover for each sub-transect. Results from 250 randomised points within each orthomosaic.

3.4.3 Coral rugosity

VRM increased as neighbourhood size increased in an asymptotic curve (Appendix 3.1). Strong linear correlation with coral counts and % cover was observed at a neighbourhood sizes of 9.5 x 9.5 cm and above (Pearson correlation plateaued at around 0.95). Beyond a neighbourhood size of 9.5 x 9.5 cm, analytical gains were negligible and thus 9.5 x 9.5 cm pixel size was used for further analysis. Rugosity index ratio and VRM were strongly correlated ($r = 0.92$, $P < 0.05$). VRM was visibly linked with coral colonies within each sub-transect whereby individual colonies observed in the orthomosaics (Figure 3.3 A) correlated with pixels indicating high VRM at all scales shown in Figure 3. VRM and Rugosity index were positively influenced by coral coverage ($R^2 = 0.914$, $p < 0.001$; $R^2 = 0.847$, $p<0.001$ respectively). VRM was chosen for the remaining analysis due to the slightly stronger relationship with coral cover than the rugosity index ratio (Figure 3.4). In addition, VRM considers the full coverage of reconstruction.

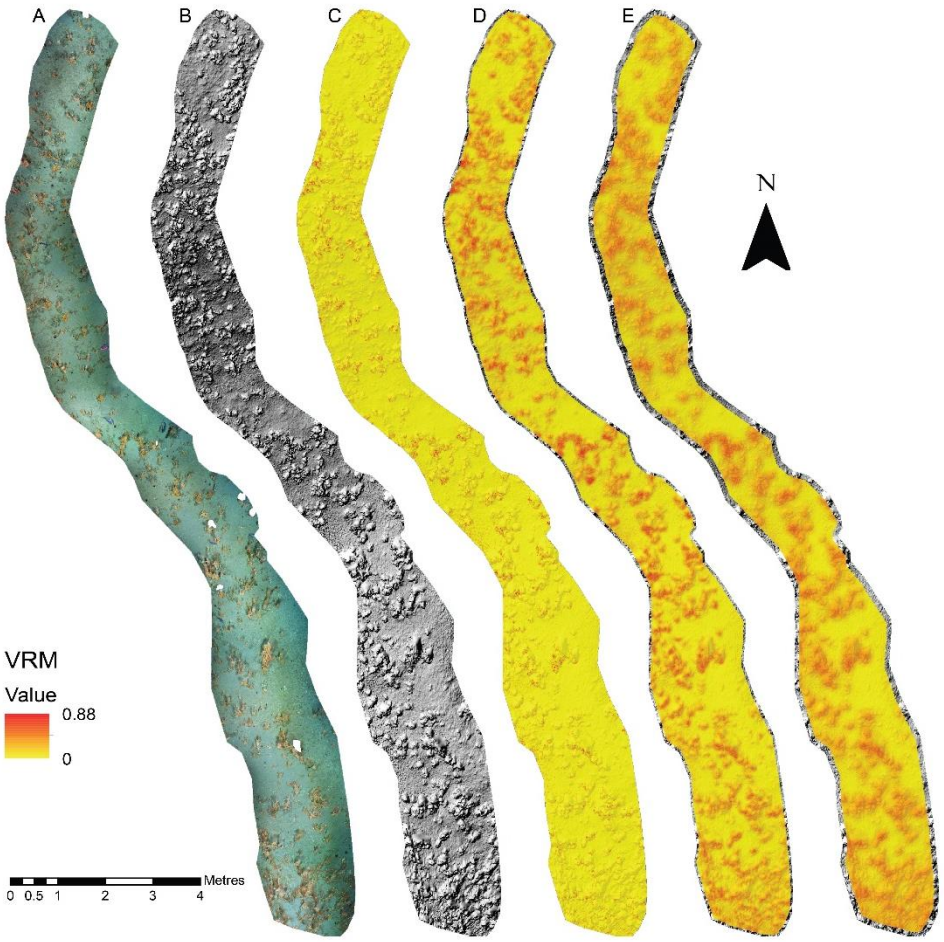

Figure 3.3. Sub-transect X as an example. A) orthomosaic, B) hillshade/digital elevation model and vector ruggedness measure values at C) 1.5, D) 9.5 and E) 19.5 cm per pixel neighbourhood analysis.

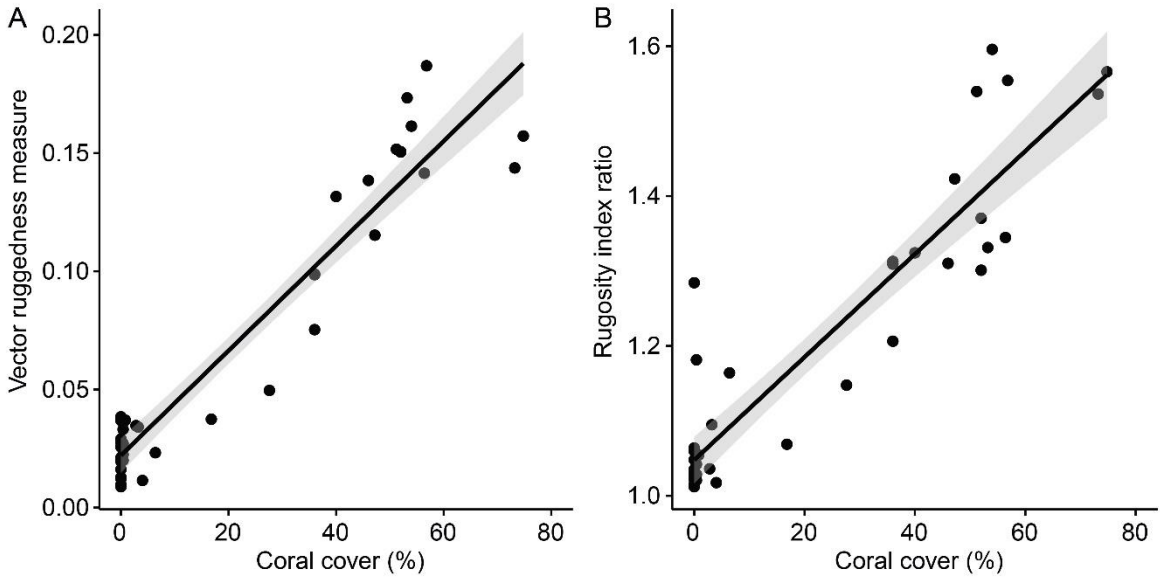

Figure 3.4. Relationship of A) vector ruggedness measure and B) rugosity index ratio with cold-water coral cover.

3.4.4 Biodiversity

A total of 17,731 individual organisms (including coral colonies of which there were 5,145 observations) from 54 morphospecies were observed within the 40 sub-transect samples. *M. oculata* (3541 colonies) and *L. pertusa* (1572 colonies) were the two most prevalent reef building scleractinians; only 32 colonies of *S. variabilis* observed.

VRM and depth influenced species richness, total abundance, Shannon-Wiener index (H') and fish abundance (Figure 3.5, Table 3.2). Species richness increased with VRM, until about 0.07 VRM, when the increase plateaued (Figure 3.5). The values of H' increased with VRM before decreasing after VRM of 0.05 (Figure 3.5). Total epifauna abundance and fish abundance positively correlated with VRM (Figure 3.5). *Lepidion lepidion* (synonym: *Lepidion eques*) represented more than 50% of the fish observed and of the 70 *L. lepidion* observed, 54 were found within a few centimetres of coral structures, six near a non-reef structure (such as mudstone outcrops and ledges) and 10 were observed on flat structureless substrate. Depth was significant for H' and total abundance, appearing to mirror the general substrate patterns seen in Figure 3.2. Spatial autocorrelation was not present in our dataset (Appendix 3.2), likely due to the inclusion of the depth variable that is intrinsically linked with latitude.

dbRDA plots revealed a partitioning between reef (>30% coral framework cover) and non-reef communities (mixed sediment and mudrock habitats) (Figure 3.6 A). Distinct clustering of mixed sediment and rock mud sub-transects was observed but the assemblages still showed 30% similarity (Figure 3.6), and sub-transects O and A11 communities were more akin to non-reef assemblages despite the presence of (mostly dead) coral structure (28 and 17% coral cover respectively), supported by ANOSIM results ($R = 0.612$; $p < 0.001$). VRM accounted for 24% of the community structure, whilst depth accounted for 12% of the variation (Table 3.3, Figure 3.6 A).

There was little to no clustering of sub-transects with coral cover assemblages (Figure 3.6 B). The DistLM found that depth and VRM accounted for 42% of the assemblage variation; depth was the strongest driving factor (26%) with VRM playing a lesser role (15%) (Table 3.3, Figure 3.6 B). The inclusion of dead:live coral ratio increased the variance explained to 46% (Table 3.4), though marginal tests deemed it non-significant, possibly due to small sample size.

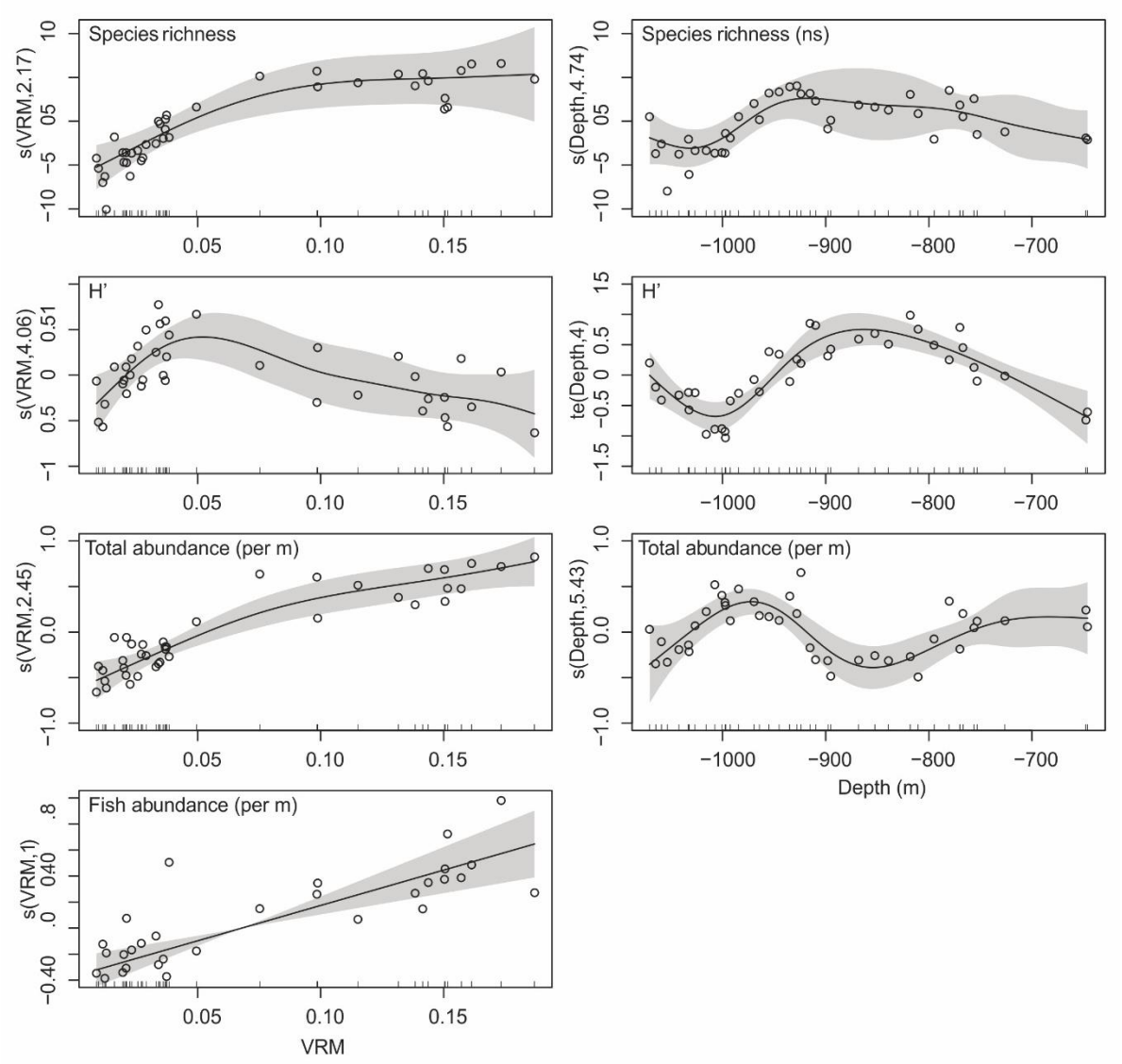

Figure 3.5. GAM smoother outputs showing the relationship between vector ruggedness measure (VRM) and depth, and biodiversity indices; species richness, Shannon–Wiener index (H'), total abundance and fish abundance

Table 3.2. Univariate biodiversity GAM results. Statistically significant (p<0.05) in bold.

	Distribution family	VRM p value	Depth p value	R^2 adjusted	Deviance explained (%)	Factors included
Species richness	Poisson	**<0.001**	0.0589	0.887	91.2	VRM + Depth
H'	Gaussian	**<0.05**	**<0.001**	0.711	77.2	VRM +Depth
Total abundance (cuberoot)	Gaussian	**<0.001**	**<0.001**	0.799	83.9	VRM + Depth
Fish abundance (sqrt)	Gaussian	**<0.001**		0.398	44.1	VRM

Table 3.3. Sequential test results from distance based linear model. All habitat community refers to figure 3.8 A and within reef community refers to figure 3.8 B.

	Variable	Pseudo-F	P	Prop	Cumulative
All habitat communities	VRM	11.994	<0.001	0.240	0.240
	Depth	7.106	<0.001	0.122	0.362
Coral reef community	Depth	5.471	<0.01	0.267	0.267
	VRM	3.693	<0.01	0.153	0.420

Table 3.4. Best model solutions for explaining community structure of transects with reef patches (Figure 3.8 B).

AICc	R^2	Selections
121.35	0.420	Depth + VRM
122.34	0.267	Depth
123.48	0.465	Depth + VRM + % dead coral

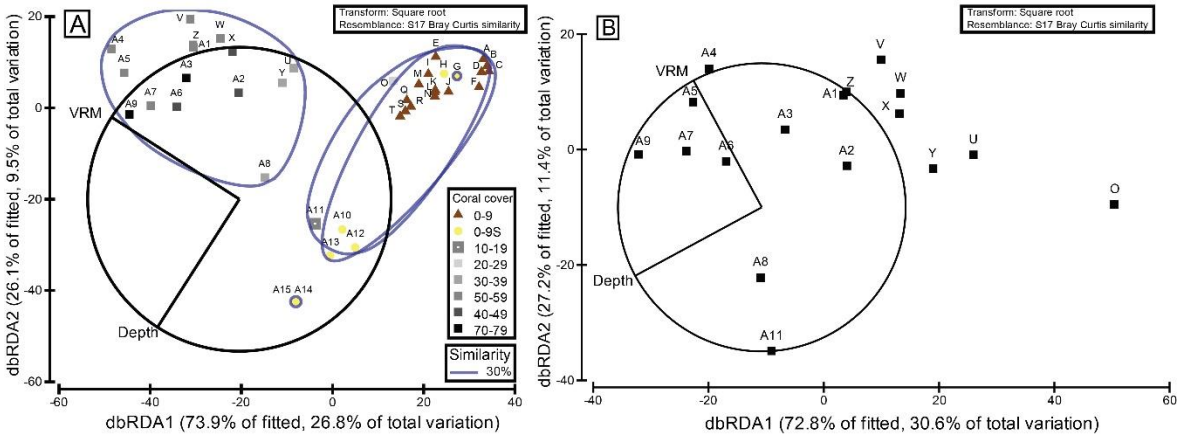

Figure 3.6. dbRDA plots based upon DistLM results (Table 3.3), with significant abiotic overlay. a) All transects. B) Transects with > 15% coral coverage. 30% similarity circles are based upon group average clustering. Coral cover as a percentage with corresponding grey gradients to match. Brown triangle represents 0–9% coral coverage with mudstone dominating the rest, yellow circle signify 0–9% coral cover with mixed sediment dominating the rest. Letters refer to sub-transect identity

3.5 Discussion

A strong linear relationship between coral cover and terrain complexity was evident, providing a strong quantitative relationship for the first time. The range of rugosity index values observed (up to 1.6) is comparable to global shallow-water coral reef rugosity index values (Graham and Nash, 2013). In shallow-water coral reefs, scale-dependant rugosity (Richardson et al., 2017; Knudby and LeDrew, 2007), is a result of diverse coral morphology diversity (Burns et al., 2015) and intra-species morphology plasticity (Todd, 2008). We did not observe comparable scale dependant patterns as the Explorer Canyon reef had relatively limited reef morphology diversity, though cauliflower-like structures found at other localities (e.g. De Clippele et al., 2018), or reefs with greater vertical relief may provide contrasting rugosity patterns.

Fine-scale structural complexity influenced biodiversity and benthic fauna abundance. However, due to a high level of collinearity we could not assess whether reef-induced complexity enhanced biodiversity or if provision of hard substrate and coral cover were the main driving factors. Yet, the reef structures observed in this study have a relatively low vertical profile, with very few colonies reaching > 50 cm tall. Thus, we suggest that reefs with greater vertical relief would display a wider rugosity range, in which case coral coverage percentage estimates from an orthogonal angle become limited as an explanatory variable. Within the rugosity values observed, our data suggest that VRM influences species richness strongly to a certain point (approximately 0.07 VRM or 1.2 rugosity index equating to approximately 25-30% coral cover), after which the structural complexity played a more limited role in promoting species richness. The strong positive relationship between species richness and rugosity at low rugosity values (indicating low coral cover) indicates sensitivity to fine-scale terrain complexity for deep sea organisms. The increasing relationship between organism abundances and rugosity suggests reef structural complexity continued to influence inhabitant density beyond our measured VRM range. In addition to shelter provision and hydrodynamic regime diversity, increased rugosity is mathematically indicative of greater surface area and thus settling availability for sessile species. Due to the strong collinearity it is likely that rugosity represented the combined effect of reef rugosity and hard substrate availability, whilst depth was a proxy for many other explanatory variables (such as temperature and substrate type in this study).

Fish-coral association studies have shown the relationship is site and species specific on a broader scale (Biber et al., 2014), but our study shows more specifically that fish utilised areas of reef-driven complexity. This is consistent with shallow-water reef research that identified a strong relationship between fish density and structural complexity (Graham and Nash, 2013). Enhanced potential prey within the reef, likely at least in part influenced by rugosity as suggested by the high abundance of

epifauna observed, could contribute to the positive fish-rugosity relationship. However, we typically observed most fish swimming and resting within centimetres of coral colonies indicating their behaviour was linked to the physical structure, likely for shelter and reproduction (Husebo, 2002; Costello, et al. 2005; Henry et al., 2013; Corbera et al., 2019).

Community assemblages in sub-transects with coral cover were driven by depth and rugosity with limited influence from the proportion of live:dead coral framework. Whilst we suggest some species such as mobile invertebrates are likely to benefit from structural complexity (Stevenson et al., 2015) independent of live:dead coral ratio, certainly for some sessile species such as *Actinaria* spp. the hard substrate provided by the dead coral framework seemed essential to their existence. However, the composition of coral framework was dominated by dead coral skeleton (49-100% dead), providing no distinct live coral dominated habitat and associated assemblages for comparison. This is consistent with Mortensen et al. (1995) who identified little difference between living and dead coral zone megafauna diversity from comparable 10 m video transects, citing the availability of dead coral framework within living reefs on the Norwegian shelf, though the threshold for living reef classification was minimal at 10% live coral cover. Conversely, De Clippele et al. (2018) noted abundances of sponge species (megafauna) differed depending on the proportion of live coral cover from video data, exemplifying that proportion of dead coral cover can influence some groups, though few sponges were observed at Explorer Canyon to enable testing of this association. Furthermore, Lessard-Pilon et al. (2010), observed that live:dead coral ratio influenced the trophic level of inhabitants suggesting a community structure difference. However, this was compared between different reef sites suggesting different inter- and intra-reef specific relationships or that local rugosity was an unquantified underlying contributing factor. This ambiguity highlights the need for further research to establish if this relationship is ecosystem wide and whether a larger live:dead coral ratio range may be required to further discriminate the influence of dead vs live coral and structural complexity. Overall, within reef influenced sub-transects, assemblage heterogeneity was present and was influenced by structural complexity and depth (and its dependents).

The techniques presented provide a novel method to quantify the role of cold-water coral in enhancing biodiversity in the deep sea on a scale of metres. Areas of high rugosity and coral cover harboured distinct communities with increased diversity and it appeared relatively little coral cover is required to influence the community. The cluster analysis grouped sub-transects A11 and O (17 and 28% coral cover respectively) distinctly from coral communities, suggesting coral cover between 28% (sub-transect O) and 36% (sub-transects U and A8) is representative of a threshold at which coral reef communities become established and distinct. Coral cover of approximately 30% may represent the point at which a group of coral colonies form a distinct habitat, at least on a scale

of 10s of metres, and support classification as a VME from imagery in Explorer Canyon. Species richness also plateaued at about 30% coral cover (0.07VRM) further supporting the suggestion that this proportion of coral represents the point at which a stable and distinct habitat is formed. This is also consistent with the position of the sub-transect in the reef, whereby distinct communities were found in the densest part of the reef at intermediate depths, with reef edges and low coral cover areas not harbouring highly distinct communities.

The implications for VME assignment are that in the absence of a large reef, it is unlikely that single colonies or very low coral coverage will support a distinct reef assemblage, thus may not fulfil the requirements for assignment. Nonetheless, if environmental conditions persist, a substantial reef may develop, meaning such areas could be considered prospective reef VME which should be taken into consideration for conservation. Furthermore, although the associated assemblages were not distinct, low coral coverage and associated rugosity still positively influenced univariate indices, and thus could still be considered biodiversity hotspots. Due to these results being based on a single reef over one time period, further research and wider application of our methods is recommended. Furthermore, these results are specific to the Explorer Canyon reef, and it is unknown how well these results would translate to different cold-water coral reefs.

Our results demonstrate how we can utilise SfM to identify fine-scale ecological drivers and quantify cold-water coral structural complexity. Furthermore, the orthomosaics produced can be useful to create high resolution substrate and habitat maps over larger areas (Lim et al. 2017; Conti et al. 2019), and the 3D models used to measure coral growth rates (Bennecke et al., 2016). This demonstrates the effectiveness of this methodology to monitor reef structures that are vulnerable to anthropogenic impacts such as fishing and shoaling aragonite saturation (Jackson et al. 2014).

To conclude, our results suggest fine-scale rugosity has an important role in community composition, which should be considered when interpreting broader-scale ecological information as ecological patterns relate to different variables at different scales, requiring multi-scale investigation. We present proof of concept that SfM can provide novel information on localised influential abiotic variables and show that reef diversity and assemblage composition is driven by intricate fine-scale drivers beyond presence and absence of coral, furthering our knowledge of cold-water coral reef ecology.

3.6 Acknowledgements

This work was undertaken as part of the European Research Council (Grant No. 258482) funded CODEMAP project (Complex Deep-sea Environments: Mapping habitat heterogeneity As Proxy for biodiversity). The JC125 cruise was funded by CODEMAP and the NERC MAREMAP programme, with

additional financial support from DEFRA. D. Price was supported by the Natural Environmental Research Council [grant number NE/N012070/1]. V. Huvenne was supported by CODEMAP, the MAREMAP programme and the NERC CLASS project (grant number NE/R015953/1). We thank the captain and crew of the RRS James Cook for their assistance during the expedition. The authors acknowledge the use of the IRIDIS High Performance Computing Facility, and associated support services at the University of Southampton. Finally, we are grateful to the three anonymous reviewers who gave constructive feedback, improving this manuscript.

Chapter 4 Fine-scale heterogeneity of a cold-water coral reef and its influence on the distribution of associated taxa.

In review (status as of 12/02/2021: Resubmitted after minor revisions): Price, D.M., Lim, A., Callaway, A., Eichhorn, M., Wheeler, A., Lo Iacono, C., Huvenne, V.A.I. Fine-scale heterogeneity of a cold-water coral biogenic reef structure and its influence on the distribution of associated taxa. Frontiers in marine science.

Author contributions: DP, AL and VH conceptualised the study. AL and AW collected data. DP generated 3D models, processed the data and undertook statistical analysis. AL created the classified substrate map. DP wrote the manuscript. All authors reviewed and commented on manuscript.

4.1 Abstract

Benthic fauna form spatial patterns which are the result of both biotic and abiotic processes, which can be quantified with a range of landscape ecology descriptors. Fine- to medium-scale spatial patterns (<1-10 metres) have seldom been quantified in deep-sea habitats, but can provide fundamental ecological insights into species' niches and interactions. Cold-water coral reefs formed by *Desmophyllum pertusum* (syn. *Lophelia pertusa*) and *Madrepora oculata* are traditionally mapped and surveyed with multibeam echosounders and video transects, which limit the ability to achieve the resolution and/or coverage to undertake fine-scale, centimetric quantification of spatial patterns. However, photomosaics constructed from imagery collected with Remotely Operated Vehicles (ROVs) are becoming a prevalent research tool and can reveal novel information at the scale of individual coral colonies.

A survey using a downwards facing camera mounted on a ROV traversed the Piddington Mound (Belgica Mound Province, NE Atlantic) in a lawnmower pattern in order to create 3D reconstructions of the reef with Structure-from-Motion techniques. Three high-resolution orthorectified photomosaics and digital elevation models (DEM) >200 m^2 were created and all organisms were geotagged in order to illustrate their point pattern. The Pair Correlation function was used to establish whether organisms were distributed with complete spatial randomness (CSR) or demonstrated a clustered pattern at various scales. We further applied a point pattern modelling approach to identify four potential point patterns: CSR, an inhomogeneous pattern influenced by environmental drivers, random clustered point pattern indicating biologically driven clustering and an inhomogeneous clustered point pattern driven by a combination of environmental drivers and biological effects. Reef framework presence and structural complexity determined inhabitant distribution with most organisms showing a departure from CSR. These clustered patterns are likely caused by affinity to local environmental drivers, growth patterns and restricted dispersion reproductive strategies within the habitat across a range of fine to medium scales. These data provide novel and detailed insights into fine-scale habitat heterogeneity and microhabitats showing that non-random distributions are apparent and detectable at these fine scales in deep-sea habitats.

4.2 Introduction

Aggregations of animals and single celled organisms have been recognised and studied for some time (Alee, 1927), in both mobile (e.g. Parrish and Edelstein-Keshet, 1999) and sessile species (e.g.

Condit et al., 2000). Aggregations may be driven by environmental heterogeneity (geological, physical and chemical) and biological factors (behaviour, dispersion method, reproduction), with different drivers affecting spatial patterns at different temporal and spatial scales (Levin, 1992). Through careful observation and quantification of faunal spatial patterns, insights can be obtained into the underlying ecological processes that influence the fine-scale dispersion of species. A range of first and second order statistical tests have been developed to assess spatial patterns as being clustered, randomly or over-dispersed distributions (Baddeley et al., 2015). These types of analyses using discrete point data have typically been applied to terrestrial systems, for example, to understand tree distributions in forests (Condit et al., 2000; Woodall and Graham 2004; Law et al., 2009), plant distribution in deserts (Eccles et al., 1999), deer distribution (Plante et al., 2004) and bird nest distributions (Melles et al., 2009; McDowall and Lynch, 2017). However, in the marine environment, quantifying spatial faunal patterns remains more challenging due to the technical difficulties of collecting precise positional data of biological observations.

Recently, point pattern analyses (PPA) have gained traction in the study of intertidal and subtidal marine habitats, in tandem with advancing technologies and survey capabilities. For example, the use of image mosaicing and 3D photogrammetry (Structure from Motion (SfM)) in shallow subtidal and intertidal waters has become more widespread, based on a range of camera platforms deployed by SCUBA diving (Burns et al., 2015), snorkelling (Leon et al., 2015; Pizzaro et al., 2017), ROVs (Remotely Operated Vehicles; Robert et al., 2017; Price et al., 2019; Lim et al., 2020), AUVs (Autonomous Underwater Vehicles; Friedman et al., 2012; Ling et al., 2016), UAVs (Unmanned Aerial Vehicles; Cassella et al., 2017; Murffit et al., 2017) and USVs (Unmanned Surface Vehicles; Raber and Schill, 2019). The use of image mosaicing and SfM has improved our ability to accurately register each organism's relative position. Using these imaging techniques, we can assess the habitat distribution with full coverage and carry out a census of all organisms present, which is required to undertake PPA. PPA, for example, has been used to quantify and characterise species-host relationships and clustering of host sponges and associated Goby species in shallow-water coral reefs (Lesneski et al., 2019). On an even finer scale, single images were used to identify clustering patterns of the acorn barnacle, *Semibalanus balanoides*, which was driven by life history and competition (Hooper and Eichhorn, 2015). Edwards et al. (2017) used image mosaics to identify various spatial patterns of scleractinian coral on a shallow-water coral reef, citing inter-specific reproduction methods that resulted in clustered patterns. In deep-sea environments, whilst aggregations of mobile benthic organisms (e.g. Morgan and Baco, 2019), and sessile organisms (e.g. Xavier et al., 2015) have been observed, quantified fine-scale knowledge derived from PPA is lacking, owing to the challenge and expense of collecting image mosaic datasets of high enough quality and resolution. However, more recent research projects using AUVs and ROVs have applied

image mosaicing techniques to assess species spatial patterns over hectares of hydrothermal vent, sponge reef and polymetallic nodule field habitats (Thornton et al., 2016; Meyer et al., 2019; Simon-Lledo et al., 2019). Each of those studies revealed species density changes and broad aggregation within the study sites which were attributed to local environmental factors such as mechanical disturbances, physical gradients and geological processes. Recently, the application of SfM has enabled the quantification of spatial patterns in deep-sea sponges, ophiuroids and gorgonians, utilising PPA (Prado et al., 2019, 2020; Mitchell and Harris et al., 2020).

Comparable studies of cold-water coral reef habitats focusing on aggregations and fine-scale spatial patterns are so far rare (e.g. Conti et al., 2019). Cold-water corals are ecosystem engineers and can form ecologically important biogenic reefs influencing local biodiversity (Jensen and Frederiksen, 1992; Mortensen et al., 1995; Costello et al., 2005; Henry and Roberts, 2007; Purser et al., 2013) by providing hard substrate and 3D structural complexity (Buhl-Mortensen et al., 2010; Price et al., 2019). Understanding ecological processes of cold-water coral reef habitats is important as they are classified as "Vulnerable Marine Ecosystems (VME)" (United Nations General Assembly Resolution 61/105; FAO, 2009), and are sensitive to anthropogenic impacts such as fishing (Wheeler et al., 2005a; Davies et al., 2007; Jackson et al., 2014; Huvenne et al., 2016) and ocean acidification (Turley et al., 2007; Hennige et al., 2014). Whilst broad-scale spatial ecological niche analyses have been used in species distribution modelling to interpolate and extrapolate observations over scales of metres to hundreds of kilometres (Davies et al., 2008; Dolan et al., 2008; Davies and Guinotte, 2012; Ross and Howell, 2013; De Clippele et al., 2017; Lo Iacono et al., 2018; Bargain et al., 2018; Barbosa et al., 2019, Pearman et al., 2020) linking the coral presence to their environment, finer scale full-coverage studies have seldom been undertaken on cold-water coral reef habitats. The scarcity of such fine-scale data is partly due to the high flow velocities, turbidity and complex terrain associated with cold-water coral reefs, which make it difficult for survey platforms such as ROVs and AUVs to navigate and collect suitable full-coverage imagery.

Nevertheless, photomosaics and 3D reconstructions have been used to visualise and characterise scleractinian cold-water coral habitats (Wheeler et al., 2005b, c; Vertino et al., 2010; Lessard-Pilson et al., 2010), derive their geomorphic properties (Robert et al., 2017; 2019; Price et al., 2019), detect size (Fabri et al., 2019) and create substrate/coral cover maps (Lim et al., 2017; Conti et al., 2019; Lim et al., 2020). However, so far these datasets have not been analysed with PPA, and thus relatively little is known about fine scale spatial organization of reef building coral and reef inhabitants. PPA and 1-D second order clustering statistics of azooxanthellate corals have been undertaken, detecting clustered patterns of soft corals and the scleractinian reef builder *Madrepora oculata* (Orejas et al., 2009; Gori et al., 2011a; Prado et al., 2019) over of tens of metres. However, these studies lacked quantitative sub-metric information of their local spatial

environment and thus the reasons for the observed clustering, such as substrate availability, hydrodynamics and food availability could only be inferred. Furthermore, it is unknown how the two main cold-water coral reef building species (*Desmophyllum pertusum*, synonym: *Lophelia pertusa* (Addamo et al., 2016) and *M. oculata*) in the NE Atlantic are organised on a fine scale. Whilst their broad scale distributions differ slightly, their ecological niches overlap in the NE Atlantic region and they are often found developing reefs together and occasionally demonstrating the ability to form "false chimaeras" and "twin colonies" (Aunaud-Haond et al., 2017; Corbera et al., 2019). However, it is unknown how the two species are distributed within a reef biogenic structure. Overall, little is known about how and if organisms found in association with reefs cluster within, towards or away from reef structures.

We addressed these knowledge gaps by applying SfM methods to create high-resolution 3D reconstructions and orthomosaics of a cold-water coral reef, in order to apply landscape ecological descriptors and statistics, based on PPA. We aimed to identify whether organisms within cold-water coral framework habitat demonstrate a random distribution, or if local scale habitat variation and biological clustering drives aggregation patterns. The Piddington Mound (NE Atlantic) was chosen for this study and the mound is dynamic having shown signs of change in terms of coral cover over the space of four years (Lim et al., 2018a; Boolukos et al., 2019). This reinforces the urgency to fully understand these habitats so that we can better discern and quantify human-related degradation, due to the habitats' vulnerability to anthropogenic impacts, distinctly from natural variation. We tested four complementary hypotheses 1) higher densities of associated species are found within the reef substrate area compared to the surrounding habitat; 2) *L. pertusa* and *M. oculata* occupy different parts of the reef; 3) organisms biologically cluster within habitats, in addition to environmentally driven clustering; 4) organisms occupying the coral framework specifically cluster in the more structurally complex areas of the reef.

4.3 Methods

4.3.1 Location

The Piddington Mound is a small cold-water coral mound (60 x 40 m laterally, 12 m in height) found in the Belgica Mound Province (BMP) in the Porcupine Seabight, NE Atlantic (Figure 4.1). The region contains many mound structures and reefs formed by *L. pertusa* and *M. oculata* (De Mol et al., 2002, Wheeler et al., 2007), including numerous mini-mounds, known as the Moira Mounds (Foubert et al., 2011, Wheeler et al., 2005b; 2011a). The mini-mounds range in height from 3 - 15 m and local currents are estimated to reach between 34 - 40 cm s^{-1} (Dorschel et al., 2007; Lim et al., 2018b), with a north-south, semi-diurnal tidal current pattern. The Piddington Mound was chosen

for this study as it (and the local area) has been extensively studied, mapped and monitored at scales from metres to centimetres (Lim et al., 2017; 2018a; 2018b; Conti et al., 2019). This work was undertaken as part of the VENTuRE survey in 2011 (Wheeler et al., 2011b), and the mound was photomosaiced using a Scale Invariant Feature Transformation algorithm (SIFT), to create a high-resolution habitat map classified into the categories "hemipelagic sediment", "hemipelagic sediment with dropstones", "live coral framework", "dead coral framework" and "coral rubble" (Lim et al., 2017).

4.3.2 Video survey

The data were acquired during the QuERCi cruise (Wheeler et al., 2015), undertaken in 2015 on *RV Celtic Explorer* with the *Holland 1* ROV. A 36-hour ROV dive was undertaken in order to collect HD video over the same area presented in Lim et al. (2017) in a lawn-mower pattern. The ROV was equipped with a vertical-downward facing HD camera (Kongsberg Maritime OE14-502a HDTV inspection camera recording at 1080 p) mounted to the front of the ROV frame. The ROV was also fitted with 8 x variable intensity 250 watt halogens, 2 x 400 watt DSPL CARC2 HMI and 2 x 25,000 Lumen APHOS LED lights (Cathx Ocean) to illuminate the seafloor and 2 red lasers spaced 10 cm apart to provide scale marks in the imagery. The ROV was manoeuvred at a low altitude using a Tritech altimeter to maintain the ROV approximately 2 m above the seafloor and ensure organisms were observed from a constant distance to make sure that species observed were of a consistent minimum resolvable size throughout the survey. The survey lines were oriented north to south where the ROV camera position would be spaced ~40 cm apart to collect >60% image overlap required for Structure from Motion processing. Currents and turbidity reduced our ability to image the entire mound and instead three areas were mapped. Site A was located on the NE part of the mound and spanned coral reef and sandy habitats (Figure 4.1D). Site B was located on the north of the mound and spanned the flank from the base to the top (Figure 4.1D). Site C was SE of the mound and consisted predominantly of sand with some coral rubble found at the base of the mound (Figure 4.1D).

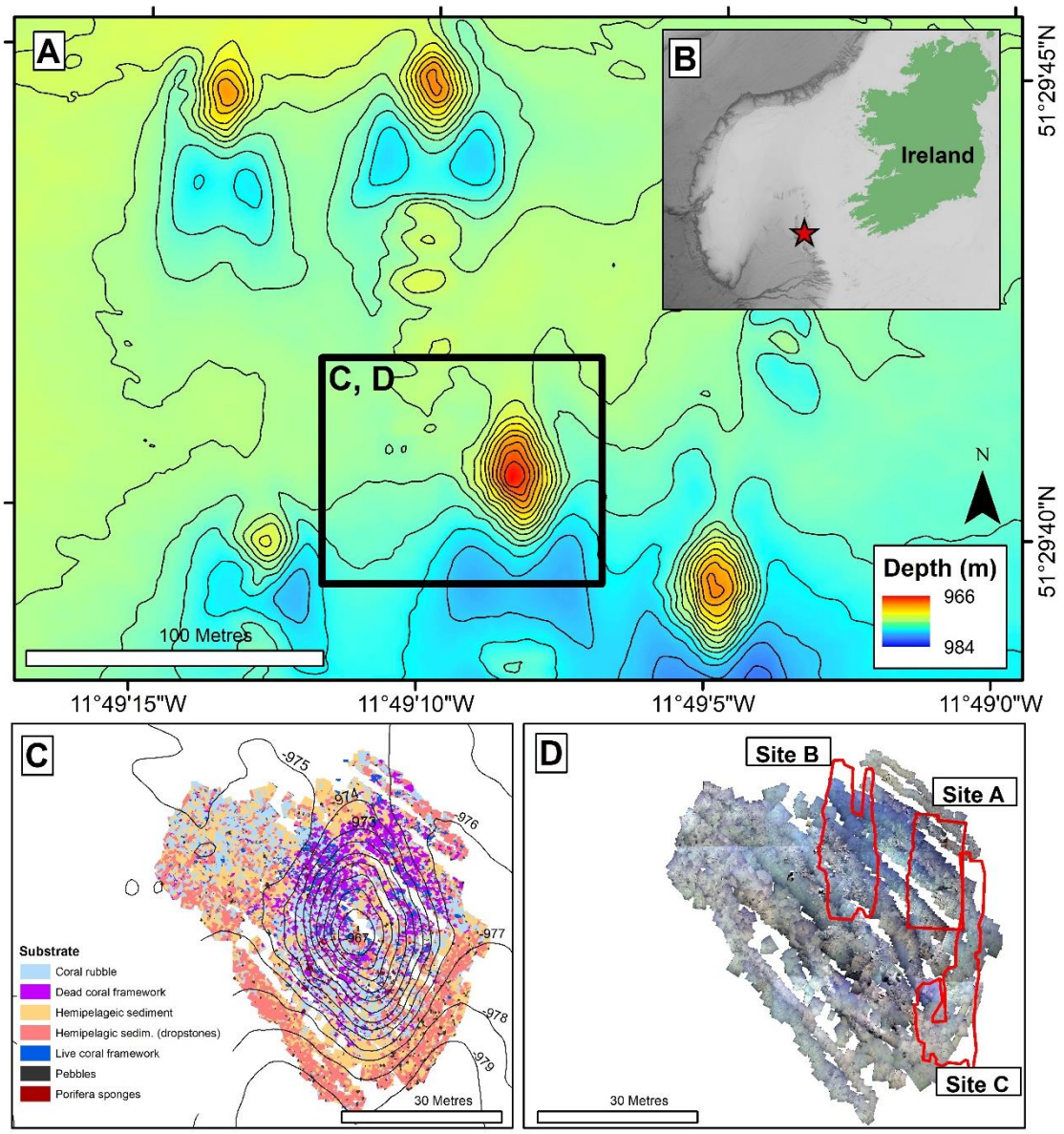

Figure 4.1 Location map: A) Bathymetry (contour interval 1 m) of Moira Mound region showing Piddington Mound (within black square). B) Location of Moira Mound region; C) Substrate map, contour interval: 1 m (data from Conti et al., 2019); D) Photomosaic of Piddington Mound (data from Lim et al., 2017), with Site A, B and C showing the area of interests for the current study.

Structure from Motion

One image per second was extracted from the video using the 3D computer graphics software Blender (V2.78) to create a ~2 megapixel image sequence. Images were enhanced in Photoshop CS6, by de-interlacing and raising the shadow values to increase exposure in the shaded areas on the periphery of the lighting and camera field of view, improving the 2D mosaic visuals. Agisoft Metashape (version 1.5.2; previously known as Photoscan) was chosen to create 3D models of the reef as it has been used in several marine habitat studies (Burns et al., 2015; Leon et al., 2015; Bennecke et al., 2016; Robert et al., 2017, 2019; Young et al., 2017; Bayley et al., 2019; Price et al.,

2019; Lim et al., 2020), proving to be reliable and accurate software (Burns and Departe, 2017). High image alignment accuracy was chosen to utilise the full resolution image. Where alignment produced artefacts between the different survey lines, alignment was reset and images added sequentially, i.e. line by line. Once aligned, dense point clouds were created, using low quality settings, as well as digital elevation models (DEM) and orthomosaics. The low quality setting was deemed sufficient as a DEM of 6 - 7 mm per pixel was produced. A minimum of 25 scaling points were distributed across each of the models based upon the laser scales (10 cm). Additionally, several georeferencing points were added by feature matching with the mosaic created by Lim et al. (2017) and a high resolution multibeam echosounder dataset (Lim et al., 2018b). This method was chosen as the navigation for this dive proved unreliable and accumulation of positioning errors tended to occur along each line as observed by Price et al. (2019). The models were then optimised, and the dense clouds recreated. Finally, the orthomosaics and DEMs were exported as geotiffs (Table 4.1). An outer boundary was used to create a window for each site within which all further analysis would be undertaken by excluding dark edges of the mosaics and areas where transect lines did not link well enough. The DEMs and orthomosaics were generated at the highest resolution (pixel size: 6 - 9 mm; Table 4.1).

Table 4.1. Meta-data of the 3D reconstructions

Site	Number of images	Total area (m^2)	Georeferencing error (m)	Scale error (mm)	DEM resolution (mm/pix)	Orthomosaic resolution (mm/pix)
Site A	4497	205.622	1.212	8.528	6.36	0.795
Site B	6491	242.676	1.648	10.824	6.51	0.814
Site C	5827	253.041	0.997	13.642	6.29	0.787

4.3.3 Substrate

The orthomosaics and DEMs were projected to UTM 29N, Datum WGS84, and derived terrain variables (Vector Ruggedness Measure (VRM), slope and aspect) were generated in ArcMap 10.4.1. Using the Estimation Scale Parameter (ESP) tool in the eCognition software (Dragut et al., 2010), a scale parameter of 300 was identified as the optimum scale value for segmentation. The data were segmented using a multi-resolution segmentation algorithm which merges pixels into “objects”.

These objects are created through merging of neighbouring pixels with similar spectral properties in each of the input data layers until a homogeneity threshold, or the value of the scale parameter, is reached.

To classify the objects within the segmented map, two classifiers were chosen: reef (substantial skeleton cover) and non-reef, rather than the detailed facies classified by Lim et al. (2017) and Conti et al. (2019). The reef class was not split into further classes such as reef rubble and 3D framework (as per Lim et al. 2017) due to the subjectivity of this classification. Instead these gradations were later visualised by the continuous rugosity measure of the VRM with a neighbourhood of ~10 cm, of the coral framework. Also, no differentiation between live or dead coral was made for the classification as live coral was manually delineated for subsequent PPA. The segmentation layer was inspected and 150 training samples, visually identified, were chosen for each class in each site, spread equally across the segmented area, similar to Conti et al. (2019). Shape (border index, area and roundness) and pixel (mean, maximum difference and standard deviation of pixel values within the objects) values for each of the layers (Red, Green, Blue, DEM, VRM, slope and aspect) within individual objects were calculated. The eCognition Nearest Neighbour classification tool was applied, which classified all objects based on their closeness to the training samples from the values defined in the Nearest Neighbour feature space. The classified objects were exported as a single substrate shapefile. Using the outputs from the substrate map in polygon format, reef and non-reef areas were isolated and frequency histograms were generated to demonstrate the different rugosity values in the form of VRM.

4.3.4 Annotation

Organisms (Table 4.2) were geotagged in Agisoft Metashape using the orthomosaic unless obscured (stitch distortion, blur or high ROV altitude), in which case the original images were used to identify the specific location of the organism. The selection of organisms analysed in this study were chosen based on their abundance to ensure a statistical robustness and on the annotators' capability to consistently identify them (Table 4.2). Some species were either too small and/or featureless (*Hexanacalida* sp.), too mobile (fishes) or rare to consider for spatial pattern analysis (e.g. *Porania cf. pulvillus*, *Ceramaster* sp., *Phelliactis* sp.). The minimum resolvable organism size was 20 mm. The point of substrate attachment was chosen to geotag elongate organisms such as *Stichopathes* sp., *Callogorgia* sp., Alcyonacea spp. and *Aphrocallistes* sp. with an elongate morphology. *Live L. pertusa* and *M. oculata* were identified by observing extruded polyps or if the tissue was orange or white; a polygon was drawn around the colony and the centre of the colony tagged to utilise as point data (Edwards et al., 2017). Creating a point pattern from these polygons was valid as all living coral patches were small and collectively cover less than 5% of Piddington Mound (Boolukos et al., 2019;

Conti et al., 2019). Finally, *Acanthogorgia* sp. and Plexauridae sp. were concatenated to Alcyonacea spp., as the image quality and angle was not conducive to a consistent identification between the two species.

Table 4.2. Organism densities and counts

	Individuals per m^2 (count) at Site A	Individuals per m^2 (count) at Site B	Individuals per m^2 (count) at Site C
Alcyonacea spp.	0.31 (64)	0.21 (52)	0.06 (14)
Anthomastus sp.	0.15 (31)	0.06 (15)	0.04 (11)
Aphrocallistes sp.	4.36 (896)	6.15 (1493)	0.38 (96)
Callogorgia sp.	0.11 (22)	0.09 (22)	0.00 (1)
Cidaris cidaris	0.20 (41)	0.23 (56)	0.10 (26)
Galatheoidae sp.	0.48 (99)	0.40 (98)	0 (0)
Gracilechinus sp. “green”	0.1 (21)	0.09 (22)	0.10 (26)
Gracilechinus sp. “pink”	0.13 (26)	0.11 (27)	0.01 (3)
Lophelia pertusa	1.37 (282)	1.46 (355)	0.06 (15)
Madrepora oculata	0.38 (78)	0.75 (181)	0.07 (17)
Psolus sp.	0.06 (13)	0.01 (2)	0.98 (249)
Stichopathes sp.	0.03 (6)	0.29 (70)	0 (0)
Zoanthidae sp.	0.22 (46)	0.27 (65)	0.02 (5)

4.3.5 Statistics

Three methods were used to describe and quantify the spatial point patterns of each species, using the spatstat package (Baddeley et al, 2015) in R-3.3.2. First, we created density plots of the organisms using a fixed-bandwidth kernel estimate of the intensity function. A sigma value of 1 m was used to create the kernel density plots. The density plots were visually assessed for affinity to regions with plentiful coral cover. Secondly, an inhomogeneous pair correlation function (PCF; Illian

et al., 2008; Law et al., 2009) was utilised as a multiscale descriptor of the point pattern. The PCF ($g(r)$) is the first derivative of Ripley's K function (Ripley et al., 1977), a descriptor used to quantify the number of points expected within distance r divided by intensity λ (equation 1). PCF ($g(r)$) reduces cumulative effects of an expanding radius, by utilising a 2-D torus shape to define a point registration field. This analysis describes the density of the species at increasing distance (r) from a representative focal point, thus providing visualisation of any clustering of the animals.

Equation 1

$$K(r) = \frac{1}{\lambda} E$$

Where $K(r)$ describes the point pattern characteristics across the scales. λ is "intensity" (number of events per unit area). E is the number of individuals within the distance r, of a randomly chosen event. $g(r)$ is calculated using equation 2.

Equation 2

$$g(r) = \frac{K'(r)}{2\pi r}$$

Where $K'(r)$ is the derivative of $k(r)$ in relation to r. The PCFs were compared to null models representing inhomogeneous point processes. An inhomogeneous PCF approach was undertaken as Pearson's X^2 goodness-of-fit and visualisation of the intensity revealed broad-scale gradients of organism distribution, likely derived from the heterogeneity of a cold-water coral reef habitat. An inhomogeneous PCF utilises the kernel bandwidth intensity to offset organism clusters that may be influenced by broader environmental drivers. A sigma value of 1 was used which was assessed visually as we have no prior knowledge of suitable values; subsequent analyses confirmed that this scale was sufficient for capturing pattern features. The point patterns were compared with 999 Monte Carlo simulations of an inhomogeneous pattern, with envelopes constructed to illustrated the 25th largest and smallest rank, thereby encompassing 95% of null model simulations ($\alpha = 0.05$). Any deviations above the envelopes would demonstrate clustering/aggregation of the species. Deviations below the critical band would infer that the species are over-dispersed, indicating their distribution is more dispersed than expected. As the point pattern process is generated within a defined region of interest, an edge correction is required to avoid biases in the PCF outputs. The command "best" implemented by spatstat was used to test each method (such as Ripley's isotrophic edge correction and translation) to identify the most statistically robust correction

(Baddeley et al., 2015). The PCF was undertaken for species of which more than 70 individuals were counted within a study site.

Point Pattern Modelling (PPM), was deployed to quantify clustering derived from underlying environmental parameters and biological mechanisms, following the outline provided by Edwards et al. (2017). We compared four species distribution patterns: 1) complete spatial randomness (CSR), 2) organism distribution and clustering driven by habitat availability and suitability creating an inhomogeneous pattern (IP), 3) biologically driven clustering influenced by biotic processes that limit or steer dispersion, e.g. fragmentation, leading to a homogeneous clustered pattern (CP) and 4) a combination of clustering driven by biological and environmental factors leading to an inhomogeneous clustered pattern (ICP). The four species patterns considered (CSR, IP, CP and ICP) directly test our hypotheses 3 and 4 by associating species point pattern with biotic and abiotic distribution drivers. PPMs are analogous to generalised linear models (GLM), and input variables (environmental drivers and clustering) can be used to improve the model where suitable. Environmental drivers were derived from the entire DEM and classification outputs. Vector ruggedness measure (VRM), a known influencer of cold-water coral reef communities (Price et al., 2019), was calculated at two scales 1) 7 mm pixel with a 15 pixel neighbourhood size and 2) 50 cm pixel with a 3 pixel neighbourhood size, in order to account for any differences related to the scale of rugosity (Richardson et al., 2017). Substrate classification was used as another layer to identify if organisms clustered towards reef substrate. Depth was used to identify if the vertical position on the mound had an influence on point patterns. Northness and eastness was calculated at 50 cm pixel as a measure of aspect because exposure to a particular current direction can influence organism distribution, especially for groups such as suspension feeders that may rely on currents to provide food and refresh intermediate water layers. The variables used depended on the number of organisms available to model. When less than 50 individuals were available, a simpler PPM including VRM (7 mm and 50 cm), depth and substrate was used to avoid inundating the model with too many variables. When more than 50 individuals were counted for a specific species at a specific study site, all variables were utilised in the model. For *L. pertusa* and *M. oculata* point patterns, the VRM at 7mm pixel with 15 pixel neighbourhood which was used to represent fine-scale rugosity, was not considered, as the rugosity was formed by the living coral themselves. The VRM calculated at 50 cm pixel was retained to account for the possibility that wider-scale underlying rugosity is likely to influence habitat suitability for live patches of reef-building coral, by baffling current velocity (Mienis et al., 2019), a known influencer of feeding efficiency and polyp behaviour (Orejas et al., 2016). The model input variables considered are summarised in Table 4.3. The models were then treated with a stepwise, drop one procedure (i.e. backward elimination) to

identify the model with the lowest Akaike information criterion (AIC) value, which was used to represent an inhomogeneous pattern driven by environmental variables.

Table 4.3. The variables considered in the PPM procedures. *except for the reef building species *Lophelia pertusa* and *Madrepora oculata*.

Variable	< 50 individuals	> 50 individuals
Substrate	✓	✓
Depth	✓	✓
VRM (7mm)	✓*	✓*
VRM (50 cm)	✓	✓
Eastness		✓
Northness		✓
Geyers point process		✓

Benthic organism patterns can be driven by biological factors such as reproductive methods (Edwards et al., 2017) and competition (Hooper and Eichhorn, 2016). To infer biologically induced clustering, interaction terms between points (i.e. the location of an individual organism) were specified in the form of Geyer's saturation process (Geyer, 1999), a modification of the Strauss process. The inclusion of a Geyer's saturation process in the PPM was undertaken on species that were represented by more than 50 individuals, as fewer data inputs led to unclear results. This technique uses the relevant point pattern to create a density field around a given point, to a maximum defined distance. Parameters distance (r) and saturation need to be specified before use in the PPM. To detect the most appropriate suitable parameters, a maximum pseudolikelihood estimator approach in an incremental, standardised procedure was undertaken. An r of 0.1 – 1 m with increments of 0.1 m, and saturation of 0.001 (equivalent of CSR) and 1 to 10 in increments of 1 were tested in all combinations. The most suitable parameters were used, based on the lowest AIC value and implemented in the PPMs that specify biological clustering (CP) and biological and environmentally driven clustering (ICP). The ICP model included the Geyers clustering and all environmental variables outlined, with a stepwise drop one procedure (i.e. backward elimination) used to find the most parsimonious model.

Finally, the best of the four models (CSR, IP, CP, ICP) determined by AIC value, was endorsed by a likelihood ratio test for the null hypothesis (CSR) against the chosen model, unless the CSR model was considered the best. The outputs provide evidence for if organism distribution is influenced by

the presence of reef substrate (Hypothesis 1), if variation within the reef habitat drives some clustering and whether there is evidence of biological clustering (Hypothesises 3 and 4).

To further inspect how variation in the structural complexity of the reef influenced organismal distribution within this coral substrate, a non-parametric curve was fitted ("rhohat"). The non-parametric estimator computes a non-parametric smoother estimate of function (ρ) which identifies how the intensity of points depends on a covariate (equation 3)

Equation 3

$$\lambda(u) = \rho(Z(u))$$

Where $\lambda(u)$ is the intensity at location u and $Z(u))$ the spatial covariate at location u. *Aphrocallistes* sp. was chosen as a model species due to its frequent occurrence on framework and its association with variation in structural complexity was tested at a VRM scale across 10.5 cm (7mm pixel with 15 pixel neighbourhood; similar to Price et al., 2019). The dependence of ρ on VRM was statistically tested using the Berman's Z1 test.

4.4 Results

The reconstructions of the seafloor were made and exported at their finest resolution (Table 4.1). Site A contained >60% coral reef substrate cover (Figure 4.2 A, B) with non-reef substrate (sand and occasional dropstones) covering the eastern-most part of the mosaic. Coral reef cover was extensive towards the shallower part of the mound with patches more isolated at the outer boundary of the mound (Figure 4.2 C). At Site B, coral reef covered more than 65% of the mapped area, mostly towards the top of the mound at the south with some non-reef sandy patches towards the north (Figure 4.3). Site C was located on the south-eastern flank of the mound and had only 14% coral reef cover with the rest consisting of non-reef substrate made up of sand and dropstones (Figure 4.4). Most VRM values of coral reef substrate typically spanned from 0 to 0.6 at Sites A and B, 0-0.4 at Site C. Overall, coral reef substrate had a greater mean VRM value at Site A and B compared site C (Figure 4.5). The highest observed VRM values were 0.8, 0.87 and 0.76 for A, B and C respectively, for the coral reef substrate. Non-reef substrate was represented with over 80%, over 70% and over 80% of the pixels between 0 and 0.05 VRM, the lowest bin, at sites A, B and C respectively (Figure 4.5). The majority of VRM values for non-reef substrate were below 0.1.

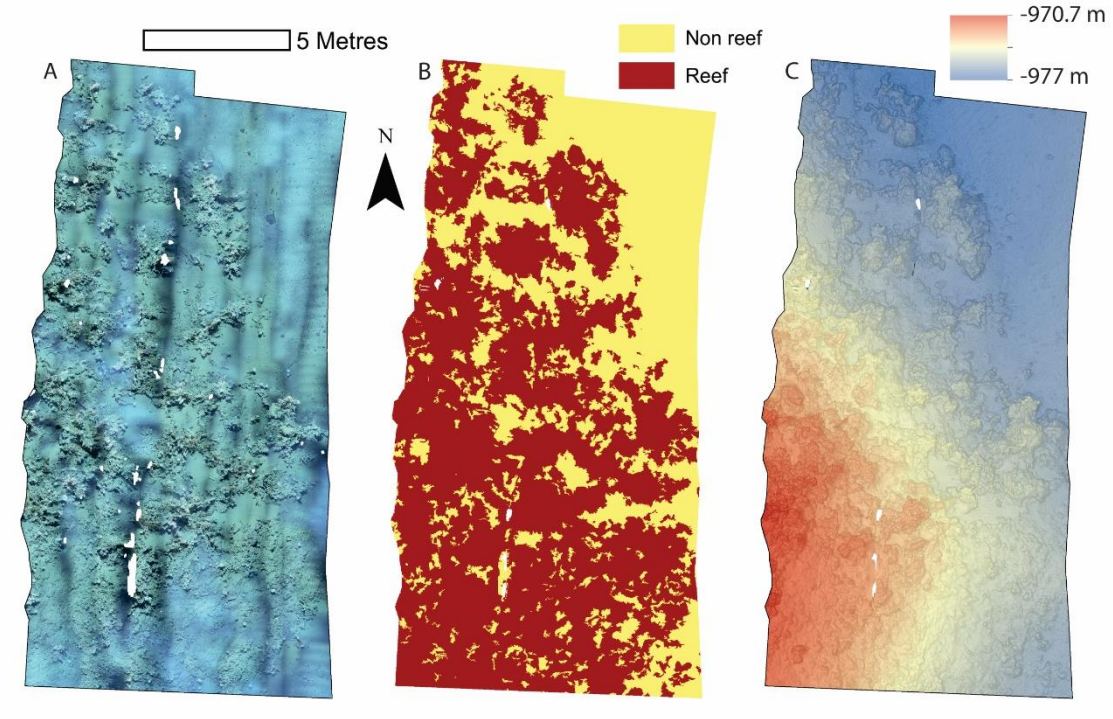

Figure 4.2. Mosaics of Site A. A) Orthorectified photomosaic; B) Classified substrate map; C) Digital Elevation Model.

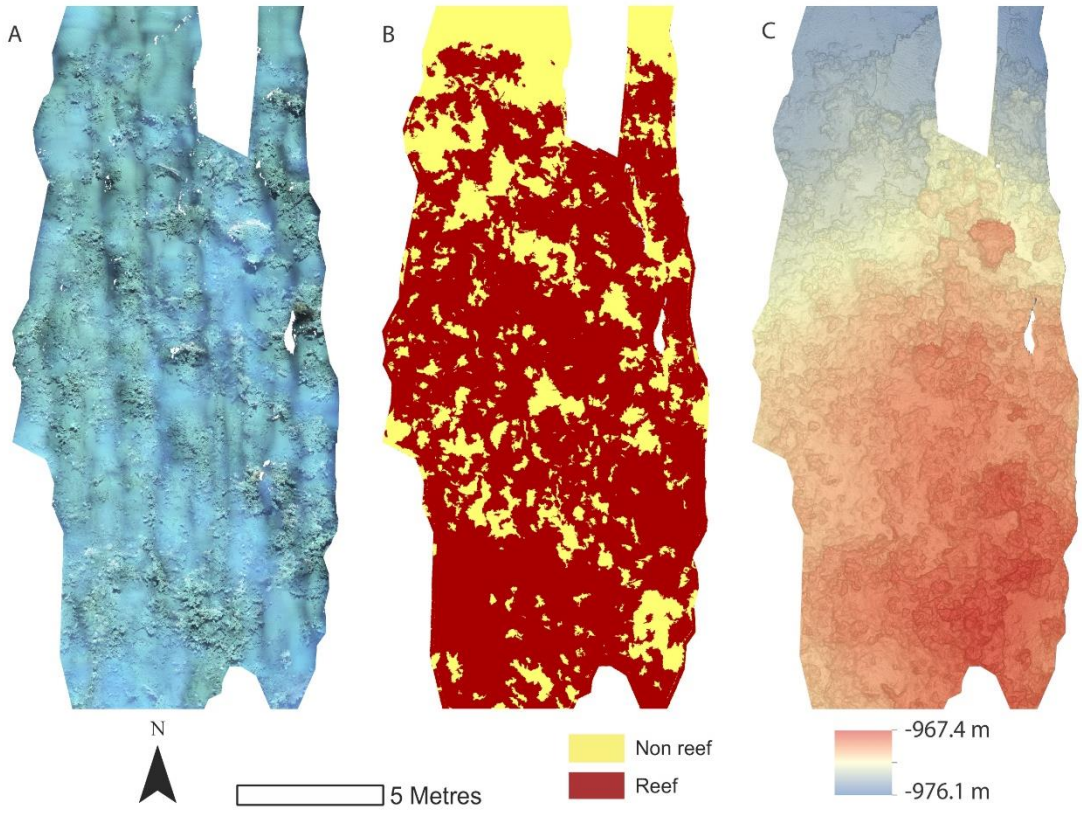

Figure 4.3. Mosaics of Site B. A) Orthorectified photomosaic; B) Classified substrate map; C) Digital Elevation Model.

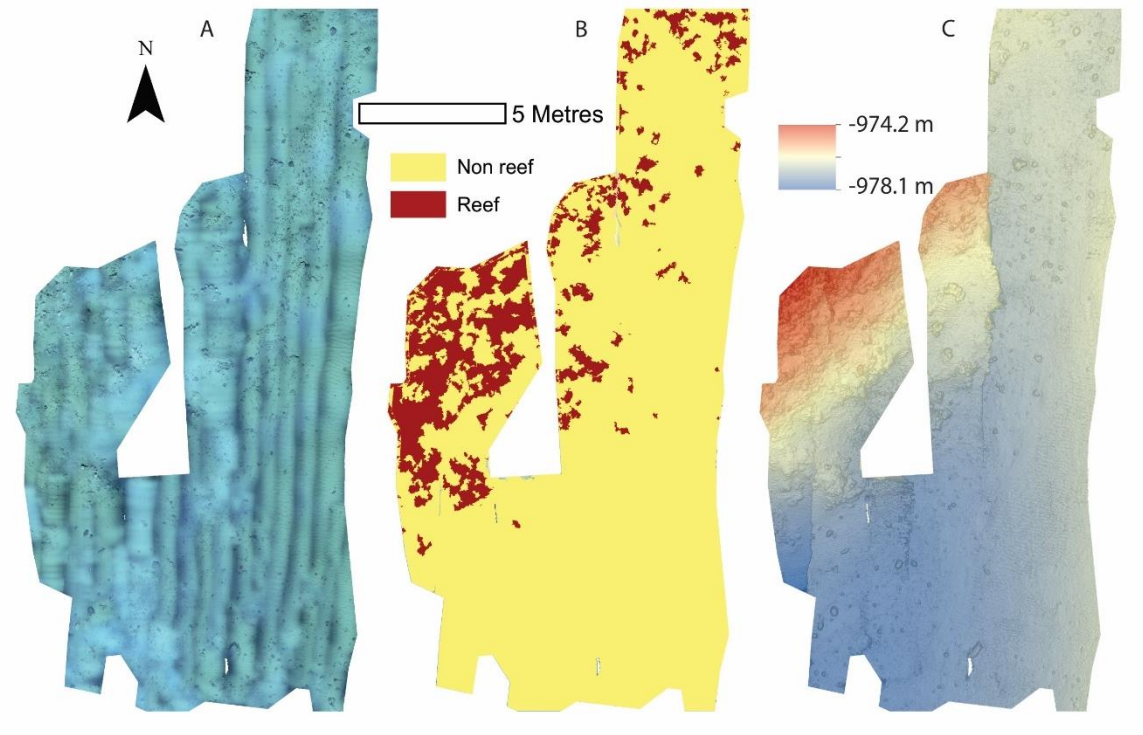

Figure 4.4. Mosaics of Site C. A) Orthorectified photomosaic; B) Classified substrate map; C) Digital Elevation Model.

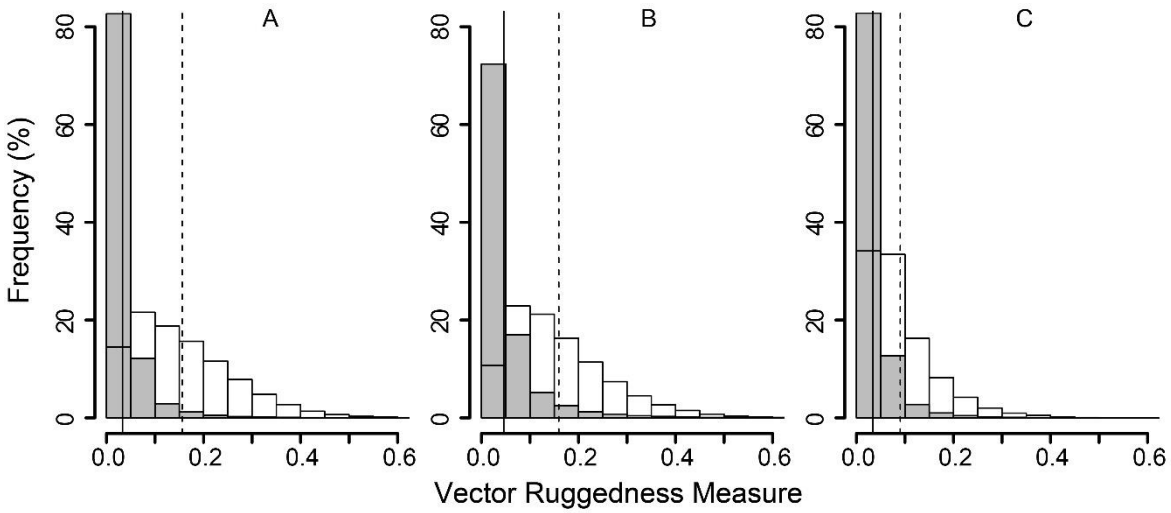

Figure 4.5. Histogram of all Vector Ruggedness Measure (VRM) values of all pixels in the non-reef class (grey) and reef class (clear) at sites A (A), B (B) and C (C). Vertical lines indicate mean VRM values for non-reef (dashed) and reef substrate (solid).

A total of 4,546 individuals from 13 taxa were counted and geotagged over the three mosaiced sites (Table 4.2; Figure 4.6). Different densities of organisms were observed between the mosaics (Table 4.2). Site C typically contained the lowest density of species, except for *Psolus* sp.. Site B contained nearly twice the density of *M. oculata*, and 9.7 times the density of *Stichopathes* sp. compared to Site A (Table 4.2).

A visual inspection of the density plots indicated that most organisms showed an affinity towards the reef part of the mosaiced areas, except for *Psolus* sp., which were generally low in density at site A and B (Appendix 4.2, 4.3). The highest densities of living patches of *L. pertusa* and *M. oculata* were located on towards the west side of the reef substrate at Site A, towards the summit of the mound. *Aphrocallistes* sp. and Alcyonacea spp. at Site A were higher in areas of coral cover towards the west side of the site where coral reef substrate was observed (Figure 4.7). Notably, typical reef associated species such as *Aphrocallistes* sp. were indeed more common at the centre of the reef, which was where the more structurally complex reef substrate (indicated by high VRM) was located. The south part of the reef which had low VRM, indicative of coral rubble due to the lack of structural complexity, harboured a low density of most species (Figure 4.7). *M. oculata* and *L. pertusa* appeared to have a slightly different distribution to each other with live *M. oculata* more densely aggregated towards the outskirts of the reef showing only minor overlap with *L. pertusa* (Figure 4.7 B,C). Hotspots of Alcyonacea spp. and *Stichopathes* sp. were evident at Site B (Figure 4.8 E,F). *Aphrocallistes* sp. appear more spread out at site B, though a distinct dense patch is evident at the south part of the site (Figure 4.8). Like Site A, *M. oculata* and *L. pertusa* density hotspots were generally located in different places. It appears that *L. pertusa* tends to cluster towards the top of the mound whereas *M. oculata* clusters towards the base. *Psolus* sp. and *Aphrocallistes* sp. showed distinct density hotspots at Site C with *Aphrocallistes* sp. showing an affinity for coral covered areas towards the base of the mound (Figure 4.9).

The inhomogeneous PCF plots revealed *L. pertusa* clustered between ~0.1 m to 0.6 m at both sites A and B (Figure 4.10 A, B). *M. oculata* displayed clustered patterns up to ~0.5 and 0.6 m at Sites A and B respectively (Figure 4.10 C, D), *Aphrocallistes* sp. consistently clustered at sites A and B up to approximately 0.7 m whilst clustering was restrained to approximately 0.4 m at Site C (Figure 4.10 E, F). There was evidence that *Stichopathes* sp. clustered at site B at ~0.1 to 0.4 m (Figure 4.10 G, H) where it was 9.7 times more abundant than site A (Table 4.2, Figure 4.10). *Psolus* sp. strongly clustered up to ~0.25 m with a second clustering r of ~0.4 – 0.7 m at site C where it was the most abundant (Table 4.2, Figure 4.10 G).

Minor reconstruction errors on the Z axis observed at Site C (Figure 4.4), where images did not stitch correctly, were amplified when calculating environmental drivers from the DEM. Thus for site C, only substrate and VRM at 7mm pixel were considered. VRM was included as the vertical errors remained very localised and had little effect on the outputs. A total of 94 PPMs were created to represent the distribution patterns (CSR, IP, CP, ICP) of each species when possible (for < 50 individuals, only CSR and ICP were considered; Table 4.3), with the lowest AIC scoring model displayed in Figure 4.11. An example of a single theoretical simulation of *Aphrocallistes* sp. point pattern is depicted in Figure 4.11. Generally, most species distributions were driven by environmental factors independently (IP) with indication of additional biological clustering for some organisms (ICP) (Figure 4.11). *Anthomastus* sp. was the only organism to consistently show a CSR distribution with no models indicating an influence of environmental factors driving their distribution. No groups showed any evidence of only biological clustering (CP) influencing the organism's distribution and aggregation patterns (Figure 4.11). Substrate (reef or non-reef) was consistently included as a variable in the most parsimonious environmental models (Figure 4.11), providing statistical support for the visual observations from the density plots that many species were attracted to reef substrate. Secondly, VRM was considered a significant predictor variable in the most parsimonious distribution models for most organisms. The other environmental factors depth, northness and eastness were also considered significant predictors, however their influence was inconsistent. The inclusion of Geyer's interactions supported the influence of biological clustering in the ICP models for *M. oculata*, *L. pertusa*, *Aphrocallistes* sp., Alcyonacea spp., *Stichopathes* sp., Zoanthidae sp., Galatheoidae sp. and *C. cidaris*. Geyer's interaction parameters specified by the maximum pseudolikelihood indicated most clustering observed was within 1 m. The strongest clustering was observed in *Aphrocallistes* sp., whereby the saturation of clustering was specified at 7 and 6 for sites A and B. Further clustering parameters utilised in the Geyers cluster process are outlined in Figure 4.11.

The coral reef substrate with low VRM values appeared unsuitable for *Aphrocallistes* sp., a species frequently found within the coral reef substrate. *Aphrocallistes* sp. was positively influenced by VRM, peaking at around 0.3 and beyond, which is in the upper regions of VRM values for coral substrate (Figures 4.12), which was statistically supported by a Berman's Z1 test (Z1 = 10.3; p-value < 0.001). At site B, a similar pattern was observed with the highest density of *Aphrocallistes* sp. occurring between 0.2 and 0.4 VRM which is near the upper end of reef substrate complexity (Figure 4.12; Bermans Z1 test; Z1 = 6.5, p-value < 0.001).

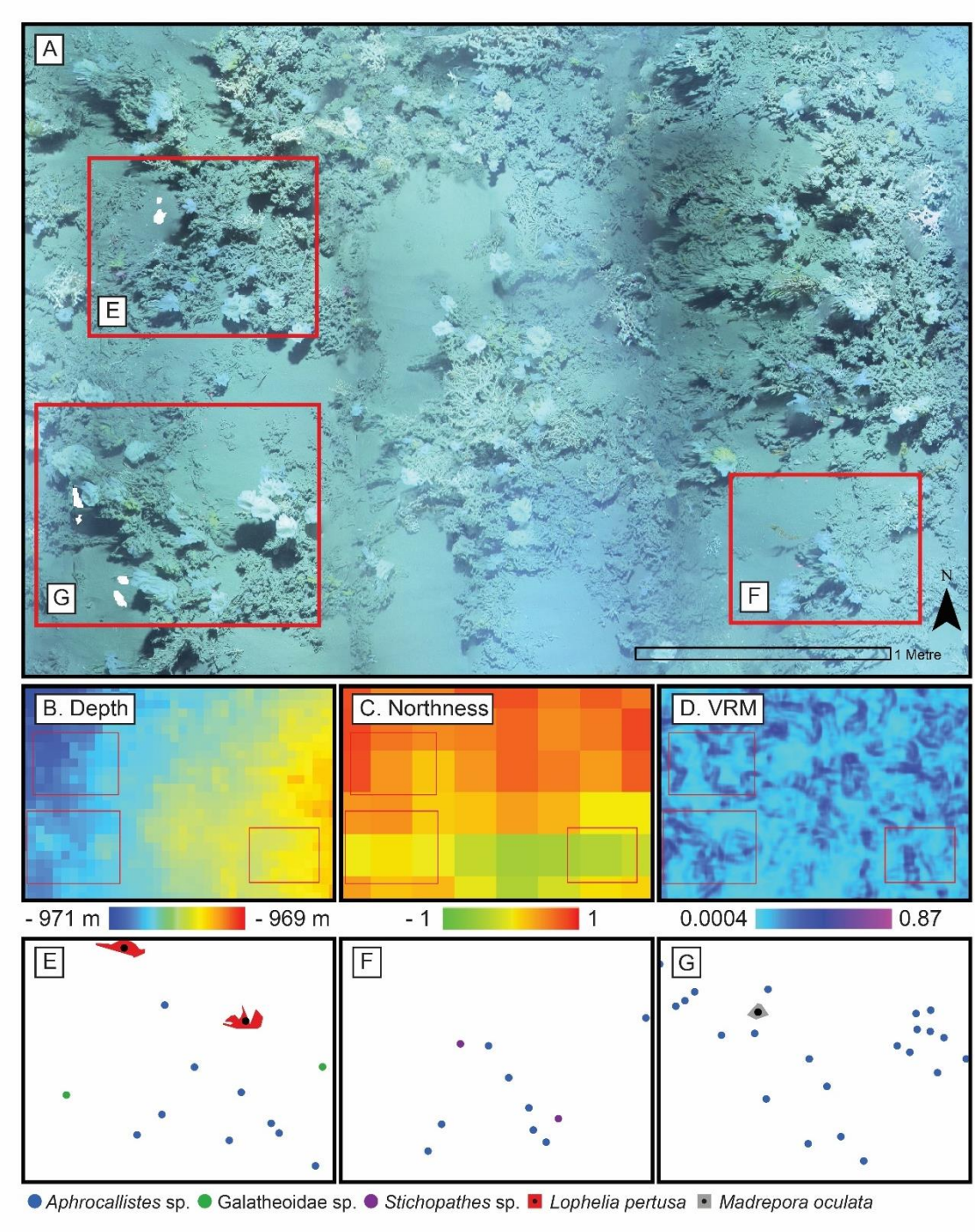

Figure 4.6 Close up of the photomosaic at Site B. Environmental drivers derived from the Digital Elevation Model (DEM) of the same area: B) depth, C) northness and D) Vector Ruggedness Measure (VRM) at 7mm pixel with 15 pixel neighbourhood. Corresponding point patterns of species generated by geotagging each relevant individual is depicted in E, F, G with their respective inset marked in red in panel A.

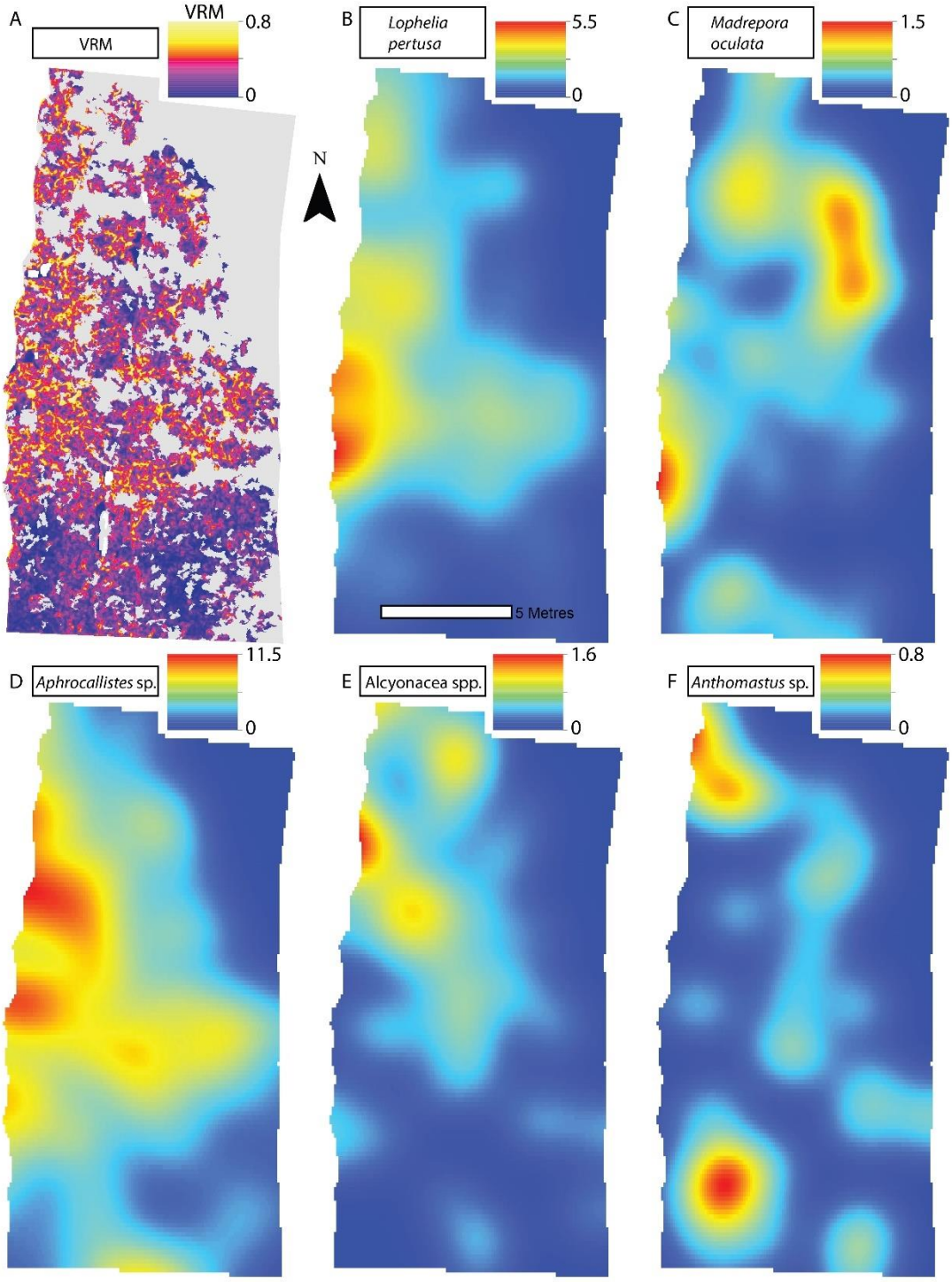

Figure 4.7 Site A Vector Ruggedness Measure (VRM) and density plots. A) Vector Ruggedness Measure values for reef facies at Site A. Density plots in the form of kernel estimate of intensity (number of individuals per m^2 and sigma = 1) B) *Lophelia pertusa* C) *Madrepora oculata* D) *Aphrocallistes* sp. E) Alcyonacea spp. and F) *Anthomastus* sp. for Site A. Note varying colour scale between the different plots.

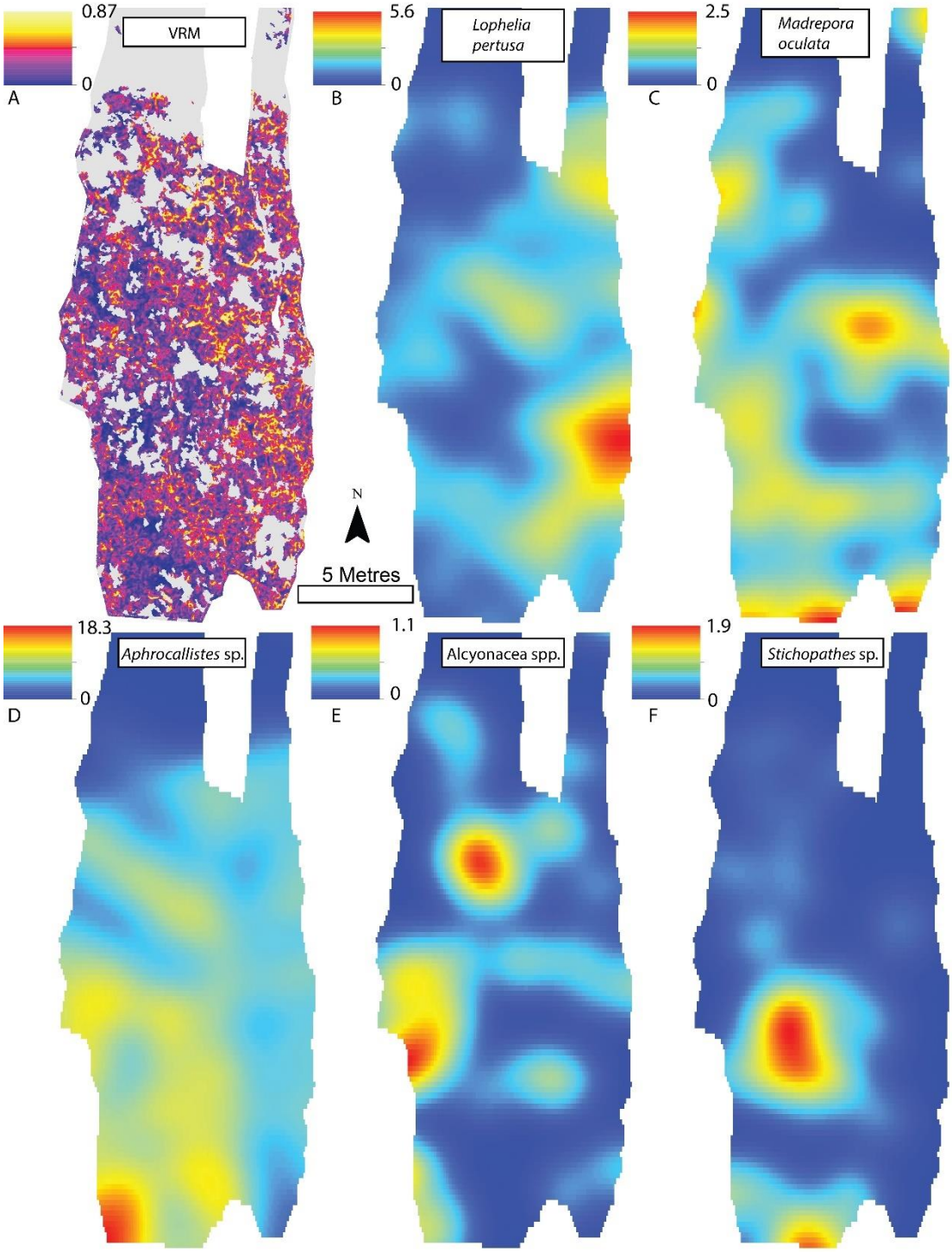

Figure 4.8. Site B Vector Ruggedness Measure (VRM) and density plots. A) Vector Ruggedness Measure values for reef facies. Density plots in the form of kernel estimate of intensity (number of individuals per m^2 and sigma = 1) B) *Lophelia pertusa* C) *Madrepora oculata* D) *Aphrocallistes* sp. E) Alcyonacea spp. and F) *Stichopathes* sp. for Site B. The non-reef substrate is in grey. Note varying colour scale between the different plots.

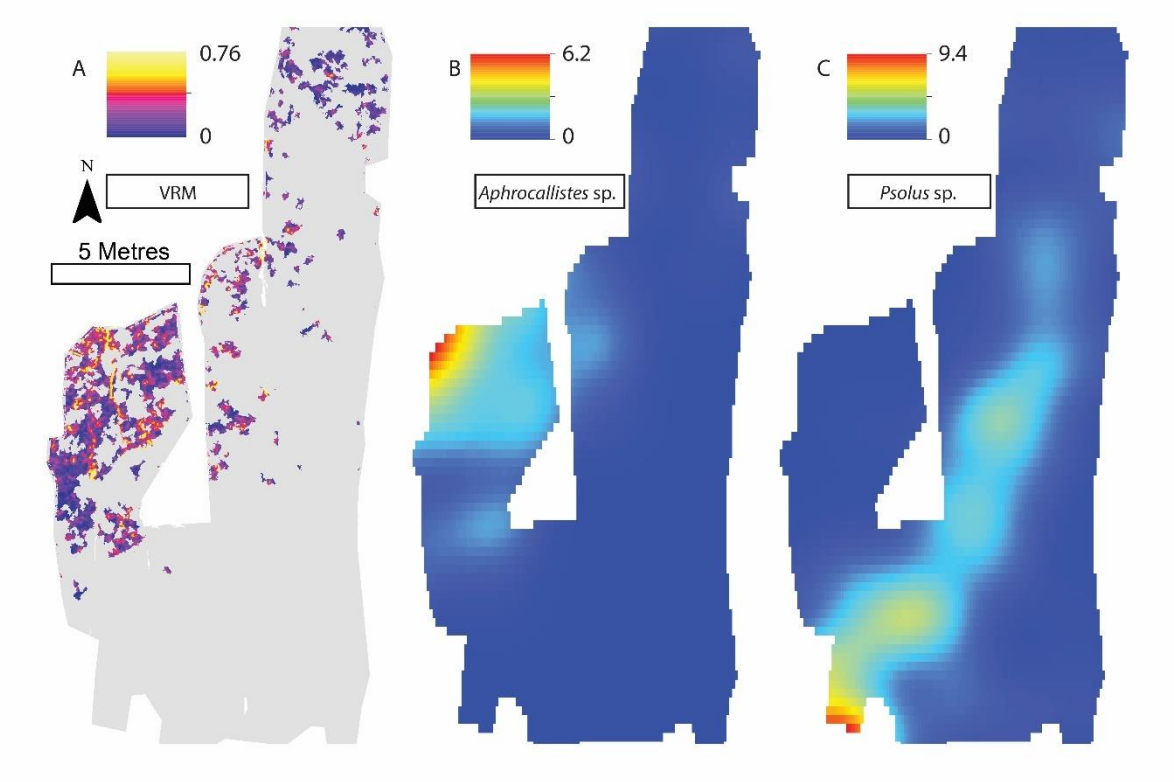

Figure 4.9. Site C Vector Ruggedness Measure (VRM) and density plots. A) Vector Ruggedness Measure values for reef facies. Density plots in the form of kernel estimate of intensity (number of individuals per m^2 and sigma = 1) B) *Aphrocallistes* sp. C) *Psolus* sp. for Site C. Note varying colour scale between the different plots.

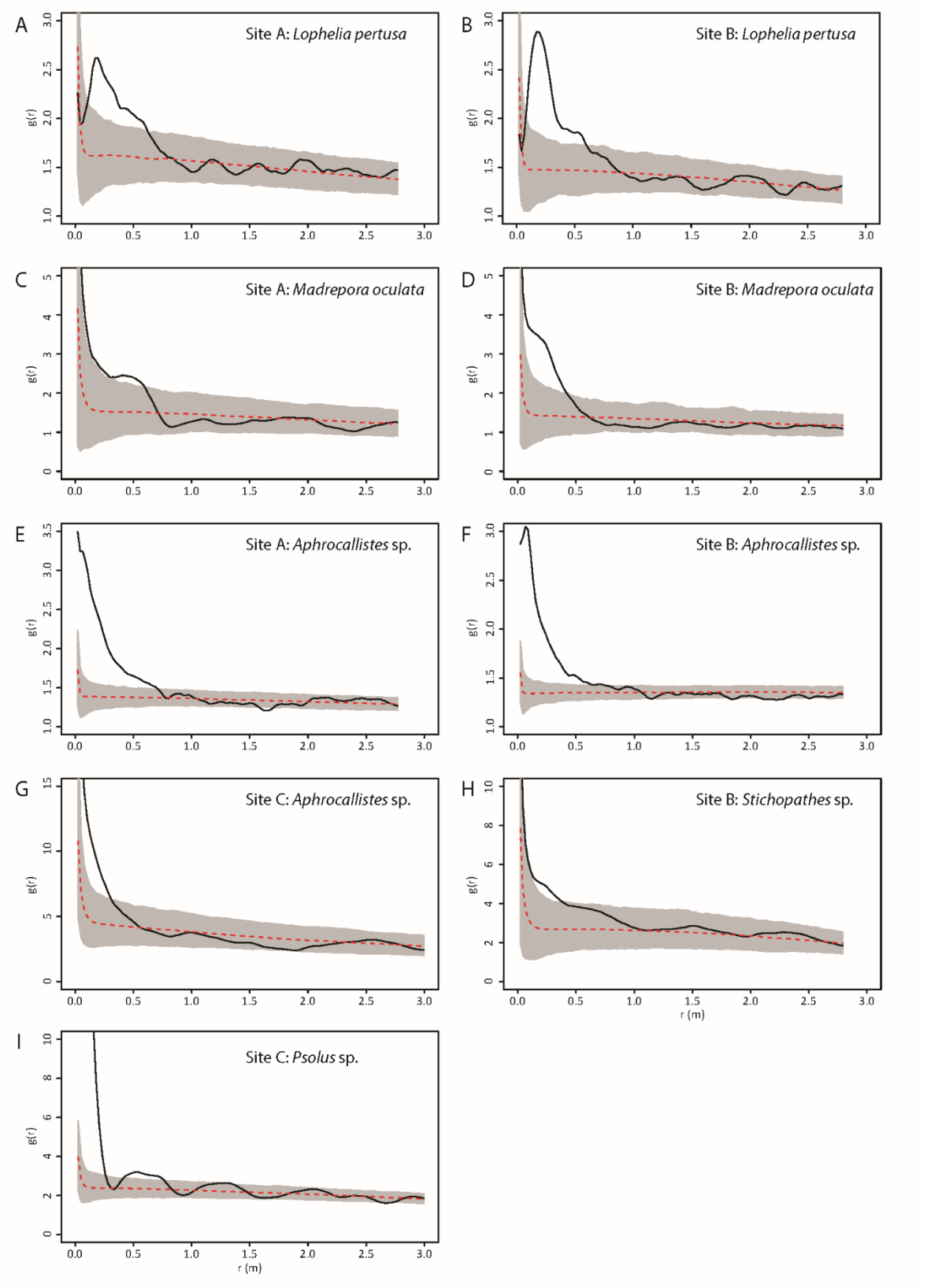

Figure 4.10. Inhomogeneous Pair Correlation Function results for specific species at specific study sites. Grey area represents simulation envelope. A) *Lophelia pertusa* at Site A. B) *L. pertusa* at Site B. C) *Madrepora oculata* at Site A. D) *M. oculata* at Site B. E) *Aphrocallistes* sp. at Site A. F)

Aphrocallistes sp. at Site B. G) *Aphrocallistes* sp. at Site C H) *Stichopathes* sp. at Site B I) *Psolus* sp. at Site C.

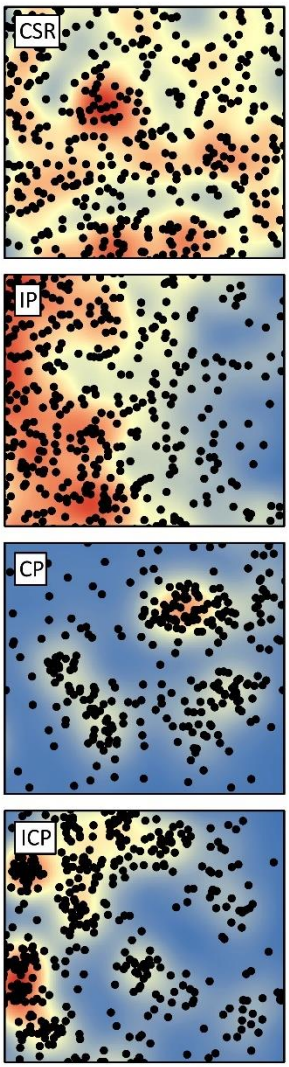

Species	Site	Model	Environmental (clustering parameters)
Lophelia pertusa	A	ICP	Northness and Substrate. (r = 0.5, sat = 3)
	B	ICP	Eastness, Northness, Depth, Substrate. (r = 0.36, sat = 4)
Madrepora oculata	A	ICP	Northness and Substrate. (r = 0.72, sat = 5)
	B	ICP	VRM (50 cm) and Substrate. (r = 0.39, sat = 3)
Aphrocallistes sp.	A	ICP	Northness, VRM (7mm), VRM (50 cm), Substrate. (r = 0.23, sat = 7)
	B	ICP	Eastness, VRM (7 mm), VRM (50 cm), depth, Substrate. (r = 0.22, sat = 6)
	C	ICP	VRM (7 mm), Substrate. (r = 0.3, sat = 2)
Alcyonacea spp.	A	ICP	VRM (7 mm), Depth, Substrate. (r = 0.3, sat = 3)
	B	IP	Northness, VRM (7 mm), VRM (50 cm), Depth, Substrate.
Psolus sp.	C	ICP	VRM (7 mm). (r = 0.15, sat = 4)
Stichopathes sp.	B	ICP	Northness, VRM (7 mm), VRM (50 cm), Substrate. (r = 0.92, sat = 5)
Zoanthidae sp.	B	ICP	Eastness, Substrate. (r = 0.79, sat = 2)
Cidaris cidaris	B	ICP	Eastness, Northness, VRM (7 mm), Substrate. (r = 0.42, sat = 3)
Galatheoidae sp.	A	ICP	VRM (50 cm), Substrate. (r = 0.78, sat = 6)
	B	IP	VRM (50 cm), Depth, Substrate.
< 50 individuals			
Lophelia pertusa	C	IP	Substrate.
Madrepora oculata	C	IP	Substrate.
Alcyonacea spp.	C	IP	VRM (7 mm), Substrate.
Callogorgia spp.	A	IP	VRM (7mm), Substrate.
	B	IP	VRM (7mm), Substrate.
Psolus sp.	A	IP	VRM (7 mm), Depth.
Zoanthidae sp.	A	IP	VRM (7 mm), VRM (50 cm), Substrate.
Anthomastus sp.	A	CSR	
	B	CSR	
	C	CSR	
Cidaris cidaris	A	IP	VRM (7 mm), VRM (50 cm), Depth, Substrate.
	C	IP	Substrate.
Gracilechinus sp. "green"	A	IP	VRM (50 cm), substrate.
	B	IP	VRM (7 mm), VRM (50 cm), Substrate.
	C	CSR	
Gracilechinus sp. "pink"	A	IP	VRM (7 mm), Substrate.
	B	IP	VRM (7 mm), VRM (50 cm), substrate.

Figure 4.11. Point Pattern Modelling results. Single simulation of *Aphrocallistes* sp. distribution from Site A assuming Complete spatial randomness (CSR), Inhomogeneous point pattern (IP), Clustering point pattern (CP) Inhomogeneous clustering point pattern (ICP). Kernel density is plotted in the background. Most parsimonious models for 13 species based on the lowest AIC score are listed in the accompanying table with environmental and Geyer's point interaction (r = distance (m), sat = saturation threshold) parameters specified where relevant.

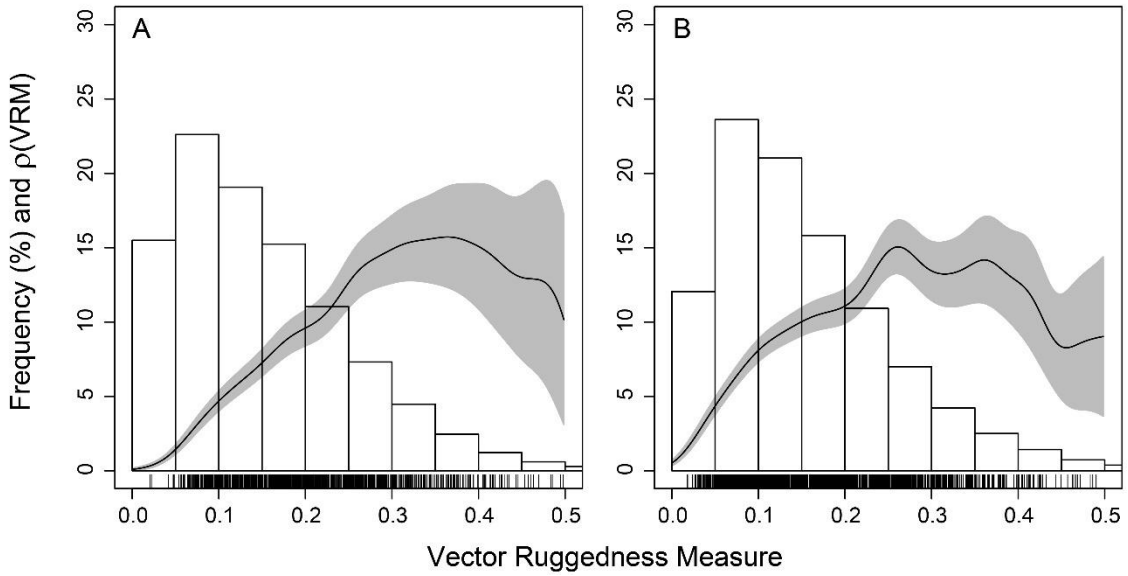

Figure 4.12. Estimated function ρ(VRM) of *Aphrocallistes* sp. intensity as a function of VRM at Site A (A) and B (B). Grey represents 95% confidence bands. Bars refers to frequency as a percentage of coral substrate VRM.

4.5 Discussion

The majority of benthic organisms were found aggregated on reef structures with further clustering at scales below 1 m. Clustering was partly influenced by the local features such as coral skeleton presence, reef rugosity at multiple scales and other geomorphic variables, and for some taxa partly by biological processes. This study demonstrates a novel use of PPA in deep-sea ecology through the utilisation of high resolution photomosaics and DEMs created from ROV video, to map and analyse reef heterogeneity and the spatial organisation of reef-building coral and associated taxa. The statistics used have so far been typically applied to terrestrial and shallow-water habitats and while applied here in a cold-water coral environment, it is clear that a similar approach can also be applied across a range of marine environments.

The benefit of undertaking PPA is the ability to identify how organisms are responding to variability in their habitats. The terrain metrics derived from Structure from Motion allowed quantification of

coral framework rugosity, provided mainly by framework-building corals *L. pertusa* and *M. oculata*. These metrics showed a wide variety of VRM values that captured the structural complexity of the seafloor, including from the coral rubble to the 3D framework. Whilst the rugosity value at which coral is considered rubble or framework remains ambiguous, the variety of VRM values showed that coral-related geomorphic metrics span a wide range of values. This habitat heterogeneity was first reported by Lim et al. (2017), who observed heterogeneity of substrate facies across the entire mound, a variable known to drive organism distribution (e.g. Corbera et al., 2019). Here, variability in organism distribution was determined in the form of general density trends and clustering, that may have been driven by both environmental and biological processes. Furthermore, the lack of consistency between the sites in terms of live *M. oculata* and *Stichopathes* sp. densities (Table 2), also infers different conditions between the northern side of the mound and the north-eastern flank of the mound, despite being located metres away from each other, showcasing the heterogeneity of mini-mound habitats.

Most organisms showed an affinity for the reef substrate, supporting our prediction (Hypothesis 1) that a higher density of certain species are found within the reef substrate compared to the surrounding non-reef substrate. The density plots reveal an abrupt decrease in some species densities between these coral- and sand-dominated habitats. The abrupt change is in contrast to mounds the northern Ionian Sea where the changes between macrohabitats were described as gradual (Vertino et al., 2010), showing the natural variability of habitat provision by biogenic reefs between regions and areas. The association with coral was particularly evident for sessile organisms, with the exception of *Psolus* sp. which was typically found on dropstones at Site C and of *Anthomastus* sp. which displayed an apparently random distribution. The association of species and reef substrate is unsurprising considering many sessile organisms use the dead coral skeleton framework as the point of attachment for stability (Henry and Roberts, 2017). These organisms may also benefit from the localised alteration of hydrodynamics influenced by cold-water coral reef framework (Buhl-Mortensen et al., 2010; Mienis et al., 2019). Mobile species such as *C. cidaris* and *Gracilechinus* spp. (Appendix 4.2, 4.3, 4.4) however displayed a slightly more cosmopolitan distribution within the mosaics, with less robust evidence of clustering, though were still associated with reef substrate and some environmental variables. This less defined clustering pattern seen in the density plots could indicate that they may move from the coral structure. However, the three urchin (*C. cidaris*, *Gracilechinus* sp 'pink', *Gracilechinus* sp 'green') species showed associations with rugged parts of the reef substrate (Figure 11), possibly utilising the 3D structure (Stevenson et al., 2015).

Further clustering was evident for the reef-building corals *L. pertusa*, *M. oculata* supporting our predictions that *L. pertusa* and *M. oculata* would occupy different parts of the reef (Hypothesis 2),

and that organisms biologically cluster within habitats, specifically cold-water coral reef framework, in addition to the terrain variable driven distribution (Hypothesis 3). Live *M. oculata* and *L. pertusa* clusters were formed distinctly from each other (Figure 7, 8), rather than being evenly or randomly distributed amongst each other. This pattern is likely caused by a combination of environmental drivers, initial settling position, growth patterns and restrictive reproductive dispersal such as fragmentation. Similar PPM fitting methods revealed clustering patterns indicating spatially constrained dispersal or fragmentation of coral in shallow-water scleractinians (Edwards et al., 2017). However, it is also known that localised abiotic drivers may influence shallow-water and cold-water scleractinian distribution (Dana 1976; Orejas et al., 2009), as also shown by our study (e.g., currents; as indicated by the importance of aspect variables in the PPM models). The facilitative mechanisms behind the clustered patterns observed in this study are ambiguous, owing to a lack of knowledge on the dominant reproductive strategy of deep-sea coral in situ at Piddington Mound. The growth patterns of dendritic scleractinians such as *L. pertusa* and *M. oculata* is conducive to senescence through abandonment of the old skeleton which can lead to separate genetically identical colonies partitioned by dead skeleton. This process can result in so-called Wilson rings (Wilson, 1979), and is likely a prominent driver of the patterns in the distribution of the framework-building corals observed in our study, as both species tended to form clusters at distances less than approximately 0.6 m. This growth pattern could be considered a biologically driven pattern, but sustaining living parts of the colony ultimately relies on underlying suitable conditions not measured in this study, such as oxygen supply, water movement, sedimentation and food supply on a sub-metric scale. Although *L. pertusa* and *M. oculata* are successful broadcast spawners, spatially restrictive asexual reproductive strategies in cold-water coral have been identified, such as cloning and fragmentation (Rogers, 1999). Dahl et al. (2012) and Le Goff-Vitry et al. (2004) demonstrated that the predominant reproductive strategy can vary from reef to reef and can result in a relatively high proportion of clones within the reef. Further, it could be argued that the low coverage of live scleractinian coral on the Piddington Mound (< 5% for the entire mound; Boolukos et al., 2019; Conti et al., 2019) is indicative of a lack of larval supply, suitable settling sites or survival conditions. Similar patterns of clustering were observed in the other cold-water corals, Alyconacea spp. ('gorgonian' octocorals) and *Stichopathes* sp. (antipatharian coral), at our study site, with evidence for biological clustering at site A and B respectively. Comparable patterns have been noted in shallow water gorgonians, attributed to localised environmental factors (Yoshiokoa and Yoshioka, 1989). However, it is well established that asexual reproduction is one form of reproduction (Wagner et al., 2011) that is likely to lead to clustering, as well as philopatric larval dispersion that has been noted in antipatharians and gorgonians (Miller et al., 1998; Gori et al., 2011a). Whilst localised, favourable abiotic conditions are a prerequisite for colony longevity and influencing fine-scale cold-water coral distribution, it is likely growth patterns and reproductive

methods are also an underlying driver contributing to the clustering patterns of all cold-water coral observed.

The clustering of *Aphrocallistes* sp., consistently observed at all three sites, reflects previously quantified sponge hotspots on the north, west and the peak of Piddington Mound (Conti et al., 2019), as well as revealing finer-scale, centimetric clustering. Similar, albeit unquantified clustering reported in previous studies of *Aphrocallistes* sp. has been attributed to both asexual reproduction and environmental drivers. Chu and Leys (2010) suggested that asexual budding of glass sponges and local larvae retention may contribute to the patchy structure of sponge reefs, although Brown et al. (2017) observed distinct, non-related sponge colonies clustering, citing local environmental conditions such as flow velocity and substrate availability as the drivers of clustering, rather than cloning. We observe evidence for both strategies whereby *Aphrocallistes* sp. aggregated in the more rugged part of the coral substrate (supporting Hypothesis 4), taking advantage of the structurally complex substrate, but the modelling approach provided strong evidence for biologically driven clustering as well. Several mechanisms such as enhanced larval entrainment and settling cues in the rugged part of the reef as well as cloning reproductive strategies may contribute to the highly clustered patterns we observed. *Aphrocallistes* sp. and colonies of scleractinians appeared to coincide with the more structurally complex portion of the reef substrate which may suggest a positive feedback mechanism for reef growth, as it is likely large *Aphrocallistes* sp. colonies contribute to the reef structure. *Aphrocallistes* sp. were found at higher densities when the VRM was above 0.1, indicating a preference against reef substrate with low VRM values, that likely represented reef rubble and low-profile coral framework with minimal structural complexity. Large colonies of *Aphrocallistes* sp. likely contribute to the rugosity values observed which could not be accounted for in the analysis, though we observed that the majority of individuals were small in size or were not detectable in the DEM, and likely had a limited influence. To support this observation, we analysed lower resolution data (which smoothed the presence of larger *Aphrocallistes* sp. individuals) in the same way which yielded a similar pattern (Appendix 4.8).

4.5.1 Future research

The combination of unmanned robotics and application of terrestrial ecological analysis approaches in deep-sea environments is progressing our understanding of fine-scale deep-sea organism distribution. However, it must be noted that, whilst great care was taken to avoid annotator bias, processing of images from unmanned vehicles tends to underestimate megafauna due to low image resolution and high camera altitude, undermining and compromising the quality of deep-sea datasets (Meyer et al., 2019). Further, it must be considered that the mobile species may move between survey lines and may have been double counted or not at all depending on the organisms'

movement direction and speed. In fact, the ROV light may also disperse some species and attract others directly or indirectly to feed on light attracted prey. Future studies should focus on collecting data for the wider area which can be achieved by using autonomous vehicles in order to liberate the research vessel for other valuable operations (Wynn et al., 2014), whilst collecting hectares of photomosaics (Simon-Lledo et al., 2019; Meyer et al., 2019) or achieving greater replication. Such large datasets however, present challenges for the annotation of such vast quantities of data. It is expected that machine learning may improve our ability to rapidly generate datasets through the annotation of images (e.g. Piechaud et al., 2019) and the automated classification of benthic habitat which is becoming a more common mapping technique (Lim et al., 2021). In addition, the mosaics presented provide an opportune dataset for temporal studies which can inform on the natural temporal variability of mound surface composition and coral growth patterns. Time-scale studies are lacking in cold-water coral habitats on a scale of years, but recent studies have shown a decline of live coral at the Piddington Mound (Boolukus et al., 2019) and lack of recovery following disturbance at the Darwin Mounds (Huvenne et al., 2016).

4.6 Acknowledgements

These data were collected during the QUERCII expedition, funded by the Marine Institute under the Ship Time Programme of the National Development Plan. We thank the officers, crew, ROV technical team and scientific party of cruise of the RV Celtic Explorer and Holland I ROV, of whom this would could not have been undertaken. D. Price is funded by the Natural Environmental Research Council (grant number NE/N012070/1) and University of Southampton GSNOCS European Exchange Programme. V. Huvenne is funded by the NERC CLASS project (grant number NE/R015953/1). A. Lim and V. Huvenne are supported by the iAtlantic project of the EU H2020 Research & Innovation Programme (grant number 818123). Finally, we thank the 2 reviewers for their detailed comments which improved the quality of the paper.

Chapter 5 Synthesis

5.1 Summary

With the increasing reach of anthropogenic impacts in the marine environment, understanding the ecological role and distribution of cold-water corals, key ecosystem engineers, is important. Cold-water coral distribution is shaped, amongst others, by the physical environment which can be quantified through so-called “abiotic variables”, that can be used in predictive spatial modelling. However, such models rarely capture fine-scale processes affecting coral distribution, nor the subsequent effects of cold-water coral reef structure on the organisation of associated benthic taxa. To address these issues, we undertook several novel analyses which were only made possible by recent advancement in technology, to capture fine-scale ecological observations. This was achieved on a scale of millimetres to tens of metres using acoustic and optical datasets. With the use of an Autonomous Underwater Vehicle (AUV), high-resolution bathymetric data were collected and used to predict cold-water coral distribution in a submarine canyon. Furthermore, the application of Structure from Motion (SfM) photogrammetry resulted in millimetric resolution data of cold-water coral habitat in 3D, paving the way for a plethora of statistical approaches to identify benthic faunal patterns.

5.2 Research aims and key results

Chapter 2 - High-resolution predictions of cold-water coral distribution in Explorer Canyon (NE Atlantic) with the use of an Autonomous Underwater Vehicle (AUV).

The aim of chapter 2 was to obtain high-resolution (metre-scale) predictive maps of reef-building cold-water coral distribution in a submarine canyon. We achieved this by deploying the *Autosub6000* AUV, producing a 5 x 5 m pixel resolution bathymetry map. This was used to derive environmental variables for Species Distribution Modelling (SDM), which was achieved using Random Forest and Generalised Additive Models. The models performed well (AUC score >0.8), though not as accurate as SDM performed on 50 m resolution data likely due to unquantifiable variables at the fine-scale and geographical errors. However, the predictions at 5 m resolution identified more precisely a series of geomorphological features that may support cold-water coral habitats such as mounds, ridges and walls. Models performed on 50 m resolution data tended to predict coral over large areas, perhaps a sign of over-predicting, but missed important geomorphic features. This analysis may be useful for planning future survey locations and ultimately for supporting marine spatial planning.

Chapter 3 - Using 3D photogrammetry from ROV video to quantify cold-water coral reef structural complexity and investigate its influence on biodiversity and community assemblage

The aim of chapter 3 was to quantify structural complexity created by cold-water coral framework, and its importance for local community assemblages. We successfully achieved this aim by creating 40 3D models from linear Remotely Operated Vehicle (ROV) video sub-transects using SfM. Digital Elevation Models (DEMs) were used to quantify structural complexity of cold-water coral framework with two rugosity measures: 1) Rugosity Index Ratio and 2) Vector Ruggedness Measure. These data were used to highlight the importance of the reef and its structural complexity to local biodiversity, by using multivariate statistics. The results show that species richness and abundance increased with greater coral cover and structural complexity, forming a distinct cold-water coral reef assemblage from approximately 30% coral cover (0.07 VRM). The data demonstrated how Vulnerable Marine Ecosystem (VME) indicator taxa can be quantified with SfM and how imagery could be used as a repeatable method to detect a VME from imagery by identifying the coral cover threshold at which VME indicator taxa form a VME, and eventually monitoring its variability.

Chapter 4 - Fine-scale heterogeneity of a cold-water coral reef and its influence on the distribution of associated taxa.

The aim of chapter 4 was to investigate the role of cold-water coral coverage and structure in the fine-scale distribution of associated taxa. We achieved the aim of quantifying the benthic organisation of a cold-water coral mound by applying SfM and Point Pattern Analysis (PPA) over a large area (~200 – 250 m^2) to identify specimen locations and reef characteristics. Geomorphic derivatives and specified Geyers clustering were used to infer abiotic and biotic drivers of the clustering of associated taxa. Geomorphic variability within the reef and clustered patterns of benthic taxa demonstrated the heterogeneous nature of cold-water coral reefs.

5.3 Scientific contributions

The results obtained in this thesis demonstrate how novel technology and image analysis can improve our understanding of cold-water coral ecology and distribution. Through the multi-scale quantification of cold-water coral habitat, we have demonstrated how a range of biotic and abiotic drivers influence the distribution of cold-water coral and its associated communities across a range of scales.

By deploying an AUV equipped with a Multibeam Echosounder (MBES), high-resolution bathymetry was generated which could be used in tandem with video ground truthing to produce spatial predictions of cold-water coral. These data show that high-resolution bathymetry can resolve

geomorphological features that may be important habitats for cold-water corals, that otherwise would have been missed. These features include vertical walls and localised bathymetric highs which may represent coral mounds. In particular, the spatial predictions highlighted the importance of vertical walls as potential cold-water coral habitats in canyon systems, supporting other observations (Huvenne et al., 2011; Robert et al., 2019). The spatial predictions are useful in marine spatial planning, demonstrated by the identification of areas that hold high potential for supporting other cold-water coral assemblages in the vicinity, which were not identified with lower resolution datasets.

In tandem with the AUV derived bathymetry of Explorer Canyon, SfM surveys of the cold-water coral reefs broadened our knowledge of cold-water coral distribution and ecological functioning. The SfM approach was amongst the first of its kind in cold-water coral reef research (e.g. Robert et al., 2017, 2019; Lim et al., 2020). Our results demonstrated the first known rugosity index values of cold-water coral reef, which were comparable with shallow-water coral rugosity values (Graham and Nash, 2013). Furthermore, by analysing orthomosaics and DEMs, continuous metrics of characteristics such as rugosity and coral cover can be generated and incorporated into statistical analysis, instead of using subjective categorical data. This analysis revealed that the most structurally complex parts of the reef, which had high coral framework cover, supported the highest fauna abundance and species richness demonstrating that the reef is a localised driver of biodiversity.

The results showed that the community became a distinct cold-water coral reef assemblage when cold-water coral covered more than 30% of the seafloor on a scale of tens of metres. This was the first published attempt at quantifying cold-water coral coverage and structural complexity values to define a threshold at which the habitat forms a distinct community assemblage. The threshold values presented in chapter 3 (Price et al., 2019) were subsequently reinforced by Rowden et al. (2020), who noted that biodiversity peaked at approximately 30% *Solenosmilia variabilis* coverage of the seafloor on a seamount. These results build a strong argument that VMEs can be designated based on imagery alone, through the quantification of cold-water coral extent, coverage and structural complexity. This supports ongoing work to identify how we can classify VMEs from imagery (Baco-Taylor et al., 2020). Understanding thresholds can also be useful in prioritising important habitats and can be incorporated within spatial planning by applying SDM with known threshold values based on scientific evidence (Rowden et al., 2017; Rowden et al., 2020).

The results from chapter 4 built upon chapter 3 by applying SfM techniques over a larger footprint and utilised for the first time PPA to study a cold-water coral reef habitat. In chapter 3 we showed that biodiversity increased with rugosity of the cold-water coral habitat, but in chapter 4 we

demonstrated that sessile species such as *Aphrocallistes* sp. were indeed attracted to the more structurally complex parts of the dead framework. This example removed any ambiguity over the importance of structural complexity by identifying specific organism locations rather than relying on habitat-wide, averaged assessments (i.e. reef over a 25 m sub-transect). Chapter 4 built upon the methods utilised by Edwards et al. (2017) in shallow-water coral reefs by using geomorphic variables and parameterised clustering to represent biological clustering. Through these methods we showed how the reef framework, local environment and species life history may determine species dispersion and distribution. Furthermore, the apparent clustering of organisms pointed to a complex system influenced by both biotic and abiotic factors which can be quantified with high quality SfM outputs.

5.3.1 Explorer Canyon as a Marine Protected Area (MPA)

The research undertaken in this thesis (specifically chapter 2 and 3), has developed a robust argument for further exploration of Explorer Canyon to support detailed VME designation. By utilising novel technology and analysis techniques, we show that the coral reef discovered by Davies et al. (2014) and Stewart et al. (2014) introduces structural complexity into the environment. Biodiversity metrics increase with coral cover and rugosity, resulting in a distinct community assemblage shaped by the reef. This directly supports the argument that the cold-water coral reef is an important component of biodiversity within Explorer Canyon.

At present Explorer Canyon is part of a Marine Conservation Zone (MCZ), specifically designated to protect, among other habitats, cold-water coral reef. Without sufficient protection, monitoring and spatial planning, MPAs can be less effective in preventing fishing damage (e.g. Reed et al., 2005; 2007). Our spatial predictions and evidence of the importance of the reef can support future policy, protection and monitoring. According to the MCZ assessment report, confidence of cold-water coral presence and spatial extent is “high”, but confidence in “feature condition” is “low” (JNCC, 2013). Our results show that cold-water coral presence is likely in other parts of the canyon in addition of the known reef system, suggesting the initial “high” confidence assessment of spatial extent is perhaps superficial and our results advocate further investigation. Our results reveal that the reef formation is structurally complex, suggesting minimal trawling impacts and active growth, supporting high biodiversity with distinct communities. This would suggest that the cold-water coral reef habitat is in good condition, although we have no baseline data to compare this with, requiring a more focussed analysis of coral health and growth.

The results indicate that coral is likely to be found in other, unexplored locations of Explorer Canyon which contrasts with the JNCC report which stated that confidence of coral spatial extent was high.

Therefore, our results justify and encourage the use of AUVs to collect high-resolution data in MPAs to investigate the distribution of cold-water coral and other species of interest. Future targeted surveys using ROVs or AUVs to collect even higher resolution data such as SfM surveys, can now be prioritised in order to assess potential habitat importance and to gauge the true scale of cold-water coral extent and condition, saving resources by avoiding less-informed or randomised survey locations.

Overall, the results from chapters 2 and 3 demonstrate the usefulness of 1) using high-resolution bathymetry to estimate coral locations and 2) using SfM outputs to perform feature condition checks and potentially monitor benthic habitat change.

5.4 Future direction

The results presented in this thesis shine a light on a plethora of potential future studies by applying our analytical approach to other cold-water coral reef locations and over large areas, through embracing emerging technology to facilitate a greater understanding of deep-sea ecology at multiple scales.

5.4.1 SDM: development and application

The SDM modelling undertaken in this thesis demonstrates the power of analysing high-resolution data, but we still lack environmental variables that may improve spatial prediction accuracy. Ecological processes occur across multiple scales (Levin, 1992) and thus species-environment relationships must be investigated using different resolutions of data. Whilst our data show that 5 m resolution bathymetric data is useful in submarine canyons as topographical variation is present on a comparable scale, additional scales (both broader and finer) may represent further scale-dependent relationships. For example, higher resolution bathymetry data could be achieved using an ROV or setting the AUV MBES to have a narrower swath. In addition, considering broader scales of analysis (>hundreds of metres) may be useful in the context of high-resolution surveys that cover a sufficiently large area. The next steps in SDM are to incorporate multiple resolution predictions into a single ensemble model. This is however difficult due to the different transect lengths of ground truthing data, resulting in non-standardised modelling between dataset resolutions.

Incorporating hydrodynamic models into SDM also improves accuracy of cold-water coral distribution predictions (Pearman et al., 2020). However, very high-resolution hydrodynamic models are rarely achieved, and models with a resolution of hundreds of metres are typically incorporated in cold-water coral studies (Navas et al., 2014; Pearman et al., 2020). Generating hydrodynamic models on a scale of metres and tens of metres, whilst difficult and costly to achieve,

would enhance our ability to predict coral and associated taxa with precision, in high-resolution, as well as aiding our fundamental understanding of cold-water coral reef ecological functioning. This is supported by Lim et al. (2020) who noted that cold-water coral reef macro-habitat composition (live coral, dead framework and coral rubble) and live coral positioning on a scale of metres were linked with local current velocity and direction. In addition, quantifying fine-scale hydrodynamics around reefs may reveal mechanisms for how food particles are delivered to live reef patches.

SDM can be useful in marine spatial planning and can contribute to other aspects of habitat conservation, such as active restoration. Reef restoration has been suggested as a viable solution to restore degraded cold-water coral reefs (van Dover et al., 2014), and recent restoration studies on deep-sea gorgonians have shown promise (Montseny et al., 2019; 2020). However, knowledge on locations that are suitable for coral growth is required to ensure optimal environmental conditions for the success of transplantation to justify harvesting from extant or lab reared colonies. This is challenging in the deep-sea and it is possible that high-resolution SDM can contribute in identifying locations that are suitable for transplantation of corals. Future studies would need to test the effectiveness of this approach to evaluate its worth.

5.4.2 SfM: development and application

The analytical gains from SfM datasets can be scaled up by collecting data over large areas using recent technological advances. The next logical step would be to deploy AUVs to collect imagery for SfM surveys over large areas of cold-water coral habitat. Huvenne and Thornton (2020) deployed the *Autosub6000* AUV in the Darwin Mounds region for this reason. By combining a laser line scanner and stereo camera, mosaics and DEMs were produced over large areas (e.g. ca. 300 m x 900 m surveyed in one 24h mission). Huvenne and Thornton (2020) noted that the horizontal collision avoidance sonar was relatively insensitive to the Darwin Mounds, which protrude ~5 m into the water column, when acquiring data from a high altitude (~5 m above seafloor). However, larger mounds may present collision hazards that may cause AUVs fitted with collision avoidance sensors to take evasive manoeuvres which is likely to lead to gaps in the dataset. One solution is the deployment of a hover-AUV to slowly navigate features and track the seafloor terrain with a closer proximity, which has already been successfully tested in shallow water reef systems (Friedman et al., 2012). Furthermore, combining the outputs of large area SfM surveys and broader bathymetry may provide a multi-resolution overview which could be analysed with advanced landscape ecological analysis such as PPA to build a fully integrated multi-resolution distribution model. The value of ecological knowledge from such analysis is very high and would provide insight into what drives cold-water coral and their associated taxa distribution, as well as providing an ecosystem-wide baseline dataset in which monitoring programs can be instigated.

By utilising robotics with sufficiently accurate navigation systems, scientists can revisit the same cold-water coral reef over time and develop a monitoring system. Huvenne et al. (2016b) already demonstrated the power of repeat surveys to test the effectiveness of MPAs. By producing a photomosaic and DEM, coral growth and structural complexity could be monitored on an individual colony scale over a large area. This is pertinent as cold-water coral mounds can change in a short space of time. For example, an increase in coral rubble due to biological and physical erosion (Lim et al., 2018b), and a decrease in live coral cover at Piddington Mound was observed over the course of 4 years (Boolukos et al., 2019). Whilst it is expensive to undertake ROV and ship board surveys, it is important to develop high-resolution spatial and temporal data in order to monitor cold-water coral reef formations in the face of anthropogenic pressure. The possibility of running AUVs from distal bases or supported with other autonomous vehicles, could deem high-frequency and high-resolution repeatable surveys invaluable, if achievable in the future. The ability of SfM to monitor coral growth and benthic change has already been demonstrated in shallow-water coral reefs using diver and drone surveys (Ferrari et al., 2017; Rossi et al., 2020; Fallati et al., 2020) and on one occasion measuring cold-water coral growth (Benneke et al., 2016). In tandem with time series studies, volumetric growth can be incorporated as a dependant variable with the use of PPM to identify hotspots of successful organisms to understand where on coral mounds is the best for coral and other sessile species.

Further investigation into the patterns of benthic organisation in other locations, larger areas and additional environmental variables may improve our fundamental knowledge of cold-water coral reef ecology. For example, measuring additional geometric variables and scales of rugosity metrics may improve our explanations of associated taxa distribution. Chapter two and three briefly explored different rugosity measures and scales to a degree, but further consideration should be given as they are influential on shallow-water coral reef biodiversity (e.g. Torres-Pulliza et al., 2020), a pattern that may be mirrored in the deep-sea coral reefs.

Finally, by utilising orthomosaics and SfM, it is clear that habitat coverage threshold and VME identification is possible. However, our studies cover only one locality. Rowden et al. (2020) have drawn similar conclusions from a different cold-water coral reef habitat, but two studies are not sufficient in capturing global patterns, therefore, comparable studies in other regions would strengthen the argument of our conclusions. Furthermore, other VME's such as sponge grounds may act functionally similar to cold-water coral reefs by introducing structural complexity. They may, however, be characterised by different thresholds. Applying our methods to sponge grounds and other deep-sea habitats will bring further insights into the functioning of deep-water VMEs. The use of SfM to identify VMEs and important habitats are not limited to the deep-sea but is applicable to shelf sea research which also support VMEs and other protected benthic habitats. For

example, Benoist et al. (2019) utilised *Autosub6000* to undertake a MBES, SSS and photographic survey of an area within a MCZ, providing a multi-faceted view on the environment. As shelf sea habitats are nearer shore, frequent independent visits of AUVs form nearby shores is a tantalising prospect and would provide invaluable data in by means of monitoring, to gauge the effectiveness of MPAs.

5.4.3 Technological and analytical advances

AUV MBES surveys cover a relatively large area, but a gap between shipboard survey and AUV survey footprint still exists. The recent development of AUVs such as *Autosub Long Range* (Furlong et al., 2012) which has a range of 6,000 km, could be used to map large areas of important habitat such as cold-water coral. As acoustic payloads draw a lot of power, 6,000 km is unlikely for the time being, but a significant range increase could still be expected. However, in order to counteract Doppler dead-reckoning navigation drift, either Terrain Aided Navigation (Salavasidis et al., 2016) or co-deployment of static beacons (Paull et al., 2014), or surface vehicles as beacons, is required to increase the accuracy in locating the AUV's precise position.

Survey AUVs and ROVs are typically expensive and require specific operational expertise, which confine their use to research groups in developed nations. Low-cost and more readily available "eyeball class" ROVs such as OpenROV (self-assembly) or the Deep trekker mini-ROV are becoming more common and are capable of SfM surveys (Obanawa et al., 2019). However, these small ROVs are typically limited in depth rating and are susceptible to destabilisation by current flow. However, if the technological development seen in aerial drones in recent years is transferred to ROV development, small accessible ROVs may become a useful survey tool for some shallower cold-water coral habitats. Whilst low-cost and easy access AUVs are not available yet, the recent development of micro-AUVs such as the ecoSUB25 (ecosub.ac.uk) shows that it may be possible to create cheaper alternatives to large survey AUVs. Micro-AUVs can be equipped with cameras which we speculate may be suitable for collecting images for SfM. Furthermore, the possibility of creating a swarm of AUVs to survey large areas and improve navigation with multiple vehicles is becoming a more likely prospect (Leblond et al., 2019).

The advancement of remote sensing technologies such as SfM, has generated massive datasets which are time consuming to analyse manually. Artificial Intelligence or Machine Learning is gradually becoming more accessible as a means to annotate large numbers of images that would otherwise take a large amount of time to process. In benthic habitat mapping, deep learning techniques have been deployed for benthic substrate classification within mosaics (Conti et al., 2019) and habitat detection from images (Yamada et al., 2021). Machine learning is also being

developed to annotate deep-sea benthic fauna from imagery (Piechaud et al., 2019) and benthic fauna behaviour (Osterloff et al., 2019). These techniques are not readily available yet or ready to fully replace manual annotation of images (Piechaud et al., 2019), but they will save time and future proof our ability to cope with large datasets once fully developed and readily available.

5.5 Conclusion

Submarine canyons are ecologically productive habitats that can provide a natural shelter for important benthic habitats such as cold-water coral reefs. These cold-water coral reefs introduce fine-scale structural complexity into the environment, which is beneficial to the local fauna. Habitats such as cold-water are vulnerable to anthropogenic disturbances, and thus protection and monitoring of these habitats are required, across multiple scales of analysis. In this thesis, we identify drivers of cold-water coral and their inhabitants' distribution on a scale of 10's of metres to centimetres by harnessing advancement in acoustic and optical technology and processing. By deploying an AUV into Explorer Canyon, this thesis reveals geomorphological features that are suitable for supporting cold-water coral growth that would have otherwise not been detected and considered in spatial predictions. This is essential as we demonstrate that coral cover and associated structural complexity is influential on the local biodiversity of Explorer Canyon. We quantify this using SfM and show that approximately 30% of the seafloor needs to be covered with cold-water coral to form a distinct habitat and that the most structural complex part of the reef framework attracts sessile organisms. These results can feed into effective spatial planning and underpin future legislation for conservation of deep-sea ecosystems.

Appendix A Chapter 2

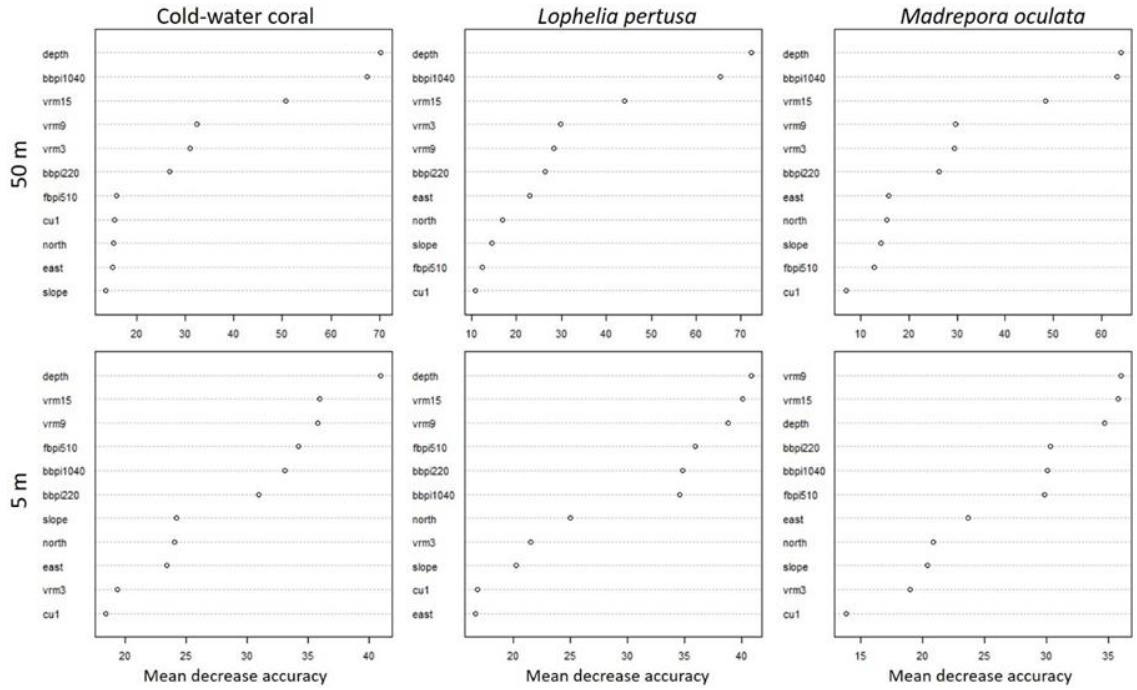

Appendix 2.1. Variable importance for Random Forest models by means of expressing loss of accuracy when each variable is removed.

Appendix A

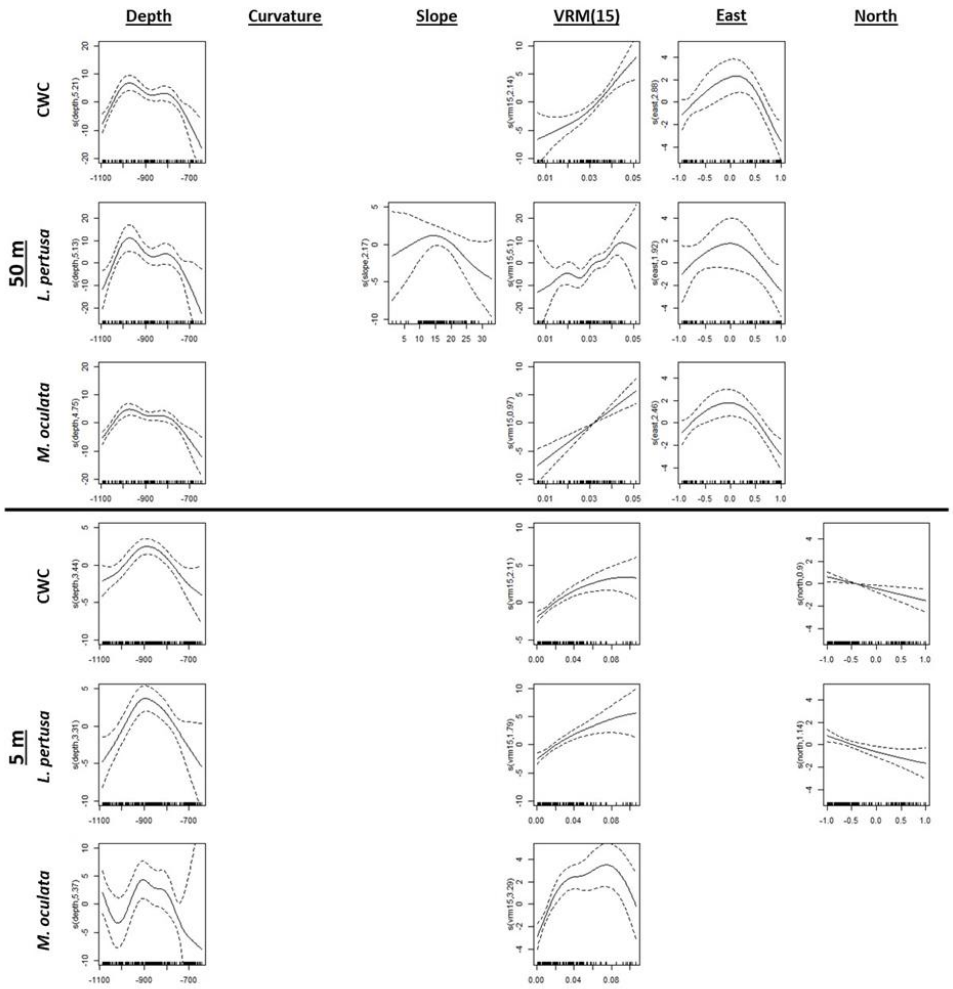

Appendix 2.2. GAM smoother to indicate the relationship between selected environmental variables and response groups.

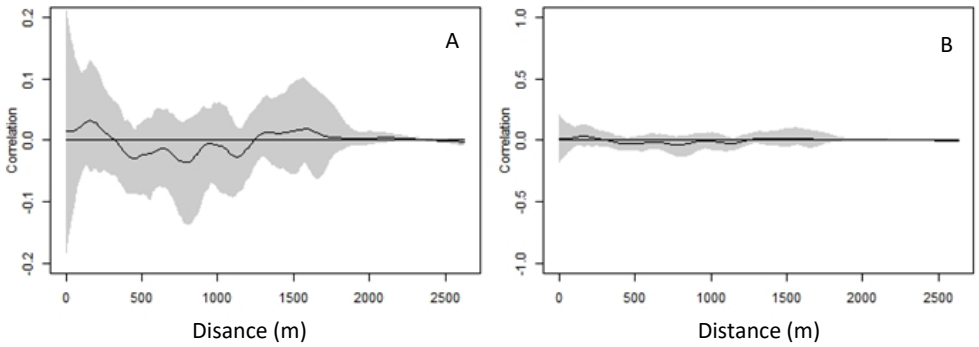

Appendix 2.3. Spatial autocorrelation tested with spline correlograms for cold-water coral models based upon 50 m resolution dataset. Grey area indicates 95% confidence intervals.

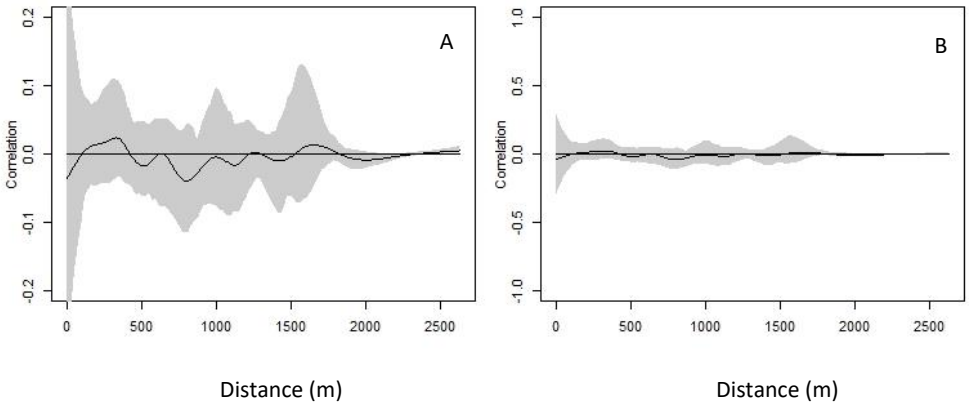

Appendix 2.4. Spatial autocorrelation tested with spline correlograms for *Lophelia pertusa* models based upon 50 m resolution dataset. Grey area indicates 95% confidence intervals.

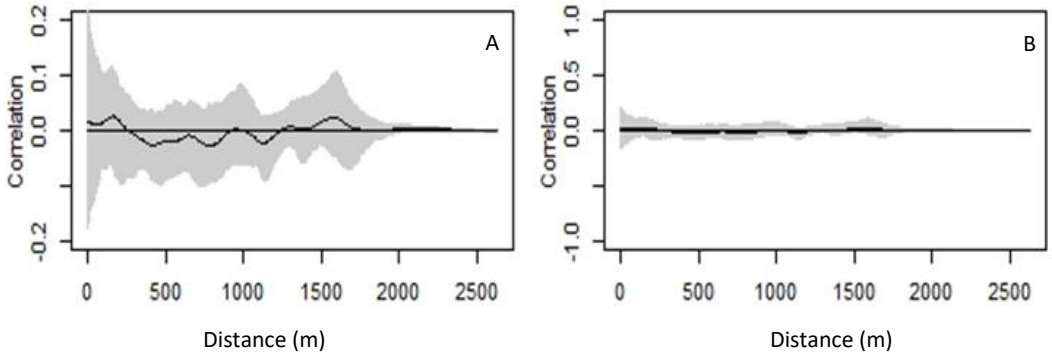

Appendix 2.5. Spatial autocorrelation tested with spline correlograms for *Madrepora oculata* models based upon 50 m resolution dataset. Grey area indicates 95% confidence intervals.

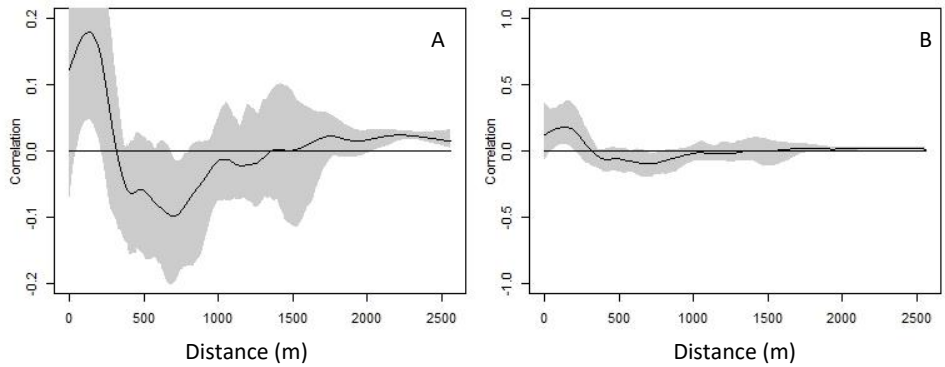

Appendix 2.6. Spatial autocorrelation tested with spline correlograms for cold-water coral models based upon 5 m resolution dataset. Grey area indicates 95% confidence intervals.

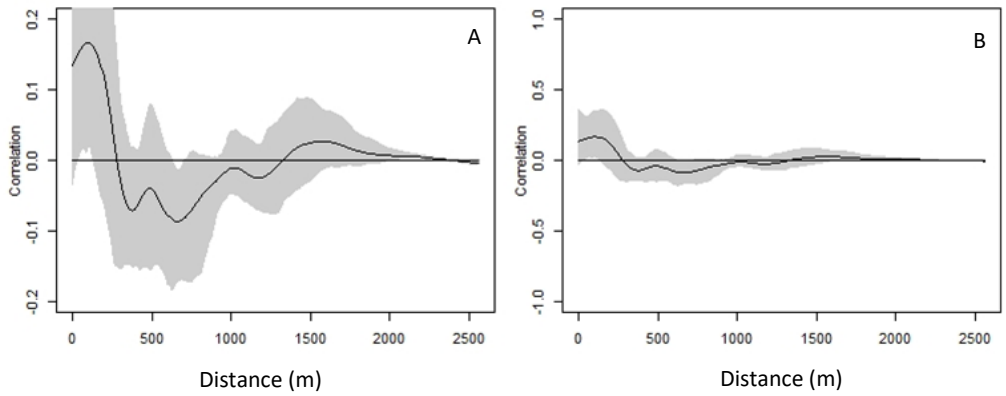

Appendix 2.7. Spatial autocorrelation tested with spline correlograms for *Lophelia pertusa* models based upon 5 m resolution dataset. Grey area indicates 95% confidence intervals.

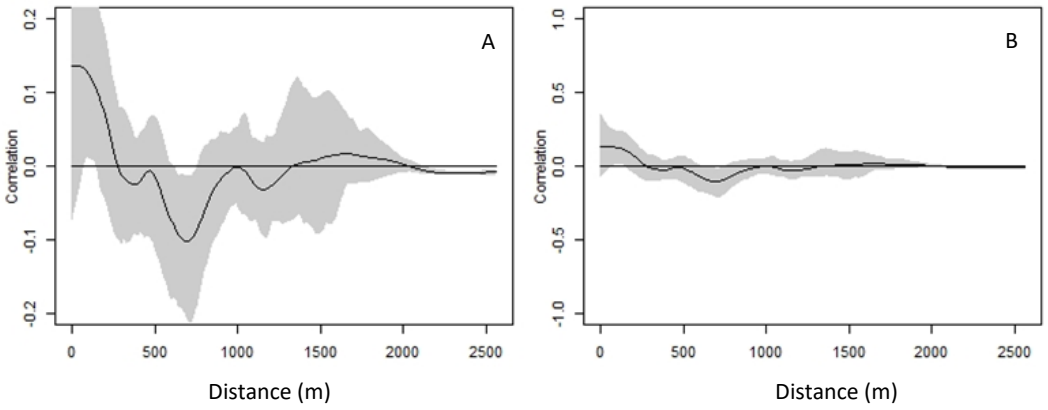

Appendix 2.8. Spatial autocorrelation tested with spline correlograms for *Madrepora oculata* models based upon 5 m resolution dataset. Grey area indicates 95% confidence intervals.

Appendix B Chapter 3

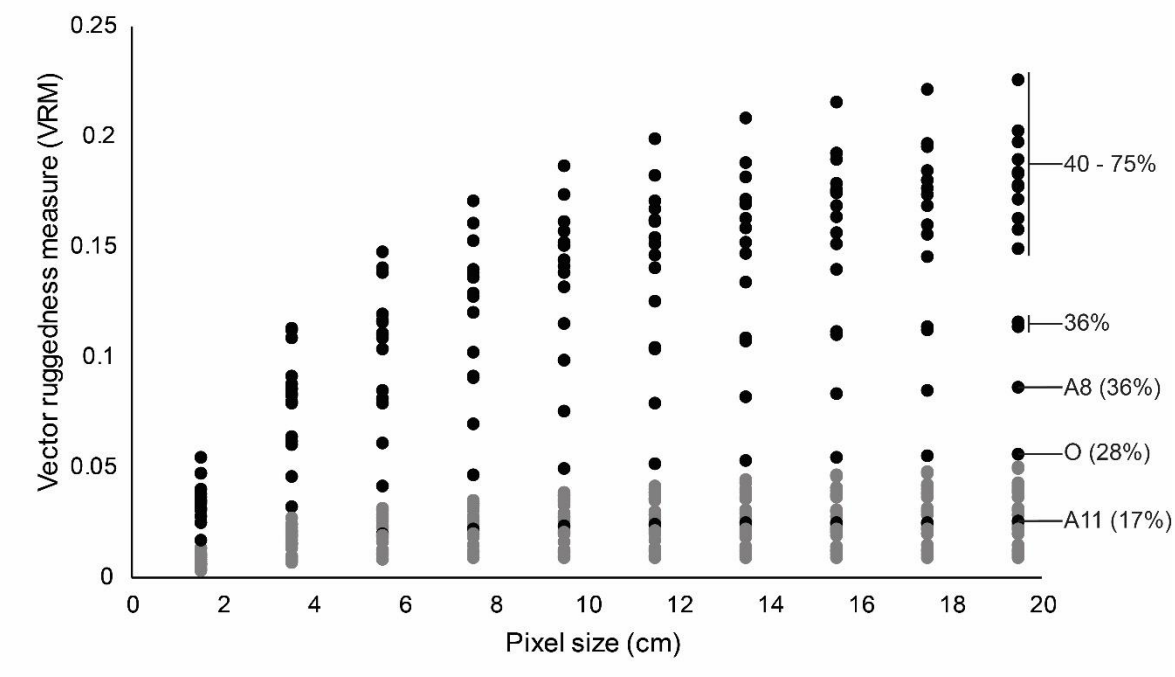

Appendix 3.1. Relationship between vector ruggedness measure and scale of neighbourhood size. Black circles depict transects that have more than 15% coral cover (both living and dead), with individual sub-transects and groups annotated with coral cover (%).

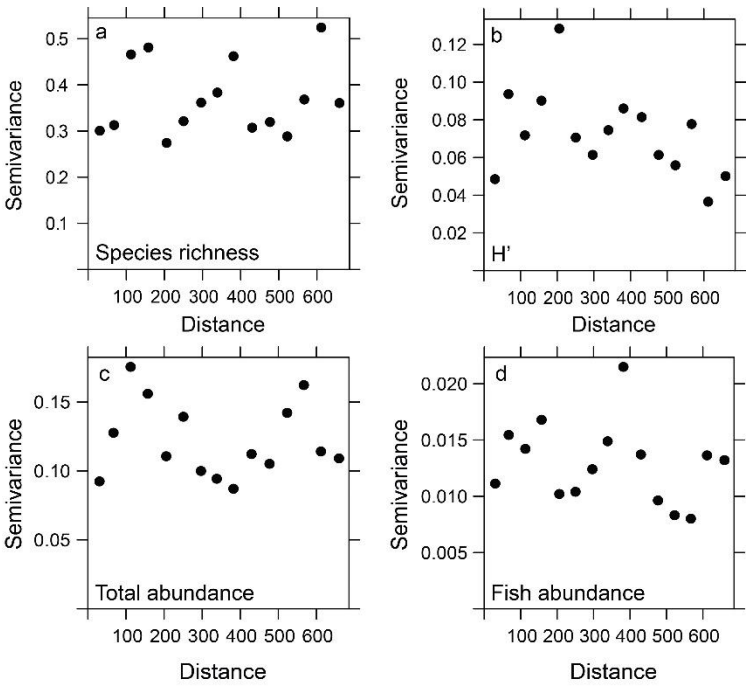

Appendix 3.2. Variogram outputs from fitted GAM model of univariate indices. If spatial autocorrelation existed within the model, an upward trend would be observed at low distances.

Appendix B

Despite the potential of spatial autocorrelation in our survey design (continuous sub-transects), the inclusion of Depth as a variable which is strongly linked with latitude, likely accounted for this in the model.

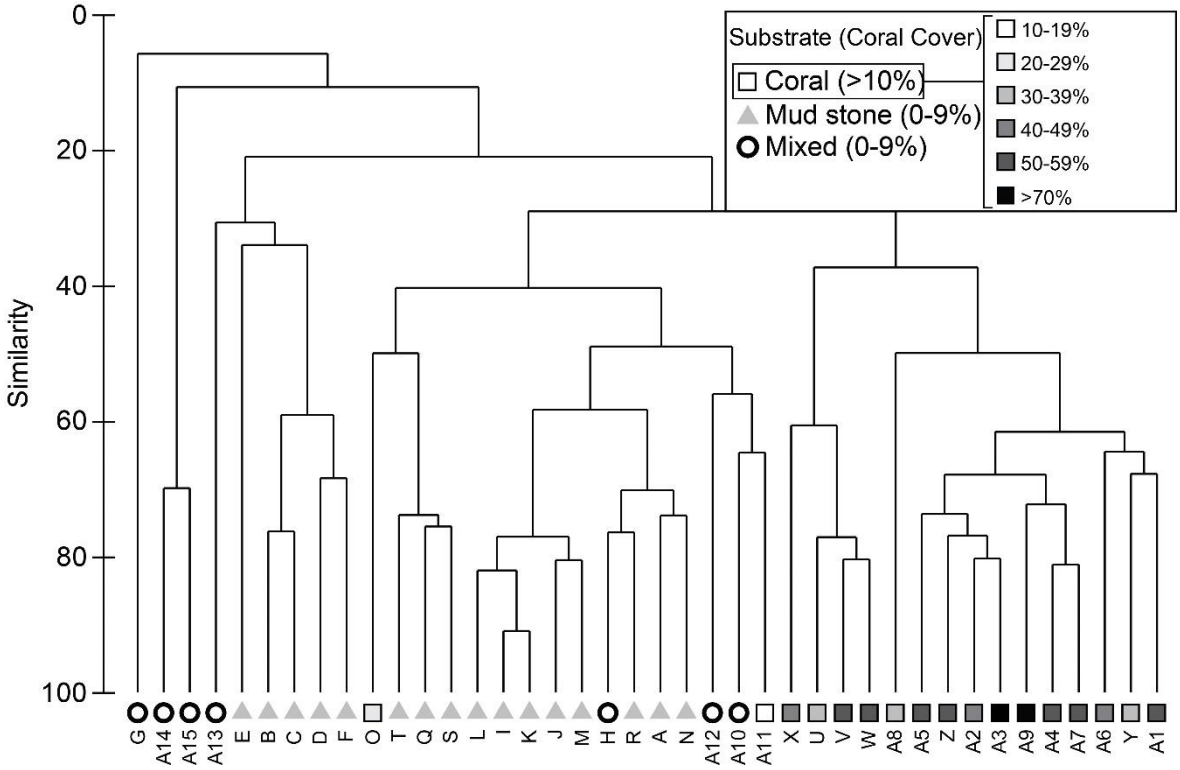

Appendix 3.3. Dendrogram of sub-transect communities based on group average similarity.

Appendix 3.4. Significance of smooth terms for Species richness GAM including sub-transect length (Species richness = VRM + Depth + sub-transect length). *** p<0.001 *p<0.05

Variable	edf	Ref.df	Chi.sq	p-value
VRM	2.244	2.812	16.892	0.000708***
Depth	4.491	5.439	10.904	0.048456*
Sub-transect length	1	1	2.067	0.150495

Appendix C Chapter 4

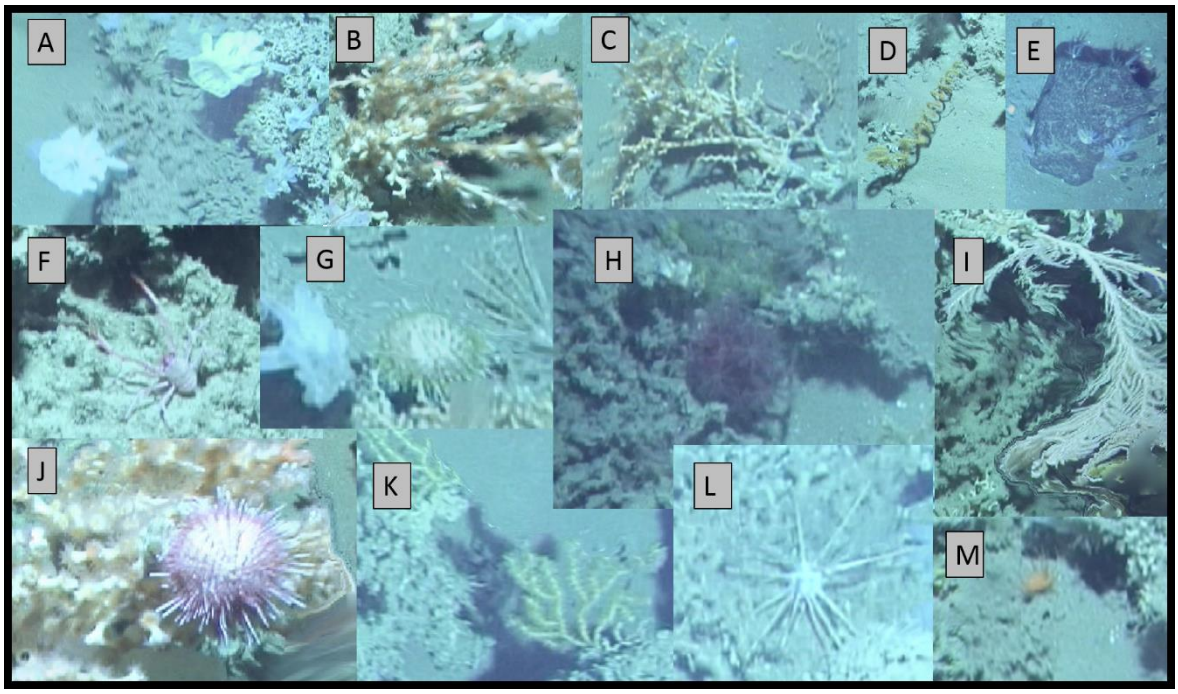

Appendix 4.1. Images of all species. A) *Aphrocallistes* sp. B) *Lophelia pertusa* C) *Madrepora oculata* D) *Stichopathes* sp. E) *Psolus* sp. F) Galatheoidae sp. G) *Gracilechinus* sp. "green" H) *Anthomastus* sp. I) *Callogorgia* sp. J) *Gracilechinus* sp. "pink" K) Alcyonacea spp. L) *Cidaris cidaris* M) Zoanthidae sp.

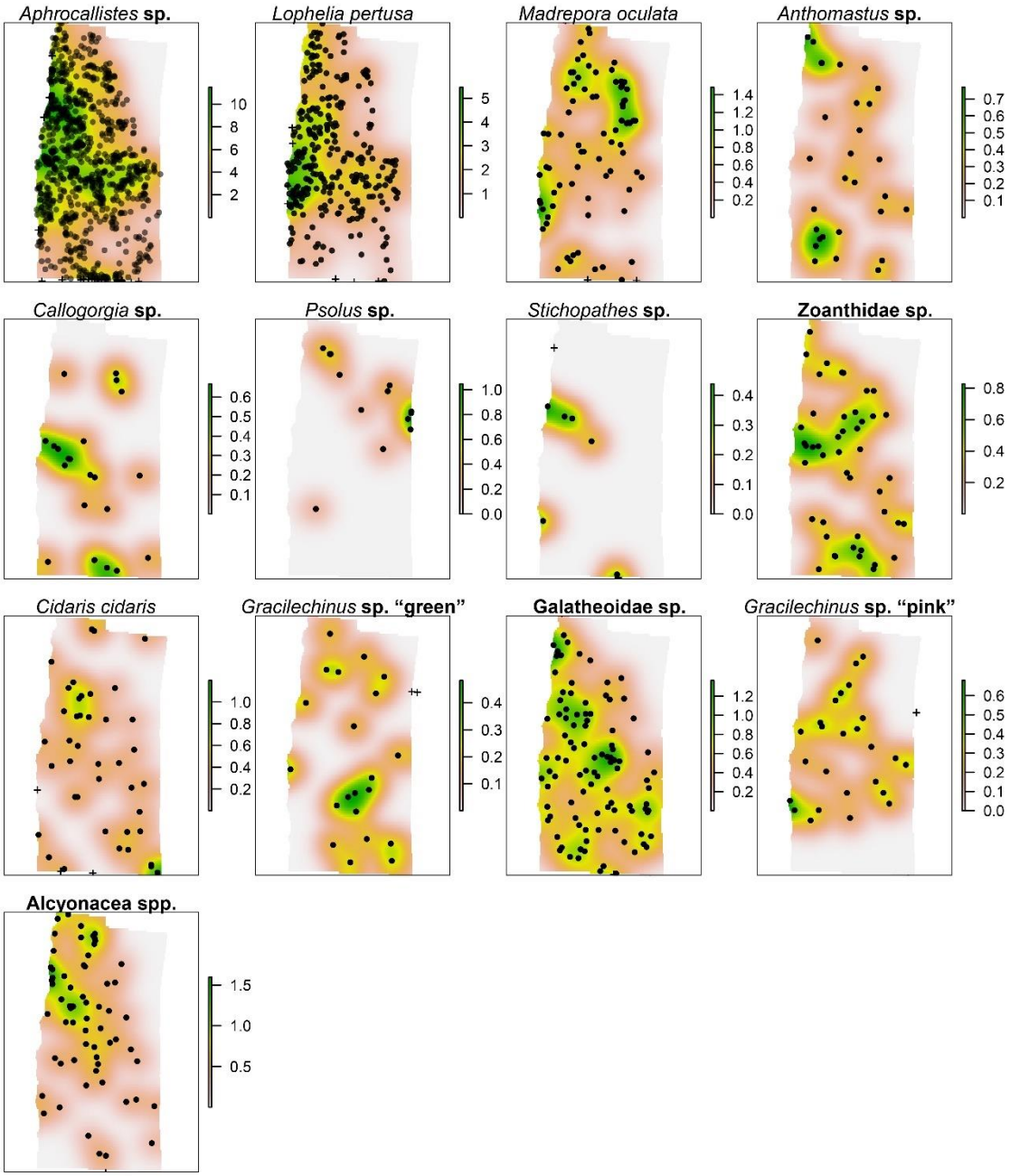

Appendix 4.2. Kernel density plots for all species at A Site A.

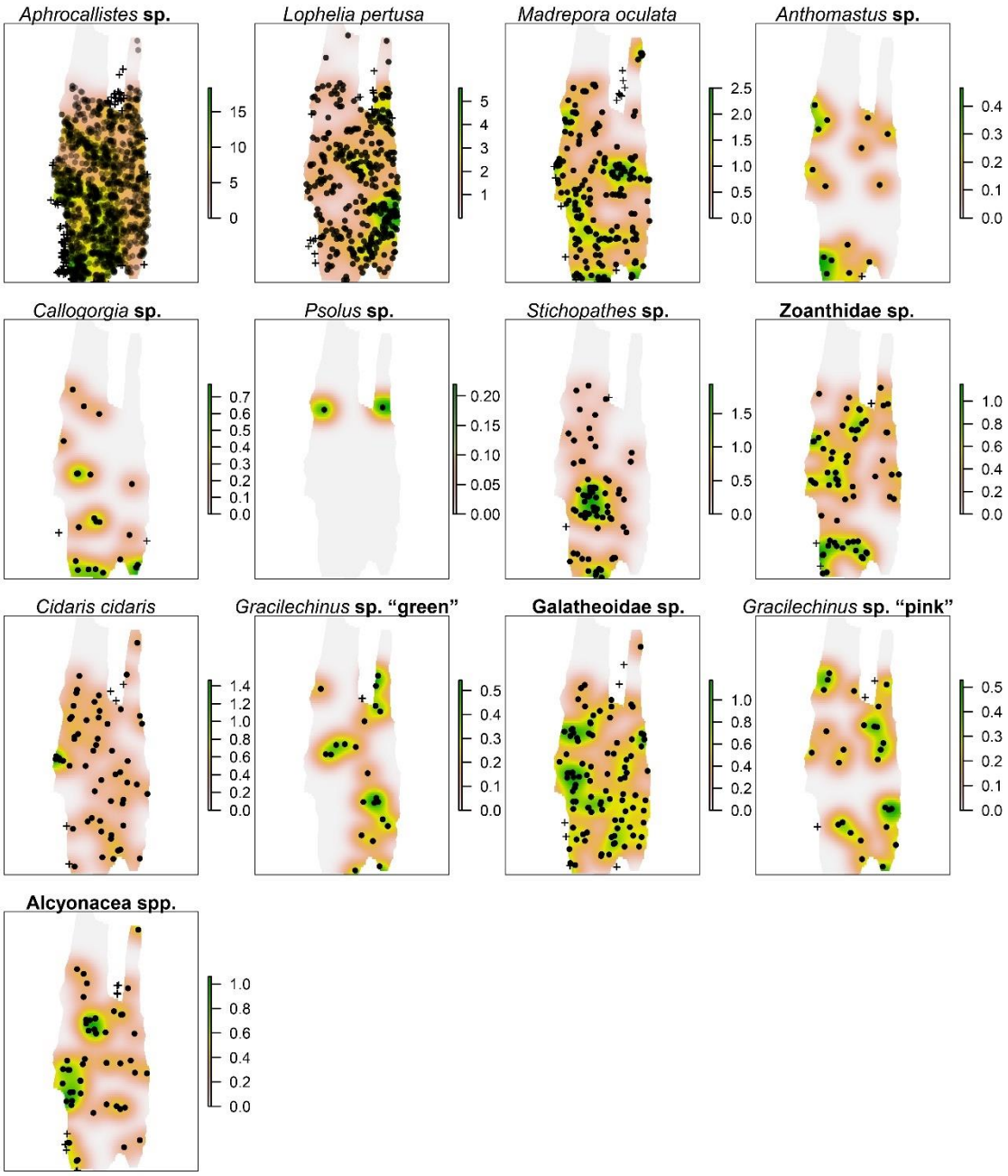

Appendix 4.3. Kernel density plots for all species at Site B.

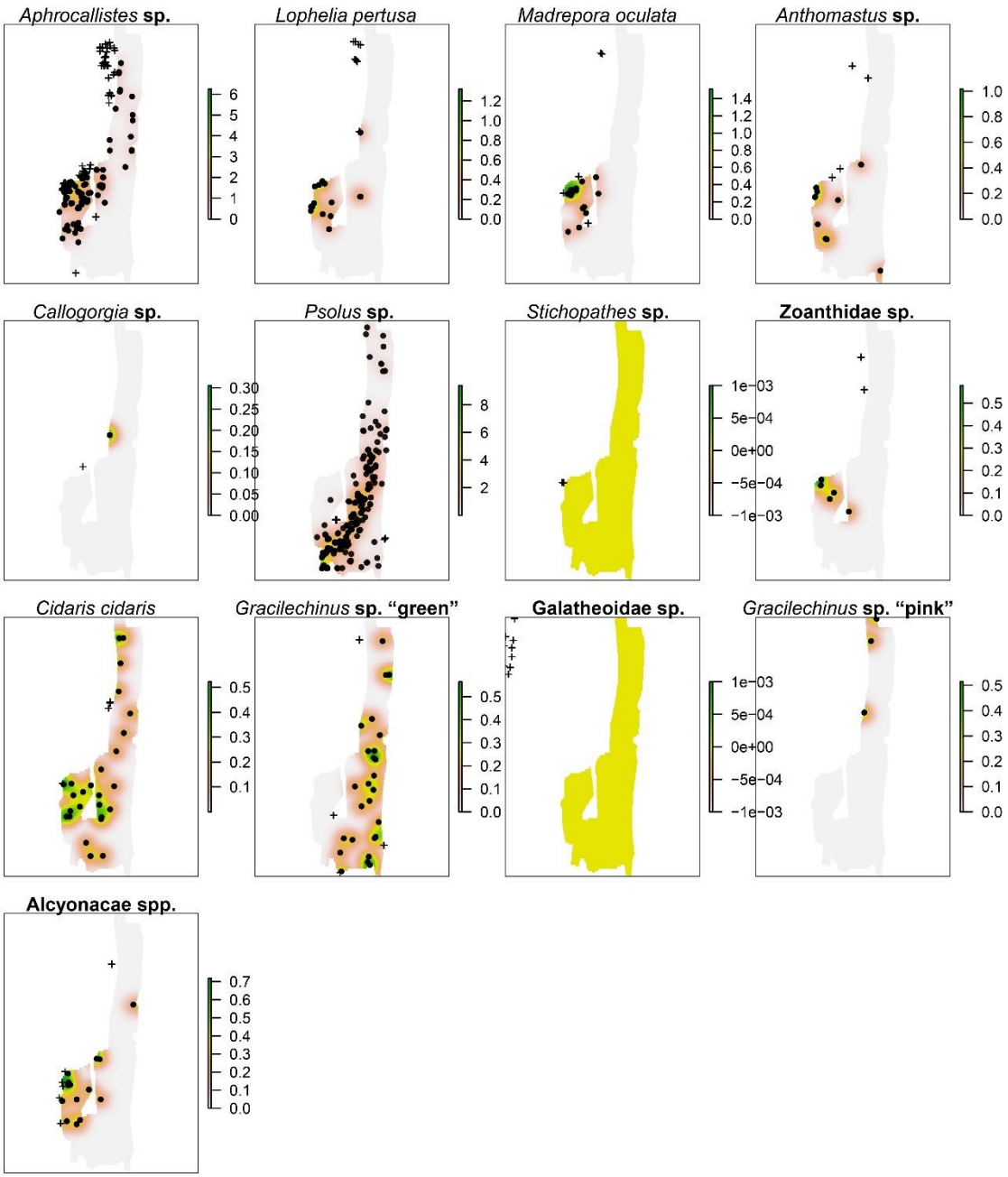

Appendix 4.4. Kernel density plots for all species at Site C.

Appendix 4.5. Results from chi squared goodness of fit test. Bold indicates P<0.05.

	Site A						Site B						Site C					
	0.5 (820 df)		1 (219 df)		2 (df: 54)		0.5 (df: 1047)		1 (df: 285)		2 (df: 87)		0.5(df: 1103)		1 (df: 308)		2 (df: 83)	
	X^2	P-values	X^2	P-values	X^2	P-values	X^2	P-values	X^2	P-values	X^2	P-values	X^2	P-values	X^2	P-values	X^2	P-values
Alcyonacea spp	**951**	**0.002**	260	0.058	**92**	**0.002**	**1191**	**0.003**	**371**	**<0.001**	**139**	**<0.001**	1117	0.755	**361**	**0.04**	**117**	**0.018**
Aphrocallistes sp.	**1945**	**<0.001**	**823**	**<0.001**	**484**	**<0.001**	**2413**	**<0.001**	**1186**	**<0.001**	**784**	**<0.001**	**1988**	**<0.001**	**1093**	**<0.001**	**626**	**<0.001**
Anthomastus sp.	**934**	**0.005**	235	0.45	**94**	**0.001**	**949**	**0.028**	**232**	**0.0196**	72	0.231	**1834**	**<0.001**	**753**	**<0.001**	**123**	**0.006**
Callogorgia sp.	888	0.099	**312**	**<0.001**	**80**	**0.025**	**1203**	**0.001**	331	0.065	**125**	**0.009**						
Cidaris cidaris	791	0.483	226	0.7	67	0.224	1010	0.424	309	0.323	89	0.825	**966.6**	**<0.002**	275.6	0.185	66	0.17
Galatheoidae sp.	796	0.208	233	0.473	72	0.111	1113	0.155	302	0.458	87	0.946						
Gracilechinus (G)	763	0.156	196	0.272	43	0.266	1084	0.417	295	0.665	94	0.582	1092.1	0.828	**402.5**	**<0.001**	78	0.728
Gracilechinus (P)	765	0.168	188	0.128	65	0.288	1023	0.56	327	0.086	81	0.663						
Psolus sp.	**953**	**0.002**	**564**	**<0.001**	**81**	**0.02**							**4003**	**<0.001**	**1645**	**<0.001**	**1031**	**<0.001**
Lophelia pertusa	**1139**	**<0.001**	**470**	**<0.001**	**237**	**<0.001**	**1479**	**<0.001**	**599**	**<0.001**	**313**	**<0.001**	**1653**	**<0.001**	**853**	**<0.001**	**154**	**<0.001**
Madrepora oculata	**998**	**<0.001**	**269**	**0.025**	**87**	**0.006**	**1432**	**<0.001**	**584**	**<0.001**	**154**	**<0.001**	**1445**	**<0.001**	**572**	**<0.001**	**186**	**<0.001**
Stichopathes sp.	**1115**	**<0.001**	**318**	**<0.001**	64	0.319	**1229**	**<0.001**	**455**	**<0.001**	**183**	**<0.001**						
Zoanthidae sp.	870	0.216	210	0.693	68	0.1907	1118	0.126	284	0.975	112	0.078						

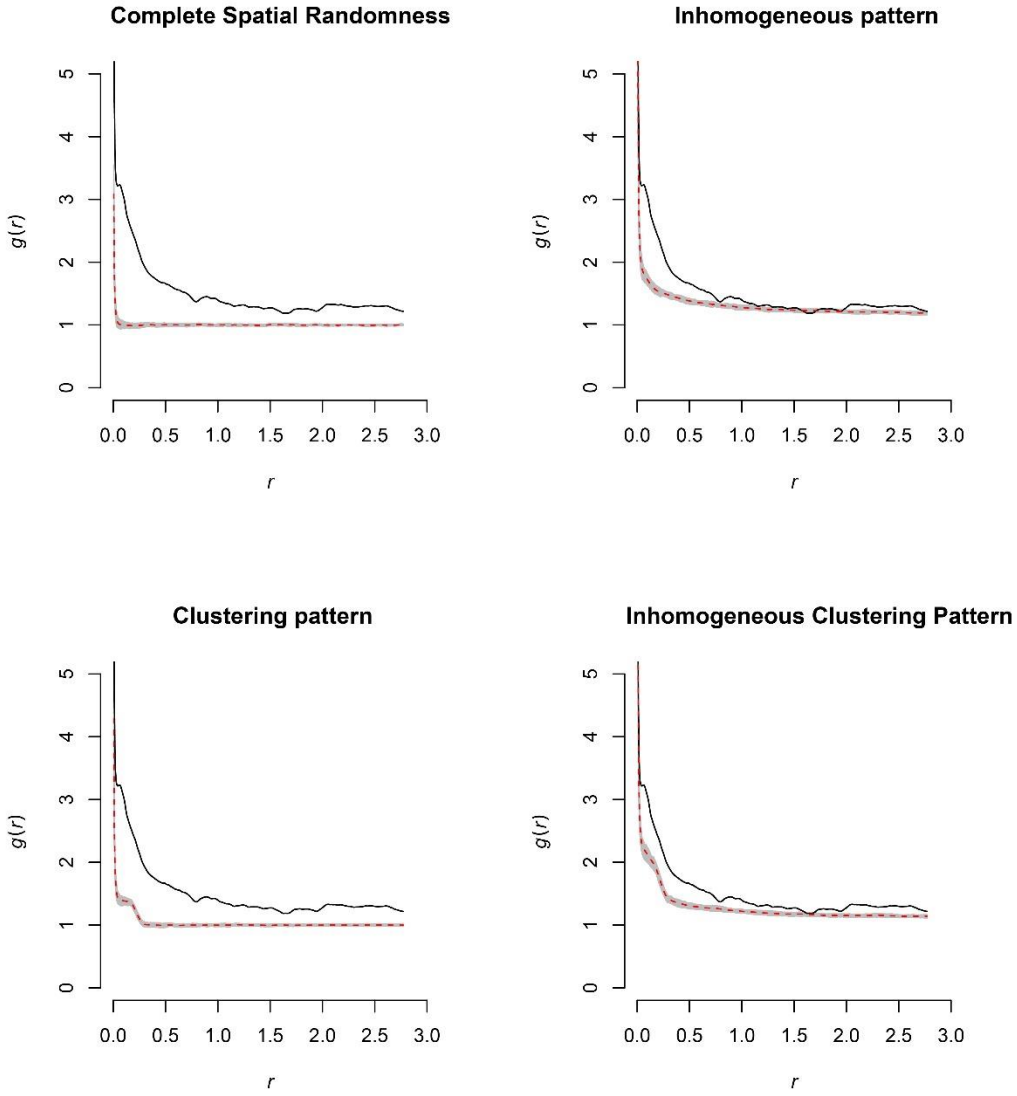

Appendix. 4.6. PCF of *Aphrocallistes* sp. at Site A compared to the null models representing CSR, IP, CP and ICP.

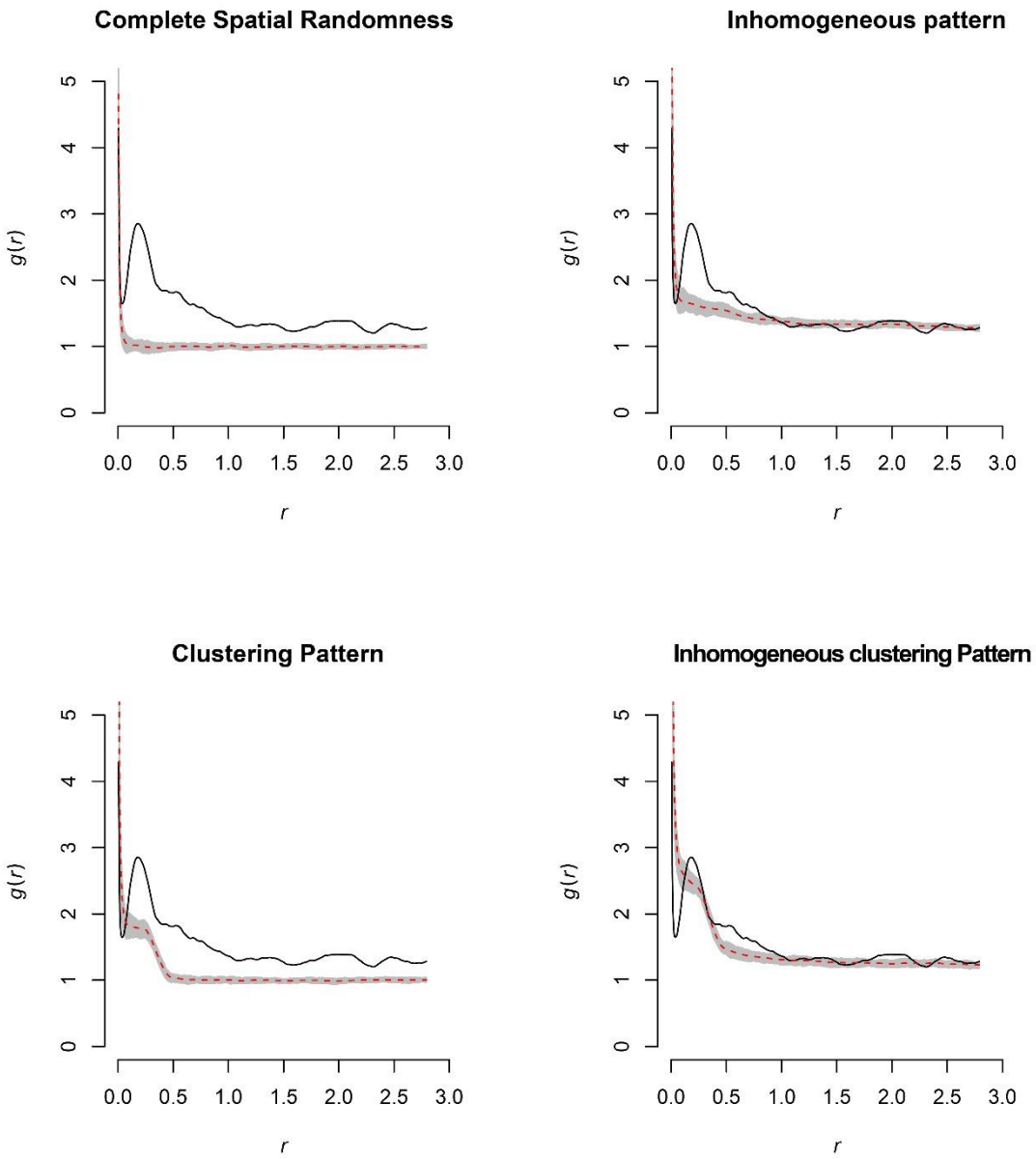

Appendix 4.7. PCF of *Lophelia pertusa* at Site A compared to the null models representing CSR, IP, CP and ICP.

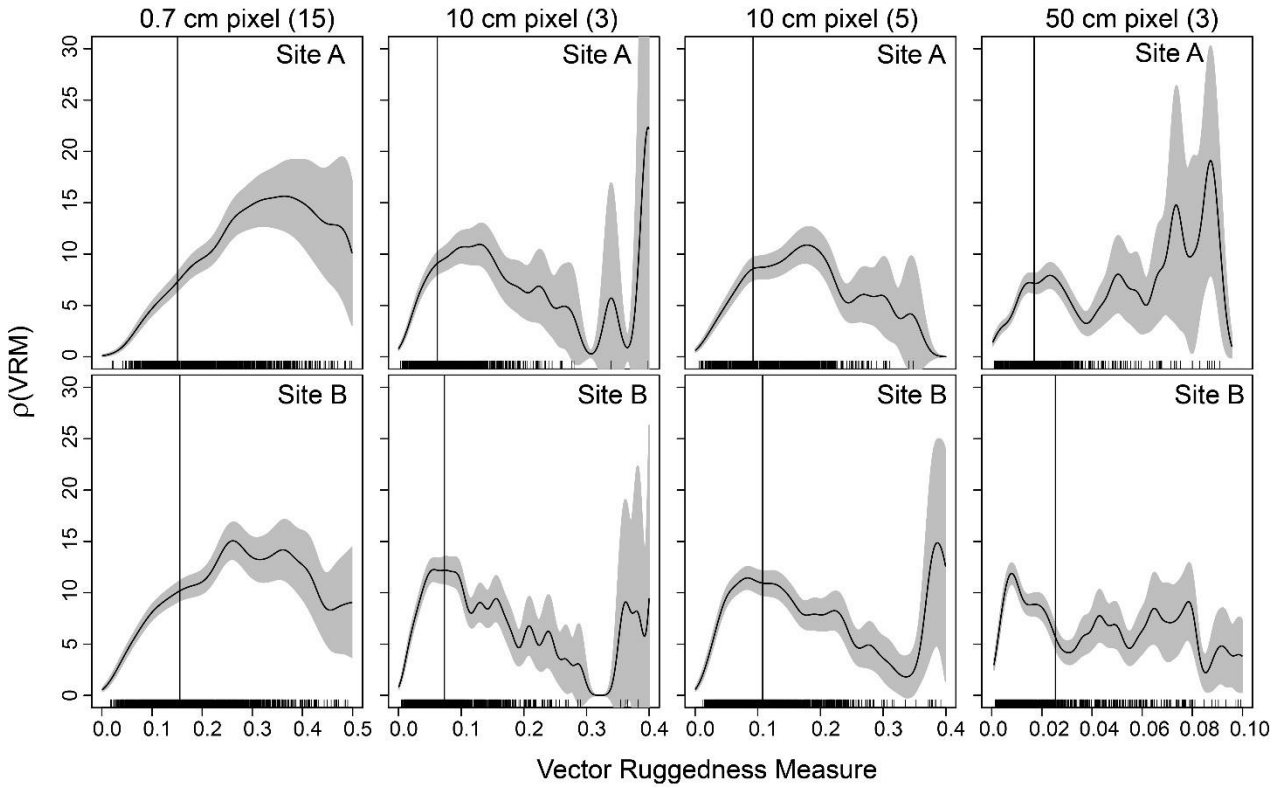

Appendix 4.8. Estimated function ρ(VRM) giving the estimated *Aphrocallistes* sp. intensity as a function of Vector Ruggedness Measure (VRM) at Site A. VRM was calculated at multiple resolutions and neighbourhood scales (indicated in brackets following pixel size). Vertical solid line represents the mean VRM value of the reef substrate.

Appendix E Research papers co-authored during the course of this PhD

Lim, A., Wheeler, A. J., Price, D. M., O'Reilly, L., Harris, K., & Conti, L. 2020. Influence of benthic currents on cold-water coral habitats: a combined benthic monitoring and 3D photogrammetric investigation. Scientific Reports, 10(1), 1-15.

Haalboom, S., Price, D. M., Mienis, F., Van Bleijswijk, J. D., Stigter, H. C. D., Witte, H. J., ... & Duineveld, G. C. 2020. Patterns of (trace) metals and microorganisms in the Rainbow hydrothermal vent plume at the Mid-Atlantic Ridge. Biogeosciences, 17(9), 2499-2519.

Clare, M. A., Le Bas, T., Price, D. M., Hunt, J. E., Sear, D., Cartigny, M. J., ... & Cronin, S. 2018. Complex and cascading triggering of submarine landslides and turbidity currents at volcanic islands revealed from integration of high-resolution onshore and offshore surveys. Frontiers in Earth Science, 6, 223.

List of References

Addamo, A.M., Vertino, A., Stolarski, J., García-Jiménez, R., Taviani, M., Machordom, A., 2016. Merging scleractinian genera: the overwhelming genetic similarity between solitary *Desmophyllum* and colonial *Lophelia*. BMC evolutionary biology 16, 108.

Allee, W.C., 1927. Animal aggregations. The Quarterly Review of Biology 2, 367-398.

Althaus, F., Williams, A., Schlacher, T.A., Kloser, R.J., Green, M.A., Barker, B.A., Bax, N.J., Brodie, P., Schlacher-Hoenlinger, M.A., 2009. Impacts of bottom trawling on deep-coral ecosystems of seamounts are long-lasting. Mar Ecol Prog Ser 397, 279-294.

Amaro, T., Huvenne, V.A.I., Allcock, A.L., Aslam, T., Davies, J.S., Danovaro, R., De Stigter, H.C., Duineveld, G.C.A., Gambi, C., Gooday, A.J., Gunton, L.M., Hall, R., Howell, K.L., Ingels, J., Kiriakoulakis, K., Kershaw, C.E., Lavaleye, M.S.S., Robert, K., Stewart, H., Van Rooij, D., White, M., Wilson, A.M., 2016. The Whittard Canyon - A case study of submarine canyon processes. Progress in Oceanography 146, 38-57.

Anderson, O.F., Guinotte, J.M., Rowden, A.A., Clark, M.R., Mormede, S., Davies, A.J., Bowden, D.A., 2016. Field validation of habitat suitability models for vulnerable marine ecosystems in the South Pacific Ocean: Implications for the use of broad-scale models in fisheries management. Ocean Coast Manage 120, 110-126.

Anderson, O.F., Guinotte, J.M., Rowden, A.A., Tracey, D.M., Mackay, K.A., Clark, M.R., 2016. Habitat suitability models for predicting the occurrence of vulnerable marine ecosystems in the seas around New Zealand. Deep-Sea Res Pt I 115, 265-292.

Arnaud-Haond, S., van den Beld, I.M.J., Becheler, R., Orejas, C., Menot, L., Frank, N., Grehan, A., Bourillet, J.F., 2017. Two "pillars" of cold-water coral reefs along Atlantic European margins: Prevalent association of *Madrepora oculata* with *Lophelia pertusa*, from reef to colony scale. Deep-Sea Res Pt Ii 145, 110-119.

Aslam, T., Hall, R.A., Dye, S.R., 2018. Internal tides in a dendritic submarine canyon. Progress in Oceanography 169, 20-32.

Auster, P.J., 2005. Are deep-water corals important habitats for fishes?. In Cold-water corals and ecosystems (747-760). Springer, Berlin, Heidelberg.

Baco, A.R., Morgan, N., Roark, E.B., Silva, M., Shamberger, K.E.F., Miller, K., 2017. Defying Dissolution: Discovery of Deep-Sea Scleractinian Coral Reefs in the North Pacific. Sci Rep-Uk 7.

Baco-Taylor, A., Ross, R., Althaus, F., Bridges, A., Brix, S., Colaço, A., Clark, M.R., Du Preez, C., Franken, M.L., Gonzalez-Mirelis, G., Kenchington, E., Levin, L.A., Lindsay, D., Molodtsova, T., Morgan, N., Morato, T., Meija-Mercado, B.E., O'sullivan, D., Olu, K., Pearman, T.R.R., Price, D.M., Robert, K., Rowden, A.A., 2020, Taylor, J., Victorero, L., Watling, L., Williams, A., Yesson, C., 2020. A Community Consensus on Designating Vulnerable Marine Ecosystems From Imagery. In Ocean Sciences Meeting 2020. AGU.

Baddeley, A., Rubak, E., Turner, R., 2015. Spatial Point Patterns: Methodology and Applications with R. Chap Hall Crc Interd, 1-810.

Barbosa, R., Davies, A., Sumida, P., 2019. Habitat suitability and environmental niche comparison of cold-water coral species along the Brazilian continental margin. Deep Sea Research Part I: Oceanographic Research Papers, 103147.

Bargain, A., Foglini, F., Pairaud, I., Bonaldo, D., Carniel, S., Angeletti, L., Taviani, M., Rochette, S., Fabri, M.C., 2018. Predictive habitat modeling in two Mediterranean canyons including hydrodynamic variables. Progress in Oceanography 169, 151-168.

Barnett, T.P., Pierce, D.W., AchutaRao, K.M., Gleckler, P.J., Santer, B.D., Gregory, J.M., Washington, W.M., 2005. Penetration of human-induced warming into the world's oceans. Science 309, 284-287.

Bas, T.P., 2016. RSOBIA-A new OBIA Toolbar and Toolbox in ArcMap 10. x for Segmentation and Classification.

Bayley, D.T.I., Mogg, A.O.M., Koldewey, H., Purvis, A., 2019. Capturing complexity: field-testing the use of 'structure from motion' derived virtual models to replicate standard measures of reef physical structure. Peerj 7.

Bennecke, S., Kwasnitschka, T., Metaxas, A., Dullo, W.C., 2016. In situ growth rates of deep-water octocorals determined from 3D photogrammetric reconstructions. Coral Reefs 35, 1227-1239.

Benoist, N.M.A., Morris, K.J., Sett, B.J., Durden, J.M., Huvenne, V.A.I., Le Sas, T.P., Wynn, R.B., Ware, S.J., Ruhl, H.A., 2019. Monitoring mosaic biotopes in a marine conservation zone by autonomous underwater vehicle. Conserv Biol 33, 1174-1186.

Beuck, L., Vertino, A., Stepina, E., Karolczak, M., Pfannkuche, O., 2007. Skeletal response of Lophelia pertusa (Scleractinia) to bioeroding sponge infestation visualised with micro-computed tomography. Facies 53, 157-176.

Biber, M.F., Duineveld, G.C.A., Lavaleye, M.S.S., Davies, A.J., Bergman, M.J.N., van den Beld, I.M.J., 2014. Investigating the association of fish abundance and biomass with cold-water corals in the deep Northeast Atlantic Ocean using a generalised linear modelling approach. Deep-Sea Res Pt Ii 99, 134-145.

Boavida, J., Becheler, R., Choquet, M., Frank, N., Taviani, M., Bourillet, J.F., Meistertzheim, A.L., Grehan, A., Savini, A., Arnaud-Haond, S., 2019. Out of the Mediterranean? Post-glacial colonization pathways varied among cold-water coral species. J Biogeogr 46, 915-931.

Bongiorni, L., Mea, M., Gambi, C., Pusceddu, A., Taviani, M., Danovaro, R., 2010. Deep-water scleractinian corals promote higher biodiversity in deep-sea meiofaunal assemblages along continental margins. Biol Conserv 143, 1687-1700.

Boolukos, C.M., Lim, A., O'Riordan, R.M., Wheeler, A.J., 2019. Cold-water corals in decline - A temporal (4 year) species abundance and biodiversity appraisal of complete photomosaiced cold-water coral reef on the Irish Margin. Deep-Sea Res Pt I 146, 44-54.

Boswarva, K.L., Howe, J.A., Obando, R., Fox, C., Narayanaswamy, B.E., Haussermann, V., Abernethy, C., 2020. Habitat mapping in the fjords of the Chilean Patagonia using an autonomous underwater vehicle. Seafloor Geomorphology as Benthic Habitat: Geohab Atlas of Seafloor Geomorphic Features and Benthic Habitats, 2nd Edition, 337-353.

Bourque, J.R., Demopoulos, A.W.J., 2018. The influence of different deep-sea coral habitats on sediment macrofaunal community structure and function. Peerj 6.

Bowen, A.D., Jakuba, M.V., Farr, N.E., Ware, J., Taylor, C., Gomez-Ibanez, D., Machado, C.R., Pontbriand, C., 2013. An un-tethered rov for routine access and intervention in the deep sea, 2013 oceans-san diego, IEEE, pp. 1-7.

Boxshall, A.J., 2000. The importance of flow and settlement cues to larvae of the abalone, Haliotis rufescens Swainson. J Exp Mar Biol Ecol 254, 143-167.

Brooke, S., Jarnegren, J., 2013. Reproductive periodicity of the scleractinian coral *Lophelia pertusa* from the Trondheim Fjord, Norway. Mar Biol 160, 139-153.

Brooke, S., Ross, S.W., 2014. First observations of the cold-water coral *Lophelia pertusa* in mid-Atlantic canyons of the USA. Deep-Sea Res Pt Ii 104, 245-251.

Brooke, S., Young, C.M., 2009. In situ measurement of survival and growth of *Lophelia pertusa* in the northern Gulf of Mexico. Mar Ecol Prog Ser 397, 153-161.

Brown, R.R., Davis, C.S., Leys, S.P., 2017. Clones or clans: the genetic structure of a deep-sea sponge, *Aphrocallistes vastus*, in unique sponge reefs of British Columbia, Canada. Mol Ecol 26, 1045-1059.

Bryson, M., Johnson-Roberson, M., Pizarro, O., Williams, S.B., 2013. Colour-consistent structure-from-motion models using underwater imagery. Robotics: Science and Systems VIII, 33.

Buhl-Mortensen, L., Vanreusel, A., Gooday, A.J., Levin, L.A., Priede, I.G., Buhl-Mortensen, P., Gheerardyn, H., King, N.J., Raes, M., 2010. Biological structures as a source of habitat heterogeneity and biodiversity on the deep ocean margins. Marine Ecology 31, 21-50.

Buhl-Mortensen, L., Olafsdottir, S.H., Buhl-Mortensen, P., Burgos, J.M. and Ragnarsson, S.A., 2015. Distribution of nine cold-water coral species (Scleractinia and Gorgonacea) in the cold temperate North Atlantic: effects of bathymetry and hydrography. Hydrobiologia, 759(1), 39-61.

Buhl-Mortensen, L., Serigstad, B., Buhl-Mortensen, P., Olsen, M.N., Ostrowski, M., Blazewicz-Paszkowycz, M., Appoh, E., 2017. First observations of the structure and megafaunal community of a large *Lophelia* reef on the Ghanaian shelf (the Gulf of Guinea). Deep-Sea Res Pt Ii 137, 148-156.

Burdon-Jones, C., Tambs-Lyche, H., 1960. Observations on the fauna of the North Brattholmen stone-coral reef near Bergen. Norwegian Universities Press.

Burns, J.H.R., Delparte, D., 2017. Comparison of Commercial Structure-from-Motion Photogrammety Software Used for Underwater Three-Dimensional Modeling of Coral Reef Environments. 3d Virtual Reconstruction and Visualization of Complex Architectures 42-2, 127-131.

Burns, J.H.R., Delparte, D., Gates, R.D., Takabayashi, M., 2015. Integrating structure-from-motion photogrammetry with geospatial software as a novel technique for quantifying 3D ecological characteristics of coral reefs. Peerj 3.

Buscher, J.V., Wisshak, M., Form, A.U., Titschack, J., Nachtigall, K., Riebesell, U., 2019. In situ growth and bioerosion rates of Lophelia pertusa in a Norwegian fjord and open shelf cold-water coral habitat. Peerj 7.

Cairns, S.D., 2007. Deep-water corals: An overview with special reference to diversity and distribution of deep-water Scleractinian corals. B Mar Sci 81, 311-322.

Cairns, S.D. and Hourigan, T.F., 2020. Deep-Sea Coral Taxa in the US Caribbean Region: Depth and Geographical Distribution. Order, 6, 73-567.

Carter, G.D., Huvenne, V.A., Gales, J.A., Iacono, C.L., Marsh, L., Ougier-Simonin, A., Robert, K., Wynn, R.B., 2018. Ongoing evolution of submarine canyon rockwalls; examples from the Whittard Canyon, Celtic Margin (NE Atlantic). Progress in Oceanography.

Casella, E., Collin, A., Harris, D., Ferse, S., Bejarano, S., Parravicini, V., Hench, J.L., Rovere, A., 2017. Mapping coral reefs using consumer-grade drones and structure from motion photogrammetry techniques. Coral Reefs 36, 269-275.

CBD, 2010. Convention on Biological Diversity Conference of the Parties (COP) 10 Decision X/29. Marine and Coastal Biodiversity.

Chamberlain, J.A., Graus, R.R., 1975. Water-Flow and Hydromechanical Adaptations of Branched Reef Corals. B Mar Sci 25, 112-125.

Chapron, L., Peru, E., Engler, A., Ghiglione, J.F., Meistertzheim, A.L., Pruski, A.M., Purser, A., Vetion, G., Galand, P.E., Lartaud, F., 2018. Macro- and microplastics affect cold-water corals growth, feeding and behaviour. Sci Rep-Uk 8.

Chirayath, V., Earle, S.A., 2016. Drones that see through waves - preliminary results from airborne fluid lensing for centimetre-scale aquatic conservation. Aquat Conserv 26, 237-250.

Chirayath, V., Instrella, R., 2019. Fluid lensing and machine learning for centimeter-resolution airborne assessment of coral reefs in American Samoa. Remote Sens Environ 235.

Collin, A., Dubois, S., James, D., Houet, T., 2019. Improving Intertidal Reef Mapping Using UAV Surface, Red Edge, and Near-Infrared Data. Drones 3, 67.

Condit, R., Ashton, P.S., Baker, P., Bunyavejchewin, S., Gunatilleke, S., Gunatilleke, N., Hubbell, S.P., Foster, R.B., Itoh, A., LaFrankie, J.V., Lee, H.S., Losos, E., Manokaran, N., Sukumar, R., Yamakura, T., 2000. Spatial patterns in the distribution of tropical tree species. Science 288, 1414-1418.

Conti, L.A., Lim, A., Wheeler, A.J., 2019. High resolution mapping of a cold water coral mound. Sci Rep-Uk 9.

Corbera, G., Lo Iacono, C., Gracia, E., Grinyo, J., Pierdomenico, M., Huvenne, V.A.I., Aguilar, R., Gili, J.M., 2019. Ecological characterisation of a Mediterranean cold-water coral reef: Cabliers Coral Mound Province (Alboran Sea, western Mediterranean). Progress in Oceanography 175, 245-262.

Cordes, E.E., McGinley, M.P., Podowski, E.L., Becker, E.L., Lessard-Pilon, S., Viada, S.T., Fisher, C.R., 2008. Coral communities of the deep Gulf of Mexico. Deep Sea Research Part I: Oceanographic Research Papers 55, 777-787.

Costello, M.J., McCrea, M., Freiwald, A., Lundalv, T., Jonsson, L., Bett, B.J., van Weering, T.C.E., de Haas, H., Roberts, J.M., Allen, D., 2005. Role of cold-water *Lophelia pertusa* coral reefs as fish habitat in the NE Atlantic. Erlangen Earth C Ser, 771-805.

Cyr, F., van Haren, H., Mienis, F., Duineveld, G., Bourgault, D., 2016. On the influence of cold-water coral mound size on flow hydrodynamics, and vice versa. Geophys Res Lett 43, 775-783.

Dahl, M.P., Pereyra, R.T., Lundalv, T., Andre, C., 2012. Fine-scale spatial genetic structure and clonal distribution of the cold-water coral Lophelia pertusa. Coral Reefs 31, 1135-1148.

Dana, T.F., 1976. Reef-Coral Dispersion Patterns and Environmental Variables on a Caribbean Coral-Reef. B Mar Sci 26, 1-13.

Davies, A.J., Duineveld, G.C.A., Lavaleye, M.S.S., Bergman, M.J.N., van Haren, H., Roberts, J.M., 2009. Downwelling and deep-water bottom currents as food supply mechanisms to the cold-water coral *Lophelia pertusa* (Scleractinia) at the Mingulay Reef complex. Limnol Oceanogr 54, 620-629.

Davies, A.J., Duineveld, G.C.A., van Weering, T.C.E., Mienis, F., Quattrini, A.M., Seim, H.E., Bane, J.M., Ross, S.W., 2010. Short-term environmental variability in cold-water coral habitat at Viosca Knoll, Gulf of Mexico. Deep-Sea Res Pt I 57, 199-212.

Davies, A.J., Guinotte, J.M., 2011. Global Habitat Suitability for Framework-Forming Cold-Water Corals. Plos One 6.

Davies, A.J., Roberts, J.M., Hall-Spencer, J., 2007. Preserving deep-sea natural heritage: Emerging issues in offshore conservation and management. Biol Conserv 138, 299-312.

Davies, A.J., Wisshak, M., Orr, J.C., Roberts, J.M., 2008. Predicting suitable habitat for the cold-water coral *Lophelia pertusa* (Scleractinia). Deep-Sea Res Pt I 55, 1048-1062.

Davies, J.S., Guillaumont, B., Tempera, F., Vertino, A., Beuck, L., Olafsdottir, S.H., Smith, C.J., Fossa, J.H., van den Beld, I.M.J., Savini, A., Rengstorf, A., Bayle, C., Bourillet, J.F., Arnaud-Haond, S., Grehan, A., 2017. A new classification scheme of European cold-water coral habitats: Implications for ecosystem-based management of the deep sea. Deep-Sea Res Pt Ii 145, 102-109.

Davies, J.S., Howell, K.L., Stewart, H.A., Guinan, J., Golding, N., 2014. Defining biological assemblages (biotopes) of conservation interest in the submarine canyons of the South West Approaches (offshore United Kingdom) for use in marine habitat mapping. Deep Sea Research Part II: Topical Studies in Oceanography 104, 208-229.

De Clippele, L.H., Gafeira, J., Robert, K., Hennige, S., Lavaleye, M.S., Duineveld, G.C.A., Huvenne, V.A.I., Roberts, J.M., 2017. Using novel acoustic and visual mapping tools to predict the small-scale spatial distribution of live biogenic reef framework in cold-water coral habitats. Coral Reefs 36, 255-268.

De Clippele, L.H., Huvenne, V.A., Molodtsova, T.N., Roberts, J.M., 2019. The Diversity and Ecological Role of Non-scleractinian Corals (Antipatharia and Alcyonacea) on Scleractinian Cold-Water Coral Mounds. Frontiers in Marine Science 6.

De Clippele, L.H., Huvenne, V.A.I., Orejas, C., Lundalv, T., Fox, A., Hennige, S.J., Roberts, J.M., 2018. The effect of local hydrodynamics on the spatial extent and morphology of cold-water coral habitats at Tisler Reef, Norway. Coral Reefs 37, 253-266.

De Mol, B., Henriet, J.-P., Canals, M., 2005. Development of coral banks in Porcupine Seabight: do they have Mediterranean ancestors?, Erlangen Earth C Ser, Springer, pp. 515-533.

De Mol, B., Van Rensbergen, P., Pillen, S., Van Herreweghe, K., Van Rooij, D., McDonnell, A., Huvenne, V., Ivanov, M., Swennen, R., Henriet, J., 2002. Large deep-water coral banks in the Porcupine Basin, southwest of Ireland. Mar Geol 188, 193-231.

De Mol, L., Van Rooij, D., Pirlet, H., Greinert, J., Frank, N., Quemmerais, F., Henriet, J.P., 2011. Cold-water coral habitats in the Penmarc'h and Guilvinec Canyons (Bay of Biscay): Deep-water versus shallow-water settings. Mar Geol 282, 40-52.

Dodds, L.A., Roberts, J.M., Taylor, A.C., Marubini, F., 2007. Metabolic tolerance of the cold-water coral *Lophelia pertusa* (Scleractinia) to temperature and dissolved oxygen change. J Exp Mar Biol Ecol 349, 205-214.

Dolan, M.F.J., Grehan, A.J., Guinan, J.C., Brown, C., 2008. Modelling the local distribution of cold-water corals in relation to bathymetric variables: Adding spatial context to deep-sea video data. Deep-Sea Res Pt I 55, 1564-1579.

D'Onghia, G., Maiorano, P., Carlucci, R., Capezzuto, F., Carluccio, A., Tursi, A., Sion, L., 2012. Comparing Deep-Sea Fish Fauna between Coral and Non-Coral "Megahabitats" in the Santa Maria di Leuca Cold-Water Coral Province (Mediterranean Sea). Plos One 7.

Dons, C., 1934. Zoologische Notizen XXV. Über die nördlichsten Korallenriffe der Welt. Det Kongelige Norske Videnskabers Selskab, Forhandl 6, 206-209.

Dorschel, B., Hebbeln, D., Foubert, A., White, M., Wheeler, A.J., 2007. Hydrodynamics and cold-water coral facies distribution related to recent sedimentary processes at Galway Mound west of Ireland. Mar Geol 244, 184-195.

Dove, D., Weijerman, M., Grüss, A., Acoba, T., Smith, J., 2020. Substrate mapping to inform ecosystem science and marine spatial planning around the main Hawaiian Islands, Seafloor Geomorphology as Benthic Habitat, Elsevier, pp. 619-640.

Dragut, L., Tiede, D., Levick, S.R., 2010. ESP: a tool to estimate scale parameter for multiresolution image segmentation of remotely sensed data. Int J Geogr Inf Sci 24, 859-871.

Du Preez, C., Swan, K.D., Curtis, J.M.R., 2020. Cold-Water Corals and Other Vulnerable Biological Structures on a North Pacific Seamount After Half a Century of Fishing. Frontiers in Marine Science 7.

Duineveld, G.C.A., Jeffreys, R.M., Lavaleye, M.S.S., Davies, A.J., Bergman, M.J.N., Watmough, T., Witbaard, R., 2012. Spatial and tidal variation in food supply to shallow cold-water coral reefs of the Mingulay Reef complex (Outer Hebrides, Scotland). Mar Ecol Prog Ser 444, 97-115.

Duineveld, G.C.A., Lavaleye, M.S.S., Berghuis, E.M., 2004. Particle flux and food supply to a seamount cold-water coral community (Galicia Bank, NW Spain). Mar Ecol Prog Ser 277, 13-23.

Duineveld, G.C.A., Lavaleye, M.S.S., Bergman, M.I.N., De Stigter, H., Mienis, F., 2007. Trophic structure of a cold-water coral mound community (Rockall Bank, NE Atlantic) in relation to the near-bottom particle supply and current regime. B Mar Sci 81, 449-467.

Dullo, W.C., Flogel, S., Ruggeberg, A., 2008. Cold-water coral growth in relation to the hydrography of the Celtic and Nordic European continental margin. Mar Ecol Prog Ser 371, 165-176.

Dunn, D.C., Halpin, P.N., 2009. Rugosity-based regional modeling of hard-bottom habitat. Mar Ecol Prog Ser 377, 1-11.

Eccles, N.S., Esler, K.J., Cowling, R.M., 1999. Spatial pattern analysis in Namaqualand desert plant communities: evidence for general positive interactions. Plant Ecol 142, 71-85.

Edwards, C.B., Eynaud, Y., Williams, G.J., Pedersen, N.E., Zgliczynski, B.J., Gleason, A.C.R., Smith, J.E., Sandin, S.A., 2017. Large-area imaging reveals biologically driven non-random spatial patterns of corals at a remote reef. Coral Reefs 36, 1291-1305.

Fabri, M.C., Pedel, L., Beuck, L., Galgani, F., Hebbeln, D., Freiwald, A., 2014. Megafauna of vulnerable marine ecosystems in French mediterranean submarine canyons: Spatial distribution and anthropogenic impacts. Deep-Sea Res Pt Ii 104, 184-207.

Fabri, M.C., Vinha, B., Allais, A.G., Bouhier, M.E., Dugornay, O., Gaillot, A., Arnaubec, A., 2019. Evaluating the ecological status of cold-water coral habitats using non-invasive methods: An example from Cassidaigne canyon, northwestern Mediterranean Sea. Progress in Oceanography 178.

FAO, 2009. International Guidelines for the Management of Deep-Sea Fisheries in the High Seas. Report of the Technical Consultation on International Guidelines for the Management of Deep-sea Fisheries in the High Seas, Rome, 4–8 February and 25–29 August 2008. FAO Fisheries and Aquaculture Report.

Fallati, L., Saponari, L., Savini, A., Marchese, F., Corselli, C., Galli, P., 2020. Multi-Temporal UAV Data and Object-Based Image Analysis (OBIA) for Estimation of Substrate Changes in a Post-Bleaching Scenario on a Maldivian Reef. Remote Sens-Basel 12.

Fernandez-Arcaya, U., Ramirez-Llodra, E., Aguzzi, J., Allcock, A.L., Davies, J.S., Dissanayake, A., Harris, P., Howell, K., Huvenne, V.A.I., Macmillan-Lawler, M., Martin, J., Menot, L., Nizinski, M., Puig, P., Rowden, A.A., Sanchez, F., Van den Beld, I.M.J., 2017. Ecological Role of Submarine Canyons and Need for Canyon Conservation: A Review. Frontiers in Marine Science 4.

Fernholm, B., Quattrini, A., 2008. A new species of hagfish (Myxinidae : Eptatretus) associated with deep-sea coral habitat in the Western North Atlantic. Copeia, 126-132.

Ferrari, R., Figueira, W.F., Pratchett, M.S., Boube, T., Adam, A., Kobelkowsky-Vidrio, T., Doo, S.S., Atwood, T.B., Byrne, M., 2017. 3D photogrammetry quantifies growth and external erosion of individual coral colonies and skeletons. Sci Rep-Uk 7.

Flot, J.-F., Dahl, M., André, C., 2013. *Lophelia pertusa* corals from the Ionian and Barents seas share identical nuclear ITS2 and near-identical mitochondrial genome sequences. BMC research notes 6, 1.

Fossa, J.H., Mortensen, P.B., Furevik, D.M., 2002. The deep-water coral *Lophelia pertusa* in Norwegian waters: distribution and fishery impacts. Hydrobiologia 471, 1-12.

Foubert, A., Huvenne, V.A.I., Wheeler, A., Kozachenko, M., Opderbecke, J., Henriet, J.P., 2011. The Moira Mounds, small cold-water coral mounds in the Porcupine Seabight, NE Atlantic: Part B Evaluating the impact of sediment dynamics through high-resolution ROV-borne bathymetric mapping. Mar Geol 282, 65-78.

Fox, A.D., Henry, L.-A., Corne, D.W., Roberts, J.M., 2016. Sensitivity of marine protected area network connectivity to atmospheric variability. Royal Society Open Science 3.

Frederiksen, R., Jensen, A., Westerberg, H., 1992. The Distribution of the Scleractinian Coral *Lophelia-Pertusa* around the Faroe Islands and the Relation to Internal Tidal Mixing. Sarsia 77, 157-171.

Freiwald, A., Fossa, J.H., Grehan, A., Koslow, T., Roberts, J.M., 2004. Cold-water coral reefs: out of sight-no longer out of mind. UNEP-WCMC.

Freiwald, A., Huhnerbach, V., Lindberg, B., Wilson, J.B., Campbell, J., 2002. The Sula Reef Complex, Norwegian shelf. Facies 47, 179-200.

Friedlander, A.M., Parrish, J.D., 1998. Habitat characteristics affecting fish assemblages on a Hawaiian coral reef. J Exp Mar Biol Ecol 224, 1-30.

Friedman, A., Pizarro, O., Williams, S.B., Johnson-Roberson, M., 2012. Multi-Scale Measures of Rugosity, Slope and Aspect from Benthic Stereo Image Reconstructions. Plos One 7.

Furlong, M.E., Paxton, D., Stevenson, P., Pebody, M., McPhail, S.D., Perrett, J., 2012. Autosub Long Range: A Long Range Deep Diving AUV for Ocean Monitoring. Ieee Auto under Veh.

Gass, S.E., Roberts, J.M., 2006. The occurrence of the cold-water coral *Lophelia pertusa* (Scleractinia) on oil and gas platforms in the North Sea: colony growth, recruitment and environmental controls on distribution. Marine Pollution Bulletin 52, 549-559.

Genin, A., Dayton, P.K., Lonsdale, P.F., Spiess, F.N., 1986. Corals on Seamount Peaks Provide Evidence of Current Acceleration over Deep-Sea Topography. Nature 322, 59-61.

Georgian, S.E., Shedd, W., Cordes, E.E., 2014. High-resolution ecological niche modelling of the cold-water coral *Lophelia pertusa* in the Gulf of Mexico. Mar Ecol Prog Ser 506, 145-U454.

Gerdes, K., Arbizu, P.M., Schwarz-Schampera, U., Schwentner, M., Kihara, T.C., 2019. Detailed Mapping of Hydrothermal Vent Fauna: A 3D Reconstruction Approach Based on Video Imagery. Frontiers in Marine Science 6.

Geyer, C., 1999. Likelihood inference for spatial point processes. Mg Stat Pro 80, 79-140.

Glenn, M.F., 1970. Introducing an Operational Multi-Beam Array Sonar. Int Hydrogr Rev 47, 35-&.

Gori, A., Rossi, S., Linares, C., Berganzo, E., Orejas, C., Dale, M.R. and Gili, J.M., 2011a. Size and spatial structure in deep versus shallow populations of the Mediterranean gorgonian *Eunicella singularis* (Cap de Creus, northwestern Mediterranean Sea). Mar Biol 158, 1721-1732.

Gori, A., Rossi, S., Berganzo, E., Pretus, J.L., Dale, M.R.T., Gili, J.M., 2011b. Spatial distribution patterns of the gorgonians *Eunicella singularis*, *Paramuricea clavata*, and *Leptogorgia sarmentosa* (Cape of Creus, Northwestern Mediterranean Sea). Mar Biol 158, 143-158.

Gori, A., Orejas, C., Madurell, T., Bramanti, L., Martins, M., Quintanilla, E., Marti-Puig, P., Lo Iacono, C., Puig, P., Requena, S., Greenacre, M., Gili, J.M., 2013. Bathymetrical distribution and size structure of cold-water coral populations in the Cap de Creus and Lacaze-Duthiers canyons (northwestern Mediterranean). Biogeosciences 10, 2049-2060.

Gori, A., Reynaud, S., Orejas, C. and Ferrier-Pagès, C., 2015. The influence of flow velocity and temperature on zooplankton capture rates by the cold-water coral Dendrophyllia cornigera. Journal of Experimental Marine Biology and Ecology, 466, 92-97.

Graham, N.A.J., Nash, K.L., 2013. The importance of structural complexity in coral reef ecosystems. Coral Reefs 32, 315-326.

Grasmueck, M., Eberli, G.P., Viggiano, D.A., Correa, T., Rathwell, G., Luo, J.G., 2006. Autonomous underwater vehicle (AUV) mapping reveals coral mound distribution, morphology, and oceanography in deep water of the Straits of Florida. Geophys Res Lett 33.

Gratwicke, B., Speight, M.R., 2005. The relationship between fish species richness, abundance and habitat complexity in a range of shallow tropical marine habitats. J Fish Biol 66, 650-667.

Guihen, D., White, M., Lundalv, T., 2013. Boundary layer flow dynamics at a cold-water coral reef. J Sea Res 78, 36-44.

Guinan, J., Brown, C., Dolan, M.F.J., Grehan, A.J., 2009. Ecological niche modelling of the distribution of cold-water coral habitat using underwater remote sensing data. Ecol Inform 4, 83-92.

Guinotte, J.M., Davies, A.J., 2014. Predicted Deep-Sea Coral Habitat Suitability for the US West Coast. Plos One 9.

Guinotte, J.M., Orr, J., Cairns, S., Freiwald, A., Morgan, L., George, R., 2006. Will human-induced changes in seawater chemistry alter the distribution of deep-sea scleractinian corals? Front Ecol Environ 4, 141-146.

Hall, R.A., Aslam, T., Huvenne, V.A.I., 2017. Partly standing internal tides in a dendritic submarine canyon observed by an ocean glider. Deep-Sea Res Pt I 126, 73-84.

Hanz, U., Wienberg, C., Hebbeln, D., Duineveld, G., Lavaleye, M., Juva, K., Dullo, W.C., Freiwald, A., Tamborrino, L., Reichart, G.J., Flogel, S., Mienis, F., 2019. Environmental factors influencing benthic communities in the oxygen minimum zones on the Angolan and Namibian margins. Biogeosciences 16, 4337-4356.

Harii, S., Kayanne, H., 2002. Larval settlement of corals in flowing water using a racetrack flume. Marine Technology Society Journal 36, 76-79.

Harter, S.L., Ribera, M.M., Shepard, A.N., Reed, J.K., 2009. Assessment of fish populations and habitat on *Oculina* Bank, a deep-sea coral marine protected area off eastern Florida. Fish B-Noaa 107, 195-206.

Hata, T., Madin, J.S., Cumbo, V.R., Denny, M., Figueiredo, J., Harii, S., Thomas, C.J., Baird, A.H., 2017. Coral larvae are poor swimmers and require fine-scale reef structure to settle. Sci Rep-Uk 7.

Heifetz, J., Stone, R.P., Shotwell, S.K., 2009. Damage and disturbance to coral and sponge habitat of the Aleutian Archipelago. Mar Ecol Prog Ser 397, 295-303.

Hennige, S.J., Wicks, L.C., Kamenos, N.A., Bakker, D.C.E., Findlay, H.S., Dumousseaud, C., Roberts, J.M., 2014. Short-term metabolic and growth responses of the cold-water coral Lophelia pertusa to ocean acidification. Deep-Sea Res Pt Ii 99, 27-35.

Hennige, S., Wicks, L., Kamenos, N., Perna, G., Findlay, H., Roberts, J., 2015. Hidden impacts of ocean acidification to live and dead coral framework. Proc. R. Soc. B 282, 20150990.

Hennige, S.J., Wolfram, U., Wickes, L., Murray, F., Roberts, J.M., Kamenos, N.A., Schofield, S., Groetsch, A., Spiesz, E.M., Aubin-Tam, M.E., Etnoyer, P.J., 2020. Crumbling Reefs and Cold-

Water Coral Habitat Loss in a Future Ocean: Evidence of "Coralporosis" as an Indicator of Habitat Integrity. Frontiers in Marine Science 7.

Henry, L.A., Roberts, J.M., 2007. Biodiversity and ecological composition of macrobenthos on cold-water coral mounds and adjacent off-mound habitat in the bathyal Porcupine Seabight, NE Atlantic. Deep-Sea Res Pt I 54, 654-672.

Henry, L.A., Navas, J.M., Hennige, S.J., Wicks, L.C., Vad, J., Roberts, J.M., 2013. Cold-water coral reef habitats benefit recreationally valuable sharks. Biol Conserv 161, 67-70.

Henry, L.-A., Frank, N., Hebbeln, D., Wienberg, C., Robinson, L., van de Flierdt, T., Dahl, M., Douarin, M., Morrison, C.L., Correa, M.L., 2014. Global ocean conveyor lowers extinction risk in the deep sea. Deep Sea Research Part I: Oceanographic Research Papers 88, 8-16.

Henry, L.-A., Roberts, J.M., 2017. Global biodiversity in cold-water coral reef ecosystems. Marine Animal Forests: the Ecology of Benthic Biodiversity Hotspots, 1-21.

Hooper, R.C., Eichhorn, M.P., 2016. Too close for comfort: spatial patterns in acorn barnacle populations. Popul Ecol 58, 231-239.

Hovland, M., Croker, P.F., Martin, M., 1994. Fault-Associated Seabed Mounds (Carbonate Knolls) Off Western Ireland and North-West Australia. Mar Petrol Geol 11, 232-246.

Hovland, M., Mortensen, P.B., Brattegard, T., Strass, P., Rokoengen, K., 1998. Ahermatypic coral banks off Mid-Norway: Evidence for a link with seepage of light hydrocarbons. Palaios 13, 189-200.

Howell, K.L., Holt, R., Endrino, I.P., Stewart, H., 2011. When the species is also a habitat: Comparing the predictively modelled distributions of Lophelia pertusa and the reef habitat it forms. Biol Conserv 144, 2656-2665.

Husebø, Å., Nøttestad, L., Fosså, J., Furevik, D., Jørgensen, S., 2002. Distribution and abundance of fish in deep-sea coral habitats. Hydrobiologia 471, 91-99.

Huvenne, V.A.I., Blondel, P. and Henriet, J.P., 2002. Textural analyses of sidescan sonar imagery from two mound provinces in the Porcupine Seabight. Marine Geology, 189(3-4), 323-341.

Huvenne, V.A.I., De Mol, B., Henriet, J.P., 2003. A 3D seismic study of the morphology and spatial distribution of buried coral banks in the Porcupine Basin, SW of Ireland. Mar Geol 198, 5-25.

Huvenne, V.A.I., Tyler, P.A., Masson, D.G., Fisher, E.H., Hauton, C., Huhnerbach, V., Le Bas, T.P., Wolff, G.A., 2011. A Picture on the Wall: Innovative Mapping Reveals Cold-Water Coral Refuge in Submarine Canyon. Plos One 6.

Huvenne, V.A.I. and Davies, J.S., 2014. Towards a new and integrated approach to submarine canyon research. Introduction. Deep Sea Research Part II: Topical Studies in Oceanography, 104, 1-5.

Huvenne, V.A.I., Bett, B.J., Masson, D.G., Le Bas, T.P., Wheeler, A.J., 2016. Effectiveness of a deep-sea cold-water coral Marine Protected Area, following eight years of fisheries closure. Biol Conserv 200, 60-69.

Huvenne, V.A., Robert, K., Marsh, L., Iacono, C.L., Le Bas, T., Wynn, R.B., 2018. Rovs and auvs, Submarine Geomorphology, Springer, pp. 93-108.

Huvene, V., Thornton, B., 2020. 2020 RRS Discovery Cruise DY108-109, 6 Sept-2 Oct 2019. CLASS–Climate-linked Atlantic System Science Darwin Mounds Marine Protected Area habitat monitoring, BioCAM-first equipment trials. BLT-Recipes: pilot study.

Illian, J., Penttinen, A., Stoyan, H., Stoyan, D., 2008. Statistical analysis and modelling of spatial point patterns. John Wiley & Sons.

Ismail, K., Huvenne, V.A.I., Masson, D.G., 2015. Objective automated classification technique for marine landscape mapping in submarine canyons. Mar Geol 362, 17-32.

Jackson, E.L., Davies, A.J., Howell, K.L., Kershaw, P.J., Hall-Spencer, J.M., 2014. Future-proofing marine protected area networks for cold water coral reefs. Ices J Mar Sci 71, 2621-2629.

Jackson, T.D., Williams, G.J., Walker-Springett, G., Davies, A.J., 2020. Three-dimensional digital mapping of ecosystems: a new era in spatial ecology. P Roy Soc B-Biol Sci 287.

Jennings, S., Kaiser, M.J., 1998. The effects of fishing on marine ecosystems. Adv Mar Biol 34, 201-+.

Jensen, A., Frederiksen, R., 1992. The Fauna Associated with the Bank-Forming Deep-Water Coral *Lophelia-Pertusa* (Scleractinaria) on the Faroe Shelf. Sarsia 77, 53-69.

JNCC, 2012. JNCC and Natural England's advice to Defra on recommended Marine Conservation Zones.

JNCC, 2013. JNCC's advice on offshore Marine Conservation Zones proposed for designation in 2013.

Johnson, M.P., White, M., Wilson, A., Wurzberg, L., Schwabe, E., Folch, H., Allcock, A.L., 2013. A Vertical Wall Dominated by *Acesta excavata* and *Neopycnodonte zibrowii*, Part of an Undersampled Group of Deep-Sea Habitats. Plos One 8.

Johnson-Roberson, M., Pizarro, O., Williams, S.B., Mahon, I., 2010. Generation and Visualization of Large-Scale Three-Dimensional Reconstructions from Underwater Robotic Surveys. J Field Robot 27, 21-51.

Jones, C.G., Lawton, J.H., Shachak, M., 1994. Organisms as Ecosystem Engineers. Oikos 69, 373-386.

Jonsson, L.G., Nilsson, P.G., Floruta, F., Lundalv, T., 2004. Distributional patterns of macro- and megafauna associated with a reef of the cold-water coral Lophelia pertusa on the Swedish west coast. Mar Ecol Prog Ser 284, 163-171.

Keller, N., 1976. The deep-sea madreporarian corals of the genus *Fungiacyathus* from the Kurile-Kamchatka, Aleutian Trenches and other regions of the world oceans. Trudy Instituta Okeanologii 99, 31-44.

Kenyon, N.H., Akhmetzhanov, A.M., Wheeler, A.J., van Weering, T.C.E., de Haas, H., Ivanov, M.K., 2003. Giant carbonate mud mounds in the southern Rockall Trough. Mar Geol 195, 5-30.

Keutterling, A., Thomas, A., 2006. Monitoring glacier elevation and volume changes with digital photogrammetry and GIS at Gepatschferner glacier, Austria. Int J Remote Sens 27, 4371-4380.

Knudby, A., LeDrew, E., Newman, C., 2007. Progress in the use of remote sensing for coral reef biodiversity studies. Prog Phys Geog 31, 421-434.

Koslow, J.A., Gowlett-Holmes, K., Lowry, J.K., O'Hara, T., Poore, G.C.B., Williams, A., 2001. Seamount benthic macrofauna off southern Tasmania: community structure and impacts of trawling. Mar Ecol Prog Ser 213, 111-125.

Krosley, L., Oerter, E., Ortiz, T., Ortiz, T., 2006. Digital ground-based photogrammetry for measuring discontinuity orientations in steep rock exposures, Golden Rocks 2006, The 41st US Symposium on Rock Mechanics (USRMS), American Rock Mechanics Association.

Kutti, T., Bergstad, O.A., Fossa, J.H., Helle, K., 2014. Cold-water coral mounds and sponge-beds as habitats for demersal fish on the Norwegian shelf. Deep-Sea Res Pt Ii 99, 122-133.

Kwasnitschka, T., Hansteen, T.H., Devey, C.W., Kutterolf, S., 2013. Doing fieldwork on the seafloor: Photogrammetric techniques to yield 3D visual models from ROV video. Comput Geosci-Uk 52, 218-226.

Lane, S.N., 2000. The measurement of river channel morphology using digital photogrammetry. Photogramm Rec 16, 937-957.

Larsson, A.I., Jarnegren, J., Stromberg, S.M., Dahl, M.P., Lundalv, T., Brooke, S., 2014. Embryogenesis and Larval Biology of the Cold-Water Coral Lophelia pertusa. Plos One 9.

Lartaud, F., Meistertzheim, A.L., Peru, E., Le Bris, N., 2017. In situ growth experiments of reef-building cold-water corals: The good, the bad and the ugly. Deep-Sea Res Pt I 121, 70-78.

Laughton, A., Hill, M., Allan, T., 1960. Geophysical investigations of a seamount 150 miles north of Madeira. Deep Sea Research (1953) 7, 117-141.

Law, R., Illian, J., Burslem, D.F.R.P., Gratzer, G., Gunatilleke, C.V.S., Gunatilleke, I.A.U.N., 2009. Ecological information from spatial patterns of plants: insights from point process theory. J Ecol 97, 616-628.

Le Goff-Vitry, M.C., Pybus, O.G., Rogers, A.D., 2004. Genetic structure of the deep-sea coral Lophelia pertusa in the northeast Atlantic revealed by microsatellites and internal transcribed spacer sequences. Mol Ecol 13, 537-549.

Leblond, I., Tauvry, S., Pinto, M., 2019. Sonar image registration for swarm AUVs navigation: Results from SWARMs project. J Comput Sci-Neth 36.

Lecours, V., Devillers, R., Schneider, D.C., Lucieer, V.L., Brown, C.J., Edinger, E.N., 2015. Spatial scale and geographic context in benthic habitat mapping: review and future directions. Mar Ecol Prog Ser 535, 259-284.

Lecours, V., Dolan, M.F.J., Micallef, A., Lucieer, V.L., 2016. A review of marine geomorphometry, the quantitative study of the seafloor. Hydrol Earth Syst Sc 20, 3207-3244.

Leon, J.X., Roelfsema, C.M., Saunders, M.I., Phinn, S.R., 2015. Measuring coral reef terrain roughness using 'Structure-from-Motion' close-range photogrammetry. Geomorphology 242, 21-28.

Lesneski, K.C., D'Aloia, C.C., Fortin, M.J., Buston, P.M., 2019. Disentangling the spatial distributions of a sponge-dwelling fish and its host sponge. Mar Biol 166.

Lessard-Pilon, S.A., Podowski, E.L., Cordes, E.E., Fisher, C.R., 2010. Megafauna community composition associated with *Lophelia pertusa* colonies in the Gulf of Mexico. Deep-Sea Res Pt Ii 57, 1882-1890.

Levin, S.A., 1992. The Problem of Pattern and Scale in Ecology. Ecology 73, 1943-1967.

Levitus, S., Antonov, J., Boyer, T., 2005. Warming of the world ocean, 1955-2003. Geophys Res Lett 32.

Lim, A., Wheeler, A.J., Arnaubec, A., 2017. High-resolution facies zonation within a cold-water coral mound: The case of the Piddington Mound, Porcupine Seabight, NE Atlantic. Mar Geol 390, 120-130.

Lim, A., Huvenne, V.A.I., Vertino, A., Spezzaferri, S., Wheeler, A.J., 2018a. New insights on coral mound development from groundtruthed high-resolution ROV-mounted multibeam imaging. Mar Geol 403, 225-237.

Lim, A., Kane, A., Arnaubec, A., Wheeler, A.J., 2018b. Seabed image acquisition and survey design for cold water coral mound characterisation. Mar Geol 395, 22-32.

Lim, A., Wheeler, A.J., Price, D.M., O'Reilly, L., Harris, K., Conti, L., 2020. Influence of benthic currents on cold-water coral habitats: a combined benthic monitoring and 3D photogrammetric investigation. Sci Rep-Uk 10.

Lim, A., Wheeler, A.J., Conti, L., 2021. Cold-Water Coral Habitat Mapping: Trends and Developments in Acquisition and Processing Methods. Geosciences 11.

Ling, S.D., Mahon, I., Marzloff, M.P., Pizarro, O., Johnson, C.R., Williams, S.B., 2016. Stereo-imaging AUV detects trends in sea urchin abundance on deep overgrazed reefs. Limnol Oceanogr-Meth 14, 293-304.

Lo Iacono, C., Robert, K., Gonzalez-Villanueva, R., Gori, A., Gili, J.-M., Orejas, C., 2018. Predicting cold-water coral distribution in the Cap de Creus Canyon (NW Mediterranean): Implications for marine conservation planning. Progress in Oceanography.

Ludvigsen, M., Johnsen, G., Sorensen, A.J., Lagstad, P.A., Odegard, O., 2014. Scientific Operations Combining ROV and AUV in the Trondheim Fjord. Marine Technology Society Journal 48, 59-71.

Lundblad, E.R., Wright, D.J., Miller, J., Larkin, E.M., Rinehart, R., Naar, D.F., Donahue, B.T., Anderson, S.M., Battista, T., 2006. A benthic terrain classification scheme for American Samoa. Mar Geod 29, 89-111.

Mackay, K.A., Rowden, A.A., Bostock, H.C., Tracey, D.M., 2014. Revisiting Squires' Coral Coppice, Campbell Plateau, New Zealand. New Zeal J Mar Fresh 48, 507-523.

Maier, C., Weinbauer, M.G., Gattuso, J.-P., 2019. 44 Fate of Mediterranean Scleractinian Cold-Water Corals as a Result of Global Climate Change. A Synthesis, Mediterranean cold-water corals: Past, present and future, Springer, pp. 517-529.

Marsh, L., Copley, J.T., Huvenne, V.A.I., Linse, K., Reid, W.D.K., Rogers, A.D., Sweeting, C.J., Tyler, P.A., 2012. Microdistribution of Faunal Assemblages at Deep-Sea Hydrothermal Vents in the Southern Ocean. Plos One 7.

Marsh, L., Copley, J.T., Huvenne, V.A.I., Tyler, P.A., Facility, I.R., 2013. Getting the bigger picture: Using precision Remotely Operated Vehicle (ROV) videography to acquire high-definition mosaic images of newly discovered hydrothermal vents in the Southern Ocean. Deep-Sea Res Pt Ii 92, 124-135.

Martin, J., Puig, P., Palanques, A., Ribo, M., 2014. Trawling-induced daily sediment resuspension in the flank of a Mediterranean submarine canyon. Deep-Sea Res Pt Ii 104, 174-183.

Marzolff, I., Poesen, J., 2009. The potential of 3D gully monitoring with GIS using high-resolution aerial photography and a digital photogrammetry system. Geomorphology 111, 48-60.

Masson, D.G., Arzola, R.G., Wynn, R.B., Hunt, J.E., Weaver, P.P.E., 2011. Seismic triggering of landslides and turbidity currents offshore Portugal. Geochem Geophy Geosy 12.

Masson, D.G., Bett, B.J., Billett, D.S.M., Jacobs, C.L., Wheeler, A.J., Wynn, R.B., 2003. The origin of deep-water, coral-topped mounds in the northern Rockall Trough, Northeast Atlantic. Mar Geol 194, 159-180.

Matos, F.L., Ross, S.W., Huvenne, V.A.I., Davies, J.S., Cunha, M.R., 2018. Canyons pride and prejudice: Exploring the submarine canyon research landscape, a history of geographic and thematic bias. Progress in Oceanography 169, 6-19.

Matos, L., Wienberg, C., Titschack, J., Schmiedl, G., Frank, N., Abrantes, F., Cunha, M.R., Hebbeln, D., 2017. Coral mound development at the Campeche cold-water coral province, southern Gulf of Mexico: implications of Antarctic Intermediate Water increased influence during interglacials. Mar Geol 392, 53-65.

McDowall, P., Lynch, H.J., 2017. Ultra-Fine Scale Spatially-Integrated Mapping of Habitat and Occupancy Using Structure-From-Motion. Plos One 12.

McPhail, S., 2009. Autosub6000: A Deep Diving Long Range AUV. J Bionic Eng 6, 55-62.

Melles, S.J., Badzinski, D., Fortin, M.J., Csillag, F., Lindsay, K., 2009. Disentangling habitat and social drivers of nesting patterns in songbirds. Landscape Ecology 24, 519-531.

Meyer, H.K., Roberts, E.M., Rapp, H.T., Davies, A.J., 2019. Spatial patterns of arctic sponge ground fauna and demersal fish are detectable in autonomous underwater vehicle (AUV) imagery. Deep-Sea Res Pt I 153.

Mienis, F., Bouma, T.J., Witbaard, R., van Oevelen, D., Duineveld, G.C.A., 2019. Experimental assessment of the effects of cold-water coral patches on water flow. Mar Ecol Prog Ser 609, 101-117.

Mienis, F., de Stigter, H.C., de Haas, H., van Weering, T.C.E., 2009. Near-bed particle deposition and resuspension in a cold-water coral mound area at the Southwest Rockall Trough margin, NE Atlantic. Deep-Sea Res Pt I 56, 1026-1038.

Mienis, F., de Stigter, H.C., White, M., Dulneveldc, G., de Haas, H., van Weering, T.C.E., 2007. Hydrodynamic controls on cold-water coral growth and carbonate-mound development at the SW and SE rockall trough margin, NE Atlantic ocean. Deep-Sea Res Pt I 54, 1655-1674.

Mienis, F., Duineveld, G.C.A., Davies, A.J., Lavaleye, M.M.S., Ross, S.W., Seim, H., Bane, J., van Haren, H., Bergman, M.J.N., de Haas, H., Brooke, S., van Weering, T.C.E., 2014. Cold-water coral growth under extreme environmental conditions, the Cape Lookout area, NW Atlantic. Biogeosciences 11, 2543-2560.

Miller, K.J., 1998. Short-distance dispersal of black coral larvae: inference from spatial analysis of colony genotypes. Mar Ecol Prog Ser 163, 225-233.

Miller, R.J., Hocevar, J., Stone, R.P., Fedorov, D.V., 2012. Structure-Forming Corals and Sponges and Their Use as Fish Habitat in Bering Sea Submarine Canyons. Plos One 7.

Ministerial order/DEFRA, 2013. The Canyons Marine Conservation Zone Designation Order, Ministerial order 2013 No. 4, [Accessed 2018/08/29: http://www.legislation.gov.uk/ukmo/2013/4/pdfs/ukmo_20130004_en.pdf].

Ministerial order/DEFRA, 2019. The Canyons Marine Conservation Zone Designation (Amendment) Order 2019. [Accessed 2021/02/10: https://www.legislation.gov.uk/ukmo/2019/7/pdfs/ukmo_20190007_en.pdf]

Mitchell, E.G., Harris, S., 2020. Mortality, Population and Community Dynamics of the Glass Sponge Dominated Community "The Forest of the Weird" From the Ridge Seamount, Johnston Atoll, Pacific Ocean. Frontiers in Marine Science 7.

Moccia, D., Cau, A., Bramanti, L., Carugati, L., Canese, S., Follesa, M.C., Cannas, R., 2020. Spatial distribution and habitat characterization of marine animal forest assemblages along nine submarine canyons of Eastern Sardinia (central Mediterranean Sea). Deep Sea Research Part I: Oceanographic Research Papers, 103422.

Mohamed, H., Nadaoka, K., Nakamura, T., 2020. Towards Benthic Habitat 3D Mapping Using Machine Learning Algorithms and Structures from Motion Photogrammetry. Remote Sens-Basel 12.

Mohn, C., Rengstorf, A., White, M., Duineveld, G., Mienis, F., Soetaert, K., Grehan, A., 2014. Linking benthic hydrodynamics and cold-water coral occurrences: A high-resolution model study at three cold-water coral provinces in the NE Atlantic. Progress in Oceanography 122, 92-104.

Monismith, S.G., 2007. Hydrodynamics of coral reefs. Annu Rev Fluid Mech 39, 37-55.

Morato, T., Gonzalez-Irusta, J.M., Dominguez-Carrio, C., Wei, C.L., Davies, A., Sweetman, A.K., Taranto, G.H., Beazley, L., Garcia-Alegre, A., Grehan, A., Laffargue, P., Murillo, F.J., Sacau, M., Vaz, S., Kenchington, E., Arnaud-Haond, S., Callery, O., Chimienti, G., Cordes, E., Egilsdottir, H., Freiwald, A., Gasbarro, R., Gutierrez-Zarate, C., Gianni, M., Gilkinson, K., Hayes, V.W.E., Hebbeln, D., Hedges, K., Henry, L.A., Johnson, D., Koen-Alonso, M., Lirette, C., Mastrototaro, F., Menot, L., Molodtsova, T., Munoz, P.D., Orejas, C., Pennino, M.G., Puerta, P., Ragnarsson, S.A., Ramiro-Sanchez, B., Rice, J., Rivera, J., Roberts, J.M., Ross, S.W., Rueda, J.L., Sampaio, I., Snelgrove, P., Stirling, D., Treble, M.A., Urra, J., Vad, J., van Oevelen, D., Watling, L., Walkusz, W., Wienberg, C., Woillez, M., Levin, L.A., Carreiro-Silva, M., 2020. Climate-induced changes in the suitable habitat of cold-water corals and commercially important deep-sea fishes in the North Atlantic. Global Change Biol 26, 2181-2202.

Morato, T., Pham, C.K., Pinto, C., Golding, N., Ardron, J.A., Munoz, P.D., Neat, F., 2018. A Multi Criteria Assessment Method for Identifying Vulnerable Marine Ecosystems in the North-East Atlantic. Frontiers in Marine Science 5.

Morgan, N.B., Baco, A.R., 2019. Observation of a high abundance aggregation of the deep-sea urchin *Chaetodiadema pallidum* A. Agassiz and HL Clark, 1907 on the Northwestern Hawaiian Island Mokumanamana. Deep-Sea Res Pt I 150.

Morris, K.J., Bett, B.J., Durden, J.M., Huvenne, V.A.I., Milligan, R., Jones, D.O.B., McPhail, S., Robert, K., Bailey, D.M., Ruhl, H.A., 2014. A new method for ecological surveying of the abyss using autonomous underwater vehicle photography. Limnol Oceanogr-Meth 12, 795-809.

Morrison, C.L., Ross, S.W., Nizinski, M.S., Brooke, S., Jarnegren, J., Waller, R.G., Johnson, R.L., King, T.L., 2011. Genetic discontinuity among regional populations of *Lophelia pertusa* in the North Atlantic Ocean. Conserv Genet 12, 713-729.

Mortensen, P.B., Hovland, M., Brattegard, T., Farestveit, R., 1995. Deep water bioherms of the scleractinian coral *Lophelia pertusa* (L.) at 64 N on the Norwegian shelf: structure and associated megafauna. Sarsia 80, 145-158.

Mortensen, P.B., Rapp, H.T., 1998. Oxygen and carbon isotope ratios related to growth line patterns in skeletons of *Lophelia pertusa* (L) (Anthozoa, Scleractinia): Implications for determination of linear extension rates. Sarsia 83, 433-446.

Mortensen, P.B., Roberts, J.M., Sundt, R.C., 2000. Video-assisted grabbing: a minimally destructive method of sampling azooxanthellate coral banks. J Mar Biol Assoc Uk 80, 365-366.

Mortensen, P.B., 2001. Aquarium observations on the deep-water coral *Lophelia pertusa* (L., 1758) (scleractinia) and selected associated invertebrates. Ophelia 54, 83-104.

Mortensen, P.B., Fosså, J.H., 2006. Species diversity and spatial distribution of invertebrates on deep-water Lophelia reefs in Norway.

Murfitt, S.L., Allan, B.M., Bellgrove, A., Rattray, A., Young, M.A., Ierodiaconou, D., 2017. Applications of unmanned aerial vehicles in intertidal reef monitoring. Sci Rep-Uk 7.

Navas, J.M., Miller, P.L., Henry, L.A., Hennige, S.J., Roberts, J.M., 2014. Ecohydrodynamics of Cold-Water Coral Reefs: A Case Study of the Mingulay Reef Complex (Western Scotland). Plos One 9.

O'Reilly, B.M., Readman, P.W., Shannon, P.M., Jacob, A.W.B., 2003. A model for the development of a carbonate mound population in the Rockall Trough based on deep-towed sidescan sonar data. Mar Geol 198, 55-66.

Orejas, C., Gori, A. and Gili, J.M., 2008. Growth rates of live Lophelia pertusa and Madrepora oculata from the Mediterranean Sea maintained in aquaria. Coral Reefs, 27(2), 255.

Orejas, C., Gori, A., Lo Iacono, C., Puig, P., Gili, J.M., Dale, M.R.T., 2009. Cold-water corals in the Cap de Creus canyon, northwestern Mediterranean: spatial distribution, density and anthropogenic impact. Mar Ecol Prog Ser 397, 37-51.

Orejas, C., Ferrier-Pages, C., Reynaud, S., Gori, A., Beraud, E., Tsounis, G., Allemand, D., Gili, J.M., 2011. Long-term growth rates of four Mediterranean cold-water coral species maintained in aquaria. Mar Ecol Prog Ser 429, 57-65.

Orejas, C., Gori, A., Rad-Menendez, C., Last, K.S., Davies, A.J., Beveridge, C.M., Sadd, D., Kiriakoulakis, K., Witte, U., Roberts, J.M., 2016. The effect of flow speed and food size on the capture efficiency and feeding behaviour of the cold-water coral Lophelia pertusa. J Exp Mar Biol Ecol 481, 34-40.

Osterloff, J., Nilssen, I., Jarnegren, J., Van Engeland, T., Buhl-Mortensen, P., Nattkemper, T.W., 2019. Computer vision enables short- and long-term analysis of *Lophelia pertusa* polyp behaviour and colour from an underwater observatory. Sci Rep-Uk 9.

Palanques, A., Martin, J., Puig, P., Guillen, J., Company, J.B., Sarda, F., 2006. Evidence of sediment gravity flows induced by trawling in the Palamos (Fonera) submarine canyon (northwestern Mediterranean). Deep-Sea Res Pt I 53, 201-214.

Parrish, J.K., Edelstein-Keshet, L., 1999. Complexity, pattern, and evolutionary trade-offs in animal aggregation. Science 284, 99-101.

Paull, C.K., Caress, D.W., Ussler, W., Lundsten, E., Meiner-Johnson, M., 2011. High-resolution bathymetry of the axial channels within Monterey and Soquel submarine canyons, offshore central California. Geosphere 7, 1077-1101.

Paull, C.K., Caress, D.W., Lundsten, E., Gwiazda, R., Anderson, K., McGann, M., Conrad, J., Edwards, B., Sumner, E.J., 2013. Anatomy of the La Jolla Submarine Canyon system; offshore southern California. Mar Geol 335, 16-34.

Paull, L., Saeedi, S., Seto, M., Li, H., 2014. AUV Navigation and Localization: A Review. Ieee Journal of Oceanic Engineering 39, 131-149.

Pearman, T.R.R., Robert, K., Callaway, A., Hall, R., Lo Iacono, C., Huvenne, V.A.I., 2020. Improving the predictive capability of benthic species distribution models by incorporating

oceanographic data - Towards holistic ecological modelling of a submarine canyon. Progress in Oceanography 184.

Pham, C.K., Ramirez-Llodra, E., Alt, C.H.S., Amaro, T., Bergmann, M., Canals, M., Company, J.B., Davies, J., Duineveld, G., Galgani, F., Howell, K.L., Huvenne, V.A.I., Isidro, E., Jones, D.O.B., Lastras, G., Morato, T., Gomes-Pereira, J.N., Purser, A., Stewart, H., Tojeira, I., Tubau, X., Van Rooij, D., Tyler, P.A., 2014. Marine Litter Distribution and Density in European Seas, from the Shelves to Deep Basins. Plos One 9.

Piechaud, N., Hunt, C., Culverhouse, P.F., Foster, N.L., Howell, K.L., 2019. Automated identification of benthic epifauna with computer vision. Mar Ecol Prog Ser 615, 15-30.

Pizarro, O., Friedman, A., Bryson, M., Williams, S.B., Madin, J., 2017. A simple, fast, and repeatable survey method for underwater visual 3D benthic mapping and monitoring. Ecol Evol 7, 1770-1782.

Plante, M., Lowell, K., Potvin, F., Boots, B., Fortin, M.J., 2004. Studying deer habitat on Anticosti Island, Quebec: relating animal occurrences and forest map information. Ecol Model 174, 387-399.

Pontoppidan, E., 1755. The Natural History of Norway...: Translated from the Danish Original.

Porter, M., Inall, M.E., Hopkins, J., Palmer, M.R., Dale, A.C., Aleynik, D., Barth, J.A., Mahaffey, C., Smeed, D.A., 2016. Glider observations of enhanced deep water upwelling at a shelf break canyon: A mechanism for cross-slope carbon and nutrient exchange. J Geophys Res-Oceans 121, 7575-7588.

Prado, E., Sanchez, F., Rodriguez-Basal, A., Altuna, A., Cobo, A., 2019. Analysis of the population structure of a gorgonian forest (*Placogorgia* sp.) using a photogrammetric 3D modeling approach at Le Danois Bank, Cantabrian Sea. Deep-Sea Res Pt I 153.

Prado, E., Rodriguez-Basalo, A., Cobo, A., Rios, P., Sanchez, F., 2020. 3D Fine-scale Terrain Variables from Underwater Photogrammetry: A New Approach to Benthic Microhabitat Modeling in a Circalittoral Rocky Shelf. Remote Sens-Basel 12.

Price, D.M., Robert, K., Callaway, A., Lo Lacono, C., Hall, R.A., Huvenne, V.A.I., 2019. Using 3D photogrammetry from ROV video to quantify cold-water coral reef structural complexity and investigate its influence on biodiversity and community assemblage. Coral Reefs 38, 1007-1021.

Purser, A., Larsson, A.I., Thomsen, L., van Oevelen, D., 2010. The influence of flow velocity and food concentration on Lophelia pertusa (Scleractinia) zooplankton capture rates. J Exp Mar Biol Ecol 395, 55-62.

Purser, A., Orejas, C., Gori, A., Tong, R.J., Unnithan, V., Thomsen, L., 2013. Local variation in the distribution of benthic megafauna species associated with cold-water coral reefs on the Norwegian margin. Cont Shelf Res 54, 37-51.

Purser, A., Marcon, Y., Dreutter, S., Hoge, U., Sablotny, B., Hehemann, L., Lemburg, J., Dorschel, B., Biebow, H., Boetius, A., 2018. Ocean Floor Observation and Bathymetry System (OFOBS): A new Towed Camera/Sonar System for Deep-Sea Habitat Surveys. IEEE Journal of Oceanic Engineering, 1-13.

Raber, G.T., Schill, S.R., 2019. Reef Rover: A Low-Cost Small Autonomous Unmanned Surface Vehicle (USV) for Mapping and Monitoring Coral Reefs. Drones 3, 38.

Raddatz, J., Titschack, J., Frank, N., Freiwald, A., Conforti, A., Osborne, A., Skornitzke, S., Stiller, W., Rueggeberg, A., Voigt, S., Albuquerque, A.L.S., Vertino, A., Schroeder-Ritzrau, A., Bahr, A., 2020. Solenosmilia variabilis-bearing cold-water coral mounds off Brazil. Coral Reefs 39, 69-83.

Rakka, M., Orejas, C., Maier, S.R., Van Oevelen, D., Godinho, A., Bilan, M. and Carreiro-Silva, M., 2020. Feeding biology of a habitat-forming antipatharian in the Azores Archipelago. Coral Reefs, 39(5), 1469-1482.

Raoult, V., Reid-Anderson, S., Ferri, A., Williamson, J.E., 2017. How Reliable Is Structure from Motion (SfM) over Time and between Observers? A Case Study Using Coral Reef Bommies. Remote Sens-Basel 9.

Reed, J.K., Shepard, A.N., Koenig, C.C., Scanlon, K.M. and Gilmore, R.G., 2005. Mapping, habitat characterization, and fish surveys of the deep-water Oculina coral reef Marine Protected Area: a review of historical and current research. Cold-water Corals and Ecosystems, 443-465.

Reed, J.K., Koenig, C.C. and Shepard, A.N., 2007. Impacts of bottom trawling on a deep-water Oculina coral ecosystem off Florida. Bulletin of Marine Science, 81(3), 481-496.

Reiss, H., Birchenough, S., Borja, A., Buhl-Mortensen, L., Craeymeersch, J., Dannheim, J., Darr, A., Galparsoro, I., Gogina, M., Neumann, H., Populus, J., Rengstorf, A.M., Valle, M., van Hoey, G.,

Zettler, M.L., Degraer, S., 2015. Benthos distribution modelling and its relevance for marine ecosystem management. Ices J Mar Sci 72, 297-315.

Rengstorf, A.M., Grehan, A., Yesson, C., Brown, C., 2012. Towards High-Resolution Habitat Suitability Modeling of Vulnerable Marine Ecosystems in the Deep-Sea: Resolving Terrain Attribute Dependencies. Mar Geod 35, 343-361.

Rengstorf, A.M., Yesson, C., Brown, C., Grehan, A.J., 2013. High-resolution habitat suitability modelling can improve conservation of vulnerable marine ecosystems in the deep sea. J Biogeogr 40, 1702-1714.

Rengstorf, A.M., Mohn, C., Brown, C., Wisz, M.S., Grehan, A.J., 2014. Predicting the distribution of deep-sea vulnerable marine ecosystems using high-resolution data: Considerations and novel approaches. Deep-Sea Res Pt I 93, 72-82.

Reolid, J., Reolid, M., Betzler, C., Lindhorst, S., Wiesner, M.G., Lahajnar, N., 2017. Upper Pleistocene cold-water corals from the Inner Sea of the Maldives: taphonomy and environment. Facies 63.

Richardson, L.E., Graham, N.A.J., Hoey, A.S., 2017. Cross-scale habitat structure driven by coral species composition on tropical reefs. Sci Rep-Uk 7.

Rigaud, V., 2007. Innovation and operation with robotized underwater systems. J Field Robot 24, 449-459.

Rios, P., Prado, E., Carvalho, F.C., Sanchez, F., Rodriguez-Basalo, A., Xavier, J.R., Ibarrola, T.P., Cristobo, J., 2020. Community Composition and Habitat Characterization of a Rock Sponge Aggregation (Porifera, Corallistidae) in the Cantabrian Sea. Frontiers in Marine Science 7.

Ripley, B.D., 1977. Modelling spatial patterns. Journal of the Royal Statistical Society: Series B (Methodological) 39, 172-192.

Robert, K., Jones, D.O. and Huvenne, V.A., 2014. Megafaunal distribution and biodiversity in a heterogeneous landscape: the iceberg-scoured Rockall Bank, NE Atlantic. Marine Ecology Progress Series, 501, 67-88.

Robert, K., Jones, D.O., Tyler, P.A., Van Rooij, D., Huvenne, V.A., 2015. Finding the hotspots within a biodiversity hotspot: fine-scale biological predictions within a submarine canyon using high-resolution acoustic mapping techniques. Marine ecology 36, 1256-1276.

Robert, K., Huvenne, V.A.I., Georgiopoulou, A., Jones, D.O.B., Marsh, L., Carter, G.D.O., Chaumillon, L., 2017. New approaches to high-resolution mapping of marine vertical structures. Sci Rep-Uk 7.

Robert, K., Jones, D.O.B., Georgiopoulou, A., Huvenne, V.A.I., 2019. Cold-water coral assemblages on vertical walls from the Northeast Atlantic. Divers Distrib.

Roberts, J.M., Peppe, O.C., Dodds, L.A., Mercer, D.J., Thomson, W.T., Gage, J.D., Meldrum, D.T., 2005. Monitoring environmental variability around cold-water coral reefs: the use of a benthic photolander and the potential of seafloor observatories. Erlangen Earth C Ser, 483-502.

Roberts, J.M., Wheeler, A.J., Freiwald, A., 2006. Reefs of the deep: the biology and geology of cold-water coral ecosystems. Science 312, 543-547.

Roberts, J.M., Henry, L.A., Long, D., Hartley, J.P., 2008. Cold-water coral reef frameworks, megafaunal communities and evidence for coral carbonate mounds on the Hatton Bank, north east Atlantic. Facies 54, 297-316.

Roberts, J.M., Wheeler, A.J., Freiwald, A., Cairns, S.D., 2009. Cold-Water Corals: The Biology and Geology of Deep-Sea Coral Habitats. Cold-Water Corals: The Biology and Geology of Deep-Sea Coral Habitats, 1-334.

Roberts, J.M., Cairns, S.D., 2014. Cold-water corals in a changing ocean. Curr Opin Env Sust 7, 118-126.

Rogers, A.D., 1999. The biology of *Lophelia pertusa* (LINNAEUS 1758) and other deep-water reef-forming corals and impacts from human activities. Int Rev Hydrobiol 84, 315-406.

Ross, L.K., Ross, R.E., Stewart, H.A., Howell, K.L., 2015. The Influence of Data Resolution on Predicted Distribution and Estimates of Extent of Current Protection of Three 'Listed' Deep-Sea Habitats. Plos One 10.

Ross, R.E., Howell, K.L., 2013. Use of predictive habitat modelling to assess the distribution and extent of the current protection of 'listed' deep-sea habitats. Divers Distrib 19, 433-445.

Ross, S.W., Quattrini, A.M., 2007. The fish fauna associated with deep coral banks off the southeastern United States. Deep-Sea Res Pt I 54, 975-1007.

Rossi, P., Castagnetti, C., Capra, A., Brooks, A.J., Mancini, F., 2020. Detecting change in coral reef 3D structure using underwater photogrammetry: critical issues and performance metrics. Appl Geomat 12, 3-17.

Rowden, A.A., Anderson, O.F., Georgian, S.E., Bowden, D.A., Clark, M.R., Pallentin, A., Miller, A., 2017. High-Resolution Habitat Suitability Models for the Conservation and Management of Vulnerable Marine Ecosystems on the Louisville Seamount Chain, South Pacific Ocean. Frontiers in Marine Science 4, 335.

Rowden, A.A., Pearman, T.R.R., Bowden, D.A., Anderson, O.F., Clark, M.R., 2020. Determining Coral Density Thresholds for Identifying Structurally Complex Vulnerable Marine Ecosystems in the Deep Sea. Frontiers in Marine Science 7.

Salavasidis, G., Harris, C., McPhail, S., Phillips, A.B., Rogers, E., 2016. Terrain Aided Navigation for Long Range AUV Operations at Arctic Latitudes. 2016 Ieee/Oes Autonomous Underwater Vehicles (Auv), 115-123.

Sappington, J.M., Longshore, K.M., Thompson, D.B., 2007. Quantifying landscape ruggedness for animal habitat analysis: a case study using bighorn sheep in the Mojave Desert. The Journal of wildlife management 71, 1419-1426.

Sars, M., 1864. Om de i Norge forekommende fossile dyrelevninger fra Quartaerperioden: Christiania. Universitetsprogram for forste halvaar.

Sedlazeck, A., Koser, K., Koch, R., 2009. 3D Reconstruction Based on Underwater Video from ROV Kiel 6000 Considering Underwater Imaging Conditions. Oceans-Ieee, 1367-1376.

Simon-Lledo, E., Bett, B.J., Huvenne, V.A.I., Koser, K., Schoening, T., Greinert, J., Jones, D.O.B., 2019. Biological effects 26 years after simulated deep-sea mining. Sci Rep-Uk 9.

Sinha, P., Gaughan, A.E., Stevens, F.R., Nieves, J.J., Sorichetta, A., Tatem, A.J., 2019. Assessing the spatial sensitivity of a random forest model: Application in gridded population modeling. Comput Environ Urban 75, 132-145.

Soares, M.O., Matos, E., Lucas, C., Rizzo, L., Allcock, L., Rossi, S., 2020. Microplastics in corals: An emergent threat. Mar Pollut Bull 161, 111810.

Soetaert, K., Mohn, C., Rengstorf, A., Grehan, A., van Oevelen, D., 2016. Ecosystem engineering creates a direct nutritional link between 600-m deep cold-water coral mounds and surface productivity. Sci Rep-Uk 6.

Soffker, M., Sloman, K.A., Hall-Spencer, J.M., 2011. In situ observations of fish associated with coral reefs off Ireland. Deep-Sea Res Pt I 58, 818-825.

Squires, D.F., 1964. Fossil coral thickets in Wairarapa, New Zealand. Journal of Paleontology, 904-915.

Steinmann, L., Baques, M., Wenau, S., Schwenk, T., Spiess, V., Piola, A.R., Bozzano, G., Violante, R., Kasten, S., 2020. Discovery of a giant cold-water coral mound province along the northern Argentine margin and its link to the regional Contourite Depositional System and oceanographic setting. Mar Geol 427.

Stevenson, A., Mitchell, F.J.G., Davies, J.S., 2015. Predation has no competition: factors influencing space and resource use by echinoids in deep-sea coral habitats, as evidenced by continuous video transects. Mar Ecol-Evol Persp 36, 1454-1467.

Stewart, H.A., Davies, J.S., Guinan, J., Howell, K.L., 2014. The Dangeard and Explorer canyons, South Western Approaches UK: Geology, sedimentology and newly discovered cold-water coral mini-mounds. Deep-Sea Res Pt Ii 104, 230-244.

Storlazzi, C.D., Dartnell, P., Hatcher, G.A., Gibbs, A.E., 2016. End of the chain? Rugosity and fine-scale bathymetry from existing underwater digital imagery using structure-from-motion (SfM) technology. Coral Reefs 35, 889-894.

Teichert, C., 1958. Cold-and deep-water coral banks. AAPG Bulletin 42, 1064-1082.

Thiem, O., Ravagnan, E., Fossa, J.H., Berntsen, J., 2006. Food supply mechanisms for cold-water corals along a continental shelf edge. J Marine Syst 60, 207-219.

Thomson, C.W., 1974. The depths of the sea. Рипол Классик.

Thornton, B., Bodenmann, A., Pizarro, O., Williams, S.B., Friedman, A., Nakajima, R., Takai, K., Motoki, K., Watsuji, T., Hirayama, H., Matsui, Y., Watanabe, H., Ura, T., 2016. Biometric assessment of deep-sea vent megabenthic communities using multi-resolution 3D image reconstructions. Deep-Sea Res Pt I 116, 200-219.

Todd, P.A., 2008. Morphological plasticity in scleractinian corals. Biol Rev 83, 315-337.

Torres-Pulliza, D., Dornelas, M.A., Pizarro, O., Bewley, M., Blowes, S.A., Boutros, N., Brambilla, V., Chase, T.J., Frank, G., Friedman, A., Hoogenboom, M.O., Williams, S., Zawada, K.J.A., Madin, J.S., 2020. A geometric basis for surface habitat complexity and biodiversity. Nat Ecol Evol 4, 1495-+.

Tracey, D.M., Rowden, A.A., Mackay, K.A., Compton, T., 2011. Habitat-forming cold-water corals show affinity for seamounts in the New Zealand region. Mar Ecol Prog Ser 430, 1-U59.

Turley, C., Roberts, J., Guinotte, J., 2007. Corals in deep-water: will the unseen hand of ocean acidification destroy cold-water ecosystems? Coral Reefs 26, 445-448.

Turley, C.M., Roberts, J.M., Guinotte, J.M., 2007. Corals in deep-water: will the unseen hand of ocean acidification destroy cold-water ecosystems? Coral Reefs 26, 445-448.

van den Beld, I.M.J., Bourillet, J.F., Arnaud-Haond, S., de Chambure, L., Davies, J.S., Guillaumont, B., Olu, K., Menot, L., 2017. Cold-Water Coral Habitats in Submarine Canyons of the Bay of Biscay. Frontiers in Marine Science 4.

Van Dover, C.L., Aronson, J., Pendleton, L., Smith, S., Arnaud-Haond, S., Moreno-Mateos, D., Barbier, E., Billett, D., Bowers, K., Danovaro, R., Edwards, A., Kellert, S., Morato, T., Pollard, E., Rogers, A., Warner, R., 2014. Ecological restoration in the deep sea: Desiderata. Mar Policy 44, 98-106.

van Oevelen, D., Duineveld, G., Lavaleye, M., Mienis, F., Soetaert, K., Heip, C.H.R., 2009. The cold-water coral community as a hot spot for carbon cycling on continental margins: A food-web analysis from Rockall Bank (northeast Atlantic). Limnol Oceanogr 54, 1829-1844.

Van Rooij, D., De Mol, B., Huvenne, V., Ivanov, M., Henriet, J.P., 2003. Seismic evidence of current-controlled sedimentation in the Belgica mound province, upper Porcupine slope, southwest of Ireland. Mar Geol 195, 31-53.

Van Rooij, D., De Mol, L., Le Guilloux, E., Wisshak, M., Huvenne, V.A.I., Moeremans, R., Henriet, J.P., 2010. Environmental setting of deep-water oysters in the Bay of Biscay. Deep-Sea Res Pt I 57, 1561-1572.

van Soest, R.W.M., Cleary, D.F.R., de Kluijver, M.J., Lavaleye, M.S.S., Maier, C., van Duyl, F.C., 2007. Sponge diversity and community composition in Irish bathyal coral reefs. Contrib Zool 76, 121-142.

van Weering, T.C.E., de Haas, H., de Stigter, H.C., Lykke-Andersen, H., Kouvaev, I., 2003. Structure and development of giant carbonate mounds at the SW and SE Rockall Trough margins, NE Atlantic Ocean. Mar Geol 198, 67-81.

van Weering, T.C.E., de Haas, H., de Stigter, H.C., Lykke-Andersen, H., Kouvaev, I., 2003. Structure and development of giant carbonate mounds at the SW and SE Rockall Trough margins, NE Atlantic Ocean. Mar Geol 198, 67-81.

Ventura, D., Bonifazi, A., Gravina, M.F., Belluscio, A., Ardizzone, G., 2018. Mapping and Classification of Ecologically Sensitive Marine Habitats Using Unmanned Aerial Vehicle (UAV) Imagery and Object-Based Image Analysis (OBIA). Remote Sens-Basel 10.

Vertino, A., Savini, A., Rosso, A., Di Geronimo, I., Mastrototaro, F., Sanfilippo, R., Gay, G., Etiope, G., 2010. Benthic habitat characterization and distribution from two representative sites of the deep-water SML Coral Province (Mediterranean). Deep-Sea Res Pt Ii 57, 380-396.

Vierod, A.D.T., Guinotte, J.M., Davies, A.J., 2014. Predicting the distribution of vulnerable marine ecosystems in the deep sea using presence-background models. Deep-Sea Res Pt Ii 99, 6-18.

Vlasenko, V., Stashchuk, N., Inall, M.E., Hopkins, J.E., 2014. Tidal energy conversion in a global hot spot: On the 3-D dynamics of baroclinic tides at the Celtic Sea shelf break. J Geophys Res-Oceans 119, 3249-3265.

Wagner, D., Waller, R.G., Toonen, R.J., 2011. Sexual reproduction of Hawaiian black corals, with a review of the reproduction of antipatharians (Cnidaria: Anthozoa: Hexacorallia). Invertebr Biol 130, 211-225.

Wagner, H., Purser, A., Thomsen, L., Jesus, C.C., Lundalv, T., 2011. Particulate organic matter fluxes and hydrodynamics at the Tisler cold-water coral reef. J Marine Syst 85, 19-29.

Wagner, J.K., McEntee, M.H., Brothers, L.L., German, C.R., Kaiser, C.L., Yoerger, D.R. and Van Dover, C.L., 2013. Cold-seep habitat mapping: High-resolution spatial characterization of the Blake Ridge Diapir seep field. Deep Sea Research Part II: Topical Studies in Oceanography, 92, 183-188.

Westoby, M.J., Brasington, J., Glasser, N.F., Hambrey, M.J., Reynolds, J.M., 2012. 'Structure-from-Motion' photogrammetry: A low-cost, effective tool for geoscience applications. Geomorphology 179, 300-314.

Wheeler, A.J., Bett, B.J., Billett, D.S.M., Masson, D.G., Mayor, D., 2005a. The impact of demersal trawling on northeast Atlantic deepwater coral habitats: The case of the Darwin mounds, United Kingdom. Am Fish S S 41, 807-817.

Wheeler, A.J., Kozachenko, M., Beyer, A., Foubert, A., Huvenne, V.A.I., Klages, M., Masson, D.G., Olu-Le Roy, K., Thiede, J., 2005b. Sedimentary processes and carbonate mounds in the Belgica Mound province, Porcupine Seabight, NE Atlantic. Erlangen Earth C Ser, 571-603.

Wheeler, A.J., Beck, T., Thiede, J., Klages, M., Grehan, A., Monteys, F.X., Pa, P.A.X.a.S., 2005c. Deep-water coral mounds on the Porcupine Bank, Irish Margin: preliminary results from the Polarstern ARK-XIX/3a ROV cruise. Erlangen Earth C Ser, 393-402.

Wheeler, A.J., Beyer, A., Freiwald, A., de Haas, H., Huvenne, V.A.I., Kozachenko, M., Roy, K.O.L., Opderbecke, J., 2007. Morphology and environment of cold-water coral carbonate mounds on the NW European margin. Int J Earth Sci 96, 37-56.

Wheeler, A.J., Kozachenko, M., Masson, D.G., Huvenne, V.A.I., 2008. Influence of benthic sediment transport on cold-water coral bank morphology and growth: the example of the Darwin Mounds, north-east Atlantic. Sedimentology 55, 1875-1887.

Wheeler, A.J., Kozachenko, M., Henry, L.A., Foubert, A., de Haas, H., Huvenne, V.A.I., Masson, D.C., Olu, K., 2011. The Moira Mounds, small cold-water coral banks in the Porcupine Seabight, NE Atlantic: Part A an early stage growth phase for future coral carbonate mounds? Mar Geol 282, 53-64.

Wheeler, A.J., shipboard party, 2011a. Vents & reefs deep-sea ecosystem study of the 45° North MAR hydrothermal vent field and the cold-water coral Moira Mounds, Porcupine Seabight.

Wheeler, A.J., shipboard party, 2015. Quantifying environmental controls on cold-water coral reef growth.

White, M., Dorschel, B., 2010. The importance of the permanent thermocline to the cold water coral carbonate mound distribution in the NE Atlantic. Earth and Planetary Science Letters 296, 395-402.

White, M., Mohn, C., de Stigter, H., Mottram, G., 2005. Deep-water coral development as a function of hydrodynamics and surface productivity around the submarine banks of the Rockall Trough, NE Atlantic. Erlangen Earth C Ser, 503-514.

Wienberg, C., Titschack, J., Freiwald, A., Frank, N., Lundalv, T., Taviani, M., Beuck, L., Schroder-Ritzrau, A., Krengel, T., Hebbeln, D., 2018. The giant Mauritanian cold-water coral mound province: Oxygen control on coral mound formation. Quaternary Sci Rev 185, 135-152.

Wilson, J.B., 1979. Patch Development of the Deep-Water Coral *Lophelia-Pertusa* (L) on Rockall Bank. J Mar Biol Assoc Uk 59, 165-&.

Wilson, M.F.J., O'Connell, B., Brown, C., Guinan, J.C., Grehan, A.J., 2007. Multiscale terrain analysis of multibeam bathymetry data for habitat mapping on the continental slope. Mar Geod 30, 3-35.

Wilson, S.K., Graham, N.A.J., Polunin, N.V.C., 2007. Appraisal of visual assessments of habitat complexity and benthic composition on coral reefs. Mar Biol 151, 1069-1076.

Wolfl, A.C., Snaith, H., Amirebrahimi, S., Devey, C.W., Dorschel, B., Ferrini, V., Huvenne, V.A.I., Jakobsson, M., Jencks, J., Johnston, G., Lamarche, G., Mayer, L., Millar, D., Pedersen, T.H., Picard, K., Reitz, A., Schmitt, T., Visbeck, M., Weatherall, P., Wigley, R., 2019. Seafloor Mapping - The Challenge of a Truly Global Ocean Bathymetry. Frontiers in Marine Science 6.

Wood, S.N., 2011. Fast stable restricted maximum likelihood and marginal likelihood estimation of semiparametric generalized linear models. J R Stat Soc B 73, 3-36.

Woodall, C.W., Graham, J.M., 2004. A technique for conducting point pattern analysis of cluster plot stem-maps. Forest Ecol Manag 198, 31-37.

Wright, D., Lundblad, E., Larkin, E., Rinehart, R., Murphy, J., Cary-Kothera, L., Draganov, K., 2005. ArcGIS benthic terrain modeler. Oregon State University, Corvallis, OR, USA.

Wynn, R.B., Huvenne, V.A.I., Le Bas, T.P., Murton, B.J., Connelly, D.P., Bett, B.J., Ruhl, H.A., Morris, K.J., Peakall, J., Parsons, D.R., Sumner, E.J., Darby, S.E., Dorrell, R.M., Hunt, J.E., 2014. Autonomous Underwater Vehicles (AUVs): Their past, present and future contributions to the advancement of marine geoscience. Mar Geol 352, 451-468.

Xavier, J.R., Tojeira, I., Van Soest, R.W.M., 2015. On a hexactinellid sponge aggregation at the Great Meteor seamount (North-east Atlantic). J Mar Biol Assoc Uk 95, 1389-1394.

Yamada, T., Prugel-Bennett, A., Thornton, B., 2021. Learning features from georeferenced seafloor imagery with location guided autoencoders. J Field Robot 38, 52-67.

Yoerger, D.R., Kelley, D.S., Delaney, J.R., 2000. Fine-scale three-dimensional mapping of a deep-sea hydrothermal vent site using the Jason ROV system. Int J Robot Res 19, 1000-1014.

Yoshioka, P.M., Yoshioka, B.B., 1989. A Multispecies, Multiscale Analysis of Spatial Pattern and Its Application to a Shallow-Water Gorgonian Community. Mar Ecol Prog Ser 54, 257-264.

Young, G.C., Dey, S., Rogers, A.D., Exton, D., 2017. Cost and time-effective method for multiscale measures of rugosity, fractal dimension, and vector dispersion from coral reef 3D models. Plos One 12.

Zeleda Leon, A.Z., Huvenne, V.A.I., Benoist, N.M.A., Ferguson, M., Bett, B.J., Wynn, R.B., 2020. Assessing the Repeatability of Automated Seafloor Classification Algorithms, with Application in Marine Protected Area Monitoring. Remote Sens-Basel 12.

Zuur, A., Ieno, E.N., Smith, G.M., 2007. Analyzing ecological data. Springer Science & Business Media.

Zuur, A.F., 2012. A beginner's guide to generalized additive models with R. Highland Statistics Limited Newburgh.